Effectiveness of Automatic Emergency Braking for Protection of Pedestrians and Bicyclists in the U.S.

Samantha H. Haus

Thesis submitted to the faculty of the Virginia Polytechnic Institute and State University in partial fulfillment of the requirement for the degree of

Doctor of Philosophy
In
Biomedical Engineering

Hampton C. Gabler, Co-Chair
Miguel Perez, Co-Chair
Zachary Doerzaph
F. Scott Gayzik
Jessica Jermakian

October 12th, 2021

Blacksburg, Virginia

Keywords: Vulnerable Road Users, Active Safety, AEB, U.S., Benefits

Effectiveness of Automatic Emergency Braking for Protection of Pedestrians and Bicyclists in the U.S.

Samantha H. Haus

Abstract (Academic)

In the United States, there were 36,560 traffic-related fatalities in 2018, of which 20% were pedestrians, bicyclists, and other vulnerable road users (VRUs) [1]. Vulnerable road users are non-vehicle occupants who, because they are not enclosed in a vehicle, are at higher risk of injury in traffic crashes. While overall traffic fatalities in the US have been decreasing, pedestrian and bicyclist fatalities have been trending upward. Vehicle-based active safety features could avoid or mitigate crashes with VRUs, but are highly dependent on the ability to detect a VRU with enough time or distance. This work presents methods to examine the characteristics of vehicle-pedestrian and vehicle-bicycle crashes and near-crashes using a variety of data sources, assess the potential effectiveness of Automatic Emergency Braking (AEB) in avoiding and mitigating VRU crashes through modeling and simulation, and estimate the future benefits of AEB for VRU safety in the United States. Additionally, active safety features are most effective when behavior of VRUs can be anticipated, however, the behavior of pedestrians and bicyclists is notoriously unpredictable. Therefore, an approach to examine and categorize pedestrian behavior in response to near-crashes and crashes events is presented. Overall, findings suggest that AEB has great potential to avoid and mitigate collisions with pedestrians and bicyclists, but it cannot avoid all crashes even when an idealized AEB system is assumed. Most pedestrians and bicyclists were found to be visible for at least one second prior to the crash, but obstructions, the unpredictability of VRUs, and adverse weather/lighting conditions still pose challenges in avoiding and mitigating crashes with VRUs.

Effectiveness of Automatic Emergency Braking for Protection of Pedestrians and Bicyclists in the U.S.

Samantha H. Haus

Abstract (General Audience)

In the United States, there were 36,560 traffic-related fatalities in 2018, of which 20% were pedestrians, bicyclists, and other vulnerable road users (VRUs) [1]. Vulnerable road users are non-vehicle occupants who, because they are not enclosed in a vehicle, are at higher risk of injury in traffic crashes. While overall traffic fatalities in the US have been decreasing, pedestrian and bicyclist fatalities are trending upward. Vehicle-based countermeasures, such as Automatic Emergency Braking (AEB), could avoid or mitigate crashes with VRUs, but are highly dependent on the ability to detect a VRU with enough time or distance. My work presents methods to examine the characteristics of vehicle-pedestrian and vehicle-bicycle crashes and near-crashes using a variety of data sources, assess the potential effectiveness of AEB in avoiding and mitigating VRU crashes through modeling and simulation, and estimate the future benefits of AEB for VRU safety in the United States. Additionally, crash avoidance technologies are most effective when behavior of VRUs can be anticipated, however, the behavior of pedestrians and bicyclists is notoriously unpredictable. Therefore, I examined and categorized pedestrian behavior in response to near-crashes and crashes events. Overall, we found that AEB has great potential to avoid and mitigate collisions with pedestrians and bicyclists, but it cannot avoid all crashes even when assuming an idealized AEB system. Most pedestrians and bicyclists were found to be visible for at least one second prior to the crash, but obstructions, the unpredictability of VRUs, and adverse weather/lighting conditions still pose challenges in avoiding and mitigating crashes with VRUs.

Acknowledgements

I would like to thank the many people who supported me during my PhD journey. I would like to start by thanking my advisor Dr. Gabler. While he is no longer with us, I hope to carry on his legacy of kindness and curiosity. He is truly missed and I am grateful that I had a chance to work with and learn from him. I would also like to thank Dr. Perez for stepping up as my co-chair. He welcomed me into his lab and generously supported me while I finished my dissertation. I would like to thank my committee members, Dr. Doerzaph, Dr. Gayzik, and Dr. Jermakian, for their guidance and constructive feedback on my dissertation, and the BEAM department for supporting and teaching me during my time at Virginia Tech.

I would like to thank my family for always encouraging me to pursue my goals and always believing in me. To Kyle, thank you for supporting me and giving me a kick in the butt when I needed it (even if I wasn't happy about it). Thank you to my friends who were there when I needed a distraction from my PhD work and made graduate school fun.

To my lab mates, thank you for always being there to brainstorm (no matter how tangential), lend a hand, and keep me sane. Thank you to the undergraduate researchers in the lab for their assistance. I would especially like to thank Jordan Moon for her help digitizing all the PCDS trajectories, Ryan Anderson for his help analyzing vehicle-bicycle crashes, and Jeremy Decker for his creative approach to analyzing vehicle-animal crashes (not included in this dissertation).

Finally, thank you to the Toyota Collaborative Safety Research center for funding much of this work and Rini Sherony for her technical guidance.

.

Attribution

This dissertation contains three published journal papers and three published conference proceedings. While I was the primary contributor to these works, other authors contributed to the final manuscripts. Below are the author contributions for the individual works.

1. Estimated Benefit of Automated Emergency Braking Systems for Vehicle-Pedestrian Crashes in the U.S. [2]. Rini Sherony and Hampton C. Gabler provided technical feedback and editorial comments.
2. Differential Benefit of Sensor System Field-of-View and Range in Pedestrian Automated Emergency Braking Systems[3]. Rini Sherony and Hampton C. Gabler provided technical feedback and editorial comments.
3. Potential Effectiveness of Bicycle-Automatic Emergency Braking using the WATS Dataset [4]. Ryan M. Anderson assisted in collection of additional variables from dataset and data analysis. Rini Sherony and Hampton C. Gabler provided technical feedback and editorial comments.
4. Feasibility of using Naturalistic Driving Data to Characterize Vehicle-Pedestrian Crashes and Near Crashes [5]. Rini Sherony and Hampton C. Gabler provided technical feedback and editorial comments.
5. Automatic Emergency Braking Sensor Configuration Effect on the Detection of U.S. Pedestrians [6]. Rini Sherony and Hampton C. Gabler provided technical feedback and editorial comments.
6. Characteristics of vehicle-bicycle crashes and near-crashes using naturalistic driving data [7]. Hampton C. Gabler provided technical feedback and editorial comments.

TABLE OF CONTENTS

1 Introduction 1
1.1 Problem Definition 1
1.2 Injury Factors 1
1.3 Vehicle Based Countermeasures 4
1.4 Consumer Information Programs 8
1.5 Research Goal 10
2 Data Sources 11
2.1 FARS 11
2.2 GES 11
2.3 CRSS 12
2.4 PCDS 12
2.5 SHRP 2 13
2.6 WATS 13
3 Pedestrian AEB Target Population 14
3.1 Research Objective 14
3.2 Approach 14
3.3 Results 16
3.4 Conclusion 30
4 Pedestrian Earliest Detection Opportunity 32
4.1 Research Objective 32
4.2 Pedestrian trajectory derived EDO using PCDS 32
4.3 Feasibility of using Naturalistic Driving Data to Characterize Vehicle-Pedestrian Crashes and Near Crashes [5] 38
4.4 Automatic Emergency Braking Sensor Configuration Effect on the Detection of U.S. Pedestrians [6] 48
4.5 Conclusion 58
5 Pedestrian AEB Effectiveness 60
5.1 Research Objective 60
5.2 Estimated Benefit of Automated Emergency Braking Systems for Vehicle-Pedestrian Crashes in the U.S. [2] 60
5.3 Differential Benefit of Sensor System Field-of-View and Range in Pedestrian Automated Emergency Braking Systems[3] 76
5.4 Conclusion 100
6 Pedestrian AEB Predicted Benefits 102
6.1 Research objective 102
6.2 Approach 102
6.3 Results 106
6.4 Discussion 107

7 Bicyclist AEB Target Population 108
7.1 Research Objective 108
7.2 Approach 108
7.3 Results 109
7.4 Discussion 127
8 Bicyclist Earliest Detection Opportunity 130
8.1 Research Objective 130
8.2 Potential Effectiveness of Bicycle-Automatic Emergency Braking using the WATS Dataset [4] 130
8.3 Characteristics of vehicle-bicycle crashes and near-crashes using naturalistic driving data [7] 145
8.4 Conclusion 159
9 Bicyclist AEB Effectiveness 161
9.1 Research Objective 161
9.2 Approach 161
9.3 Results 163
9.4 Discussion 165
9.5 Conclusion 167
10 Bicyclist AEB Predicted Benefits 168
10.1 Research Objective 168
10.2 Approach 168
10.3 Results 169
10.4 Discussion 172
10.5 Conclusion 172
11 Understanding Pedestrian Behavior In Crash and Near-Crash Scenarios 173
11.1 Research Objective 173
11.2 Introduction 173
11.3 Methods 174
11.4 Results 176
11.5 Discussion 185
12 Conclusion 187
References 189

Table of Figures

FIGURE 1. FATALITY RISK OF PEDESTRIANS STRUCK BY THE FRONT OF A PASSENGER CAR AS A FUNCTION OF IMPACT SPEED. (A) RESULTS BASED ON BIASED DATA, (B) RESULTS ADJUSTED FOR BIAS FROM 1960S-1970S, AND (C) LESS BIASED OR ADJUSTED DATA RESULTING FROM CRASHES IN THE 1990S AND 2000S. [10]..... 3

FIGURE 2. THE NUMBER OF PEDESTRIAN FATALITIES IN THE U.S. FROM 2011 – 2015 COMPARED TO THE TARGET POPULATION (FARS).....17

FIGURE 3. THE NUMBER OF POLICE REPORTED VEHICLE-PEDESTRIAN CRASHES FROM 2011 – 2015 COMPARED TO THE TARGET POPULATION (GES). 17

FIGURE 4. THE NUMBER OF PEDESTRIAN FATALITIES IN THE U.S. FROM 2011-2015. DATA SOURCE: FARS 19

FIGURE 5. THE NUMBER AND SEVERITY OF POLICE REPORTED VEHICLE-PEDESTRIAN CRASHES FROM 2011-2015. DATA SOURCE: GES.....19

FIGURE 6. THE AGE DISTRIBUTION OF PEDESTRIANS FROM FARS AND GES.....20

FIGURE 7. DISTRIBUTION OF PEDESTRIANS INVOLVED IN VEHICLE-PEDESTRIAN COLLISIONS, BY GENDER.....21

FIGURE 8. DISTRIBUTION OF CASES IN WHICH PEDESTRIAN WAS INVOLVED WITH ALCOHOL. DATA SOURCE: FARS 21

FIGURE 9. DISTRIBUTION OF CASES IN WHICH PEDESTRIAN WAS INVOLVED WITH ALCOHOL. DATA SOURCE: GES.22

FIGURE 10. AGE DISTRIBUTION OF DRIVERS. DATA SOURCE: FARS, GES.....23

FIGURE 11. DISTRIBUTION OF DRIVER GENDER IN FATAL PEDESTRIAN CRASHES (FARS) AND IN ALL PEDESTRIAN CRASHES (GES).....23

FIGURE 12. DISTRIBUTION OF CASES IN WHICH THE DRIVER WAS INVOLVED WITH ALCOHOL. DATA SOURCE: FARS 24

FIGURE 13. DISTRIBUTION OF CASES IN WHICH THE DRIVER WAS INVOLVED WITH ALCOHOL. DATA SOURCE: GES 24

FIGURE 14. LIGHTING CONDITION DISTRIBUTION AT TIME OF COLLISION. DATA SOURCE: FARS, GES 26

FIGURE 15. WEATHER CONDITION DISTRIBUTION AT TIME OF COLLISION. DATA SOURCE: FARS, GES 27

Figure 16. Distribution of speed limit in incident locations. Data source: FARS.....27
Figure 17. Distribution of speed limit in incident locations. Data source: GES.....28
Figure 18. Distribution of collisions in relation to junction. Data source: FARS and GES.....28
Figure 19. Comparison of two methods of detection time calculation.....37
Figure 20. Cumulative distribution plot of the estimated time pedestrian was detectable using three different methods. Time on Road (red) and Time Visible (green) assume a pedestrian speed of 1.2m/s whereas Time Visible (blue) adjusted walking speed by pedestrian age.....37
Figure 21. Crash Modes from SHRP 2 video analysis.....39
Figure 22. Incidence rates of crash modes in SHRP 2.....42
Figure 23. Duration pedestrian was visible by crash mode. The points above and below the box and whisker plots are outliers which were defined as points greater than 1.5 times the interquartile range away from the median.....43
Figure 24. Distribution plot of duration visible for the total time the pedestrian was visible and the duration visible only for when the pedestrian was on the road. The dotted line is located at one second duration visible which is the assumed minimum time needed for injury mitigation. 43
Figure 25. Braking Time-To-Collision (TTC) by crash mode. The points above and below the box and whisker plots are outliers which were defined as points greater than 1.5 times the interquartile range away from the median.....44
Figure 26. Comparison of vehicle speed at 1 second before the impact proximity point (IPP). The dotted line is the points were the speed before and at the impact proximity point were the same indicating no braking occurred.....45
Figure 27. Time-to-collision of braking compared to the subject vehicle speed at the onset of braking.....45

FIGURE 28. CUMULATIVE DISTRIBUTION PLOT OF TIME-TO-COLLISION OF BRAKING FOR DAYLIGHT AND NON-DAYLIGHT LIGHTING. 46
FIGURE 29. VEHICLE (BLUE) AND PEDESTRIAN (RED) TRAJECTORIES IN GLOBAL COORDINATES FOR THE EARLY/WEAK (LEFT) AND LATE/HARD (RIGHT) BRAKING DRIVER. 49
FIGURE 30. PERCENTAGE OF CASES IN WHICH THE PEDESTRIAN WAS DETECTED FOR SENSOR FOVS FROM ±10° TO ±90° AND SENSOR RANGES FROM 20M – 100M. 53
FIGURE 31. PEDESTRIAN LOCATION WHEN FIRST DETECTED BY SENSOR SYSTEM WITH SENSOR FOVS FROM ±10° TO ±90° AND SENSOR RANGES FROM 20M – 100M. BLUE POINTS INDICATE CASES WITH OBSTRUCTIONS AND GREEN POINTS INDICATE CASES WITH NO KNOWN OBSTRUCTION. 54
FIGURE 32 CUMULATIVE DISTRIBUTION OF TTC AT PEDESTRIAN DETECTION BY SENSOR SYSTEM WITH SENSOR FOVS FROM ±10° TO ±90° AND SENSOR RANGES FROM 20M – 100M. 55
FIGURE 33. CUMULATIVE DISTRIBUTION OF PEDESTRIAN ANGLE RELATIVE TO HYPOTHETICAL AEB SYSTEM AT A TTC OF 1 (RED), 2 (GREEN), AND 3 (BLUE) SECONDS. 56
FIGURE 34. CUMULATIVE DISTRIBUTION OF PEDESTRIAN DISTANCE RELATIVE TO HYPOTHETICAL AEB SYSTEM AT A TTC OF 1 (RED), 2 (GREEN), AND 3 (BLUE) SECONDS. 56
FIGURE 35. STUDY APPROACH OVERVIEW. 61
FIGURE 36. POTENTIAL AEB BRAKING PROFILE CASES. 64
FIGURE 37. DECELERATION PROFILES FOR (A) EARLY/WEAK BRAKING DRIVER AND (B) LATE/HARD BRAKING DRIVER WITH RAMP-UP BRAKING. 65
FIGURE 38. CUMULATIVE DISTRIBUTION PLOT OF IMPACT SPEEDS FOR BRAKING AND NON-BRAKING DRIVERS IN THE AEB-RELEVANT CASES. 66
FIGURE 39. FATALITY RISK CURVE FOR CARS (RED) AND LTVS (BLUE) COMPARED TO ROSÉN, ET AL. [10](BLACK). THE FATALITY RISKS ARE SHOWN IN RELATION TO IMPACT SPEED ASSUMING A PEDESTRIAN AGE OF 30. THE DOTTED AND DASHED LINES CORRESPOND TO A 95% CONFIDENCE INTERVAL. 69

FIGURE 40. MAIS3+F INJURY RISK CURVE FOR CARS (RED) AND LTVS (BLUE) COMPARED TO ROSÉN, ET AL. [10](BLACK). THE INJURY RISKS ARE SHOWN IN RELATION TO IMPACT SPEED ASSUMING A PEDESTRIAN AGE OF 30. THE DOTTED AND DASHED LINES CORRESPOND TO A 95% CONFIDENCE INTERVAL.....69
FIGURE 41. CUMULATIVE DISTRIBUTION OF CALCULATED TRAVEL SPEEDS FOR ALL AEB-RELEVANT CASES (LEFT) AND DEPICTION OF DECELERATION PROFILES (RIGHT).....71
FIGURE 42. AEB SYSTEM EFFECTIVENESS AT A RANGE OF TTC VALUES AND LATENCY VALUES FOR BOTH THE LATE/HARD BRAKING DRIVER SCENARIO AND THE EARLY/WEAK BRAKING DRIVER SCENARIO. 72
FIGURE 43. AEB SYSTEM AVERAGE CHANGE IN VELOCITY FOR UNAVOIDED CASES FOR A RANGE OF TTC AND LATENCY VALUES FOR BOTH THE LATE/HARD BRAKING DRIVER SCENARIO AND THE EARLY/WEAK BRAKING DRIVER SCENARIO. THE NUMBER ON THE BAR CORRESPONDS TO THE NUMBER OF UNAVOIDED CASES. 73
FIGURE 44. PERCENT CHANGE IN FATALITY RISK (LEFT) AND MAIS3+F INJURY RISK (RIGHT) FOR A RANGE OF TTC AND LATENCY VALUES FOR BOTH THE LATE/HARD BRAKING DRIVER SCENARIO AND THE EARLY/WEAK BRAKING DRIVER SCENARIO.....74
FIGURE 45. SCHEMATIC OF AEB MODEL. 84
FIGURE 46. IMPACT DETECTION METHOD SCHEMATIC.....87
FIGURE 47. PERCENT OF CRASHES AVOIDED FOR A SET OF SENSOR HALF ANGLES AND RANGES.....90
FIGURE 48. PERCENT OF CRASHES AVOIDED FOR A SET OF SENSOR HALF ANGLES AND RANGES BY WHETHER THE VEHICLE HAD A STRAIGHT OR CURVED TRAJECTORY.....91
FIGURE 49. AVERAGE IMPACT SPEED (M/S) OF UNAVOIDED CRASHES FOR A SET OF SENSOR HALF ANGLES AND RANGES.....92
FIGURE 50. RISK OF FATAL INJURY FOR THE RANGE OF IMPACT SPEEDS AND PEDESTRIAN WEIGHT FOR CHILDREN (A), ADULTS (B), AND SENIORS (C). PURPLE CORRESPONDS TO LOW INJURY RISK WHILE YELLOW CORRESPONDS TO HIGH INJURY RISK. THE CONTOUR LINES (WHITE) ARE SPACED AT 10% INJURY RISK INTERVALS. RISKS SHOWN WERE LIMITED TO THE RANGE OF OBSERVED DATA WITHIN EACH AGE GROUP. 93

FIGURE 51. RISK OF FATAL INJURY CONTOUR LINES FOR CHILD (GREEN), ADULT (RED), AND SENIORS (BLUE). DARKER CONTOUR LINES CORRESPOND TO HIGHER INJURY RISK. LINE LENGTH CORRESPONDS TO THE DATA AVAILABLE WITHIN EACH AGE GROUP. 94
FIGURE 52. RISK OF FATAL INJURIES FOR THE CHILD, ADULT AND SENIOR GROUPS. WEIGHT WAS SET AS THE MEDIAN WEIGHT IN EACH GROUP: 70 KG FOR ADULT AND SENIOR AND 37 KG FOR CHILD. DOTTED LINES CORRESPOND TO 95 PERCENTILE CONFIDENCE INTERVALS. LOGISTIC REGRESSION EQUATIONS ARE PROVIDED WITH THE COEFFICIENTS ROUNDED TO TWO DECIMAL PLACES. 94
FIGURE 53. RISK OF MAIS 3+F INJURY FOR CHILD, ADULT AND SENIOR AGE GROUPS. DOTTED LINES CORRESPOND TO 95 PERCENTILE CONFIDENCE INTERVALS. LOGISTIC REGRESSION EQUATIONS ARE PROVIDED WITH THE COEFFICIENTS ROUNDED TO TWO DECIMAL PLACES. 95
FIGURE 54. RISK OF MAIS2+F INJURY FOR CHILD, ADULT, AND SENIOR AGE GROUPS. DOTTED LINES CORRESPOND TO 95 PERCENTILE CONFIDENCE INTERVALS. LOGISTIC REGRESSION EQUATIONS ARE PROVIDED WITH THE COEFFICIENTS ROUNDED TO TWO DECIMAL PLACES. 96
FIGURE 55. PROPORTION OF FATAL INJURIES PREVENTED BY P-AEB WITH 70%, 80%, 90%, AND 100% SENSORS. ERROR BARS REPRESENT ONE STANDARD DEVIATION CHANGE IN THE INJURY RISK MODEL 97
FIGURE 56. PROPORTION OF MAIS3+F INJURIES PREVENTED BY P-AEB WITH 70%, 80%, 90%, AND 100% SENSORS. ERROR BARS REPRESENT ONE STANDARD DEVIATION CHANGE IN THE INJURY RISK MODEL 97
FIGURE 57. PROPORTION OF MAIS2+F INJURIES PREVENTED BY P-AEB WITH 70%, 80%, 90%, AND 100% SENSORS. ERROR BARS REPRESENT ONE STANDARD DEVIATION CHANGE IN THE INJURY RISK MODEL 97
FIGURE 58. ESTIMATED PEDESTRIAN-AEB MARKET PENETRATION BASED ON THE IIHS AEB MARKET PENETRATION ESTIMATES AND SHIFTED TO REFLECT BICYCLIST-AEB ENTERING THE MARKET IN 2011. .. 103
FIGURE 59. CRASH (A), FATAL INJURY (B), AND MAIS3+F INJURY (C) REDUCTION EFFECTIVENESS BY MARKET PENETRATION. 104
FIGURE 60. CRASH (A), FATAL INJURY (B) AND MAIS3+F INJURY (C) REDUCTION EFFECTIVENESS OVER TIME. 105

FIGURE 61. ESTIMATE OF VEHICLE-PEDESTRIAN CRASHES WITHOUT PEDESTRIAN-AEB (BLACK LINE) COMPARED TO SPATIOTEMPORAL MODEL (PINK LINE) AND TEMPORAL MODEL (BLUE LINE) WITH THE "BEST" (SOLID LINE) AND "WORST" (DOTTED LINE) PERFORMING PEDESTRIAN-AEB. ASSUMED CONSTANT VMT (LEFT) AND GROWING VMT (RIGHT)..... 106
FIGURE 62. ESTIMATE OF VEHICLE-PEDESTRIAN FATAL INJURIES WITHOUT PEDESTRIAN-AEB (BLACK LINE) COMPARED TO SPATIOTEMPORAL MODEL (PINK LINE) AND TEMPORAL MODEL (BLUE LINE) WITH THE "BEST" (SOLID LINE) AND "WORST" (DOTTED LINE) PERFORMING PEDESTRIAN-AEB. ASSUMED CONSTANT VMT (LEFT) AND GROWING VMT (RIGHT)..... 106
FIGURE 63. ESTIMATE OF VEHICLE-PEDESTRIAN MAIS3+F INJURIES WITHOUT PEDESTRIAN-AEB (BLACK LINE) COMPARED TO SPATIOTEMPORAL MODEL (PINK LINE) AND TEMPORAL MODEL (BLUE LINE) WITH THE "BEST" (SOLID LINE) AND "WORST" (DOTTED LINE) PERFORMING PEDESTRIAN-AEB. ASSUMED CONSTANT VMT (LEFT) AND GROWING VMT (RIGHT)..... 107
FIGURE 64. VEHICLE-BICYCLE FATALITIES FROM 2011-2015 (FARS)..... 109
FIGURE 65. VEHICLE-BICYCLE POLICE-REPORTED CRASHES FROM 2011-2015 (GES)..... 110
FIGURE 66. DISTRIBUTION OF IMPACT LOCATIONS VEHICLE-BICYCLE FATALITIES (FARS) AND POLICE-REPORTED CRASHES (GES)..... 111
FIGURE 67. BREAKDOWN OF TARGET POPULATION EXCLUSION CRITERIA FOR BICYCLISTS..... 113
FIGURE 68. THE TOTAL VEHICLE-BICYCLE FATALITIES (FARS) COMPARED TO THE TARGET POPULATION THAT COULD BE AFFECTED BY BICYCLIST AEB..... 113
FIGURE 69. THE TOTAL VEHICLE-BICYCLE CRASHES (GES) COMPARED TO THE TARGET POPULATION THAT COULD BE AFFECTED BY BICYCLIST AEB..... 114
FIGURE 70. DISTRIBUTION OF BICYCLIST AGES FOR VEHICLE-BICYCLE FATALITIES FROM 2011-2015 (FARS). 114
FIGURE 71. DISTRIBUTION OF BICYCLIST AGES FOR VEHICLE-BICYCLE POLICE-REPORTED CRASHES FROM 2011-2015 (GES)..... 115

FIGURE 72. DISTRIBUTION OF BICYCLIST GENDER FOR ALL VEHICLE-BICYCLIST FATALITIES (FARS) AND CRASHES (GES) FROM 2011-2015. 115
FIGURE 73. DISTRIBUTION OF BICYCLISTS THAT HAD EVIDENCE OF ALCOHOL INVOLVEMENT FOR FATAL (FARS) AND POLICE-REPORTED CRASHES (GES) FROM 2011-2015 116
FIGURE 74. DISTRIBUTION OF DRIVER AGES FOR VEHICLE-BICYCLE FATALITIES FROM 2011-2015 (FARS). 117
FIGURE 75. DISTRIBUTION OF DRIVER AGES FOR VEHICLE-BICYCLE CRASHES FROM 2011-2015 (GES). 117
FIGURE 76. DISTRIBUTION OF DRIVER GENDER FOR ALL VEHICLE-BICYCLIST FATALITIES (FARS) AND CRASHES (GES) FROM 2011-2015. 118
FIGURE 77. DISTRIBUTION OF DRIVERS THAT HAD REPORTED ALCOHOL INVOLVEMENT FOR FATAL (FARS) AND POLICE-REPORTED CRASHES (GES) FROM 2011-2015. 118
FIGURE 78. DISTRIBUTION OF SPEED LIMITS FOR FATAL (FARS) AND POLICE-REPORTED CRASHES (GES) FROM 2011-2015. 119
FIGURE 79. DISTRIBUTION OF LIGHTING CONDITIONS FOR FATAL (FARS) AND POLICE-REPORTED CRASHES (GES) FROM 2011-2015. 120
FIGURE 80. DISTRIBUTION OF WEATHER CONDITIONS FOR FATAL (FARS) AND POLICE-REPORTED CRASHES (GES) FROM 2011-2015. 121
FIGURE 81. DISTRIBUTION OF BICYCLIST RELATION TO THE ROAD FOR FATAL (FARS) AND POLICE-REPORTED CRASHES (GES) FROM 2011-2015 122
FIGURE 82. DISTRIBUTION OF CRASH LOCATION IN RELATION TO JUNCTION FOR FATAL (FARS) AND POLICE-REPORTED CRASHES (GES) FROM 2011-2015. 123
FIGURE 83. DISTRIBUTION OF BICYCLIST INITIAL TRAVEL DIRECTION FOR FATAL (FARS) AND POLICE-REPORTED CRASHES (GES) FROM 2014-2015 124
FIGURE 84. DISTRIBUTION OF BICYCLIST POSITION FOR FATAL (FARS) AND POLICE-REPORTED CRASHES (GES) FROM 2014-2015. 124

FIGURE 85. DISTRIBUTION OF BICYCLIST CRASH GROUPS FOR FATAL (FARS) AND POLICE-REPORTED CRASHES (GES) FROM 2014-2015. DESCRIPTIONS OF THE CRASH GROUPS CAN BE FOUND ON PAGES 99-102 OF THE PBCAT MANUAL [82]. 125
FIGURE 86. DISTRIBUTION OF PRE-EVENT VEHICLE MOVEMENT FOR FATAL (FARS) AND POLICE-REPORTED CRASHES (GES) FROM 2014-2015 126
FIGURE 87. SAMPLE CRASH SCENE DIAGRAM AND CAD MEASUREMENT. GREEN BRACKET INDICATES THE MEASURED DISTANCE THE BICYCLIST TRAVELED ON THE ROAD 133
FIGURE 88. RIDE THROUGH (LEFT), TURNING LEFT/RIGHT (CENTER), AND RIDE ALONG (RIGHT) DIAGRAMS. 134
FIGURE 89. DISTRIBUTION OF VEHICLE PRE-EVENT MOVEMENTS BEFORE COLLIDING WITH A BICYCLIST. 141
FIGURE 90. PERCENTAGE OF CRASH CASES FOR VARYING VEHICLE AND BICYCLING TRAVELING PATHS IN WATS. THE ANNOTATED NUMBER DENOTES THE NUMBER OF CASES EACH BAR REPRESENTS. 142
FIGURE 91. CUMULATIVE DISTRIBUTION OF EARLIEST DETECTION TIME FOR RIDE ALONG AND RIDE THROUGH CASES IN WATS. 143
FIGURE 92. THE MOST COMMON VEHICLE-BICYCLE INTERACTIONS FOUND IN THE SHRP 2 NDS DATABASE. 147
FIGURE 93. VISUAL DEPICTION OF TIME AND TOTAL TIME IN NON-OBSTRUCTED AND OBSTRUCTED CASES. 148
FIGURE 94. BREAKDOWN OF THE INCIDENCE OF THE DIFFERENT VEHICLE BICYCLE INTERACTION TYPES BY PERCENTAGE OF TOTAL CASES. 152
FIGURE 95. DISTRIBUTION OF DURATION OF BICYCLIST VISIBILITY (SECONDS) BEFORE THE PROXIMITY POINT (BLUE) COMPARED TO THE DURATION THE BICYCLIST WAS BOTH VISIBLE AND ON THE ROAD (PINK). THE DASHED LINE MARKS THE ONE SECOND THRESHOLD 153
FIGURE 96. BOX PLOTS OF THE SPEED BICYCLISTS WERE TRAVELLING GROUPED BY THE VEHICLE-BICYCLE INTERACTION TYPE. 153
FIGURE 97. BOX PLOT OF THE DURATION BICYCLISTS WERE BOTH VISIBLE AND ON THE ROAD GROUPED BY THE VEHICLE BICYCLE INTERACTION TYPE. 154

FIGURE 98. THE SPEED IN KM/H BETWEEN VEHICLES 1 SECOND BEFORE PROXIMITY POINT AND AT THE PROXIMITY POINT. THE HORIZONTAL DISTANCE BETWEEN THE DATA POINT AND THE NO BRAKE LINE (BLUE) INDICATES THE INCREASE OR DECREASE IN SPEED. 155
FIGURE 99. CUMULATIVE DISTRIBUTION PLOT OF THE MAXIMUM LONGITUDINAL DECELERATION FOR EACH EVENT. 155
FIGURE 100. CUMULATIVE DISTRIBUTION PLOT OF THE TOTAL AND ON-ROAD TIME THE BICYCLIST WAS VISIBLE BEFORE THE PROXIMITY POINT (SHRP 2) COMPARED TO THE WATS ESTIMATED EARLIEST DETECTION OPPORTUNITY. 159
FIGURE 101. DIAGRAM OF AEB SYSTEM MODELED 162
FIGURE 102. EVENTS AVOIDED THROUGH BRAKING USING DIFFERING LATENCY AND TTC VALUES. 163
FIGURE 103. AVERAGE CHANGE IN VELOCITY FOR UNAVOIDED CASES. THE NUMBER IN THE BAR CORRESPONDS TO THE NUMBER OF UNAVOIDED CASES FOR A GIVEN AEB SYSTEM CONFIGURATION. 164
FIGURE 104. COMPARISON OF AVERAGE CHANGE IN VELOCITY FOR CASES THAT COULD NOT BE AVOIDED FROM BRAKING ALONE. SPLIT BY ROAD SURFACE CONDITIONS: MU = 0.4 WAS ASSUMED FOR WET ROAD CONDITIONS, AND MU = 0.8 WAS ASSUMED FOR DRY ROAD CONDITIONS. THE NUMBER IN THE BAR CORRESPONDS TO THE NUMBER OF UNAVOIDED CASES. 165
FIGURE 105. VEHICLE SPEED (SPEED LIMIT USED AS SURROGATE) COMPARED TO EARLIEST DETECTION TIME. THE CURVED LINE DENOTES THE MAXIMUM EARLIEST DETECTION TIME NEEDED TO AVOID A CRASH FOR A GIVEN TRAVEL SPEED. THE COLOR OF THE POINT INDICATES WHETHER THAT CASES COULD BE AVOIDED (GREEN) BY A SYSTEM WITH A 1.5 SECOND TTC OF BRAKING AND 0 SECOND LATENCY, OR NOT AVOIDED (RED) 166
FIGURE 106. ESTIMATED BICYCLIST-AEB MARKET PENETRATION BASED ON THE IIHS AEB MARKET PENETRATION ESTIMATES AND SHIFTED TO REFLECT BICYCLIST-AEB ENTERING THE MARKET IN 2019. .. 169
FIGURE 107. CRASH REDUCTION BY MARKET PENETRATION. 170
FIGURE 108. CRASH REDUCTION EFFECTIVENESS BY YEAR 170

FIGURE 109. ESTIMATE OF VEHICLE-BICYCLE CRASHES WITHOUT BICYCLIST-AEB (BLACK LINE) COMPARED TO CRASHES WITH BICYCLIST-AEB (BLUE LINE) FOR THE CONSTANT (LEFT) AND INCREASING (RIGHT) VMT ASSUMPTIONS. 171
FIGURE 110. DISTRIBUTION OF PEDESTRIAN REACTIONS. THE NUMBER IN THE BAR CORRESPONDS TO THE NUMBER OF PEDESTRIAN TRAJECTORIES. 177
FIGURE 111. PEDESTRIAN SPEED PROFILES FOR SHRP 2 CRASH AND NEAR CRASH EVENTS DIVIDED BY PEDESTRIAN REACTION GROUP. A TIME OF ZERO CORRESPONDS TO THE IMPACT PROXIMITY POINT. DOTTED LINES REPRESENT EVENTS THAT WERE CRASHES. 178
FIGURE 112. PEDESTRIAN HEADING CHANGE FROM ORIGINAL TRAJECTORY FOR SHRP 2 CRASH AND NEAR CRASH EVENTS DIVIDED BY PEDESTRIAN REACTION GROUP. A TIME OF ZERO CORRESPONDS TO THE IMPACT PROXIMITY POINT. 179
FIGURE 113. DISTRIBUTION OF PEDESTRIAN LOCATIONS FOR EACH PEDESTRIAN REACTION TYPE. THE NUMBER IN THE BAR CORRESPONDS TO THE NUMBER OF PEDESTRIAN TRAJECTORIES. 180
FIGURE 114. DISTRIBUTION OF LIGHTING CONDITIONS FOR EACH PEDESTRIAN REACTION TYPE. THE NUMBER IN THE BAR CORRESPONDS TO THE NUMBER OF PEDESTRIAN TRAJECTORIES. 181
FIGURE 115. DISTRIBUTION OF ESTIMATED PEDESTRIAN AGE GROUP FOR EACH PEDESTRIAN REACTION TYPE. THE NUMBER IN THE BAR CORRESPONDS TO THE NUMBER OF PEDESTRIAN TRAJECTORIES. 182
FIGURE 116. CUMULATIVE DISTRIBUTION OF MINIMUM (BLUE), AVERAGE (RED), AND MAXIMUM (GREEN) PEDESTRIAN SPEED FOR EACH PEDESTRIAN REACTION GROUP. 183
FIGURE 117. CUMULATIVE DISTRIBUTION OF PEDESTRIAN REACTION TIME FOR EACH PEDESTRIAN REACTION GROUP. THE MINIMAL REACTION GROUP WAS NOT INCLUDED AS THERE WAS NO ESTIMATED REACTION TIME. 185

Table of Tables

TABLE 1. BREAKDOWN OF TARGET POPULATION FILTERING....16

TABLE 2. PEDESTRIAN CHARACTERISTICS OF VEHICLE–PEDESTRIAN CRASHES IN FARS AND GES....18

TABLE 3. DRIVER CHARACTERISTICS OF VEHICLE-PEDESTRIAN CRASHES IN FARS AND GES....22

TABLE 4. ENVIRONMENTAL CHARACTERISTICS OF VEHICLE-PEDESTRIAN CRASHES IN FARS AND GES....25

TABLE 5. CRASH AVOIDANCE POTENTIAL OF P-AEB SYSTEMS THAT MAY BE LIMITED BY WEATHER AND/OR LIGHTING CONDITIONS....30

TABLE 6. OVERVIEW OF PCDS PARALLEL CASES AND THE LIGHTING CONDITIONS OF THE EVENTS....33

TABLE 7. AVERAGE WALKING SPEED OF PEDESTRIANS BASED ON AGE AS RECOMMENDED BY GATES ET AL [59]. 34

TABLE 8. OVERVIEW OF PCDS CASES WITH VISUAL OBSTRUCTIONS....34

TABLE 9. PCDS CASE BREAKDOWN BY PEDESTRIAN STRUCK. 35

TABLE 10. BREAKDOWN OF CASE EXCLUSION 36

TABLE 11. SHRP 2 PEDESTRIAN EVENTS COMPARES TO US DATABASES, GES AND FARS....41

TABLE 12. BREAKDOWN OF SHRP 2 EVENTS WITH OBSTRUCTIONS. 42

TABLE 13. TABLE OF THE WEIGHTS APPLIED TO THE PCDS CASES TO MATCH GES DISTRIBUTION OF KABCO SCORES....62

TABLE 14. PEDESTRIAN INJURY MODEL COEFFICIENTS....67

TABLE 15. PCDS CASE EXCLUSION CRITERIA....76

TABLE 16. CALCULATION OF PCDS WEIGHTING FACTOR. WEIGHTING FACTOR WAS COLOR SCALED TO SHOW THE LOWEST WEIGHTING FACTORS (BLUE) AND THE HIGHEST WEIGHTING FACTORS (GREEN)....78

TABLE 17. CHI-SQUARE GOODNESS OF FIT ANALYSIS OF PEDESTRIAN CHARACTERISTICS IN PCDS DISTRIBUTION COMPARED TO GES DISTRIBUTION BEFORE WEIGHTING....79

TABLE 18. CHI-SQUARE GOODNESS OF FIT ANALYSIS OF PEDESTRIAN CHARACTERISTICS IN PCDS DISTRIBUTION COMPARED TO GES DISTRIBUTION AFTER WEIGHTING. 79

TABLE 19. CHI-SQUARE GOODNESS OF FIT ANALYSIS OF ENVIRONMENTAL CHARACTERISTICS IN PCDS DISTRIBUTION COMPARED TO GES DISTRIBUTION BEFORE WEIGHTING. 80
TABLE 20. CHI-SQUARE GOODNESS OF FIT ANALYSIS OF ENVIRONMENTAL CHARACTERISTICS IN PCDS DISTRIBUTION COMPARED TO GES DISTRIBUTION AFTER WEIGHTING. 80
TABLE 21. CHI-SQUARE GOODNESS OF FIT ANALYSIS OF PRE-CRASH CHARACTERISTICS IN PCDS DISTRIBUTION COMPARED TO GES DISTRIBUTION BEFORE WEIGHTING. 82
TABLE 22. CHI-SQUARE GOODNESS OF FIT ANALYSIS OF PRE-CRASH CHARACTERISTICS IN PCDS DISTRIBUTION COMPARED TO GES DISTRIBUTION AFTER WEIGHTING. 82
TABLE 23. MODELED SENSOR CONFIGURATIONS. 85
TABLE 24. INJURY MODEL SIGNIFICANT PARAMETERS. 88
TABLE 25. BREAK DOWN OF OCCURRENCE OF CRASH TYPES INCLUDED IN THIS STUDY BY VEHICLE TRAJECTORY AND PEDESTRIAN PATH. 89
TABLE 26. INJURY MODEL COEFFICIENTS. 92
TABLE 27. ODDS RATIOS FOR THE FATAL, MAIS3+F, AND MAIS2+F INJURY MODELS. 96
TABLE 28. CHANGE IN FATAL, MAIS3+F, AND MAIS2+F INJURY RISK. 97
TABLE 29. EFFECTIVENESS NUMBERS FOR "BEST" AND "WORST" PERFORMING SYSTEM FROM EACH AEB MODEL. 103
TABLE 30. BREAKDOWN OF TARGET POPULATION EXCLUSION CRITERIA FOR VEHICLE-BICYCLE CRASHES. 112
TABLE 31. WEIGHTED DISTRIBUTION OF CASE VEHICLE PRE-EVENT MOVEMENT AND BICYCLIST TRAVEL DIRECTION. 127
TABLE 32. OVERVIEW OF DATA SOURCES. 132
TABLE 33 AVERAGE BICYCLIST SPEEDS FOR RIDING ALONG THE ROAD AND TURNING [88, 89]. 134
TABLE 34. AVERAGE BICYCLIST SPEEDS FOR RIDING THROUGH AN INTERSECTION [91] 134
TABLE 35. RESULTS FOR DRIVER CHARACTERISTICS. 136
TABLE 36 RESULTS FOR BICYCLIST CHARACTERISTICS. 137

TABLE 37 RESULTS OF ENVIRONMENTAL CHARACTERISTICS. 138

TABLE 38 RESULTS FOR EVENT CHARACTERISTICS. 139

TABLE 39. COMPOSITION OF THE SHRP 2 DATA COMPARED TO 2015 GES AND FARS BICYCLE CRASH DATA. .. 151

TABLE 40. WATS CASE EXCLUSION CRITERIA. 161

TABLE 41. MAXIMUM SYSTEM BRAKING FORCES ASSUMED BASED ON ROAD SURFACE CONDITIONS [69]. 162

TABLE 42. ESTIMATED VEHICLE-BICYCLE CRASHES WITH AND WITHOUT BICYCLIST-AEB INTERVENTION FOR THE CONSTANT AND GROWING VMT ASSUMPTIONS. 171

1 INTRODUCTION

In the United States, there were 36,560 traffic-related fatalities in 2018, of which 20% were pedestrians, bicyclists, and other vulnerable road users (VRUs) [1]. Vulnerable road users are non-vehicle occupants who, because they are not enclosed in a vehicle, are at higher risk of injury in traffic crashes. While overall traffic fatalities in the US have been decreasing, pedestrian and bicyclist fatalities have been trending upward. The VRU classification is generally applied to pedestrians, bicyclists, and motorcyclists, but teen drivers and elderly drivers are sometimes referred to as vulnerable road users due to disproportionately high crash risk. For the purposes of this dissertation, vulnerable road users will refer to only pedestrians and bicyclists. This chapter will explore the problem of pedestrian and bicyclist safety and review current research efforts to mitigate VRU fatalities and injuries.

1.1 PROBLEM DEFINITION

VRU safety is a difficult problem to solve because pedestrians and bicyclists do not have the protective equipment to reduce the risk of injury like that of vehicle occupants. There are few countermeasures that protect pedestrians and bicyclists in the event of a crash. Infrastructure and safety equipment could help avoid or mitigate vulnerable road user injuries. However, updating infrastructure is expensive. Likewise, the protection offered by safety equipment, e.g. bicycle helmets, requires user to comply with usage regulations and properly use the safety device. Vehicle based active safety features could avoid or mitigate vulnerable road user crashes, but are most effective when behavior of VRUs can be anticipated. However, the behavior of pedestrians and bicyclists is notoriously unpredictable.

1.2 INJURY FACTORS

Once a conflict between a vehicle and a VRU occurs, a variety of factors determine the resultant injury severity. Determining when a VRU is most at risk can allow design of solutions to mitigate VRU injury severity. Mohamed, et al. [8] examined how environmental factors affected the probability of a fatal interaction as a function of accident type. Data from New York and Canada were examined using cluster regression models. It was found that heavy vehicles, dark lighting conditions, and higher speed roads such as highways increased the probability that a vehicle-pedestrian interaction will be fatal.

Fredriksson, et al. [9] used data from the German In-Depth Accident Study (GIDAS) to examine how pedestrian age and impact speeds affect resultant injury type and severity. Fredriksson, et al. [9] found that the head and chest were the most commonly injured body region, with approximately equal injury rates, when considering severely injured pedestrians. For pedestrians aged 65 and older, the chest was the most common injury location. On the other hand, it was more common for children to sustain injuries to their heads as the most common impact type in children was found to be head-to-hood.

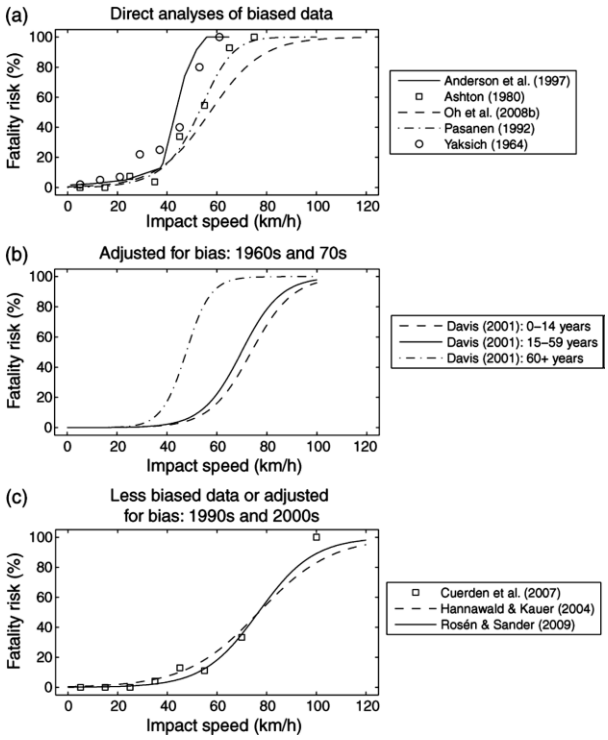

Figure 1. Fatality risk of pedestrians struck by the front of a passenger car as a function of impact speed. (A) Results based on biased data, (B) Results adjusted for bias from 1960s-1970s, and (C) Less biased or adjusted data resulting from crashes in the 1990s and 2000s. [10]

Rosén, et al. [10] compared impact speed to fatality risk using data from GIDAS. As shown in Figure 1, pedestrian fatality risk increases substantially at speeds above 50 km/h. Niebuhr, et al. [11] showed that pedestrian injury risk is dependent on pedestrian age as well as impact speed. According to Niebuhr, et al. [11], older pedestrians have a higher risk of a Maximum Abbreviated Injury Scale (MAIS) score of 3 or higher at all impact speeds compared to younger pedestrians. Children were found have lower injury risk at low speeds and higher risk of injury at higher speeds when compared to all other age groups [11].

Pedestrian injuries also vary depending on the shape of the front of vehicles. Mizuno and Kajzer [12] examined the police and in-depth accident data from accidents that occurred throughout Japan and collected by the Institute for Traffic Accident Research and Data Analysis (ITARDA). Mizuno and Kajzer [12] found that mini-vans result in higher risk of head injury and a lower risk of

lower limb injury than bonnet-type cars. They also found that the likelihood of head injury increases with contact with the cowl, windshield frame or A-pillar, and decreases with increasing distance from these elements.

In the U.S. the percentage of light truck and vans (LTVs) on the road is increasing as demand for LTVs increases. Lefler and Gabler [13] found that pedestrians struck by a LTV are two to three times more likely to be fatally injured than if they are than if they are struck by a car.

1.3 VEHICLE BASED COUNTERMEASURES

With the multitude of factors that affect vehicle-VRU incidents and resultant injury severity the question becomes how to mitigate these injuries. While there are potential solutions from the VRUs' perspective and from VRU friendly infrastructure such as sidewalks, crosswalks, etc., we will focus on the solutions applicable from the perspective of the vehicle. Vehicle based countermeasures have the potential to affect vehicle-VRU incidence much quicker than redesigning / rebuilding infrastructure or attempting to convince road users to change their behavior.

1.3.1 ACTIVE SAFETY: FORWARD COLLISION AVOIDANCE SYSTEM

Forward Collision Avoidance System (FCAS) is an active safety system that uses a suite of sensors to detect an imminent collision and through warning and or braking aids the driver in avoiding a frontal collision. Current systems are designed to alert the driver of a potential conflict through Forward Collision Warning (FCW), then institute pre-collision brake assist and finally pre-collision braking if the driver does not take action [14]. The effectiveness of these systems is highly dependent on detecting the VRU with enough time or distance to collision to avoid or mitigate the conflict. Pre-collision braking, also known as automatic emergency braking (AEB), has been shown to be effective at avoiding pedestrians when the vehicle is traveling at below 14 m/s (about 50km/h or 30 mph) [15]. While the vehicle may not be able to avoid the pedestrian at higher speeds, the

decrease in velocity of the vehicle would help mitigate the severity of the crash [10]. Although, the focus of this dissertation is vulnerable road users, forward collision avoidance systems have been assessed in many other crash modes [16-20].

User acceptance is a potential obstacle to FCAS effectiveness. Drivers may disable FCAS if they perceive that FCW is premature, or even worse if the system prematurely applies AEB. A disabled system provides no benefit. Thus, it is important to optimize the AEB activation threshold so that the vehicle has time to avoid the collision and the driver does not feel that the system unnecessarily activated. Lubbe and Rosén [21] found that the time to collision at driver brake application ranges from 2.1 to 4.3s and is independent of driving speed. Lubbe and Davidsson [22] used a high-fidelity simulator to examine the effect of pedestrian walking speed on brake onset and intensity. They found that when pedestrians were walking at slower speeds (1 m/s) the driver braked earlier that when the pedestrians were travelling at a fast walk/jog (2 m/s).

1.3.1 ACTIVE SAFETY: FORWARD COLLISION WARNING

Lubbe and Kullgren [23] used the AsPeCSS (Assessment methodologies for forward looking integrated Pedestrian, and further extension to Cyclist Safety Systems) method to compare the potential casualty reduction from AEB and forward collision warning systems. AEB systems resulted in a 25% casualty cost reduction, whereas forward collision warning systems resulted in a 0-25% casualty cost reduction depending on the type of warning system used. Lubbe [24] further explored the differences between different types of forward collision warnings. Among the warnings that were tested, brake pulse warning was the most effective type of forward collision warning, reducing the number of collisions and shortening brake reaction times. While forward collision warning can be effective, the effectiveness is limited by the driver reaction time. Driver reaction times can vary widely depending on the type of warning and if the driver is distracted. Studies have shown driver

reaction time ranging from the fastest at around half a second to the slowest at almost 2 seconds [25, 26].

1.3.2 Combined Passive and Active Safety: Pop-up bonnets and AEB

Lubbe, et al. [27] conceptualized a method for assessing both passive and active integrated pedestrian safety systems. The method they proposed included testing both the active and passive safety components in order to calculate injury risk and socio-economic cost. These results could then be weighted and applied to scenarios that were not specifically tested.

Edwards, et al. [28] further developed this methodology for testing the effectiveness of the combination of AEB and passive safety features using data from AEB tests and Euro NCAP. This study found that a combination of AEB and passive safety features resulted in improved pedestrian protection when compared to having only AEB, only passive safety systems, or neither. Edwards, et al. [28] also found that a hypothetical passive external A-pillar airbag decreased injury severity more than AEB.

1.3.3 Active Safety: Highly Automated Vehicles

Highly automated vehicles have to potential to transform transportation by making vehicular travel easier and safer than ever before, but while highly automated vehicles have the potential to substantially reduce crash risk, there is concern that they will have trouble safely operating in mixed fleets and with vulnerable road users [29, 30]. Detwiller and Gabler [31] used the NHTSA Pedestrian Crash Data Study, an in-depth analysis of over 500 vehicle-pedestrian crashes, to determine if highly automated vehicles with either a law abiding algorithm or a more cautious algorithm would be able to avoid the incidents with pedestrians. The study found that although the highly automated vehicles could potentially avoid most of the incidents using the more cautious algorithm, in 27 of the 523 events, the car would not be able to avoid the crash. Fully automated vehicles that are functional in

all scenarios may still be a long way off due to limitations in electronics, artificial intelligence, and the time it takes to validate that these systems are safe [32].

1.3.4 VRU DETECTION

While many active safety systems are adept at detecting vehicles, VRUs present a unique challenge due to their different material properties, smaller size, and unpredictable behavior. Yang, et al. [33] proposed a system that takes into account the time of day, location, weather, road type and more in order to choose the appropriate algorithm that efficiently detects pedestrians resulting in a method that is faster, more accurate, and uses less computing power. Tian, et al. [34] developed a model to estimate the likelihood that a pedestrian will have an interaction with a vehicle. This type of information is useful because it allows pedestrian detection and analysis systems to efficiently employ different pedestrian detection methods. The model achieved about 80% accuracy with consideration of the presence of right-of-way control devices, road location, pedestrian behavior, and number of pedestrians [34].

Improvement has been made in the radar detection systems as well. The earlier a pedestrian can be detected the more time an automated driving system or a human driver would have to avoid or mitigate the conflict. Newer radar detection systems may utilize a 76-78 GHz bandwidth compared to the 24 GHz bandwidth used previously. This higher frequency radar will allow detection systems to detect small objects that are further away (100-150 m) and at a better resolution, but the smaller wavelength can cause large fluctuations in the reflected signal [35]. Though the fluctuations could be problematic, there are measurable differences in the maximum radar cross section angle, differentiating between walking and standing pedestrians [35]. This information could be useful in path prediction of pedestrians.

Understanding vulnerable road user motion is an integral component of path prediction. Many groups have conducted studies to analyze vehicle-pedestrian and vehicle-bicycle interactions and actions. The Transportation Active Safety Institute (TASI) conducted a naturalistic driving study in which 110 cars were instrumented for one year in the greater Indianapolis area. This study observed that both lone children and adults in groups of three or more were at elevated risk of an incident with a vehicle [36]. Additionally, it was observed that off roadway locations such as parking lots and school areas could have a higher risk of conflict as well as actions such as a pedestrian crossing the road or walking in the road [36].

Tian, et al. [37] found that pedestrian step frequency tended to be higher when crossing the road, especially if the pedestrian was in the path of a vehicle or was violating right of way. A higher step frequency is associated with a higher walking speed. This is consistent with studies conducted in the U.S. and Sweden that were used to develop mannequins to test pedestrian pre-collision systems. Chien, et al. [38] combined the studies completed in the U.S. and Sweden and found that pedestrian walking speed ranged from 0.6m/s to 2.4 m/s and depended on the age and speed (slow, comfortable, and fast) of the pedestrian. While all pedestrians are vulnerable road users, Elderly pedestrians have at a higher risk of injury and fatality than pedestrians and vulnerable road users if they are struck. Elderly pedestrians are disproportionately killed in traffic related crashes. In 2015, only 14.8 % of the US population was considered elderly, but 18.6 percent of fatal pedestrian crashes involved elderly pedestrians [39].

1.4 Consumer Information Programs

For the cases in which the collision is unavoidable, it is vital that the vehicle is designed to mitigate pedestrian injury. A major force that drives US, European, and global vehicle safety standards is the New Car Assessment Programme (NCAP).

While the U.S. NCAP currently does not rate pedestrian or bicyclist safety, other US. Agencies have begun testing vulnerable road user safety. The Insurance Institute for Highway Safety (IIHS) is an independent institution that rates U.S. vehicles on various safety metrics with the purpose of informing consumers and improving motor vehicle safety. The IIHS began testing pedestrian AEB in 2018. IIHS tests an adult pedestrian form in a crossing and parallel path scenario and a child pedestrian form in a crossing scenario [40]. Although U.S. NCAP does not currently test pedestrian or bicyclist safety, they have announced they will be updating their testing procedure in 2020 which may include the addition of pedestrian and other vulnerable road user tests [41].

In comparison, Euro NCAP has influenced many advances in occupant protection, but pedestrian protection was not a major focus until Euro NCAP revised pedestrian assessment and testing protocols in 2002 [42]. In 2009, Euro NCAP adopted its current rating system, which rates vehicles on occupant protection (adult and child), pedestrian protection, and safety assist technology resulting in improved pedestrian subsystem test scores [42]. In 2018, Euro NCAP began testing bicyclist AEB [43].

Strandroth, et al. [44] examined the relationship between Euro NCAP pedestrian subsystem scores and pedestrian injury severity. Strandroth found that higher scoring cars reduced the risk of serious consequences more than lower scoring cars for speeds up to 50 km/h. Above 50km/h (about 30 mph) there was no significant injury reduction. This is concerning because, as shown in figure 1, fatality risk greatly increases at impact speeds greater than 50 km/h.

In 2015, Euro NCAP protocols scored pedestrian protection based on vehicle performance in passive and active safety systems. Passive safety was tested through impact tests using a head form, upper leg form, and lower leg form. Active safety tests scored the human machine interface and AEB [45]. Starting in 2018, there were changes to the active safety portion of the assessment protocol. The new protocol conducted tests with both pedestrian and bicyclist dummies, assessed the forward

collision warning system, and completed tests in both day and night lighting conditions [43]. By 2022 Euro NCAP is planning to improve their dummy model by adding an upper body mass which will result in more representative injury models. Additionally, Euro NCAP plans to modify impact tests to include pedestrians and cyclists to improve avoidance technology as well as deployable bonnets [46]. Deployable bonnets are a passive safety feature in which the hood of the vehicle rises to protect the pedestrian from striking the stiff structures on the front of the vehicle.

Euro NCAP is the most comprehensive vehicle safety assessment currently, but Japan and Korea have similar consumer information programs to test vehicle safety (JNCAP and KNCAP respectively). KNCAP testing is very similar to Euro NCAP with the major differences being that they only test AEB for pedestrians and no other types of vulnerable road users. In addition, KNCAP does not test upper leg form impacts to the vehicle bonnet. JNAP only tests AEB in response to pedestrians and doesn't does not test upper leg form impacts to the vehicle bonnet or the bumper. In addition, JNCAP only tests adult and child head forms up to 35km/h compared to the Euro NCAP and KNCAP standard of 40 km/h.

1.5 Research Goal

The overall goal of this dissertation was to estimate the potential effectiveness of automatic emergency braking at avoiding or mitigating vehicle-bicycle and vehicle-pedestrian crashes. The following chapters will propose methods using a variety of data sources to examine the characteristics of vehicle-pedestrian and vehicle-bicycle crashes and near-crashes, assess the potential effectiveness of AEB, and estimate the future benefits of AEB in the United States.

2 DATA SOURCES

Vehicle-pedestrian and vehicle-bicyclist crash data in the U.S. is limited. National databases contain information of VRU crashes, but they often lack the detail necessary for an in-depth analysis. In-depth VRU crash databases, while detailed, are not nationally representative meaning that conclusions cannot be made about the U.S. vehicle-VRU crashes as a whole. Publically available in-depth studies on VRU crashes in the U.S. are rare; most do not contain current crash data. This dissertation leveraged a variety of data sources in order to account for the limitations of each data source. Description of the data sources as well as the pros and cons of each data source are described below.

2.1 FARS

The Fatality Analysis Reporting System (FARS) is a census of all traffic crashes that resulted in a fatality [47]. FARS contains data dating back to 1975. In 2011 the FARS and National Automotive Sampling System (NASS) General Estimates System (GES) coding systems were modernized to allow for a more standardized comparison between the data sources. This prevents ready comparison with data before 2011. FARS is nationally representative because every known crash resulting in a fatality is included, but does not contain in-depth injury information or crash reconstructions.

2.2 GES

The General Estimates System (GES) is a subset of the National Automotive Sampling System (NASS) and contains a probability sample of all U.S. police reported crashes from 1988 to 2015 [48]. GES includes sampling weights, which when applied to the database, allow the calculation of the actual incidence rates of the different types of crashes. Because many data elements have large numbers of missing values, GES provides imputed variables for many data elements. Imputed variables are variables in which the unknown values have been filled in using an algorithm developed

by NASS GES. The imputed variables were used when available. GES was modernized in 2011 to improve the comparability of GES to other crash databases, like FARS, which prevents ready comparison to previous data. GES was replaced with the Crash Research Sampling System (CRSS) in 2016.

2.3 CRSS

The Crash Research Sampling System (CRSS) is a new database that has replaced the General Estimates System (GES). Similar to GES, CRSS is a sample of all police-reported motor vehicle crashes. The sampling locations have changed however in an effort to account for shifts in the US population and vehicle fleet [49]. Due to the different sampling scheme, CRSS cannot be readily compared with GES. All CRSS values reported were weighted to better reflect national estimates and imputed variables were used when available.

2.4 PCDS

The PCDS database was collected by NHTSA through adaptation of the NASS Crashworthiness Data System (CDS) methodology to assess vehicle-pedestrian collisions [50]. PCDS consists of 549 in-depth vehicle-to-pedestrian crash investigations collected from 1994 to 1998 from six U.S. urban areas. The six data collection areas for PCDS were the cities of Buffalo, NY; Ft. Lauderdale and Hollywood, FL; Dallas, TX; Chicago, IL; Seattle, WA; and San Antonio, TX. PCDS collected cases from a diverse set of urban regions with a wide range of weather conditions and roads, ensuring a broad scope of possible environments for vehicle-pedestrian encounters. PCDS is the most recent public domain pedestrian crash dataset available in the U.S. The strategy in using this older dataset is that, although vehicles in the 2011-2015 time frame were much different than in 1994-1998, the types of vehicle-pedestrian conflicts, e.g. children dodging out from between parked cars, are unlikely to have greatly changed [51].

2.5 SHRP 2

The Second Strategic Highway Research Program (SHRP 2) was a naturalistic driving study conducted in six cities across the USA from 2010 to 2013 [52]. SHRP 2 was not designed as a nationally representative sample as the project depended on volunteers that were in proximity to one of the six collection sites. The collection resulted in over 4,300 years of driving data and recorded over 1,900 crashes and 6,900 near-crashes [52]. Approximately 3,300 participant vehicles were instrumented to collect vehicle speed, acceleration, yaw rate and brake and gas pedal position in addition to forward, rear, hands and driver video. Vehicle time series data were collected asynchronously and video was captured at 15 frames per second.

For this study, the database was queried for all events that were pedestrian or bicyclist related, which resulted in 168 pedestrian events and 64 bicyclist events. Six events were excluded because the subject vehicle was a witness to the event and not directly involved in it, meaning that critical information was lacking, leaving only crashes and near-crashes. A crash was defined as an event in which the subject vehicle had any contact with a pedestrian or bicyclist. A near-crash was defined as any situation that required a rapid evasive maneuver by the subject vehicle, pedestrian, or cyclist [4].

2.6 WATS

The Washtenaw Area Transportation Study (WATS) dataset, funded by the Toyota Collaborative Safety Research Center, was a sample of vehicle-bicycle crashes that occurred in southeast Michigan from 2011 to 2013. The dataset contains both vehicle-bicycle crashes and vehicle-pedestrian crashes, but only the vehicle-bicycle crashes were analyzed for our study. Similar to PCDS, the WATS database contains detailed information not available from nationally representative datasets like FARS and GES. The WATS database contains driver and bicyclists characteristics, detailed crash scene diagrams, and a thorough recording of potential obstructions that could have affected the crash.

3 PEDESTRIAN AEB TARGET POPULATION

3.1 RESEARCH OBJECTIVE

The objective of this chapter was to determine the characteristics of the target population for a pedestrian AEB system. The target population refers to that subset of pedestrian-vehicle impacts which might be avoided or mitigated by a pedestrian AEB system. The characteristics of pedestrian, vehicle, environment, and driver conditions were examined for those crashes in the target population.

3.2 APPROACH

FARS and GES were initially filtered to include all vehicle-pedestrian crashes from 2011-2015, but not all vehicle-pedestrian crashes could be avoided by a pedestrian detecting AEB system. While AEB is being developed for large trucks and buses, their larger mass and longer required stopping distance may require a specialized AEB system [53], therefore this study only considered pedestrian AEB that would be installed in cars and light trucks and vans (LTVs). Furthermore, most AEB systems use a combination of forward facing radar, LiDAR, and/or cameras to detect pedestrians. Vehicle-pedestrian crashes in which the pedestrian was not visible to forward facing sensors, such as backing-up crashes, would not be mitigated by a pedestrian detecting AEB system. Finally, AEB systems would likely be ineffective in loss of control scenarios because they mitigate crashes by initiating evasive braking which may not be beneficial if, for example, a vehicle is sliding on ice.

Therefore, the target population for pedestrian AEB was assumed to be vehicle-pedestrian crashes in which the front of the car or LTV struck the pedestrian and loss of control was not a factor. The data was filtered to only include cases in which the striking vehicle had a car or LTV body type (*body_typ* or *bdy_typ_im < 50)*, frontal impact (*impact1 = 11, 12, or 1*), and no loss of control (*p_crash2 > 9*).

The target populations of vehicle-pedestrian crashes from GES and vehicle pedestrian fatalities from FARS were then characterized to better understand potential crash causation factors. The characterization was divided into three major categories: 1) pedestrian characteristics, 2) driver characteristics, and 3) environmental characteristics.

A Pedestrian detecting AEB system may be able to avoid or mitigate many pedestrian vehicle-related collisions in the target population, however, it is unlikely that all could be avoided. The effectiveness of a P_AEB system may be affected by environmental characteristics such as lighting conditions, and weather. For this reason, the following three P-AEB system limitations were examined to understand how each potential limitation could affect the target population:

1. Target population "daylight" includes the conditions of the target population with the limitation that only crashes in which the pedestrian struck during daylight would be avoidable.
2. Target population "clear" includes the conditions of the target population with the limitation that only crashes in which the pedestrian struck during clear weather conditions would be avoidable.
3. Target population "daylight and clear" includes the conditions of the target population with the limitations that only crashes in which the pedestrian struck during daylight and during clear weather conditions would be avoidable.

3.3 RESULTS

The following sections breakdown the target population and compare the distributions of vehicle-pedestrian crashes and vehicle-pedestrian fatalities in terms of pedestrian, driver, and environmental characteristics. The tables highlight the trends, similarities, and differences between the distributions of FARS and GES (weighted and unweighted). The trends, similarities, and differences are discussed individually in the following pedestrian characteristics, driver characteristics, and environmental characteristics sections.

3.3.1 TARGET POPULATION

The target population was defined as the subset of pedestrian-vehicle crashes which might be avoided or mitigated by a pedestrian AEB system. We assumed that a P-AEB system would be integrated into cars, light trucks, and vans, but not other vehicles such as large trucks, buses, and motorcycles. As shown in Table 1, excluding crashes with non-passenger vehicles reduced the target population by 4,068 fatal crashes (FARS cases) and 33,311 crashes (weighted GES cases) over the 5 year time frame. Additionally, we assumed a P-AEB system would only be effective in frontal impact scenarios which excluded 4,035 FARS cases and 104,994 weighted GES cases. Finally, we assumed P-AEB would not be effective in situations in which there was loss of control of the vehicle. Of the remaining cases, loss of control was present in 297 FARS cases and 4,808 weighted GES cases. As shown in Table 1, the final target population from 2011 to 2015 was estimated to be 17,775 fatal crashes (FARS) and 245,889 crashes (weighted GES cases).

Table 1. Breakdown of target population filtering

	FARS Cases (2011-2015)	**GES Cases (2011-2015)**	**GES Weighted Cases (2011-2015)**
All Pedestrians Crashes	24,459	11,897	374,645
Non-applicable Crashes			
Struck by non-passenger vehicle	4,068	620	33,311
Non-Frontal Impacts	4,035	2,962	104,994
Loss of control	297	121	4,808
Target Population	17,775	8,035	245,889

The target population relative to the total population of vehicle-pedestrian crashes is shown graphically in Figure 2 and Figure 3. The target population made up about 73% and 68% of the total population of fatal and all crashes, respectively, which indicated that P-AEB may be a promising mitigation strategy for many vehicle-pedestrian crashes. The characteristics of the pedestrian, driver, and environmental conditions were examined for those crashes in the target population.

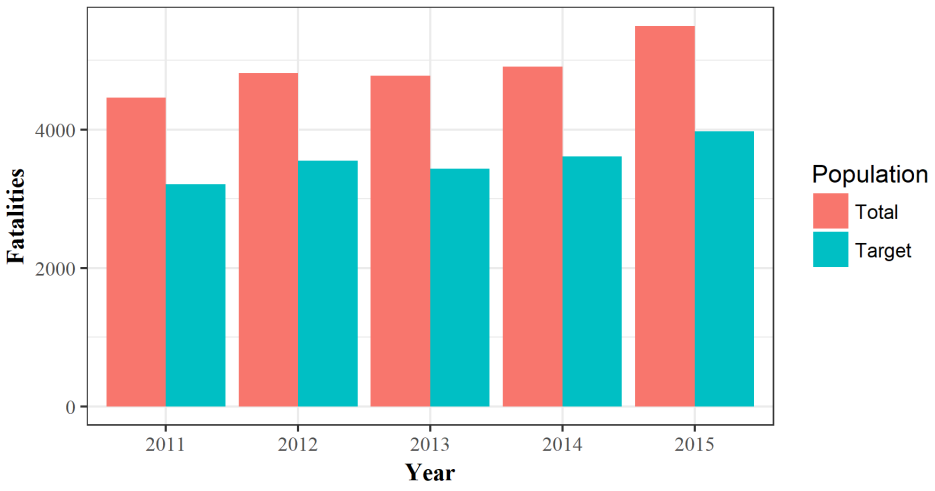

Figure 2. The number of pedestrian fatalities in the U.S. from 2011 – 2015 compared to the target population (FARS).

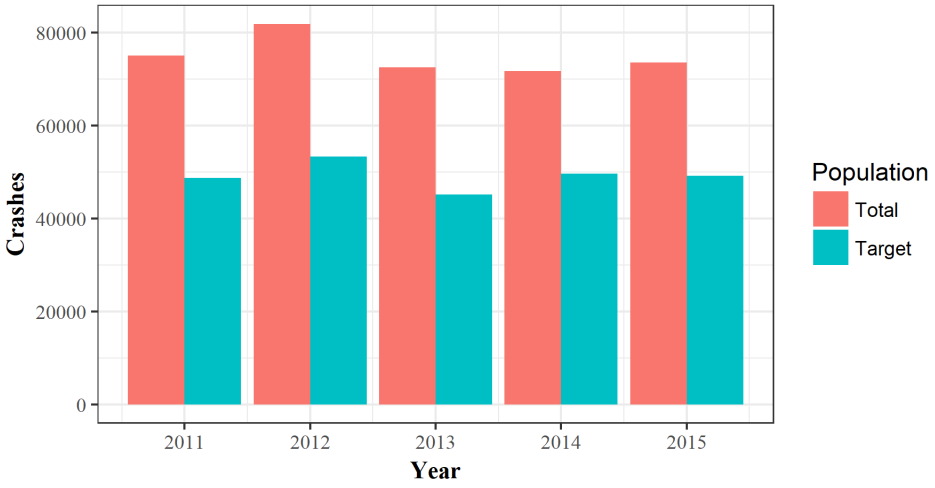

Figure 3. The number of police reported vehicle-pedestrian crashes from 2011 – 2015 compared to the target population (GES).

3.3.2 PEDESTRIAN CHARACTERISTICS

Pedestrian characteristics were examined in for both the fatal crashes (FARS) and all crashes (GES). Table 2 is an overview of the results. All analyses were conducted solely on the target population. GES imputed values were used for the analysis of gender and age.

Table 2. Pedestrian characteristics of vehicle–pedestrian crashes in FARS and GES.

Variable	FARS Cases	FARS %	GES Cases	GES %	GES Weighted Cases	GES Weighted %
Total Cases	24,459	100	11,897	100	374,645	100
Target Population	17,775	72.7	8,035	67.5	245,889	65.6
Gender						
Male	12,186	68.6	4,553	56.7	136,074	55.3
Female	5,572	31.3	3,482	43.3	109,815	44.7
Other/Unknown	17	0.0	-	-	-	-
Age						
Child (≤ 16)	1,085	6.1	1,418	17.7	39,749	16.2
Adult	13,029	73.3	5,691	70.7	177,252	72.2
Senior (≥ 65)	3,563	20.0	926	11.4	28,889	11.8
Other/Unknown	98	0.6	-	-	-	-
Alcohol Involvement						
No	5839	32.8	6,027	75	188,030	76.5
Yes	3455	19.4	618	7.7	15,711	6.4
Unknown	8481	47.7	1,390	17.3	42,147	17.1

As shown in Figure 4, the number of pedestrian fatalities in the U.S. has been increasing since 2011. This trend is not apparent however in the number of pedestrians involved in police reported crashes (Figure 5). More recent data has increased police reported injuries, but this data was collected using a new sampling scheme and therefore data between the two are not comparable [54]. Figure 5 was also separated by injury severity as reported by the police which highlights the fact that the majority of vehicle-pedestrian collisions did not result in a fatality.

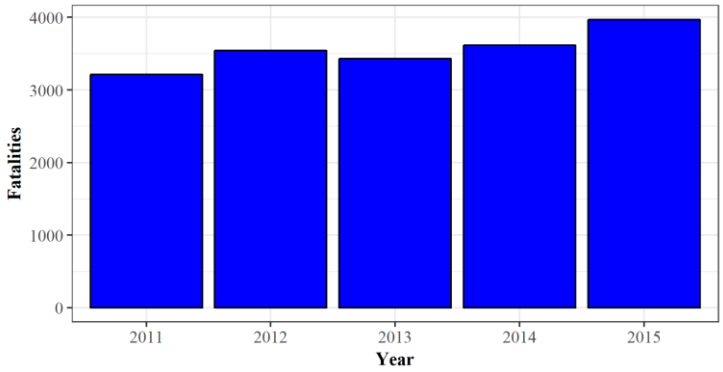

Figure 4. The number of pedestrian fatalities in the U.S. from 2011-2015. Data source: FARS

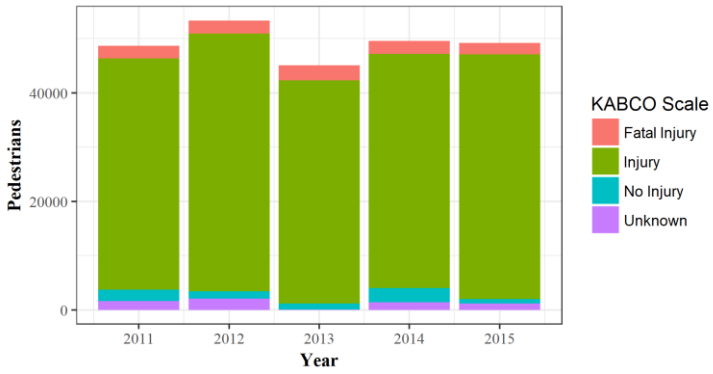

Figure 5. The number and severity of police reported vehicle-pedestrian crashes from 2011-2015. Data source: GES

Figure 6 shows the age distributions of the pedestrians involved in vehicle-pedestrian collisions. The median age of pedestrians in all police-reported pedestrian crashes (GES) was 32 years old compared to a median age of 48 years old for fatal crashes (FARS). Most fatally injured

pedestrians were older than the overall population of struck pedestrians. This difference may be due to the fact that injury tolerance declines with age.

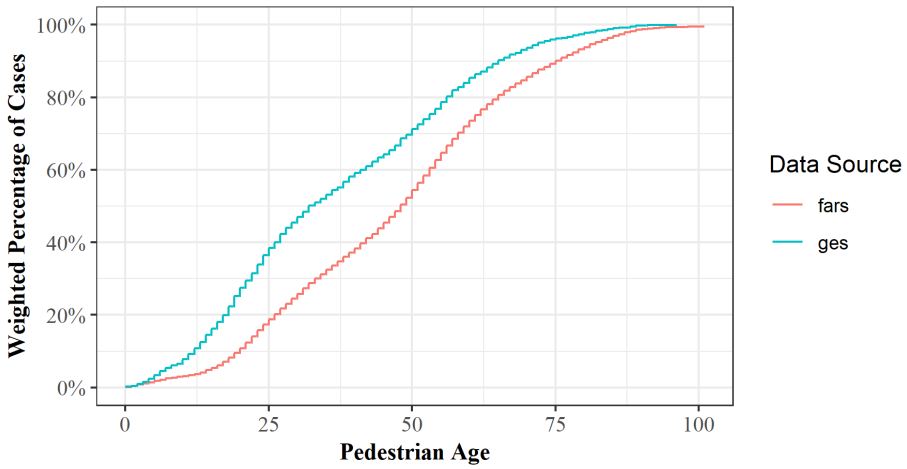

Figure 6. The age distribution of pedestrians from FARS and GES.

Figure 7 shows the gender distribution of pedestrians involved in vehicle-pedestrian collisions. Both target populations indicated that males were more likely than female pedestrians to be struck. In GES, a little more than half of struck pedestrians were male, comprising 55.3%, of the crashes. In fatal accidents this trend was much more evident with 68.6% of pedestrians being male.

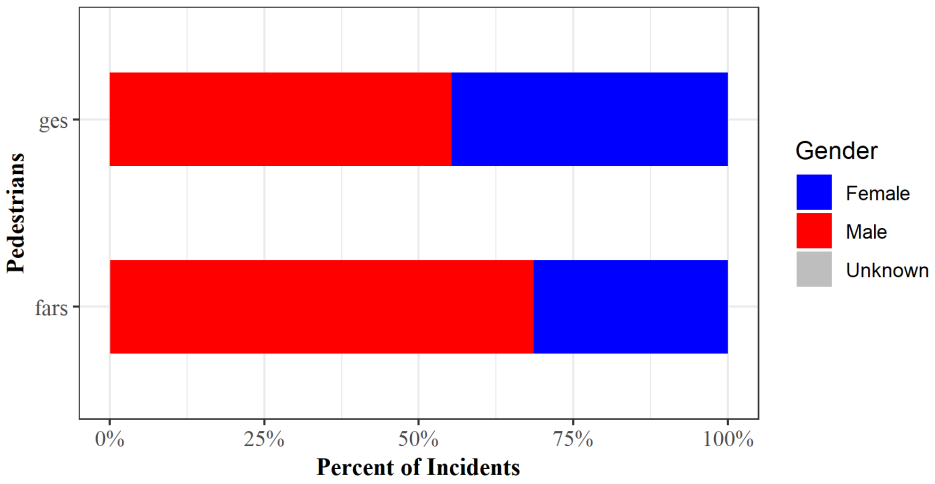

Figure 7. Distribution of pedestrians involved in vehicle-pedestrian collisions, by gender.

Figure 8 and Figure 9 show the fraction of pedestrians involved in vehicle-pedestrian collisions that were involved with alcohol prior to the incident. In both databases the majority of known pedestrians were not involved with alcohol. GES had a reported alcohol involvement of 6.4% while, FARS had a higher proportion of cases with reported alcohol involvement at 19.4% of pedestrians involved with alcohol. This was quite a large difference which may be attributed to the large number of FARS cases where alcohol involvement was unknown or may be due a difference in pedestrian behavior or environmental conditions related to drinking alcohol that lead to more fatal crashes.

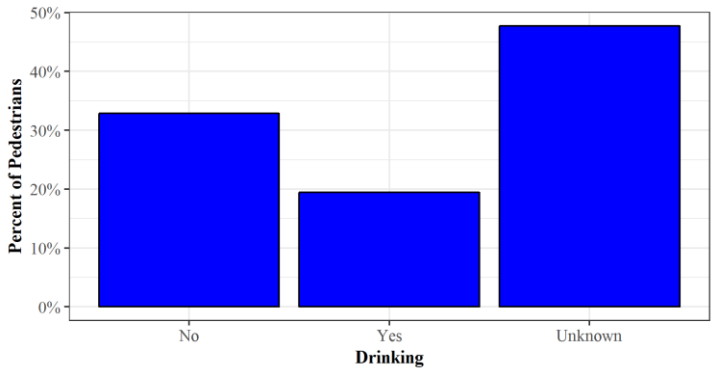

Figure 8. Distribution of cases in which pedestrian was involved with alcohol. Data source: FARS

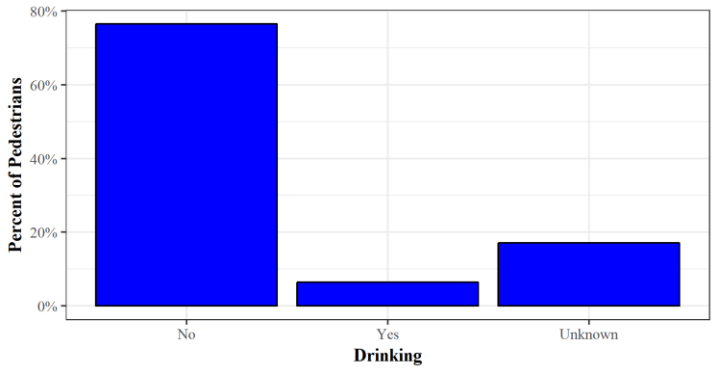

Figure 9. Distribution of cases in which pedestrian was involved with alcohol. Data source: GES

3.3.3 DRIVER CHARACTERISTICS

Driver characteristics were examined in the FARS and GES target populations. Table 3 is an overview of the results from both datasets. All analyses were conducted solely on the target population. GES imputed values were used for the analysis of driver gender and age.

Table 3. Driver characteristics of vehicle-pedestrian crashes in FARS and GES.

Variable	FARS Cases	FARS %	GES Cases	GES %	GES Weighted Cases	GES Weighted %
Total Cases	24,197	100	11,792	100	370,874	100
Target Population	17,744	73.3	8,015	68	245,177	66.1
Gender						
Male	11,993	67.6	4,811	60	148,192	60.4
Female	5,410	30.5	3,204	40	96,984	39.6
Other/Unknown	341	1.9	-	-	-	-
Age						
Young Adult (≤ 25)	4,049	22.8	2,032	25.2	59,549	24.3
Adult	11,397	64.2	5,139	64.1	155,447	63.3
Senior (≥ 65)	1,927	10.9	8,44	10.4	30,181	12.1
Other/Unknown	371	2.1	-	-	-	-
Alcohol Involvement						
No	11,498	64.8	6,322	78.9	19,4919	79.5
Yes	1,597	9	232	2.9	6,491	2.6
Unknown	4,649	26.2	1461	18.2	43767	17.9

Figure 10 shows the age distribution of drivers involved in vehicle-pedestrian collisions. The age distributions were very similar. The median age of the driver was 39 in FARS and 40 in GES. This indicates that driver age likely did not contribute to the severity of pedestrian injuries, although younger drivers were more likely to be involved in a vehicle-pedestrian crash.

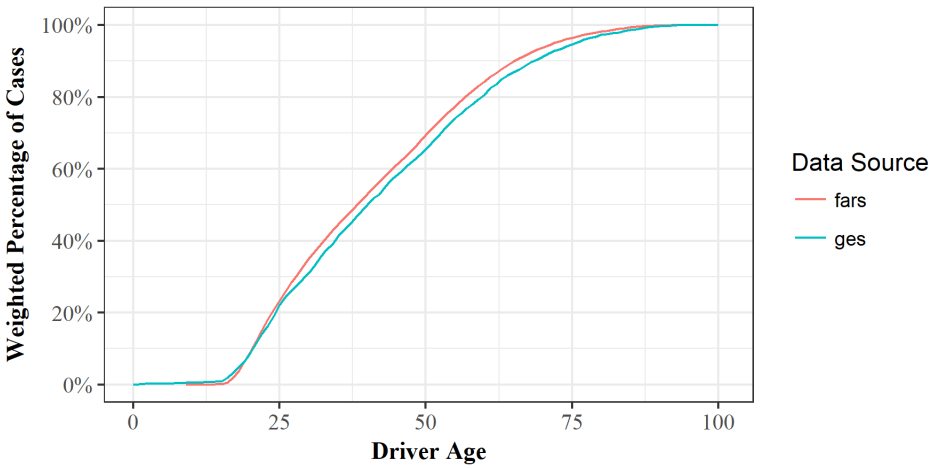

Figure 10. Age distribution of drivers. Data source: FARS, GES

Figure 11 shows the gender distribution of drivers involved in vehicle-pedestrian collisions. In both GES and FARS, male drivers made up the majority of cases, 60.4% and 67.6%, respectively.

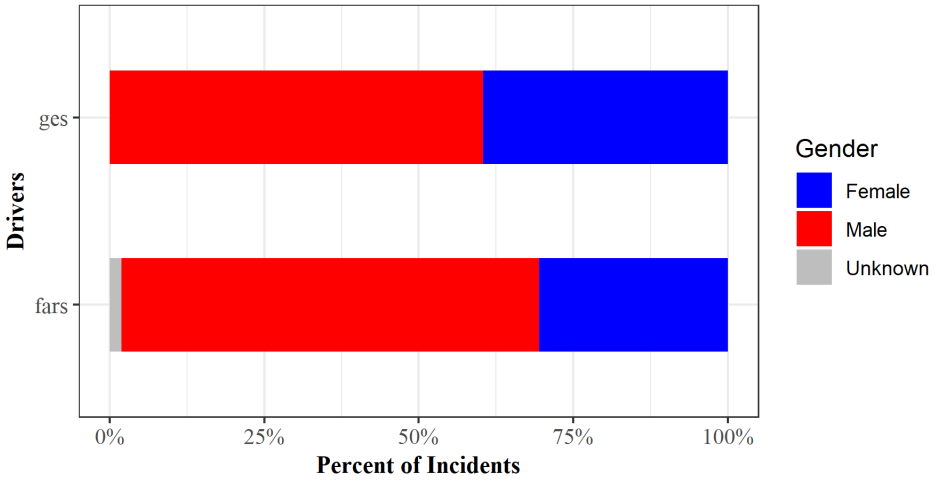

Figure 11. Distribution of driver gender in fatal pedestrian crashes (FARS) and in all pedestrian crashes (GES).

Figure 12 and Figure 13 depict the proportion of drivers, involved in vehicle-pedestrian collisions that were involved with alcohol prior to the incident. For cases in which alcohol involvement was known, in all three databases the majority of drivers were not involved with alcohol. GES target population cases had only 2.4% of the cases in which the driver was reportedly involved with alcohol, while FARS had a higher proportion of reported alcohol involvement with 7.6% of drivers involved with alcohol. This was quite a large difference which may be attributed partially to the large number of FARS cases where alcohol involvement was unknown or may be due a difference in driver behavior.

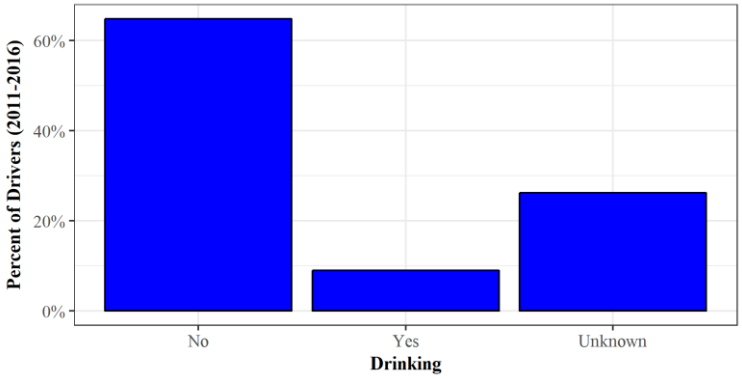

Figure 12. Distribution of cases in which the driver was involved with alcohol. Data source: FARS

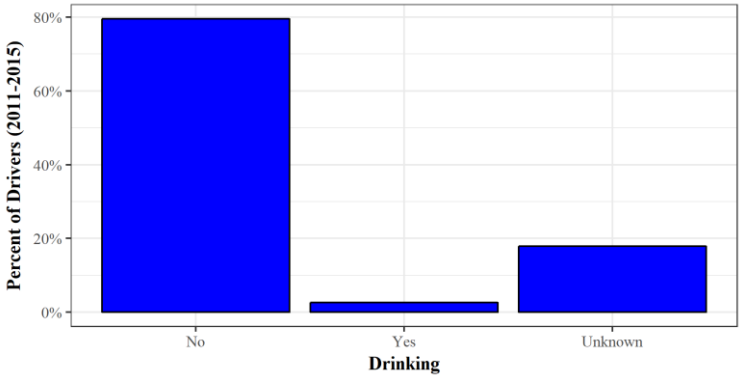

Figure 13. Distribution of cases in which the driver was involved with alcohol. Data source: GES

3.3.4 ENVIRONMENTAL CHARACTERISTICS

Environmental characteristics were examined for the target population of police-reported crashes (GES) and fatal crashes (FARS). Table 4 is an overview of the results from FARS and GES. GES imputed values were used for the analysis of lighting conditions, weather, relation to junction, and pedestrian location in relation to the road. Cold related weather conditions include weather conditions such as snow, ice, sleet, and hail.

Table 4. Environmental characteristics of vehicle-pedestrian crashes in FARS and GES.

Variable	FARS Cases	FARS %	GES Cases	GES %	GES Weighted Cases	GES Weighted %
Total Cases	24,197	100	11,792	100	370,874	100
Target Population	17,744	73.3	8,015	68	245,177	66.1
Lighting						
Daylight	3,792	21.4	4,326	54	136,008	55.5
Dark-Not Lighted	6,243	35.2	745	9.3	21,166	8.6
Dark-Lighted	6,848	38.6	2,579	32.2	76,904	31.4
Dawn	283	1.6	116	1.4	3,004	1.2
Dusk	386	2.5	197	2.46	6,949	2.8
Other	192	0.6	52	0.64	1,145	0.5
Weather						
Clear	15,841	89.3	7,012	87.5	211,158	86.2
Rain	1,434	8.1	871	10.9	28,084	11.5
Cold related	145	0.8	96	1.2	4,803	2
Other/Unknown	324	1.8	36	0.4	1,131	0.4
Crash Location						
Non-Junction	12,066	68	3,063	38.2	87,735	35.8
Intersection	2,079	11.7	1,220	15.2	44,459	18.1
Intersection Related	2,844	16	3,329	41.5	101,478	41.4
Other	755	4.2	403	4.8	11,504	4.7
Pedestrian Location						
On Roadway	16,489	92.9	7,636	95.3	232,719	94.9
On Shoulder	476	2.7	91	1.1	2,660	1.1
On Median	64	0.4	21	0.3	440	0.2
On Roadside	484	2.7	153	1.9	4,440	1.8
Other	231	1.4	114	1.3	4,918	2

Figure 14 shows the distributions of lighting conditions at the time the vehicle-pedestrian collision occurred. In GES, daylight was the most common lighting condition constituting 55.5% of the crashes. The most common lighting condition in FARS was “Dark-Lighted”, accounting for 38.6% of incidents, compared to Daylight which accounted for 21.4% of incidents. The distribution of all the lighting conditions can be found in Table 4.

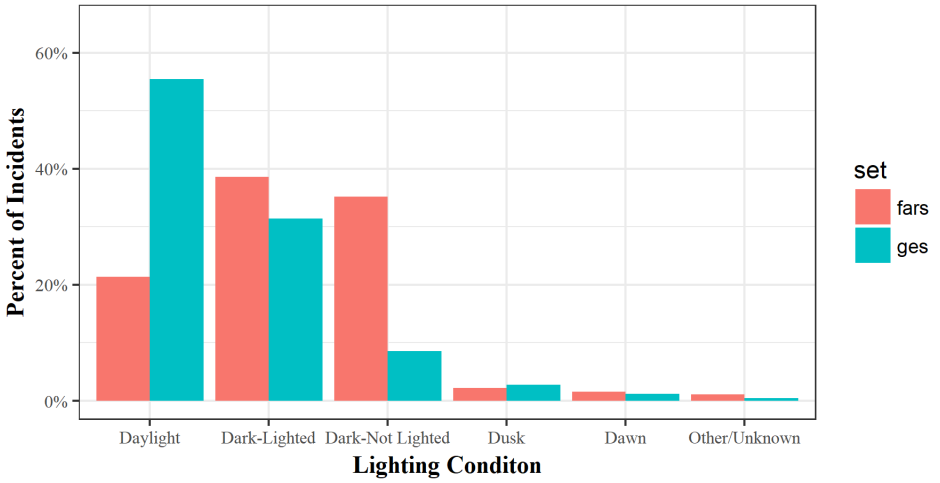

Figure 14. Lighting condition distribution at time of collision. Data Source: FARS, GES

Figure 15 shows the distribution of weather conditions at the time the vehicle-pedestrian crash occurred. For the GES and FARS databases the “No adverse” and “Cloudy” weather categories were combined into a “Clear” category because cloudiness should not have an effect on pedestrian detection using radar or LiDAR. The “Clear” weather condition was by far the most common weather

condition in all three data sources accounting for over 80% of all cases in both databases. The percentages of all weather conditions can be found in Table 4.

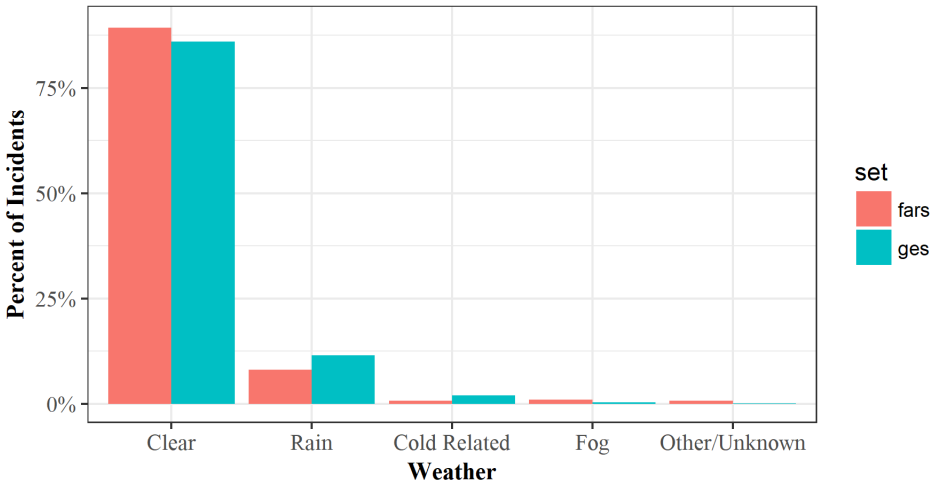

Figure 15. Weather condition distribution at time of collision. Data source: FARS, GES

Figure 16 and Figure 17 show the speed limit of the zone where the vehicle-pedestrian incident occurred. The most common FARS incident speed limit (45 mph) was faster than the GES speed limit (25 mph). It was not surprising that fatalities are more common at higher speeds because fatality risk increases as impact speed increase[55, 56].

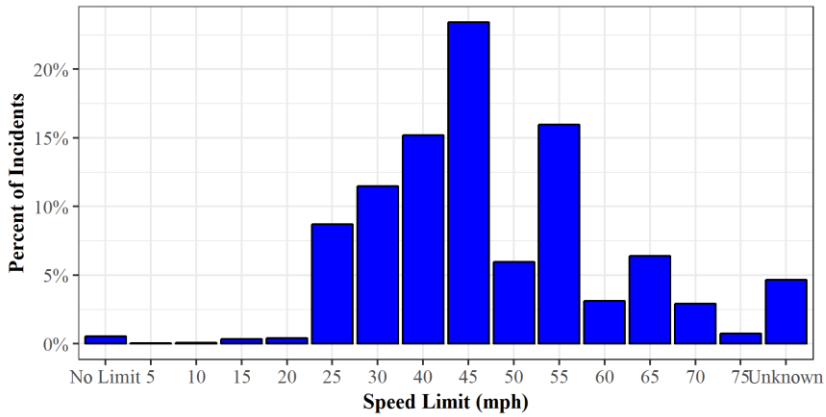

Figure 16. Distribution of speed limit in incident locations. Data source: FARS

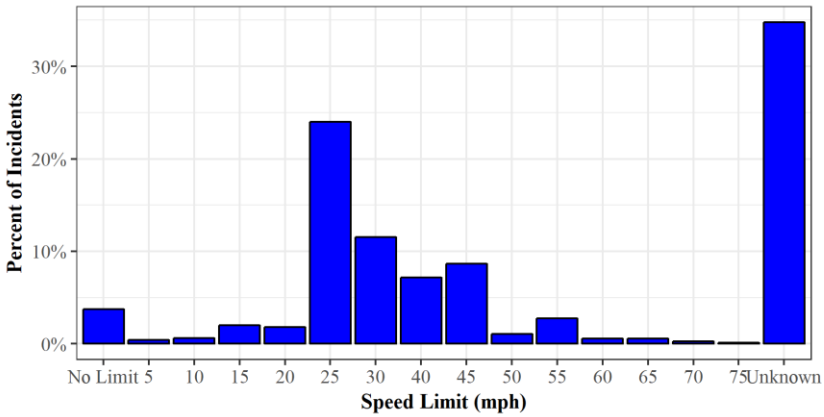

Figure 17. Distribution of speed limit in incident locations. Data source: GES

Figure 18 shows the most common vehicle-pedestrian collision locations in relation to junctions. A junction is the area formed by the connection of two roadways[50]. A junction includes intersections, connections between driveways and alleyways to roadways, and connections between alleys and driveways[50]. Non-junctions are the most common in FARS and GES constituting 68% and 35.8%, respectively. FARS most likely has a higher percentage of cases occurring at non-junctions because vehicle speeds tend to be travelling at higher speeds at non junctions than at intersections or intersection-related areas, which as discussed previously, increases pedestrian fatality risk.

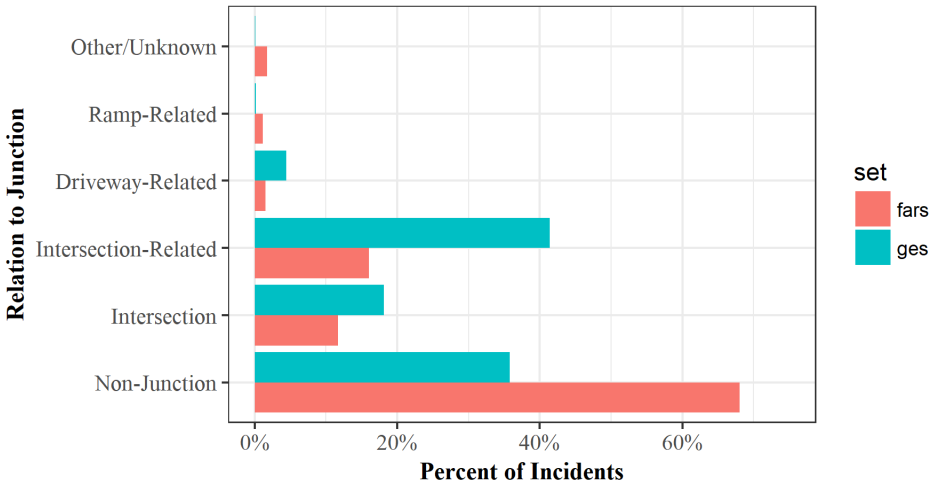

Figure 18. Distribution of collisions in relation to junction. Data source: FARS and GES

3.3.5 CHARACTERISTICS IMPACT ON TARGET POPULATION

The target population includes approximately two-thirds of all pedestrian crashes and fatalities. Realistically, not all of the target population incidents could be avoided or mitigated with current technology. Some systems are more effective during daylight conditions and when there are no adverse weather conditions that could affect the system's sensing ability. When these factors are considered the most restrictive system (target population "daylight and clear") could potentially avoid or mitigate 12% of all fatal incidents and 29% of all struck pedestrian incidents. This corresponds to approximately 600 pedestrian fatalities and 21,780 struck pedestrians per year (Table 5). Pedestrian AEB systems that are effective during low-light conditions (target population "Clear") could potentially avoid or mitigate 53% of all fatal incidents and 48% of all struck pedestrian incidents. This corresponds to approximately 2,600 pedestrian fatalities and 36,400 struck pedestrians annually (Table 5).

Table 5 also shows that there is a tremendous benefit to deploying a P-AEB system which operates in low-light conditions. If P-AEB systems were effective during low light conditions the number of pedestrian fatalities which could be potentially mitigated rises to over 2,600, a 430% increase in the target population over the most restrictive, daylight only, system. An all-weather pedestrian AEB system would further increase the number of pedestrian fatalities which could be potentially mitigated by 127%.

The target populations presented in Table 5 are an upper bound on the collisions which may be avoided or mitigated. This number does not take into account factors such as obstructions or pedestrians which dart out into traffic, leaving a P-AEB system insufficient time to react.

Table 5. Crash avoidance potential of P-AEB systems that may be limited by weather and/or lighting conditions.

Crash Type	Average Annual Pedestrian Struck	Struck %	Average Annual Pedestrian Fatalities	Fatal %
All Pedestrians Crashes	74,929	100	4,892	100
Only Passenger Vehicles	68,267	91.1	4,078	83.4
Only Passenger Vehicles Only Frontal Impacts	49,795	66.5	3,585	73.3
Target Population				
Only Passenger Vehicles Only Frontal Impacts No Loss of Control	49,178	65.6	3,555	72.7
Target Population "Daytime"				
Target Population Only Daytime	27,317	36.5	762	15.6
Target Population "Clear"				
Target Population Only Clear Weather	36,484	48.7	2,623	53.6
Target Population "Daytime and Clear"				
Target Population Only Daytime Only Clear Weather	21,781	29.1	601	12.3

3.4 CONCLUSION

This study examined two nationally representative data sources collected in the U.S. to characterize the target population for P-AEB systems.

Pedestrian Characteristics: Male pedestrians constituted the majority of collisions (52-69%). Few pedestrians were involved with alcohol prior to the incident (6-18%). These results, however, may be skewed due to a large number of pedestrians with unknown alcohol involvement. The median age of struck pedestrians was 32 years, however the median age of fatally-injured pedestrians was 48 years reflecting the lower injury tolerance of older pedestrians.

Driver Characteristics: The age distribution of drivers was similar in FARS and GES with a median age of 39 and 40, respectively. Furthermore, males made up over 60% of the drivers involved in these types of collisions. Few drivers were involved with alcohol prior to the incident (2-7%).

These results, however, may be skewed due to a large number of drivers with unknown alcohol involvement.

Environmental Characteristics: Most collisions occurred during the daylight (56-65%), however most fatalities occurred in dark conditions (71%, combined lighted and not lighted). In addition, most collisions occurred when there were no adverse weather conditions (83-89%) and at non junction locations (40-68%).

4 PEDESTRIAN EARLIEST DETECTION OPPORTUNITY

4.1 RESEARCH OBJECTIVE

The effectiveness of pedestrian AEB will be highly dependent upon whether the length of time the pedestrian is visible to sensors on the vehicle is sufficient to warn the driver and/or automatically brake. The objective of this chapter was to estimate the time of earliest detection or earliest detection opportunity (EDO) in vehicle-pedestrian collisions using three methods: 1) pedestrian trajectory derived EDO using PCDS, 2) Naturalistic Video derived EDO using SHRP 2, and 3) simulation derived EDO using PCDS.

4.2 PEDESTRIAN TRAJECTORY DERIVED EDO USING PCDS

4.2.1 APPROACH

Detection time was determined by estimating the distance the pedestrian travelled on the road and dividing the distance by the speed of the pedestrian. The distance the pedestrian travelled was calculated in two ways.

1. Used the PCDS scaled crash diagram to measure the distance along the pedestrian's path from the edge of the road to the impact point. This method relies on the accuracy of the crash investigators who made the scene diagrams.
2. Counted the lanes the pedestrian crossed between the edge of the road and the impact point. While this depends less on the accuracy of the scene diagram, this method does not account for differing lane widths. For this study, the width of a lane was estimated to be 3m as most of the cases occurred in urban or rural environments, rather than on the wider roads of the interstate highways. Typical lane widths in the U.S. range from 3-3.8m. By choosing an estimated lane width of 3m, the narrower end of the spectrum, the resulting time visible will more likely underestimate the actual time visible.

In order to determine time visible in cases in which the pedestrian was travelling parallel to the direction of traffic (24 collisions) it was assumed that the pedestrian would be visible to a driver from 40m away [57]. Bhagavathula, et al. [58] found that lighting and pedestrian motion affected detection distance, with pedestrians detectable at ranges over 200m in lighted conditions and as low as 25 m in unlighted conditions. As shown in Table 6, most parallel cases occurred during dark conditions whether that be lighted or non-lighted. A distance of 40 meters was chosen as a conservative measure of detection distance and corresponds to about half of a block. This aligned with the crossing pedestrian cases because it was assumed that the pedestrian was only detectable when they entered the road and therefore were a potential collision partner. While pedestrians may be detectable at longer distances, we assumed that they were not considered a threat until they were within 40 m.

Using the speed limit, the time it would take the vehicle to travel the 40m to the pedestrian could be calculated (t = 40m/speed limit) and substituted for the time the pedestrian was visible. This method allows the parallel cases to be included in the analysis, but does not account for differences that may arise from vehicles traveling above or below the speed limit. This method was also applied to scenarios in which the pedestrian was stationary.

Table 6. Overview of PCDS parallel cases and the lighting conditions of the events.

Lighting	Parallel Cases	Percent of Cases
All	22	4.2%
Daylight	10	1.9%
Dark (lit)	7	1.3%
Dark (unlit)	4	0.8%
Dusk	1	0.2%

The cases in which the vehicle struck a pedestrian not on a roadway fit neither of these conditions. If the case was missing a scene diagram, the pedestrian was not in the roadway, or a

parallel case had no recorded speed limit they were excluded. The final sample contained 512 applicable collisions.

Walking speed of the pedestrian was computed in two ways. Initially, the speed of the pedestrian was assumed to be 1.2 m/s as this is a common value used in pedestrian walking studies [59]. This was followed by using the average walking speeds of different age groups as recommended by Gates et al [59]. Groups of pedestrians and adults assisting children were assumed to walk at slower speeds as shown in Table 7 and recommended by Gates et al [59]. A child was defined as a pedestrian under the age of 6.

Table 7. Average Walking Speed of Pedestrians based on Age as recommended by Gates et al [59].

Age	Walking Speed (m/s)
< 30	1.45
30 - 64	1.42
> 64	1.15
Adult w/ Child	1.20
Groups 2 - 4	1.32

As shown in Table 8 visual obstructions were present in about 20% of the PCDS cases. This poses a problem for pedestrian AEB systems. To account for obstructions, duration visible was calculated in two ways. First the time on road was calculated. The time on road does not account for obstructions, but is the time from when the pedestrian enters the road until the point of impact. Then the time visible on the road was calculated. Time visible on the road is the time from when the pedestrian is both on the road and visible until the impact point.

Table 8. Overview of PCDS cases with visual obstructions.

Obstruction	Number of Cases	Percent of Cases
All	104	19.6%
Parked Vehicle	41	7.7%
Stopped Vehicle	37	7.0%
Bus	20	3.8%

Ice Cream Truck	4	0.8%
Moving Vehicle	2	0.4%

4.2.2 RESULTS

Table 9 describes the type of vehicle-pedestrian collisions investigated by the PCDS database. In the PCDS database slightly more struck pedestrians were male and pedestrians aged 16 and younger were involved in 27.9% of the PCDS cases. Alcohol involvement was low, only affecting 6.9% of pedestrians. Most cases occurred during daylight and clear weather conditions and occurred in either non-junctions or were intersection-related. Obstructions were present in 14.5% of the PCDS cases.

Table 9. PCDS case breakdown by pedestrian struck.

Variable	Cases	Percentage
Total	549	100
Pedestrian Gender		
Male	288	52.5
Female	257	46.8
Pedestrian Age		
Child (≤ 16)	154	27.9
Adult	326	59.7
Senior (≥ 65)	69	12.5
Pedestrian Alcohol Involvement		
No	362	65.9
Yes	38	6.9
Unknown	149	27.1
Lighting		
Daylight	355	64.7
Dark-Not Lighted	32	5.8
Dark-Lighted	125	22.8
Dawn	14	2.6
Dusk	23	4.2
Weather		
Clear	458	83.4
Rain	83	15.1
Cold related	6	1.1
Other/Unknown	2	0.4
Crash Location		
Non-Junction	221	40.3

Intersection	49	8.9
Intersection Related	213	38.8
Other	66	12
Occluded		
No	422	76.9
Yes	107	14.5
Unknown	20	3.6

Of the 549 pedestrians involved in the 530 PCDS cases, 8 pedestrians (from 8 cases) were excluded because there was no crash scene diagram. An additional 8 pedestrians, representing 7 cases, were excluded because they were struck when on the sidewalk or road shoulder. If a case in which the pedestrian was travelling parallel to the road did not have a speed limit recorded, the case was excluded because this value was required for the EDO estimation. There were only three pedestrians, involved in three crashes, in that were excluded for lack of reported speed limit. The remaining dataset consisted of 530 pedestrians that were involved in 512 vehicle-pedestrian crashes (Table 10).

Table 10. Breakdown of case exclusion

Reason Excluded	Number of Cases Remaining	Number of Pedestrians Remaining
None Excluded	530	549
Missing Scene Diagram	522	541
Pedestrian off Roadway	515	533
Parallel Cases with no speed limit	512	530

As shown in Figure 19, the two methods for estimation of detection time were linearly related with an r^2 value of 0.93. The remainder of this study will only consider the detection time calculated based on the number of lanes crossed because the results will be more scalable to situations in which there is no crash diagram. Additionally, the time calculation based on the scene diagram was on average 20% larger than the lanes crossed approach. Thus, using the time calculation based on lanes crossed will give a lower bound on AEB effectiveness and will therefore be more conservative.

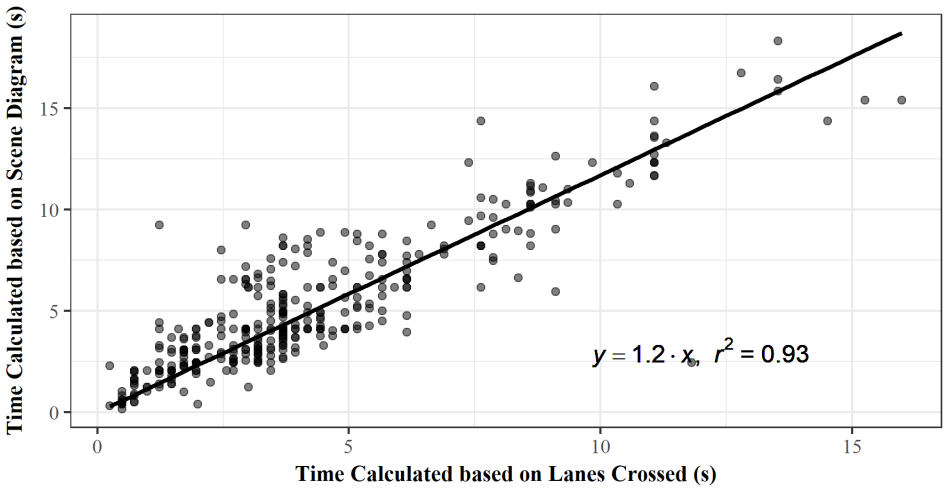

Figure 19. Comparison of two methods of detection time calculation.

As shown in Figure 20, in more than 80% of the cases the pedestrian was visible for at least one second prior to impact. This is encouraging for P-AEB systems because the longer the pedestrian in visible, the more time the system has to detect the pedestrian and take action.

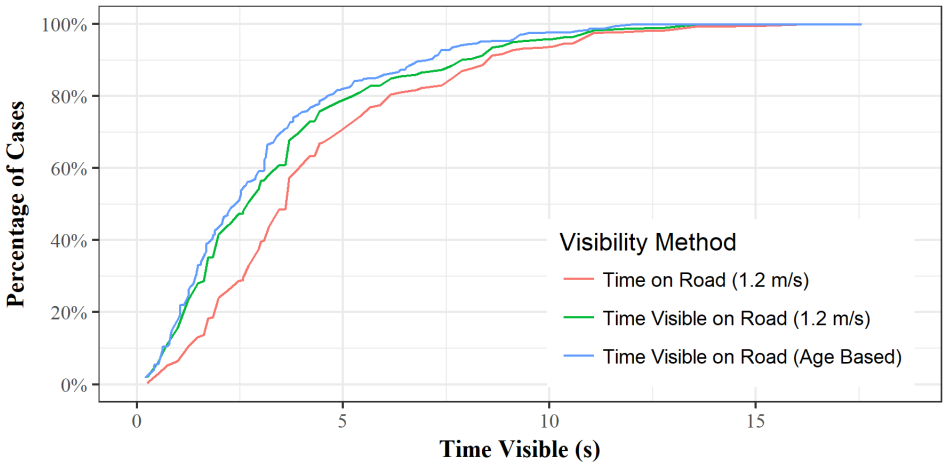

Figure 20. Cumulative distribution plot of the estimated time pedestrian was detectable using three different methods. Time on Road (red) and Time Visible (green) assume a pedestrian speed of 1.2m/s whereas Time Visible (blue) adjusted walking speed by pedestrian age.

4.3 Feasibility of using Naturalistic Driving Data to Characterize Vehicle-Pedestrian Crashes and Near Crashes [5]

4.3.1 Approach

This approach examined crashes and near-crashes from the Second Strategic Highway Research Program (SHRP 2) naturalistic driving study [52]. The database was queried for all events that were pedestrian related, which resulted in 168 events. Six events were excluded because the subject vehicle was a witness to the event and not directly involved in it, meaning that critical information was lacking, leaving only crashes and near-crashes (3 crashes and 159 near-crashes). A crash was defined as an event in which the subject vehicle had any contact with a pedestrian. A near-crash was defined as any situation that required a rapid evasive maneuver by the subject vehicle or pedestrian [4]. Additionally, four near-crashes events were excluded because either video or time series data were missing. One of the crash events was excluded after video review because it was determined that the pedestrian intentionally contacted the vehicle with their foot, which is not representative of a normal crash mode. The final data set consisted of 161 events (2 crashes and 159 near-crashes).

4.3.1.1 Classification of Interaction Types

For each event the forward-facing SHRP 2 video was examined. Events were characterized based on pedestrian, driver, and environmental factors and then compared to the nationally representative US data sets. Each event was also grouped by crash mode. If the pedestrian crossed straight in front of the subject vehicle from the left or right, the crash mode was termed as a Left/Right straight crossing path (LSCP or RSCP, respectively). If the subject vehicle was making a left turn, then the crash mode was termed as left turn across path/opposite direction or same direction (LTAP/OD, LTAP/SD), depending on the pedestrian direction of travel relative to the subject vehicle. If the subject vehicle was making a right turn, the crash mode was labelled following

the same pattern as the left-turn scenarios. These crash modes are illustrated in Figure 21. Any other crash mode was grouped in the "Other" category.

Videos were reviewed manually using a standard set of definitions for pedestrian, driver, and environmental conditions. All videos were examined by the same reviewer for consistency. For certain variables (i.e. weather conditions lighting conditions, and relation to junction) the reviewer's assessment was compared to the assessment of the SHRP 2 professional reductionists. If there was a disagreement, the video was re-examined. The proximity point was also determined by both the reviewer and the SHRP 2 reductionists, for this variable the SHRP 2 reductionist assessment was used, but it should be noted that there was very little difference in the recorded results.

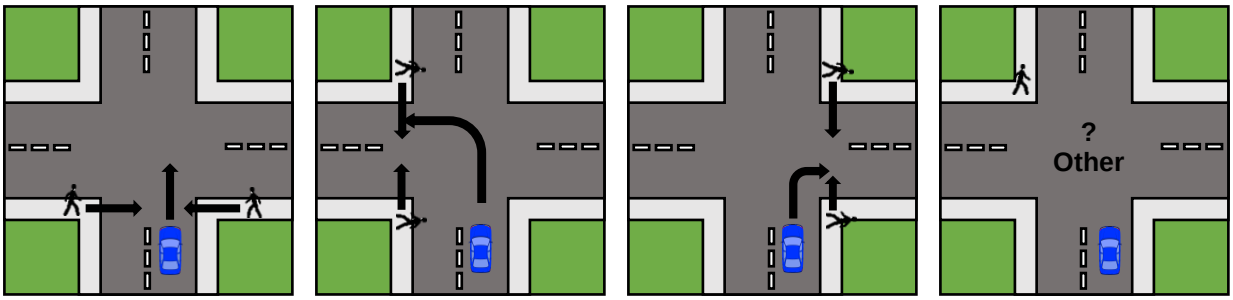

LSCP/RSCP LTAP/OD, LTAP/SD RTAP/OD, RTAP/SD Other

Figure 21. Crash Modes from SHRP 2 video analysis.

4.3.1.2 Duration Visible

The time duration that a pedestrian was visible was calculated by manual examination of the event video. The timestamp of the moment when the pedestrian was first visible was recorded, whether or not the pedestrian was on the road. If they were not on the road, meaning they were on the sidewalk or the road shoulder, for example, then the timestamp of the moment they first entered the road was also recorded. The duration visible was defined as the time from when the pedestrian was first visible until the time the pedestrian reached the impact proximity point. The impact

proximity point was defined as the time at which the subject vehicle first made contact with the pedestrian or, in the absence of contact, when the subject vehicle was closest to the pedestrian.

4.3.1.3 Vehicle Time Series Data

For each event, the subject vehicle time series data were examined. The event sample rates differed based on the vehicle and the data type. Brake activation was recorded at a rate of 10 samples per second. Vehicle speed was recorded at a rate between 1 and 10 samples per second, depending on whether the vehicle recorded vehicle speed using the vehicle network system (offering rates > 1Hz) or the speed calculated based on GPS location (collected at 1 Hz). For this study network speed was used, when possible, because it had a higher sampling rate. Where network speed was not available, GPS speeds were used instead. When determining travel speed of the vehicle, the vehicle speed was linearly interpolated between the adjacent samples in an effort to compensate for different sampling rates and correct for differences in the sampling rate of the vehicle data and the frame rate of the video. Time to collision (TTC) at braking was defined as the time from the onset of braking to the collision (or proximity impact point).

4.3.2 RESULTS

4.3.2.1 Comparison of SHRP 2 to Nationally Representative Datasets

Table 11 compares SHRP 2 to GES and FARS, two nationally representative databases. SHRP 2 follows similar trends to both GES and FARS in terms of driver age, driver gender, and weather. In general, SHRP 2 tended to be closer to GES which was expected due to the fact that GES contains incidents of all crash severities whereas FARS is only fatalities. SHRP 2 had more female drivers than GES or FARS and SHRP 2 had a higher proportion of incidents that occurred at intersections than GES or FARS. This may be because there is a higher chance of vehicle-pedestrian interaction at intersections, but these interaction do not necessarily translate to more police-reported or fatal vehicle-pedestrian crashes. The SHRP 2 “other” category is a large proportion of the observed crash

locations. This category is primarily made up of events that occurred in parking lots. The majority of the non-fatal vehicle-pedestrian incidents in both GES and SHRP 2 occurred during daylight hours whereas the majority of fatal vehicle-pedestrian interactions occurred during dark lighting conditions (Table 11).

Table 11. SHRP 2 Pedestrian events compares to US Databases, GES and FARS.

	SHRP 2 Events	SHRP 2 %	GES Cases (2011–2015)	GES %	FARS Cases (2011–2015)	FARS %
Total	161	100	370,874	100	24,197	100
Driver Age						
Young Adult (< 25)	47	29.2	73,170	19.8	8,540	35.3
Adult	68	42.2	251,573	67.9	12,546	51.7
Senior (≥ 65)	43	26.7	46,129	12.4	3,524	14.3
Driver Gender						
Male	82	50.9	229,190	61.8	15,512	64.1
Female	77	47.8	141,684	38.2	6,264	25.9
Unknown	2	1.2	-	-	2,421	9.9
Lighting						
Daylight	106	65.8	207,578	56	5,692	23.5
Dark-Not Lighted	3	1.9	33,735	9.1	8,361	34.6
Dark-Lighted	48	29.8	112,298	30.3	8,928	36.9
Dawn	1	0.6	4,401	1.2	383	1.6
Dusk	3	1.9	11,168	3	500	2.1
Other	-	-	1,694	0.4	333	1.4
Weather						
Clear	145	90.1	273,992	73.9	21,403	88.5
Rain	15	9.3	40,521	10.9	1,954	8.1
Cold related	-	-	54,434	14.7	265	1.1
Other/Unknown	1	0.6	1,044	0.3	575	2.4
Crash Location						
Non-Junction	48	29.8	153,039	41.3	16,480	68.1
Intersection	58	36	62,309	16.8	2,754	11.4
Intersection Related	16	9.9	137,461	37.1	3,700	15.3
Other	38	23.6	18,063	4.8	1,263	5.2

4.3.2.2 Analysis of SHRP 2 cases: Duration Visible

As shown in Table 12, about 33% of the incidents involved visual obstruction of the pedestrian in the time leading up to the incident. Obstructions labelled as "Other" included events in which the pedestrian was obstructed by trees, a building, a telephone pole and a dumpster.

Table 12. Breakdown of SHRP 2 Events with Obstructions.

	Events	Percent of Total
Total	161	100%
Obstructions	53	32.9%
Moving Vehicle	38	22.4%
Parked Vehicle	11	6.8%
Other	4	2.4%

LSCP and RSCP, scenarios in which the pedestrian was travelling perpendicular to the vehicle, account for over 60% of events and make up the two most common crash modes, as shown in Figure 22. Figure 23 shows that the median duration the pedestrian was visible did not differ substantially between crash modes, but that RTAP/SD tended to have lower duration visible than the other crash modes.

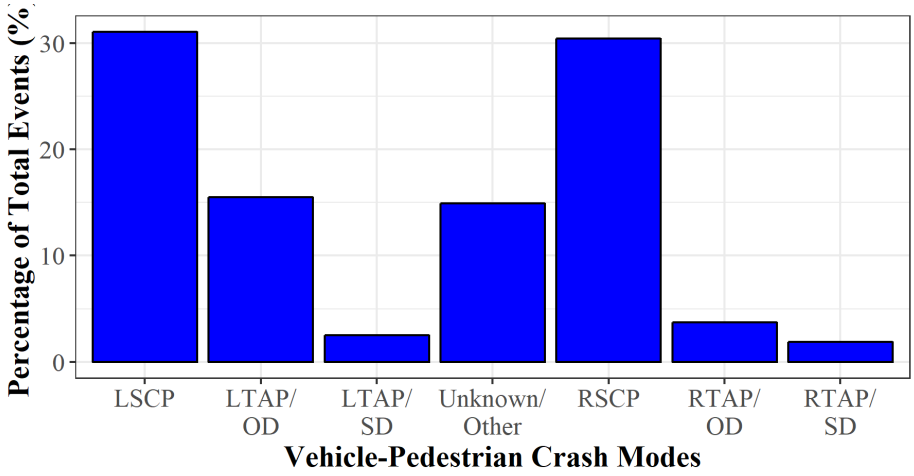

Figure 22. Incidence rates of crash modes in SHRP 2.

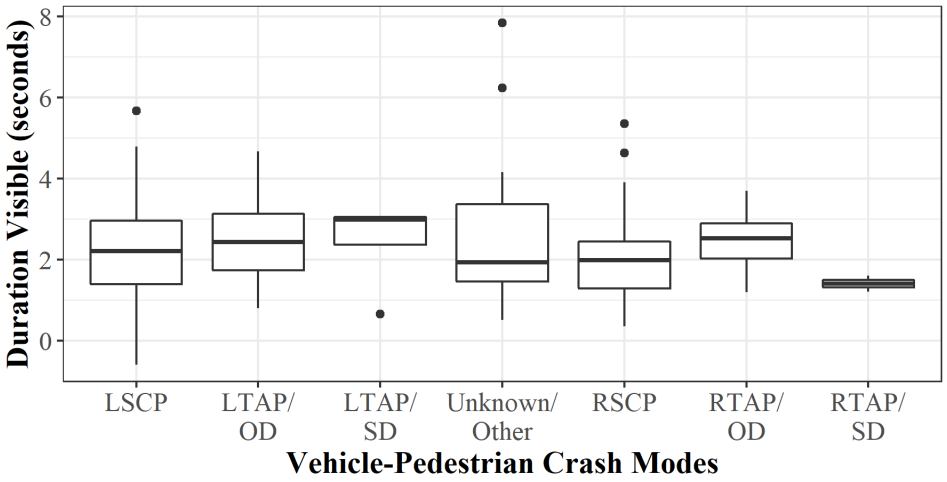

Figure 23. Duration pedestrian was visible by crash mode. The points above and below the box and whisker plots are outliers which were defined as points greater than 1.5 times the interquartile range away from the median.

As shown in Figure 24, in about 90.8% of cases, pedestrians were on the road and visible for longer than one second, 82.4% were visible for at least 1.25 seconds, and 73.2% were visible for at least 1.5 seconds. Total time the pedestrian was visible tended to be longer than the time the pedestrian was visible and on the road meaning that in many cases the pedestrian was visible before they stepped into the road.

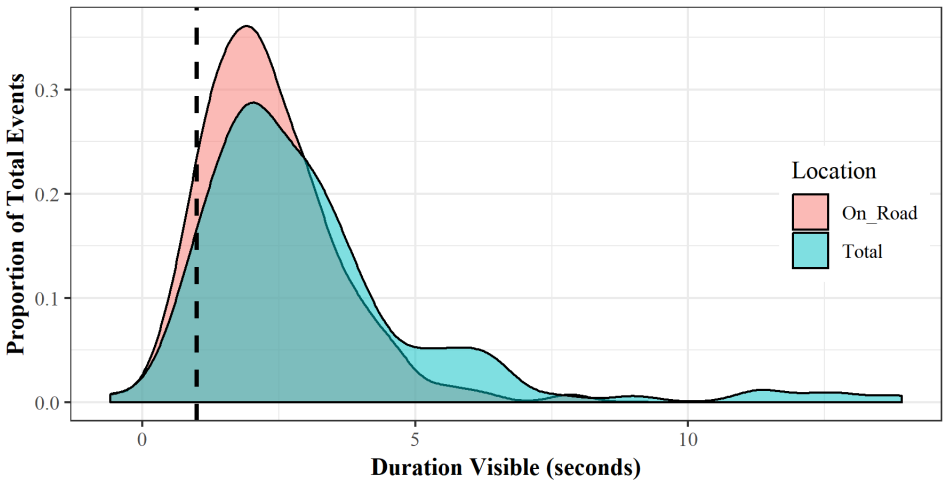

Figure 24. Distribution plot of duration visible for the total time the pedestrian was visible and the duration visible only for when the pedestrian was on the road. The dotted line is located at one second duration visible which is the assumed minimum time needed for injury mitigation.

4.3.2.3 Analysis of SHRP 2 Cases: Driver Braking TTC

As shown in Figure 25 the Braking TTC values were not substantially different between the crash modes. RTAP/OD had slightly lower Braking TTC than the other crash modes and LSCP had the largest number of outliers all above 2.5 seconds.

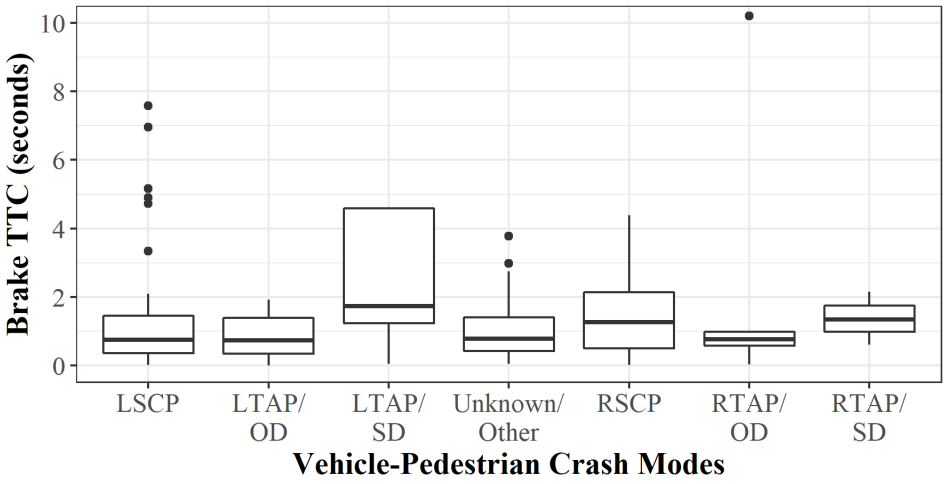

Figure 25. Braking Time-To-Collision (TTC) by crash mode. The points above and below the box and whisker plots are outliers which were defined as points greater than 1.5 times the interquartile range away from the median.

All but one of the SHRP 2 drivers involved in near-crashes braked, while in both of the pedestrian crash cases the driver took no evasive action. As shown in Figure 26, the majority of the subject vehicles decreased their travel speed in the last second preceding the impact proximity point. In 10% of the analyzed cases, drivers began evasive actions less than one second prior to the potential collision.

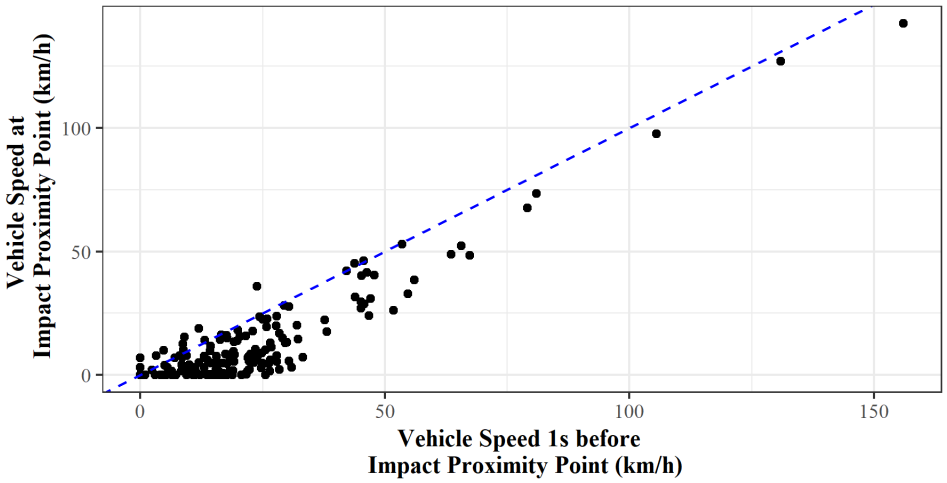

Figure 26. Comparison of vehicle speed at 1 second before the impact proximity point (IPP). The dotted line is the points were the speed before and at the impact proximity point were the same indicating no braking occurred.

On average, drivers initiated braking evasive maneuvers an estimated 1.5 s prior to the potential collision, with 50% of drivers initiating braking at a TTC of 0.97 s or less (Figure 27 and Figure 28). Assuming a threshold of one second, an AEB system would be activated before the driver's evasive action in about 52.8% of the observed events.

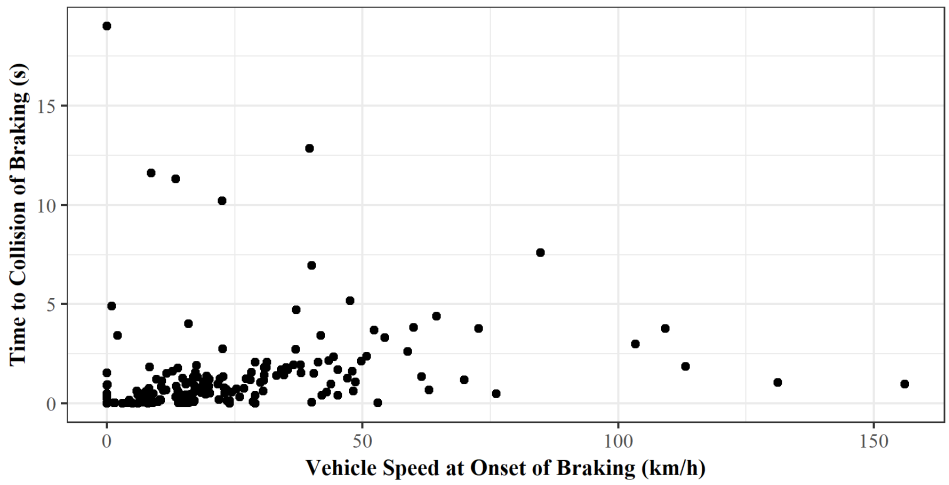

Figure 27. Time-to-collision of braking compared to the subject vehicle speed at the onset of braking.

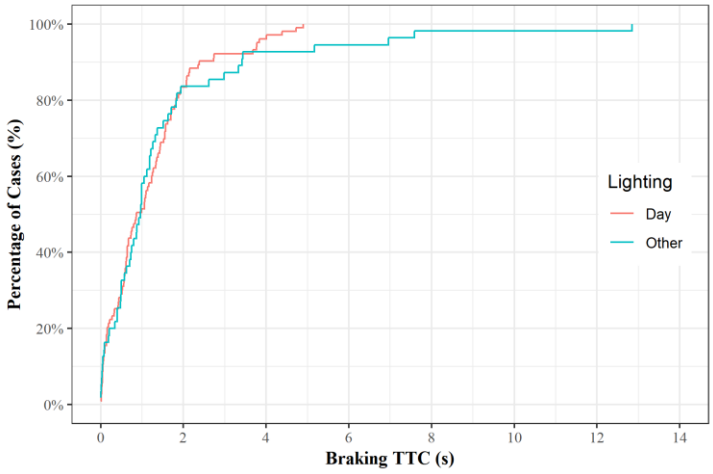

Figure 28. Cumulative distribution plot of time-to-collision of braking for daylight and non-daylight lighting.

4.3.3 DISCUSSION

The SHRP 2 naturalistic driving study is a useful tool because it contains important information (e.g. TTC at braking) which is unavailable in traditional datasets. The drawback of using a database like SHRP 2, however, is the comparatively small sample size of rare events such as crashes. To compensate for this limitation, near-crash events were included as they are much more common events. Near-crashes have been shown to be representative of crash events, but to check this assumption SHRP 2 was compared to GES and FARS. SHRP 2 events were shown to be more similar to GES than FARS, but generally followed the same trends. SHRP 2 had a larger proportion of events that occurred at intersections than GES or FARS which may be attributed to more vehicle-pedestrian interactions at intersections. GES and FARS may have lower recorded vehicle-pedestrian interactions at intersections than SHRP 2 because cars tend to go at lower speeds meaning that police-reported and fatal interactions are less likely at those locations.

One potential method to mitigate the increasing vehicle-pedestrian problem is the use of active safety systems to detect and avoid pedestrians through the use of automatic emergency braking (AEB) systems. Most AEB systems depend on a combination of radar and camera to detect pedestrians, and require at least one second to detect and initiate an evasive maneuver. To estimate the potential benefit of AEB the duration the pedestrian was visible to the forward facing camera was calculated. In about 33% of the cases there was some sort of obstruction that decreased the amount of time the pedestrian was visible. It was also found that on average the duration visible was shorter when the vehicle made a right turn into the path of a pedestrian traveling in the same direction as the vehicle (RTAP/SD). This information indicates that RTAP/SD interaction may be more difficult for AEB systems to prevent and/or mitigate than other crash modes.

Current AEB systems have a threshold TTC that must be reached before a response is initiated. This threshold is necessary in order to encourage adoption of the technology by keeping unnecessary AEB activation to a minimum. Based on the assumption that one second is needed to detect and respond to a pedestrian conflict, an AEB system would have sufficient time to mitigate approximately 80% of the events examined. Mitigation means that the severity of the crash would be reduced either by avoidance of the collision, reduction of impact speed, or another change in the crash scenario that reduces injury.

In many cases the driver initiated braking before the one second TTC threshold was reached meaning that AEB system activation would have occurred after the driver initiated evasive action. Therefore, AEB activation was examined at various AEB braking thresholds in relation to the TTC of the driver's first evasive action. For this analysis the TTC threshold refers to the amount of time before vehicle-pedestrian interaction occurs, not the amount of time the system needed to recognize and respond to the pedestrian. A limitation of this analysis is that the duration the pedestrian was visible was not considered, only the TTC of the driver's first evasive action affected the results. As

expected, the sooner the AEB system braked the more likely the AEB system would brake before the driver.

This study presents an examination of characteristics associated with real-world vehicle-pedestrian crashes and near crashes to estimate the benefit of pedestrian AEB systems in the USA. The use of naturalistic driving data allows the investigation of crucial parameters for active safety design, which are not available in retrospective police reported crash databases. These crucial parameters include the time-to-collision of driver evasive maneuvers, pedestrian evasive maneuverers, time the pedestrian was visible and the incidence of obstructions. This information can be used to estimate the benefit of active safety systems, such as AEB, on mitigating pedestrian traffic-related fatalities and injuries.

4.4 Automatic Emergency Braking Sensor Configuration Effect on the Detection of U.S. Pedestrians [6]

4.4.1 Approach

4.4.1.1 Reconstruction

To reconstruct the vehicle and pedestrian trajectories, the trajectory points were digitized from the scanned PCDS crash scene diagrams. The scene diagrams were loaded into AutoCAD, scaled, and oriented so that the origin was located at the front center of the vehicle at impact with the vehicle heading toward the positive y-axis. The vehicle and pedestrian trajectory points were then collected relative to the origin. If a crash scene diagram only had one vehicle trajectory point, a second trajectory point was extrapolated based on the impact position of the vehicle, vehicle heading, and the event summary. To create a smooth vehicle/pedestrian path, the measured trajectory points were connected together. If the trajectory was straight, a linear path was fitted to the trajectory

points using linear regression to minimize the error of the positions in the scene diagram. For curved trajectories, the measured trajectory points were fit to a curve. To fit the curved trajectories, the trajectory points were loaded into MATLAB and the curve fitting tool was used to fit the points, minimizing the root mean square error, with a variety of potential curve models including, but not limited to, exponential, power, tangent, cotangent, and secant. Two cases, where the vehicle/pedestrian was performing a "U-turn" maneuver, were fitted using a parabolic model. The models were manually inspected to ensure that they fit with the crash summary and then the model with the best R-squared value was used. The vehicle and pedestrian trajectories are shown in Figure 29 in global coordinates, where the origin was the front and center of the vehicle, the y-axis was along the vehicle longitudinal axis, and the x-axis was along the vehicle's front bumper, all at the point of impact.

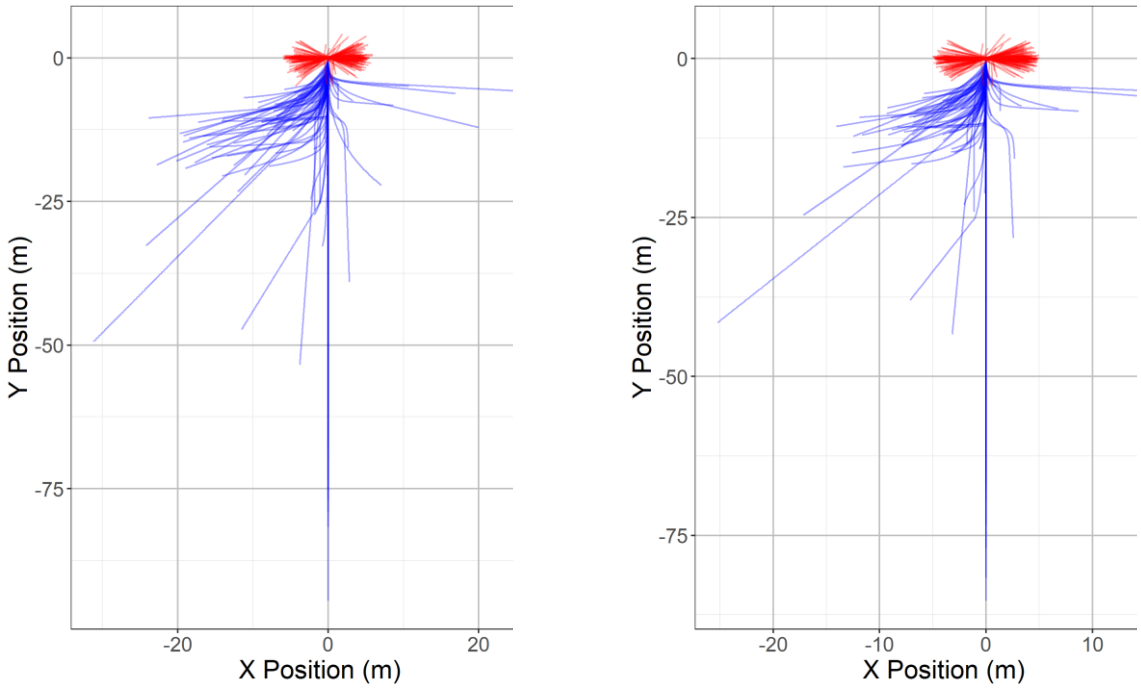

Figure 29. Vehicle (blue) and pedestrian (red) trajectories in global coordinates for the early/weak (left) and late/hard (right) braking driver.

To obtain the position and speed of the vehicle and pedestrian in the time prior to the crash, the scenario was reconstructed backwards from the point of impact based on the impact speed estimated by the crash scene investigator. The pedestrian was assumed to walk at a constant speed and take no evasive actions. Pedestrian speed was predicted based on the pedestrian's age and whether or not they were travelling in a group. The pedestrian walking speed ranged from 1.15 to 1.45 m/s based on the pedestrian age and whether or not they were walking in a group [60]. For the vehicle, if there was no evidence that the driver braked before the collision, it was assumed that the vehicle travel speed was equivalent to the impact speed. If there was evidence of braking, there were two equally likely potential driver braking patterns utilized, an early and weak braking pattern and a late and hard braking pattern. The early/weak braking driver pattern was assumed to start braking at a time-to-collision (TTC) of 2 seconds with a maximum deceleration of 0.2 g. The late/hard braking driver pattern was assumed to start braking at a time-to-collision (TTC) of 0.4 seconds with a maximum deceleration of 0.4 g. These two braking models were chosen because the true brake timing and maximum deceleration were not known. The two braking models were intended to represent an upper and lower bound with the driver's true braking profile falling within the bounds [61]. Both braking models were assumed to have a jerk, or acceleration rate, of 10.7 m/s^3. If there was braking, the braking was assumed to begin at the TTC value of the braking model whether or not the pedestrian was visible and on the road. The vehicle and pedestrian trajectories were calculated out to a TTC of 3 seconds.

For each time point we also recorded whether or not the pedestrian was on the road and whether or not the pedestrian was obstructed from the drivers' view. For this study, only physical obstructions, such as parked and moving cars and any physical objects denoted in the crash scene diagram, were considered. Visual obstructions such as glare from the sun or headlights were not considered. Similarly, darkness or lack of street lighting were not considered obstructions for this study.

4.4.1.2 Simulation

Based on the calculated vehicle and pedestrian trajectories, simulations were conducted with a hypothetical AEB model to estimate when and where various hypothetical AEB sensors could potentially detect the pedestrians. The AEB sensor was modelled on the front center edge of the vehicle with varied sensor field-of-view (FOV) and ranges. It was assumed that the sensor was attached to the front and center of the vehicle with the center axis of the FOV aligned with the longitudinal axis of the vehicle. FOV was varied from ±10° to ±90° and range was varied from 20 m to 100 m to capture a range of system specifications seen in commercially available radar and LiDAR systems [62].

The simulation was conducted using a specially developed code written in the R programming language. The code used the vehicle and pedestrian trajectories to determine the starting parameters and the path the vehicle and pedestrian would take and then it iterated forward in time. At each time point the code determined if the pedestrian was detectable based on their location relative to the vehicle, whether they were in the road, and whether they were obstructed from the sensor's view. If the pedestrian's location was within the range and FOV of the sensor and there was a direct line of sight to the pedestrian; then it was assumed that the pedestrian was detected by the sensor. This assumed that the sensor system, regardless whether radar, LiDAR, or cameras, was always capable of detecting a pedestrian in view. We assumed that an AEB system would only detect a pedestrian once it was in the road because if the pedestrian was not in the roadway, it was assumed that the system would not perceive the pedestrian as a threat.

At every time point, the code used the kinematic equations of motion to calculate the displacement over the time step (0.01 seconds) and the new velocity and acceleration for the vehicle and pedestrian. The displacement was projected onto the estimated path to calculate the new vehicle and pedestrian location. It was assumed that the front and center of the vehicle followed the

estimated path. A simple bicycle type kinetic model was used to calculate the location of the vehicle rear relative to the vehicle front as shown in equation (1) – (3) where X and Y indicate the X and Y location of the center of the vehicle rear, v represents the vehicle speed in m/s, Δt represents the time step, θ represents the heading, $steering \angle$ represents the steering angle, and L represents the vehicle length which was calculated by multiplying the vehicle wheel base by 1.2.

$$\Delta X_{rear} = v\Delta t \cos\theta \tag{1}$$

$$\Delta Y_{rear} = v\Delta t \sin\theta \tag{2}$$

$$\Delta\theta_{rear} = \frac{v\Delta t \tan(steering \angle)}{L} \tag{3}$$

For this study, the primary focus was pedestrian detection and not on avoidance/mitigation, therefore the hypothetical AEB system was designed to not activate. More details on the full code can be found in Haus, et al. [63].

Analysis was conducted by identifying whether or not the pedestrian could be detected prior to impact, the pedestrian's location relative to the hypothetical AEB system at the time of detection, and the time-to-collision (TTC) at the time of detection. The pedestrian's relative location was calculated relative to the AEB system on the vehicle meaning that the y-axis corresponds to the center forward facing axis of the sensor. The TTC at detection was calculated by dividing the linear distance to the original impact point by the vehicle speed at the moment the pedestrian was detected. In addition, the relative location of the pedestrian was calculated at TTCs of 1, 2, and 3 seconds to examine the sensor angle and range necessary to detect pedestrians over time.

4.4.2 RESULTS

Sensor effectiveness was first defined as the ability of the sensor to detect the pedestrian before impact. As shown in Figure 30, sensor range had very little effect on the ability for the sensor

to detect the pedestrian. Only the sensor with a FOV of ±10° showed any effect of sensor range with a 3 percentage point decrease in estimated detection ability for a sensor with a 20 m range compared to a range of 40 m or greater. Sensor FOV had a larger effect on the ability of the system to detect the pedestrians. The sensor with the narrowest FOV (±10°) was able to detect an estimated 58-61% of the pedestrians while the widest FOV sensor (±90°) was able to detect 99% of the pedestrians.

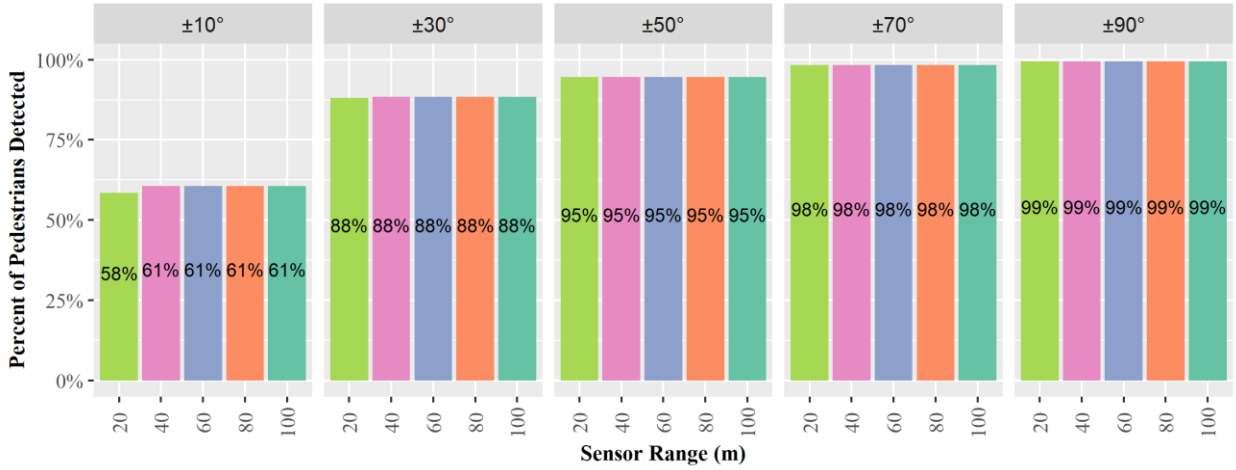

Figure 30. Percentage of cases in which the pedestrian was detected for sensor FOVs from ±10° to ±90° and sensor ranges from 20m – 100m.

While sensor range did not show a large effect on the ability to detect a pedestrian before impact it does have a substantial effect on where the pedestrian was detected. As shown in Figure 31, the AEB system with the narrower FOV and shorter range detected the pedestrian much closer to the impact point. While the pedestrian is still detected with a shorter range sensor, the system would have much less time to detect, identify, and take evasive action to avoid the collision. Also notable is that even when the FOV is wide and the range is long, many pedestrians were not detected until they were within 50 m and only a few were detectable at distances greater than 80 m. As expected, cases in which there were obstructions (Figure 31 blue points), the pedestrian tended to be detected much closer to the impact point than cases with no known obstructions.

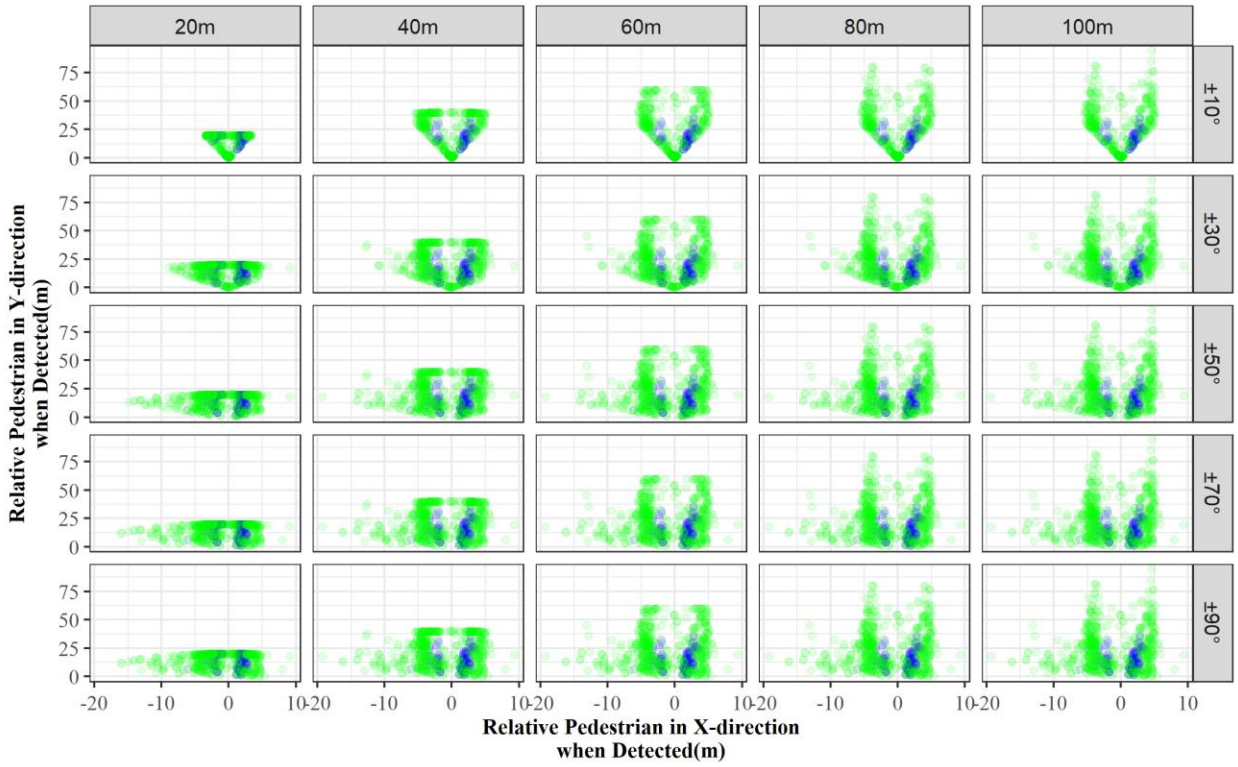

Figure 31. Pedestrian location when first detected by sensor system with sensor FOVs from ±10° to ±90° and sensor ranges from 20m – 100m. Blue points indicate cases with obstructions and green points indicate cases with no known obstruction.

The pedestrian's location when detected can indicate the urgency of the situation, but it was difficult to determine how much time the system would have to react by that metric alone because the vehicle speed was not taken into account. To account for speed the TTC was calculated at the time the pedestrian was detected. As shown in Figure 32, in less than 25% of the cases the pedestrian was estimated to be detectable at TTCs less than 1 second. The median TTC at detection increased with increasing sensor FOV and range. Increasing sensor FOV primarily increased the toe region of the graph so that there were fewer cases with a TTC of less than 1 second at detection. Increasing sensor range primarily increased the number of pedestrians that were detectable at the maximum TTC of 3 seconds. A TTC of 3 seconds was the most common detection which indicates that many pedestrians

were detected at the start of the simulation. It is possible that the pedestrians could have been detected at TTCs higher than 3 seconds, but longer TTCs were not considered in this study.

The relative pedestrian angle and distance was examined at TTCs of 1, 2, and 3 seconds (Figure 33 and Figure 34). As expected, median pedestrian distance decreased with TTC. The median distance at a TTC of 1 second was 6.4 m compared to median distances of 15.5 m and 22.4 m for TTCs of 2 and 3 seconds, respectively. There was very little difference between the relative pedestrian angles across TTC, although angles decreased slightly as TTC increased. The median pedestrian angle was 14.3°, 12.5°, and 11.5° for a TTC of 1,2, and 3 seconds, respectively.

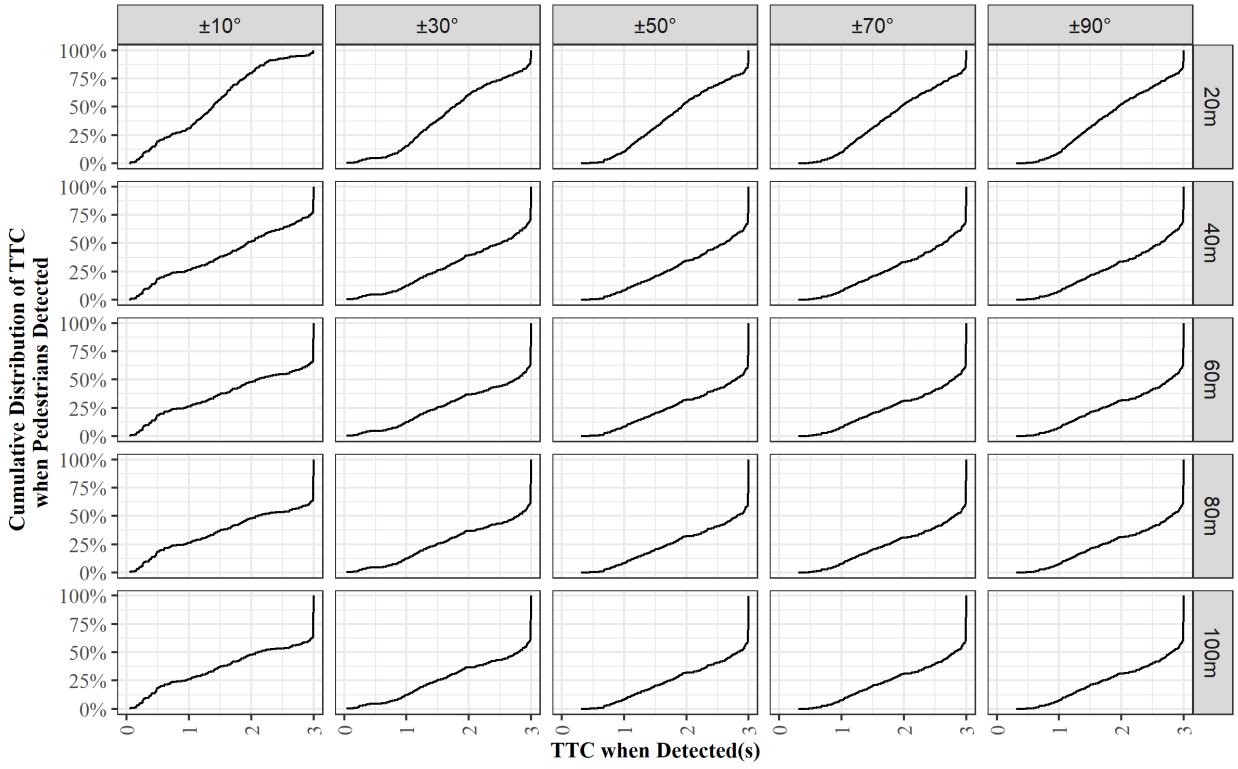

Figure 32 Cumulative distribution of TTC at pedestrian detection by sensor system with sensor FOVs from ±10° to ±90° and sensor ranges from 20m – 100m.

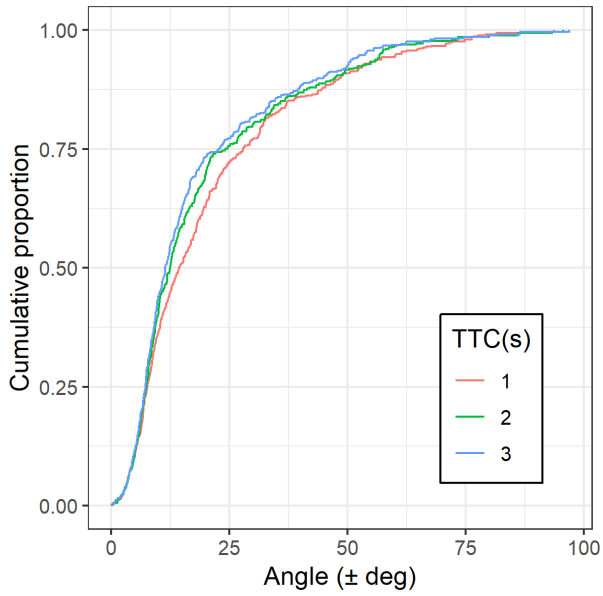

Figure 33. Cumulative distribution of pedestrian angle relative to hypothetical AEB system at a TTC of 1 (red), 2 (green), and 3 (blue) seconds.

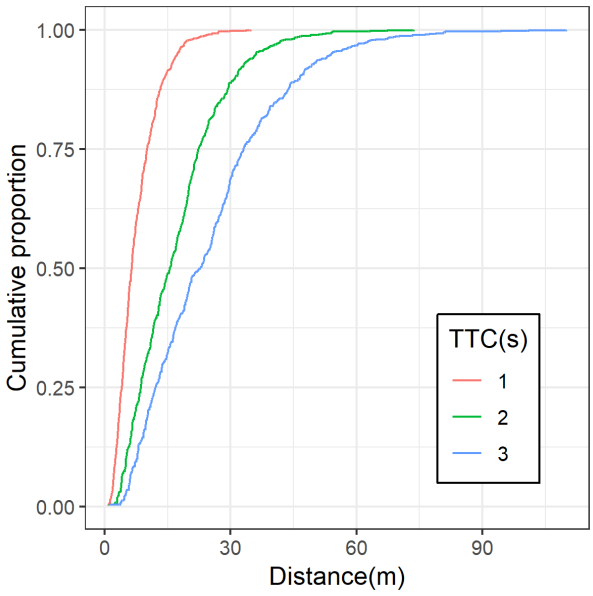

Figure 34. Cumulative distribution of pedestrian distance relative to hypothetical AEB system at a TTC of 1 (red), 2 (green), and 3 (blue) seconds.

4.4.3 DISCUSSION

In-depth vehicle-pedestrian crash data in the U.S. is limited. While PCDS is the most recent publicly available vehicle-pedestrian crash database that contains reconstructions, crash scene diagrams, detailed vehicle damage reports, and detailed injury records, the age and size of the dataset is a limitation. The data set was collected from 1994 to1998 and contains only 530 crashes. While we assumed that the crashes from the collection range resemble crashes that occur today, changes in driver or pedestrian behavior, different types of distractions, and more pedestrian friendly intersections could affect the applicability of these crashes.

The simulation model assumed that the vehicle followed the estimated trajectory and that the vehicle was able to achieve the necessary braking regardless of the lateral acceleration associated with turning. Given that the hypothetical braking forces used in this study did not exceed 0.4 g, we

believe this is a good assumption, but this assumption may not be so applicable with higher braking forces.

Time to collision (TTC) was calculated by the linear distance to the impact point by the vehicle velocity. While this assumption is reasonable for cases in which the vehicle is travelling straight, this method may underestimate the TTC for vehicles in turning cases, particularly at longer TTCs.

The sensor with the widest FOV was estimated to be able to detect 99% of pedestrians before the crash occurred. This estimate assumed an ideal sensor, i.e. a sensor that had no false positives or false negatives, was equally effective in all weather and lighting conditions, and instantly detected the pedestrian. Studies have shown that different sensors, such as camera, radar, and LiDAR may have different effectiveness based on the distance of the pedestrian, environmental conditions, and pedestrian characteristics such as height or clothing type [64]. AEB systems may also have a computational latency over which the system must identify that the pedestrian is a pedestrian and that they are on a trajectory to interact with the vehicle. These factors were not considered in this study and may reduce the detection ability of a sensor system.

In addition, we assumed the sensor was located on the front center of the vehicle. If the pedestrian became visible immediately prior to the crash the sensor cone may have missed the pedestrian. Alternate sensor placement or additional sensors, such as corner sensors, could affect the ability for the system to detect the pedestrians in these cases, but that was not examined in this study.

This work only considered pedestrian detection. While sensor FOVs above 70° showed minimal additional detection benefit in this study, wider FOV sensors may benefit other vulnerable road users such as bicyclists. Lenard, et al. [65] found that bicyclists required wider FOVs and longer ranges to be detected in the same proportions as pedestrians. US studies have examine earliest detection opportunity for bicyclist and animals [4] [19], but have not to our knowledge conducted analysis of sensor requirements necessary to detect these other road users.

The results presented in this study generally agree with similar analysis conducted using European data. Lenard, et al. [65] conducted a TTC analysis of pedestrian crashes using in-depth data from the UK and found similar distributions of distances at the TTCs leading up to the crashes, but a smaller range of pedestrian angles. Lenard, et al. [65] did not show pedestrian angles above ±45°, whereas this study shows angles as high as ±90° despite both datasets containing cases with travelling straight and turning vehicles.

4.5 Conclusion

Three different approaches were used to examine the earliest detection opportunity in vehicle pedestrian crashes.

The first method used the distance the pedestrian travelled in the road and the estimated pedestrian speed from the PCDS dataset to estimate the time the pedestrian was in the road. This method estimated that most (80%) of pedestrians were in the road for more than one second prior to the collision.

The second method examined vehicle-pedestrian crashes and near-crashes from the SHRP 2 database and estimated the duration the pedestrian was visible through manual inspection of the forward facing video camera. This method found that 90% of pedestrians were visible for at least one second and characterized the types of obstructions that may not be represented on a crash scene diagram. In addition, both the total time and the time in the road were examined and it was found that while total time increased the maximum duration visible for some cases did not have a large effect on cases in which the pedestrian was detectable for less than a second.

The third method simulated crashes from PCDS to examine the effect of a variety of sensor field-of-views and ranges on the ability to detect pedestrians. Sensor range was varied from 20 to 100m and found to have little effect on the detectability of pedestrians prior to the collision, but

increased range did cause the pedestrians to be detected sooner. Sensor range was found to have a larger effect on detectability with a ±90° degree sensor detecting up to 99% of the pedestrians compared to only 58-61% for the ±10° degree sensor. Depending on the sensor, 75-90% of the pedestrians were visible for longer than one second prior to the crash.

Despite the different methodologies, the three methods yielded similar results. All three methods found that the majority of pedestrians were visible for longer than one second prior to the crash. This is encouraging for P-AEB technology as the longer the pedestrian is detectable, the more time the system has to mitigate or avoid the crash.

5 PEDESTRIAN AEB EFFECTIVENESS

5.1 RESEARCH OBJECTIVE

Automatic emergency braking has the potential to mitigate or avoid vehicle-pedestrian crashes. This chapter seeks to estimate how effective AEB could be at mitigating crashes and injuries in the US. AEB systems may have varying sensor configurations, system parameters, and limitations. The aim of this chapter was to estimate the effectiveness of AEB in U.S. crashes for a variety of AEB systems. Two model methods were implemented. The first method estimated effectiveness by using the reconstructed impact speed and information about the scene and driver reaction to determine if the vehicle with a hypothetical P-AEB system could have avoided the crash by coming to a complete stop prior to the impact location (temporal avoidance). The second method improved upon the first by incorporating the pedestrian and vehicle trajectories from crash scene diagrams, sensor system limitations, and by considering a crash could be avoided if the vehicle braked enough to avoid striking the pedestrian, but did not come to a complete stop (spatiotemporal avoidance).

5.2 ESTIMATED BENEFIT OF AUTOMATED EMERGENCY BRAKING SYSTEMS FOR VEHICLE-PEDESTRIAN CRASHES IN THE U.S. [2]

5.2.1 APPROACH

The overall approach in this study consisted of three main components. First, the model of a hypothetical AEB system with pedestrian detection ability, henceforth referred to as pedestrian AEB, was developed to determine the system effect on the crash. Second, a pedestrian injury model was developed to quantify the effect of crash factors on injury and fatality risk for the struck pedestrians. Finally, the pedestrian AEB model and injury risk curve were applied to real-world cases to determine the benefit if all cars and light trucks and vans (LTVs) were equipped with pedestrian AEB.

A diagram depicting the approach is shown in Figure 35.

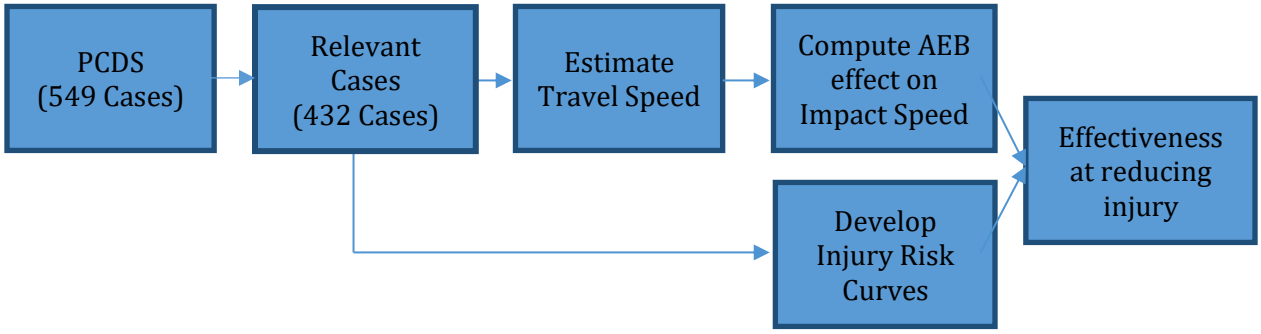

Figure 35. Study approach overview.

5.2.1.1 Data Sources

To conduct this study three U.S. databases were utilized: 1) the Pedestrian Crash Data Study (PCDS), 2) General Estimates System (GES), and 3) Fatality Analysis Reporting System (FARS).

PCDS cases were excluded if impact speeds were missing, pedestrian age was missing, if the time visible could not be determined, or if the pedestrian was a child under age 15. Of the 530 cases in PCDS, 87 were missing impact speeds. We were unable to estimate the time the pedestrian was visible in an additional 11 cases. In 94 cases, the pedestrians were under the age of 15 or were missing pedestrian age. The final sample used in this study consisted of 338 cases which involved 346 pedestrians.

PCDS is a clinical sample, and not inherently nationally representative. To correct for this potential bias, a weighting scheme was developed based on vehicle type and police reported injury severity to match the proportions seen in the General Estimates System (GES) from 2011-2015 (Table 13). Injury severity is recorded in GES using the KABCO scale. KABCO is an injury scale used by law enforcement to rank injury severity in which K (Killed) represents a fatal injury, A is a suspected serious injury, B is a suspected minor injury, C is possible injury, and O in no injury [47]. As an example, our analysis showed that PCDS under sampled low severity crashes, so the weighting

factor for low severity PCDS crashes was greater than 1. Fatal and incapacitating injury crashes were oversampled, so the weighting factor for these crashes tended to be less than 1. FARS was primarily used to find the target population so that PCDS effectiveness could be compared to real world fatality numbers.

Table 13. Table of the weights applied to the PCDS cases to match GES distribution of KABCO scores.

	KABCO Scale		PCDS Cases	PCDS Incidence Rate	GES Incidence Rate	Weighting Factor
Cars	O	No injury	2	0.013636	0.031699	2.868745
	C	Possible Injury	42	0.222727	0.349757	1.507285
	B	Non-incapacitating Injury	49	0.277273	0.347107	1.28217
	A	Incapacitating Injury	69	0.368182	0.200611	0.52624
	K	Killed	21	0.109091	0.044358	0.382324
	U	Injury, Severity Unknown	1	0.009091	0.026469	4.790844
LTVs	O	No injury	1	0.008197	0.035422	3.861007
	C	Possible Injury	27	0.213115	0.376073	1.51822
	B	Non-incapacitating Injury	33	0.311475	0.291488	0.962792
	A	Incapacitating Injury	38	0.319672	0.196567	0.563837
	K	Killed	15	0.131148	0.071357	0.51853
	U	Injury, Severity Unknown	2	0.016393	0.029093	1.585585

5.2.1.2 AEB model with pedestrian detection ability

The pedestrian AEB system was modeled to function by 1) detecting the pedestrian and 2) applying emergency braking. The system effectiveness depends primarily on the time the pedestrian was visible, vehicle travel speed, road surface conditions, system mechanical latency, and the time-to-collision (TTC) threshold at which the system initiates emergency braking. The time the pedestrian was visible, travel speed, and road surface conditions were calculated from PCDS cases.

The AEB system with pedestrian detection was modeled with a range of mechanical latencies (0 – 0.3 seconds) and braking TTC thresholds (0.5 – 1.5 seconds). Mechanical latency was defined as

the time required for the system to prepare the vehicle for braking. It was assumed that the system instantaneously identified the object as a pedestrian and determined the pedestrian was on a collision course with the vehicle. This range of latency values was chosen because braking systems can have mechanical delays in the range of about 0.2 seconds [66]. Values above and below 0.2 seconds were chosen to account for non-ideal situations and technological improvements, respectively. As shown in Equation1, TTC was defined as the distance to the pedestrian divided by the vehicle's instantaneous velocity. The TTC threshold range was adapted from typical braking thresholds reported by Rosén [67].

$$TTC = \frac{distance\ to\ pedestrian}{vehicle\ velocity} \tag{1}$$

The modeled pedestrian AEB system calculated time the pedestrian was visible (hereafter referred to as detection time) by taking into account walking speeds and obstructions. Detection time was defined as the distance the pedestrian traveled unobstructed in the road divided by the pedestrian's estimated walking speed (Equation2). Distance traveled was calculated by multiplying the number of unobstructed lanes the pedestrian crossed by an estimated lane width of 3m. The 3m width is on the shorter range of U.S. lane widths [68], but this value was conservatively chosen as a shorter lane width would result in lower detection times. Walking speed was estimated based on pedestrian age. Estimated walking speed ranged from 1.15 – 1.45 m/s [60].

$$Detection\ Time = \frac{Distance\ Traveled}{Walking\ Speed} \tag{2}$$

The pedestrian AEB system braking peak magnitude was assumed to reach 0.8g in dry road conditions, 0.4g in wet road conditions, and 0.3g in icy road conditions [69]. It was assumed that AEB would increase braking deceleration at a jerk of -30m/s^3 [23]. There were three possible braking configurations: 1) if the pedestrian was detectable for longer than the latency and threshold

combined, the system started braking at a time-to-collision (TTC) value equivalent to the TTC threshold 2) if the pedestrian was detectable for longer than the threshold but not longer than the latency and threshold combined, the system started braking once the TTC threshold was reached and latency period had elapsed 3) if the pedestrian was detectable for less than the TTC threshold, the system started braking once the latency period had elapsed (i.e. after the system had identified the pedestrian). These configurations are depicted in Figure 36.

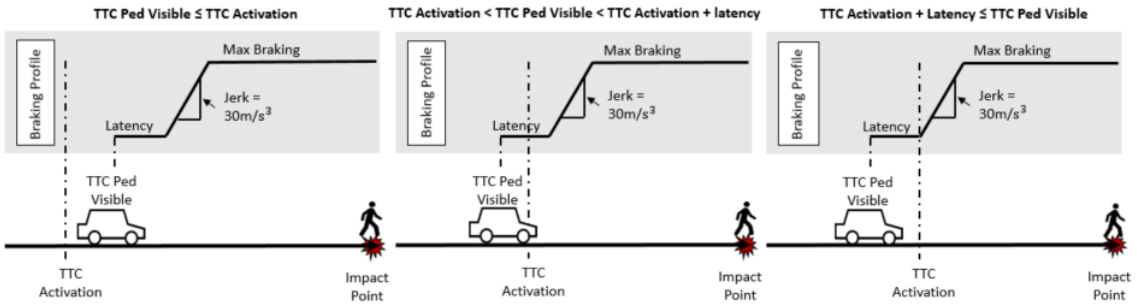

Figure 36. Potential AEB braking profile cases.

Travel speed of the vehicle was estimated by assuming two human braking patterns [61]. The method described is based on work done in estimating TTC of braking [70]. The first pattern modeled a driver who braked late, but with a hard magnitude. The late and hard braking driver braked at 0.4 seconds TTC and reached a deceleration of 0.4g. The second pattern modeled a driver who braked early, but with a weak magnitude. The early and weak braking driver braked at a TTC of 2 seconds and reached a deceleration of 0.2g. The parameters of the models, shown in Figure 37, were chosen based on previous studies in human braking application [70]. Both driver braking patterns assumed a jerk of -10.7 m/s^3 [23]. These two patterns are intended to model the range of typical driver braking and thereby form boundaries between which most drivers would fall.

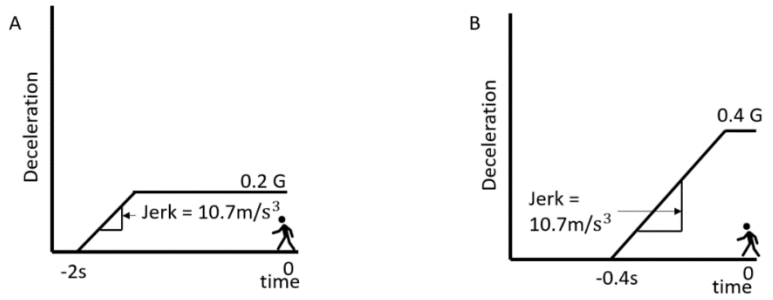

Figure 37. Deceleration profiles for (A) early/weak braking driver and (B) late/hard braking driver with ramp-up braking.

Using Equation3, travel speeds were estimated given impact speeds and whether or not there was evidence of driver braking from the PCDS database. The variables v_{travel} and v_{impact} are the calculated travel speed and impact speed in m/s, a is the maximum acceleration in m/s^2, J is the jerk or deceleration rate in m/s^3, and TTC is the time to collision in seconds.

$$v_{travel} = TTCa + \frac{\sqrt{3}}{3J}\sqrt{3J^2\left(TTC^2a^2 + v_{impact}^2\right) - a^3(3JTTC + a)} - \frac{1}{2J}a^2 \qquad (3)$$

If the case had no evidence of braking, it was assumed that the travel speed equaled the impact speed. In approximately 46% (173/416) of the cases, investigators reported no evidence of braking. As shown in Figure 38, the impact speeds for braking and non-braking drivers are similar with the braking drivers having slightly lower impact speeds than the non-braking drivers.

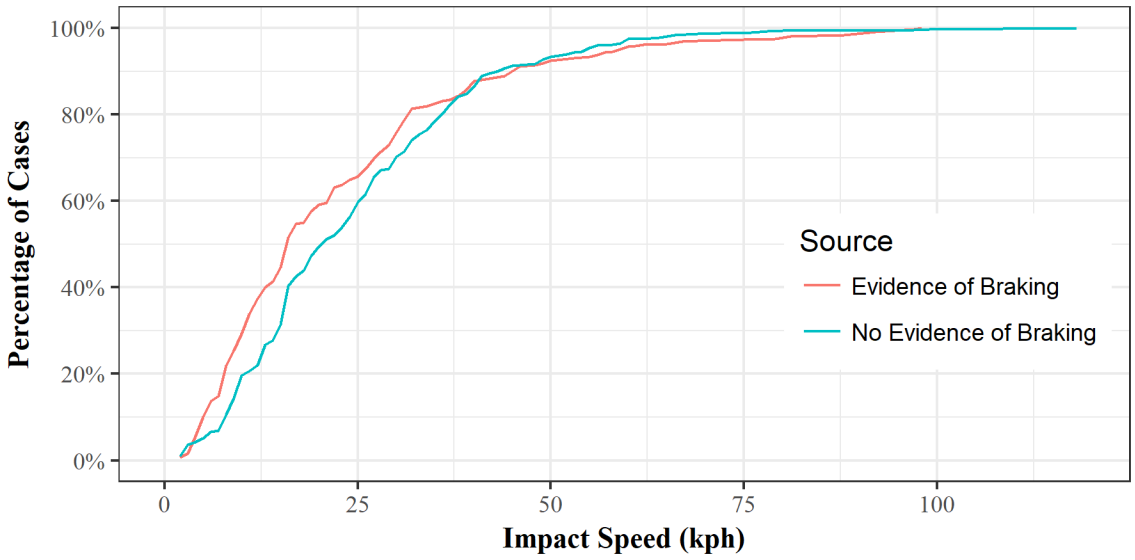

Figure 38. Cumulative distribution plot of impact speeds for braking and non-braking drivers in the AEB-relevant cases.

5.2.1.3 Pedestrian Injury Model

The pedestrian injury model was developed using the Maximum Abbreviated Injury Scale (MAIS) coding from PCDS (PCDS injury coding used AIS-90). PCDS was used for this assessment because GES and FARS do not report injury severity using AIS. AIS ranges from 1-6, AIS = 1 indicating minor injury and AIS = 6 indicating maximal injury. For this study, an MAIS score of 3 or higher, including fatalities, (MAIS3+F) injury curve and a fatal injury curve were developed for pedestrians struck by cars and LTVs separately. This approach was followed because injuries sustained from being struck by a car and a LTV are expected to be different due to different striking geometries and heights [71].

A logistic model was fit to the weighted PCDS data using impact speed and age as co-variables. The glm (generalized linear model) function in the R computing programming language was used to fit the data to the equations 4 and 5, shown below [72]. In the equations below *v* is the impact speed in kilometers/hour and *a, b,* and *c* are coefficients calculated from the logistic model. P is the probability of a fatality or injury. The model coefficients were calculated separately for cars and LTVs and are shown in Table 1.

$$P_{fatal}(v, age) = \frac{1}{1+\exp(-a_{fatal}-b_{fatal}*v-c_{fatal}*age)} \quad (4)$$

$$P_{injury}(v, age) = \frac{1}{1+\exp(-a_{injury}-b_{injury}*v-c_{injury}*age)} \quad (5)$$

Table 14. Pedestrian injury model coefficients

Vehicle Type	Severity	*a*	*b*	*c*
Car	Fatal	-8.119	0.0968	0.0364
LTV	Fatal	-7.264	0.0752	0.0527
Car	Injury (MAIS3+F)	-4.897	0.0940	0.0284
LTV	Injury (MAIS3+F)	-4.036	0.0851	0.0223

Confidence intervals were computed based on methods outlined in Kutner et al. (2004) and used in Rosén and Sander [73]. This method defines the 95% confidence interval as shown in equation 6. X is a 3x1 column vector made up of ones, *v* is the impact speed, and *age* is the age of the pedestrian. S^2 is the estimated approximate variance-covariance matrix which is a 3x3 matrix. The coefficients, *a*, *b, and c* are the maximum likelihood estimates that were previously determined. The matrices were multiplied to give equation 7 where the subscript of S^2 corresponds to the values within the S^2 matrix.

$$Confidence\ Interval = \frac{1}{1 + \exp(-a - bv - c\ age \pm 1.96(X^T S^2 X)^{\frac{1}{2}}} \tag{6}$$

$$Confidence\ Interval = \frac{1}{1 + \exp(-a - bv - c\ age \pm 1.96(S_1^2 + (S_2^2 + S_4^2) * v + (S_3^2 + S_7^2) * age + (S_6^2 + S_8^2) * v * age + S_5^2 * v^2 + S_9^2 * age^2)^{\frac{1}{2}})} \tag{7}$$

Figure 39 and Figure 40 show the fatality and injury risk curves compared to Rosén, et al. [10]. Rosén's curves were developed using data from GIDAS. The curves developed using PCDS were shifted to the left of the Rosén curves which indicates a larger risk of injury or fatality at the same impact speed. Surprisingly, the car and LTV curves were not significantly different from each other, based on the overlap between the confidence intervals. This may be due to small sample sizes or differences in injuries between car and LTV struck pedestrians that are not evident when using MAIS. A injury specific analysis may show greater differences between cars and LTVs that are not evident in these curves.

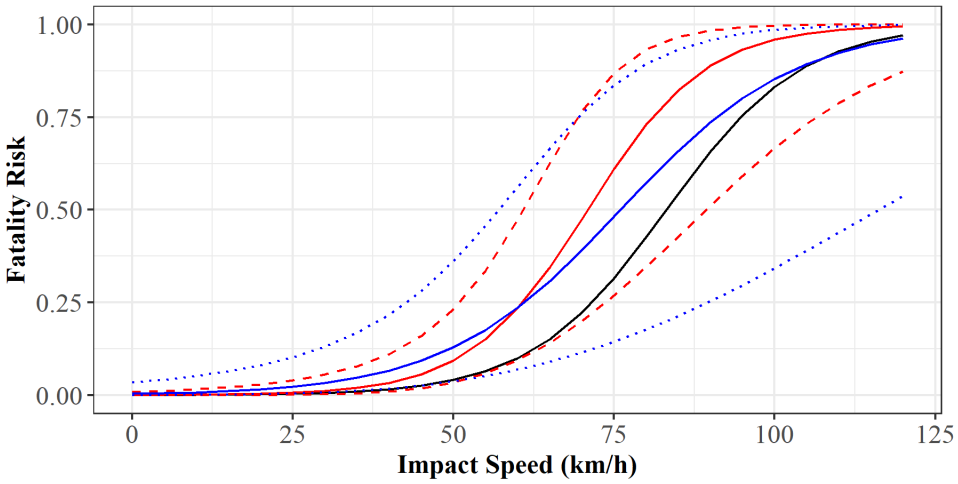

Figure 39. Fatality risk curve for cars (red) and LTVs (blue) compared to Rosén, et al. [10](black). The fatality risks are shown in relation to impact speed assuming a pedestrian age of 30. The dotted and dashed lines correspond to a 95% confidence interval.

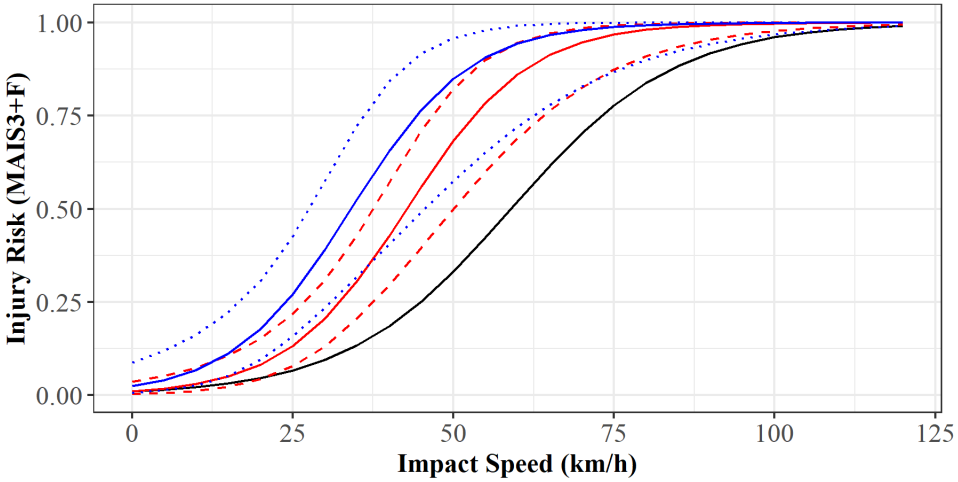

Figure 40. MAIS3+F injury risk curve for cars (red) and LTVs (blue) compared to Rosén, et al. [10](black). The injury risks are shown in relation to impact speed assuming a pedestrian age of 30. The dotted and dashed lines correspond to a 95% confidence interval.

5.2.1.4 AEB Benefits Estimation

The injury risk calculation for pedestrian AEB-equipped vehicles utilized the impact speeds calculated from the AEB model. The injury risk calculation for vehicles without AEB utilized the impact speed reported in PCDS. The fatality and MAIS3+F risks were calculated using equations 4

and 5 in which *fatal risk* and *MAIS3+F risk* were the proportions calculated from the injury models and *wt* is the case weight. If impact speed was zero, meaning the crash was avoided, then the fatal risk and MAIS3+F risk were set to zero.

$$Fatal\ Risk\ (\%) = \frac{\sum fatal\ risk * wt}{\sum wt} \times 100 \quad (6)$$

$$MAIS3^{+}F\ Risk\ (\%) = \frac{\sum MAIS3^{+}F\ risk * wt}{\sum wt} \times 100 \quad (7)$$

As shown in equations 6 and 7, the percent change in fatality and MAIS3+F injury risk was calculated by first summing the weighted injury risk across all cases if the vehicle had a pedestrian AEB system. This value was then compared to the injury risk if the vehicle did not have a pedestrian AEB system. As none of the vehicles in this study were equipped with pedestrian AEB, it was assumed that the actual event was a good estimation of a vehicle without pedestrian AEB. *Fatal risk no AEB* and *MAIS3+F risk with no AEB* were the proportions calculated from the injury models without AEB, and *wt* is the case weight.

$$\frac{Change\ in}{fatal\ risk\ (\%)} = \frac{(\sum fatal\ risk\ no\ AEB * wt) - (\sum fatal\ risk * wt)}{(\sum fatal\ risk\ no\ AEB * wt)} \times 100 \quad (8)$$

$$\frac{Change\ in}{MAIS3^{+}F\ risk\ (\%)} = \frac{(\sum MAIS3^{+}F\ \ risk\ no\ AEB * wt) - (\sum MAIS3^{+}F\ \ risk * wt)}{(\sum MAIS3^{+}F\ \ risk\ no\ AEB * wt)} \times 100 \quad (9)$$

5.2.2 RESULTS

Travel speed was estimated from the impact speed. The cumulative distribution plots show that the late/hard assumption resulted in lower estimated travel speeds than the early/weak assumption (Figure 41).

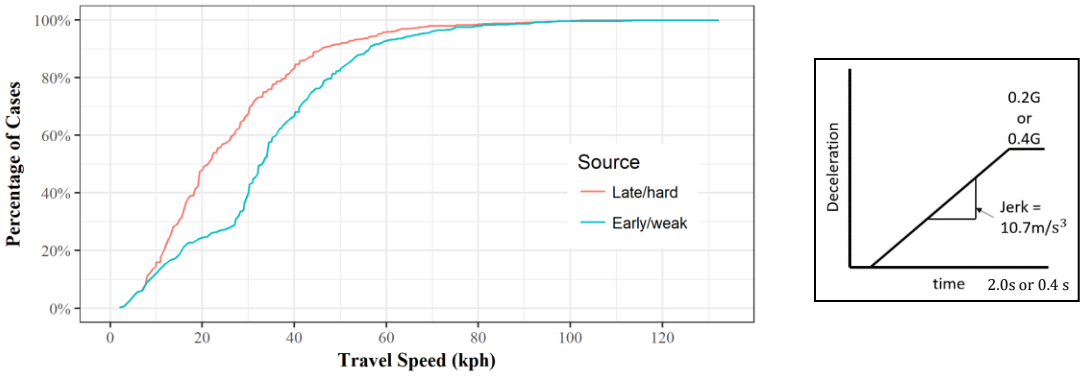

Figure 41. Cumulative distribution of calculated travel speeds for all AEB-relevant cases (left) and depiction of deceleration profiles (right).

As expected, the modeled pedestrian AEB system was more effective at avoiding crashes for system designs with a higher TTC threshold and a lower latency (Figure 42). At low TTC thresholds (below 0.75 seconds), the highest effectiveness was observed for early weak braking drivers, but at larger TTC thresholds the late hard braking drivers actually had a higher effectiveness (Figure 42). The early and weak braking driver likely showed lower effectiveness due to the method used to calculate travel speed. Early weak braking drivers' travel speeds were higher than their corresponding late hard braking drivers' travel speed.

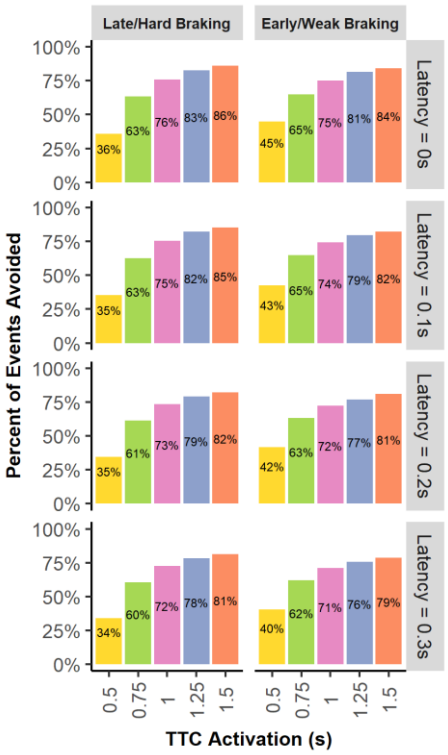

Figure 42. AEB system effectiveness at a range of TTC values and latency values for both the Late/Hard braking driver scenario and the Early/Weak braking driver scenario.

For the cases in which the crash was not avoided, Figure 43 generally showed an increase in average reduction of velocity with increased TTC and decreased latency. Early weak braking drivers resulted in larger average change in velocity compared to late hard braking drivers. This confirms that the reason early late braking drivers had lower effectiveness was due to the initial travel speed; although early weak braking drivers had larger changes in velocity, they were not able to completely avoid the crash. The average change in velocity for late/hard braking drivers and early/weak braking drivers ranged from 10 – 25 km/h and 18 – 30km/h, respectively.

Early and weak braking drivers showed slight decreases in change in velocity at a TTC value of 1.5 seconds (Figure 43). As TTC increases, more and more cases are estimated to be avoided, finally leaving only the hard to avoid cases in which AEB with pedestrian detection ability can do little to

avoid. The remaining cases have lower estimated earliest pedestrian detection opportunities and often have adverse road surface conditions (e.g. wet or icy roads) that reduce the ability of the vehicle to brake.

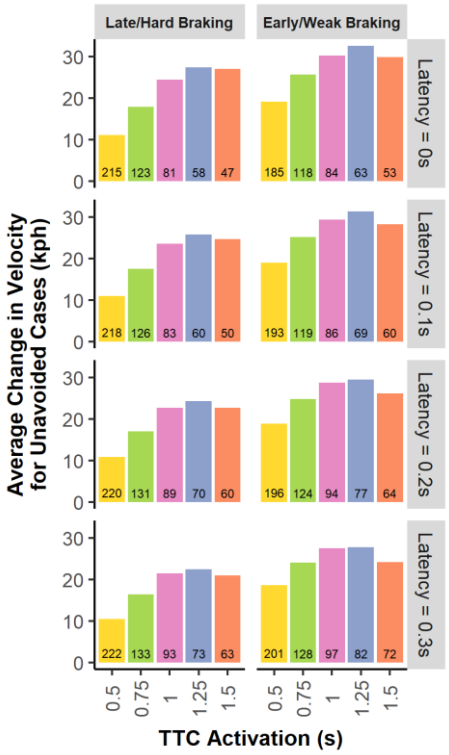

Figure 43. AEB system average change in velocity for unavoided cases for a range of TTC and latency values for both the Late/Hard braking driver scenario and the Early/Weak braking driver scenario. The number on the bar corresponds to the number of unavoided cases.

Figure 44 further shows that increasing TTC and decreasing latency, in turn increases system effectiveness at reducing pedestrian fatalities and MAIS3+F injuries. The change in fatality and MAIS3+F risk (effectiveness) was very similar. Fatality and MAIS3+F risk reduction differed by only 1% across most TTC and latency values. The most beneficial system (TTC = 1.5s and latency = 0s) was estimated to decrease fatality risk between 84 and 87% and injury risk (Maximum AIS score 3 and greater) between 83 and 87% for the target population.

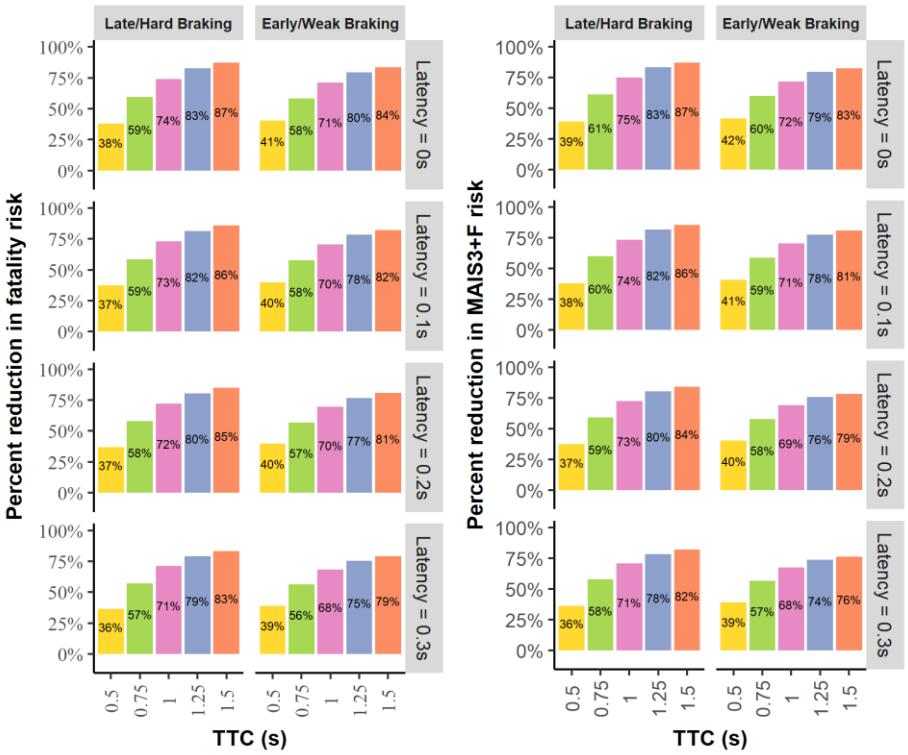

Figure 44. Percent change in fatality risk (left) and MAIS3+F injury risk (right) for a range of TTC and latency values for both the Late/Hard braking driver scenario and the Early/Weak braking driver scenario.

5.2.3 DISCUSSION

This study was limited by the in-depth pedestrian crash data available in the U.S. While PCDS was a valuable resource, the sample size was relatively small and is not nationally representative. Additionally, PCDS was collected from 1994-1998 on then late-model vehicles which may not be representative of vehicles in the current U.S. fleet. However, we compared our fatality risk curves with more recent pedestrian injury risk curves generated with the German In-Depth Accident Study (GIDAS) [10, 73]. The curves developed with PCDS tended to be shifted to the left, meaning higher injury risk at lower speeds, but this was only statistically significant for MAIS3+F injury at speeds below 73km/h. Despite these limitations, PCDS is the most recent in-depth vehicle-pedestrian

database and includes important injury information and crash reconstructions not available in GES and FARS.

This study was also limited by the lack of information concerning travel speed. The driver braking patterns used in this study were intended to act as upper and lower bounds on normal driving behavior. We expect that driver actions will fall somewhere between the early/weak braking driver and the late/hard braking driver.

The predicted fatality and MAIS3+F injury estimations used in this study did not include children due to differences in stature that could affect pedestrian vehicle interaction during collisions. In the future we would like to extend our model to include children or develop a child specific curve.

There are several important limitations to the AEB model. (1) We assumed an idealized system in which there was no sensor degradation, no mechanical failures, and no computational issues, (2) AEB algorithms are highly proprietary, therefore we analyzed a hypothetical AEB algorithm based on characterization gathered from the literature and non-confidential discussions with industry, and (3) we assumed braking performance based on literature. Consequently, the results of this investigation only represent the maximum potential of the model system which was analyzed.

While not all crashes could be avoided, AEB with pedestrian detection ability could substantially mitigate injury risk to pedestrians in the target population. The target population accounts for about 68.8% of pedestrian fatalities (FARS 2011-2015) and 56.2% of pedestrians struck (GES 2011-2015), meaning that about 31-44% of the pedestrians struck or fatality injured by vehicles annually would not be affected by AEB with pedestrian detection ability. The crashes that would be affected but could not be avoided tended to have short pedestrian detection opportunities and/or

adverse road conditions which would affect the system's ability to effectively avoid or mitigate a collision. Higher benefits were estimated for the AEB system as the TTC of braking lengthened and the latency value shortened.

5.3 Differential Benefit of Sensor System Field-of-View and Range in Pedestrian Automated Emergency Braking Systems[3]

5.3.1 Approach

5.3.1.1 Data Source

This study utilized vehicle-pedestrian crashes from the Pedestrian Crash Data Study (PCDS). The PCDS dataset includes 530 vehicle pedestrian crashes involving 549 pedestrians. For simulation, each case was only simulated once. Cases were excluded if there was not enough information in the crash scene diagram to track the pedestrian's path, resulting in 511 remaining cases. In addition, impact speed was needed to simulate the crashes, therefore, cases were excluded if impact speed was not estimated leaving 432 remaining cases. Cases were excluded if the primary damage was not to the front of the vehicle due to the differing injury mechanisms of a "cornering" crash. The case selection criteria are shown in Table 15.

Table 15. PCDS case exclusion criteria.

Reason Excluded	Number of Cases Remaining
None Excluded	549
Include only one pedestrian per event	530
Cases missing time visible	511
Cases missing impact speed	432
No damage to front of vehicle	357

PCDS selection criteria specified that the point of impact must have been in front of the A-pillar, involving a passenger vehicle in which the only impact was the pedestrian, the vehicle had to

be forward moving, and the pedestrian must have not been lying down or sitting at the time of impact [74]. To match the PCDS selection criteria, the 2011 – 2015 NASS-GES vehicle pedestrian crashes were filtered with the following conditions:

1. Only include frontal crashes (*impact1_im = 1, 11, 12*).
2. Only include passenger vehicles (*bodytyp_im < 50*).
3. Only include crashes in which the most harmful event was the impact with the pedestrian (*m_harm = 8*).
4. Excluded crashes in which the vehicle was moving backwards (*pcrash_im != 13*).

NASS-GES data did not have enough information to determine if the pedestrian was lying down or sitting.

PCDS was known to have oversampled vehicle-pedestrian crashes involving children and higher injury severity crashes. In addition, due to the age of the dataset, the U.S. fleet at the time of the crash was assumed to have a lower proportion of light trucks and vans (LTVs) than the current fleet. Injury mechanisms in LTV vehicle-pedestrian crashes have been shown to differ from those involving cars [13]. To adjust for these known discrepancies, the PCDS dataset was weighted by whether or not the pedestrian was a child (defined at less than 15 years old), the pedestrian was struck by a car or LTV, and by injury severity (defined as police reported injury). Police reported injury was used because this variable was available in both NASS-GES and PCDS. Police reported injury is reported using the KABCO scale in which police rate injury as fatal injury (K), suspected serious injury (A), suspected minor injury (B), possible injury (C), no apparent injury (O), and injured unknown severity (U) [75].

As shown in Table 16, the weighting factors were calculated by dividing the weighted proportion of NASS-GES cases in a given category by the proportion of PCDS cases in the same category. The weighting factors corroborate the expected differences between PCDS and NASS-GES. Cases involving children had lower weighting factors, cases involving cars tended to be weighted lower than their equivalent LTV weights, and higher severity crashes tended to be weighted lower.

Table 16. Calculation of PCDS weighting factor. Weighting factor was color scaled to show the lowest weighting factors (blue) and the highest weighting factors (green).

Age	Vehicle Type	KABCO	PCDS count	GES count	GES weighted	PCDS proportion	GES weighted proportion	Weight Factor
Adult (≥15)	Car	O	2	30	4190	0.006	0.017	2.974
		C	38	258	46558	0.106	0.185	1.739
		B	45	2511	45512	0.126	0.181	1.435
		A	64	1299	26798	0.179	0.107	0.594
		K	22	238	5686	0.062	0.023	0.367
		U	11	28	3979	0.031	0.016	0.513
	LTV	O	1	19	2745	0.003	0.011	3.896
		C	24	154	29293	0.067	0.116	1.732
		B	29	1485	27097	0.081	0.108	1.326
		A	33	791	16835	0.092	0.067	0.724
		K	14	244	5246	0.039	0.021	0.532
		U	5	17	2177	0.014	0.009	0.618
Child (<15)	Car	O	1	8	334	0.003	0.001	0.474
		C	12	51	7203	0.034	0.029	0.852
		B	18	526	9310	0.050	0.037	0.734
		A	16	181	3216	0.045	0.013	0.285
		K	2	13	1011	0.006	0.004	0.718
		U	3	5	508	0.008	0.002	0.240
	LTV	O	1	6	654	0.003	0.003	0.929
		C	3	23	3945	0.008	0.016	1.866
		B	8	325	5785	0.022	0.023	1.026
		A	5	127	2968	0.014	0.012	0.842
		K	NA	13	462	NA	0.002	NA
		U	NA	2	19	NA	0.000	NA

Chi-square analysis of the unweighted data shows that the PCDS distribution of pedestrian age was significantly different from NASS-GES distributions (Table 17). Weighting the PCDS data did not completely eliminate the difference between the PCDS distributions and with NASS-GES distributions (Table 18). Although the weight factors were calculated partially based on pedestrian age, the weighted distribution was still significantly different than the NASS-GES distribution, likely because the weighting factor was based on “child” or “not child” rather than the four age categories used in the chi-square analysis.

Table 17. Chi-square goodness of fit analysis of pedestrian characteristics in PCDS distribution compared to GES distribution before weighting.

	PCDS count	PCDS proportion	GES count	GES weighted	GES weighted proportion	P-value
Pedestrian Age						
Child (0 - 14)	69	0.193	1280	35416	0.141	0.001853*
Youth (15 - 24)	51	0.143	1768	52878	0.210	
Adult (25 - 64)	186	0.521	4145	126435	0.503	
Senior (65+)	51	0.143	1161	36805	0.146	
Pedestrian Sex						
Female	173	0.485	3618	110837	0.441	0.094413
Male	184	0.515	4736	140696	0.559	

*P-values ≤ 0.05 indicate the sample (PCDS) was significantly different from the population (GES).

Table 18. Chi-square goodness of fit analysis of pedestrian characteristics in PCDS distribution compared to GES distribution after weighting.

	PCDS weighted count	PCDS weighted proportion	GES count	GES weighted	GES weighted proportion	P-value
Pedestrian Age						
Child (0 - 14)	50	0.139	1280	35416	0.141	0.016006*
Youth (15 - 24)	54	0.152	1768	52878	0.210	
Adult (25 - 64)	206	0.578	4145	126435	0.503	
Senior (65+)	47	0.132	1161	36805	0.146	
Pedestrian Sex						
Female	175	0.491	3618	110837	0.441	0.057154
Male	181	0.509	4736	140696	0.559	

*P-values ≤ 0.05 indicate the sample (PCDS) was significantly different from the population (GES).

Chi-square analysis of the unweighted data shows that PCDS distributions of environmental characteristics were all significantly different from NASS-GES distributions (Table 19). Weighting the PCDS data resulted in a loss of significance when comparing the distribution of weather conditions, indicating that the PCDS sample was not significantly different from the NASS-GES distribution. Weighting PCDS did not affect the significance of the other PCDS distributions when compared with NASS-GES distributions (Table 20). Weather conditions are important for effectiveness estimations of P-AEB performance because adverse weather could affect the sensors ability to detect the

pedestrian and reduces the coefficient of friction thereby reducing the maximum braking capability of the vehicle. While lighting conditions are important for camera-based systems, they have less of an effect on radar or LiDAR.

Table 19. Chi-square goodness of fit analysis of environmental characteristics in PCDS distribution compared to GES distribution before weighting.

	PCDS count	PCDS proportion	GES count	GES weighted	GES weighted proportion	P-value
Speed Limit						
5 - 25 mph	37	0.104	1862	57681	0.339	<0.000001*
30 - 45 mph	293	0.821	3935	96746	0.568	
50 - 65 mph	17	0.048	247	7919	0.046	
> 65 mph	2	0.006	16	688	0.004	
No Limit	8	0.022	241	7289	0.043	
Weather Conditions						
Clear	293	0.821	6961	207259	0.862	0.024294*
Rain	58	0.162	854	27407	0.114	
Snow/Sleet	4	0.011	93	4732	0.020	
Fog/Other	2	0.006	39	1175	0.005	
Lighting Conditions						
Daylight	227	0.636	4230	132682	0.552	0.000009*
Dark	105	0.294	3409	98039	0.408	
Dawn/Dusk	25	0.070	306	9826	0.041	
Relation to Junction						
Non-Junction	134	0.375	3052	84803	0.353	<0.000001*
Intersection/ Intersection-Related	188	0.527	4468	144313	0.600	
Interchange	10	0.028	64	994	0.004	
Other/Unknown	25	0.070	363	10463	0.043	

*P-values ≤ 0.05 indicate the sample (PCDS) was significantly different from the population (GES).

Table 20. Chi-square goodness of fit analysis of environmental characteristics in PCDS distribution compared to GES distribution after weighting.

	PCDS weighted count	PCDS weighted proportion	GES count	GES weighted	GES weighted proportion	P-value
Speed Limit						
5 - 25 mph	37	0.103	1862	57681	0.339	<0.000001*
30 - 45 mph	298	0.837	3935	96746	0.568	

50 - 65 mph	10	0.027	247	7919	0.046	
> 65 mph	2	0.005	16	688	0.004	
No Limit	10	0.028	241	7289	0.043	
Weather Conditions						
Clear	294	0.826	6961	207259	0.862	0.074581
Rain	56	0.156	854	27407	0.114	
Snow/Sleet	6	0.016	93	4732	0.020	
Fog/Other	1	0.002	39	1175	0.005	
Lighting Conditions						
Daylight	240	0.675	4230	132682	0.552	<0.000001*
Dark	89	0.250	3409	98039	0.408	
Dawn/Dusk	27	0.075	306	9826	0.041	
Relation to Junction						
Non-Junction	118	0.331	3052	84803	0.353	0.000006*
Intersection/ Intersection-Related	206	0.579	4468	144313	0.600	
Interchange	7	0.020	64	994	0.004	
Other/Unknown	25	0.070	363	10463	0.043	

*P-values ≤ 0.05 indicate the sample (PCDS) was significantly different from the population (GES).

Chi-square analysis of the unweighted data shows that PCDS distributions of pre-crash characteristics were all significantly different from NASS-GES distributions (Table 21). Weighting the PCDS data resulted in a loss of significance when comparing pre-event movement, indicating that the PCDS sample was not significantly different from the NASS-GES distribution. Weighting PCDS did not affect the significance of the other PCDS distributions when compared with NASS-GES distributions (Table 22). This could partially be due to the large number of unknowns in the NASS-GES distribution. Pre-event movement is important because as we show in this study system performance is reduced when the vehicle has a curved trajectory. While attempted avoidance maneuver is important for developing the pre-crash vehicle trajectories, the presence of a P-AEB system would change the attempted avoidance maneuvers, particularly the proportion of crashes in which there was no avoidance action.

Table 21. Chi-square goodness of fit analysis of pre-crash characteristics in PCDS distribution compared to GES distribution before weighting.

	PCDS count	PCDS proportion	GES count	GES weighted	GES weighted proportion	P-value
Pre-Event Movement						
Straight	224	0.627	4662	126386	0.525	0.000385*
Turning	103	0.289	2716	94379	0.392	
Accel/Deccel	14	0.039	255	9228	0.038	
Lane Change	9	0.025	103	3477	0.014	
Curve	3	0.008	151	5030	0.021	
Other	4	0.011	60	2073	0.009	
Attempted Avoidance Maneuver						
No Action	140	0.392	2201	75218	0.313	<0.000001*
Braking	163	0.457	703	19128	0.080	
Steering	6	0.017	196	6160	0.026	
Braking + Steering	43	0.120	70	1562	0.006	
Other	1	0.003	54	1805	0.008	
Unknown	4	0.011	4723	136701	0.568	

*P-values ≤ 0.05 indicate the sample (PCDS) was significantly different from the population (GES).

Table 22. Chi-square goodness of fit analysis of pre-crash characteristics in PCDS distribution compared to GES distribution after weighting.

	PCDS weighted count	PCDS weighted proportion	GES count	GES weighted	GES weighted proportion	P-value
Pre-Event Movement						
Straight	196	0.549	4662	126386	0.525	0.155942
Turning	128	0.361	2716	94379	0.392	
Accel/Deccel	17	0.047	255	9228	0.038	
Lane Change	9	0.024	103	3477	0.014	
Curve	3	0.007	151	5030	0.021	
Other	4	0.012	60	2073	0.009	
Attempted Avoidance Maneuver						
No Action	139	0.391	2201	75218	0.313	<0.000001*
Braking	170	0.477	703	19128	0.080	
Steering	7	0.019	196	6160	0.026	
Braking + Steering	38	0.106	70	1562	0.006	
Other	1	0.002	54	1805	0.008	
Unknown	2	0.005	4723	136701	0.568	

*P-values ≤ 0.05 indicate the sample (PCDS) was significantly different from the population (GES).

5.3.1.2 Develop Trajectories from PCDS Data

While PCDS includes crash scene diagrams, this data was not digitized and therefore required manual collection. In AutoCAD, the PDF scene diagrams were scaled and the origin was defined from the front center of the vehicle at the impact location. In order to develop the vehicle and pedestrian trajectories needed for the simulation, the trajectory points were manually collected from the PDF scene diagrams. If the subject trajectory was straight, the trajectory was defined using a linear fit model of the extracted trajectory points. If the subject trajectory was curved, the trajectory was fit using the MATLAB curve fitting tool and a variety of potential models including exponential, power, cotangent models, and cosecant (used for U-turn cases). Generally, the model with the highest R-squared value was chosen. Due to limited available trajectory points in some cases, however, the model with highest R-squared values sometimes did not match the case narrative and/or physical constraints. In these cases the model with the next highest R-squared value was chosen.

Next, the velocity and location of both the pedestrian and vehicle was computed at 0.01 second intervals over the time leading up to the crash through simplifying assumptions of their pre-crash actions. The pedestrian was assumed to travel at a constant velocity that was estimated based on the pedestrian's age and whether or not they were traveling in a group. Pedestrian walking speeds ranged from 1.15 – 1.45 m/s [60]. The vehicle velocity was assumed to be constant if there was no reported evidence of braking prior to the crash. If there was evidence of braking, we assumed two potential driver braking models: 1) an early weak braking driver which braked at a time-to-collision (TTC) of 2 seconds and a deceleration of 0.2 g and 2) a late hard braking driver which braked at a TTC of 0.4 seconds and a deceleration of 0.4 g [2]. We assumed that both the driver braking models were equally likely to occur.

In addition to the trajectory information, we also recorded whether or not the pedestrian was in the road and/or obstructed at each time point. A pedestrian was considered to be obstructed if

there was a parked or moving vehicle in the crash scene diagram which could have blocked them from the sensor view. If an obstruction was not denoted on the crash scene diagram, then it was not considered in this study.

5.3.1.3 P- AEB Model

For the spatiotemporal approach, a computational model was developed to simulate each PCDS case with and without P-AEB. The P-AEB model was coded using the R programming language. The model was designed to iteratively step through time from before AEB system activation to impact. At each time step, the position, the velocity, and the acceleration of the vehicle and pedestrian were calculated. If we assumed that the driver braked in the trajectory calculation, then we also assumed the driver braked in the simulation. The model required the vehicle and pedestrian trajectories in addition to the case environmental characteristics and vehicle parameters.

The proposed AEB system activated when four conditions were met: 1) the pedestrian was within the road edges and not obstructed, 2) the pedestrian was within the FOV and range of the sensor system (detectable), 3) the pedestrian was detectable for the length of latency period, and 4) the time-to-collision (TTC) threshold of activation was reached. An overview of the AEB model is depicted in Figure 45.

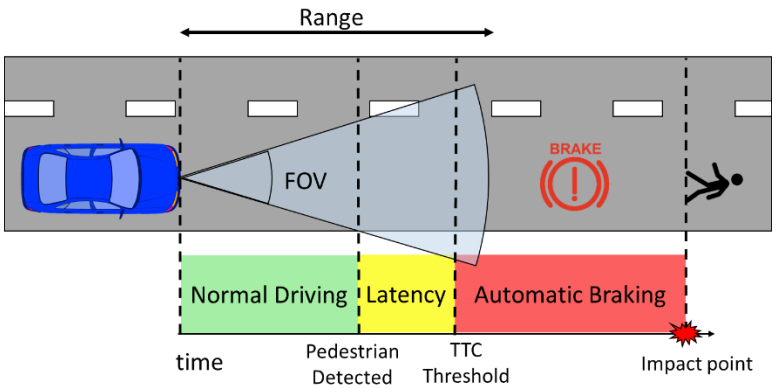

Figure 45. Schematic of AEB model.

A variety of sensor FOV and ranges were considered for analysis. According to the European Telecommunications Standards Institute, commercially available radar systems should be able to detect pedestrians at over 90 m under ideal conditions [62]. That range, however, may not be achievable under adverse conditions [64, 76]. Tang, et al. [77] examined pedestrian detection by vehicle LiDAR under different weather conditions and pedestrian distances and found that LiDAR was able to detect pedestrians at 30 m and capable of detecting pedestrians at up to 60 m. The sensor configurations examined in this study are shown in Table 23. The systems with FOVs of ±10° and ±30°, sensor half angle of 10° and 30° respectively, were intended to model a radar sensor system. The systems with FOVs of ±60° and ±90°, sensor half angle of 60° and 90° respectively, were intended to model a LiDAR or an advanced sensor system. It was assumed that the sensor was located at the front and center of the vehicle. While this is a potential location for radar and LiDAR, a camera based system would likely be located elsewhere on the vehicle.

Table 23. Modeled sensor configurations.

Configuration	Sensor Half Angle	Sensor Range
Radar	10° 30°	25 m
		50 m
		100 m
LiDAR	60° 90°	25 m
		50 m
		100 m

The latency period was defined as the time needed for the vehicle to prepare the brakes for the evasive braking maneuver. It was assumed the system instantaneously identified the object as a pedestrian and determined the pedestrian was on a collision course with the vehicle. For this study we assumed an ideal system that immediately brakes to avoid the collision, i.e. a latency of 0 seconds.

The time-to-collision (TTC) was calculated at each time step by dividing the linear distance to the impact point by the vehicle velocity. The system only activated once the TTC threshold was reached. TTC thresholds are highly proprietary and therefore unknown by the authors. A braking TTC of 1.5 seconds was chosen because this value had the highest crash/injury reduction estimation in a previous study [2].

Once all four activation conditions were met: 1) the pedestrian was visible, 2) the pedestrian was detectable, 3) the latency period elapsed, and 4) the time-to-collision (TTC) threshold of activation was reached, the AEB system was activated. The AEB system was assumed to brake at a maximum of 0.8g (dry), 0.4g (wet), or 0.3g (icy) with a jerk of -30 m/s^3 [69].

The iteration continued until the vehicle impacted the pedestrian, the vehicle came to a stop or the vehicle and pedestrian missed each other. An impact was said to have occurred if at any time in the simulation the pedestrian came into contact with any part of the vehicle. As shown in Figure 46, an impact was detected by computing the total area of the four triangles made up of the vehicle corner locations (two points) and the closest pedestrian location (one point). If the total triangle area was greater than the vehicle area, then the pedestrian was not in contact with the vehicle. If the sum of the areas was equivalent to the area of the vehicle, then an impact was assumed to have occurred. The pedestrian was assumed to have a radius of 0.3 m, while the car size was assumed to be the track width and 1.2 times the wheelbase length. If the track width was unknown, it was assumed to be 1.5 meters. If the wheelbase was unknown, it was assumed to be 3 meters.

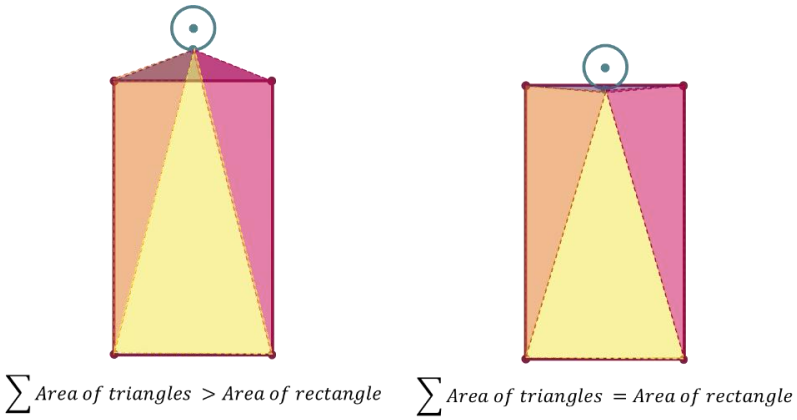

Figure 46. Impact detection method schematic.

Vehicle speed and deceleration were calculated using the kinematic equations of motion. The vehicle was assumed to follow the estimated trajectory. The vehicle rear location was calculated using a simple kinematic bicycle model shown in equation (1) – (3) where X and Y indicate the X and Y location of the center of the vehicle rear, v represents the vehicle speed in m/s, Δt represents the time step, θ represents the heading, $steering\ \angle$ represents the steering angle, and L represents the vehicle length which was calculated by multiplying the vehicle wheelbase by 1.2.

$$\Delta X_{rear} = v\Delta t \cos\theta \tag{1}$$

$$\Delta Y_{rear} = v\Delta t \sin\theta \tag{2}$$

$$\Delta\theta_{rear} = \frac{v\Delta t \tan(steering\ \angle)}{L} \tag{3}$$

5.3.1.4 Pedestrian Injury Risk Curves

The injury risk models used with the simplified P-AEB model were developed using only pedestrians that were 15 years or and older. Children are different from adults and therefore adult

injury risk curves should not be directly applied to cases involving child pedestrians. For the spatiotemporal P-AEB model three injury risk models representing different injury severities were developed using the 357 relevant cases from PCDS. Fatal cases were identified using the treatment variable. Cases with serious injuries were identified as pedestrians that had a maximum abbreviated injury score (MAIS) of 3 or higher or the cases resulted in a fatality (MAIS3+F). Cases with moderate injuries were identified as pedestrians that had a maximum abbreviated injury score (MAIS) of 2 or higher or the cases resulted in a fatality (MAIS2+F).

The data was fitted with a logistic regression model using the 'glm' function in R. Initially, pedestrian age was included as a continuous variable, but the relationship between age and injury tolerance was non-linear. Therefore, the pedestrians were categorized into three age groups: children (1-14 years old), adults (15-64 years old), and seniors (65+). As shown in Table 24, impact speed and pedestrians in the senior age group were significant in all three injury models. For the fatal injury model, pedestrians in the child age group and pedestrian weight were also significant. Weight was found to have no interaction effects with any other covariates.

Table 24. Injury model significant parameters.

Variables	Fatal Injury	MAIS3+F Injury	MAIS2+F Injury
Impact Speed (km/h)	✓	✓	✓
Pedestrian Age - Senior	✓	*	✓
Pedestrian Age - Child	*	-	-
Vehicle Type	-	-	-
Pedestrian Sex	-	-	-
Pedestrian Height	-	-	-
Pedestrian Weight	*	-	-

Significance: '✓' = P-Val < 0.001, '*' = P-Val < 0.05, '-' = P-Val > 0.1

5.3.1.5 Model Benefits Estimation

Crash avoidance potential was calculated dividing the number of crashes that did not occur over the total number of crashes that were simulated for each sensor design. The results were also split up depending on vehicle trajectory and the path of the pedestrian. A turning vehicle trajectory indicates the trajectory path of the vehicle was curved and therefore could include a vehicle traveling through a curve and/or a vehicle making a turn. A summary of the included cases, categorized by vehicle trajectory and pedestrian path, is presented in Table 25.

Table 25. Break down of occurrence of crash types included in this study by vehicle trajectory and pedestrian path.

		Pedestrian Path			
Vehicle Trajectory	Type	Straight	Curved	Stationary	Total
	Straight	230	22	2	254
	Turning	95	7	1	103
	Total	325	29	3	357

To calculate the injury reduction potential, the injury risk curves were used to estimate the risk of fatal, MAIS3+F and MAIS2+F injury for each pedestrian given their new impact speeds. If there was no impact, it was assumed that the risk of injury was 0. The injury risks for each case were then summed to get the risk of injury for each sensor design and compared to the risk of injury in the original crashes with no P-AEB systems.

5.3.2 RESULTS

5.3.2.1 Crash Avoidance Results

As shown in Figure 47, systems with a larger FOV and a longer range were estimated to be able to avoid a larger percentage of crashes. Although longer range sensor configurations performed slightly better when compared to a sensor with a 25 m range, there was no significant difference between a 50 m and 100 m range sensor. Sensors with a 50m and 100m range only performed an estimated 1-2% better than a sensor with a 25 m range. System FOV had a larger effect on system avoidance capabilities with wider sensor FOVs able to avoid a larger percentage of crashes. A system

with a 10° half FOV was estimated to avoid 46-47% of crashes while a sensor with a 90° half FOV was estimated to avoid 91-92% of crashes. The increased benefit from wider FOV appears to only marginally increase past a half FOV of 60° as there was only a 1-3 percentage point increase in avoidance between the 60° and 90° half FOV sensor systems.

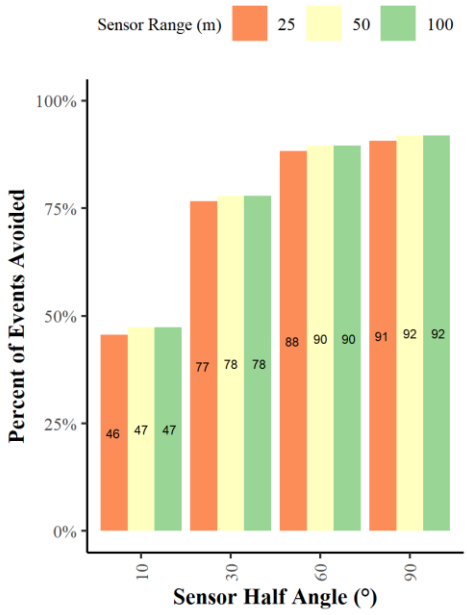

Figure 47. Percent of crashes avoided for a set of sensor half angles and ranges.

A concern with narrower sensor FOV angles is that a vehicle with forward facing sensors, may not see pedestrians when traveling on a curve or executing a turn. To examine this potential scenario we divided the cases into those in which the vehicle was traveling straight (n = 232, weighted) and compared them to those in which the vehicle had a curved trajectory (n = 123, weighted). As shown in Figure 48, the modeled P-AEB systems were able to avoid a greater percentage of the cases in which the vehicle was traveling straight for sensor half FOVs of 30° and narrower. When the vehicle was traveling straight the system with a sensor half FOV of 10° and 30° avoided an estimated 10 to 13 and 6 to 8 percentage points more crashes than the cases in which the vehicle was turning, respectively. At sensor half FOV of 60° and wider, the hypothetical AEB systems were estimated to

have higher effectiveness for cases in which the vehicle was turning than cases in which the vehicle was traveling straight. A sensor with a half FOV of 60° was estimated to avoid 4 to 6 percentage points more turning crashes than straight crashes, this difference increased to 9 to 11 percentage points for a sensor half FOV of 90°. Interestingly, range had no noticeable effect on the estimated avoidance capability of the curved crash cases.

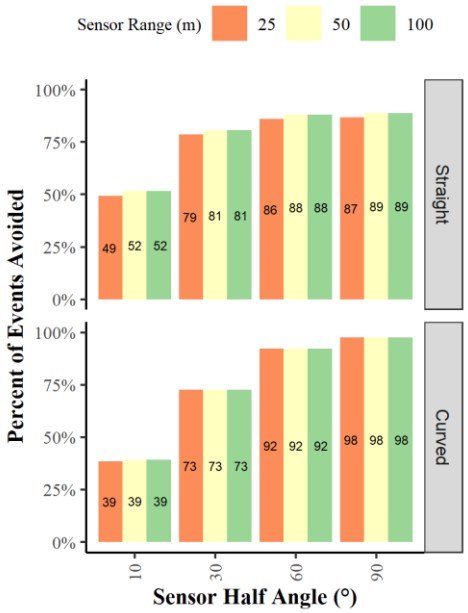

Figure 48. Percent of crashes avoided for a set of sensor half angles and ranges by whether the vehicle had a straight or curved trajectory.

Although sensor range had little effect on crash avoidance, it did have a small effect on impact speed of the crashes that were not avoided. As shown in Figure 49, the average impact speed of the unavoided crashes decreased as sensor range increased. At a sensor half angle of 90° the 100 m sensor's average impact velocity was 7.4 m/s (16.5 mph, 26.6 km/h) compared to an average impact velocity of 8.1 m/s (18 mph, 29 km/h) with a sensor range of 25 m. The average impact speed was shown to increase with FOV, likely because each bar in Figure 48 corresponds to a subset of cases

that were unavoided and the subset that makes up the larger FOV system are harder to avoid either because of adverse road conditions, higher initial speeds, and/or obstructions.

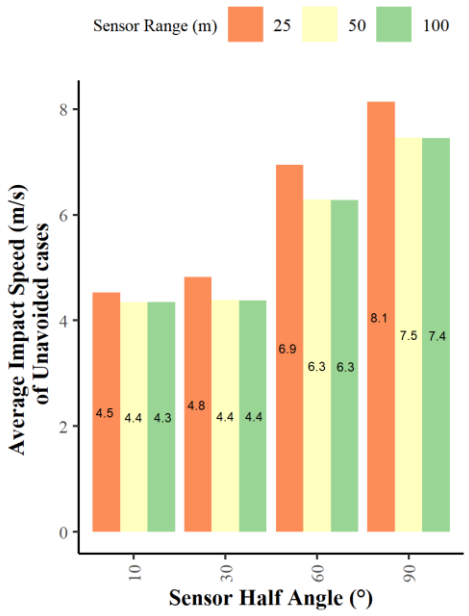

Figure 49. Average impact speed (m/s) of unavoided crashes for a set of sensor half angles and ranges.

5.3.2.2 Pedestrian Injury Risk Curve Results

While seniors were found to have a significantly higher risk of injury than adults, children were not found to have a significant difference in injury risk, except for fatal injury risk. Children are not adults, therefore it is expected that their risk of injury would be different despite the lack of significant difference.

Table 26. Injury model coefficients.

Injury Models	Impact Speed	Age: Child	Age: Senior	Pedestrian Weight	Intercept
Fatal	0.11310	2.24020	2.93552	0.03578	-10.20848
MAIS 3+F	0.09394	-0.53275	1.04428	-	-3.64599
MAIS 2+F	0.075302	0.066635	1.241275	-	-2.071403

Figure 50 shows the results of the fatality injury risk model for all the impact speeds and pedestrian weights present in each of the age groups. Seniors were at a higher risk of fatal injury at lower impact speeds. Children also had a higher risk than adults at the same impact speed. To more easily compare injury risk between the age groups, Figure 51 shows the overlaid contour plots from Figure 50 and Table 27 compares the model odds ratios.

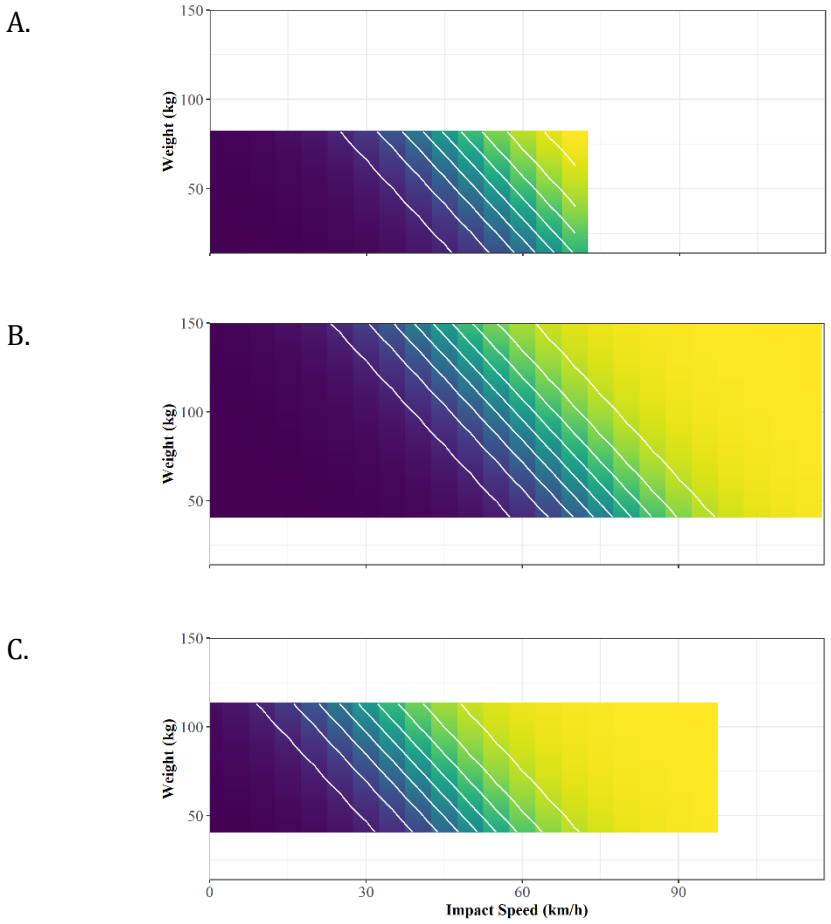

Figure 50. Risk of fatal injury for the range of impact speeds and pedestrian weight for children (A), adults (B), and seniors (C). Purple corresponds to low injury risk while yellow corresponds to high injury risk. The contour lines (white) are spaced at 10% injury risk intervals. Risks shown were limited to the range of observed data within each age group.

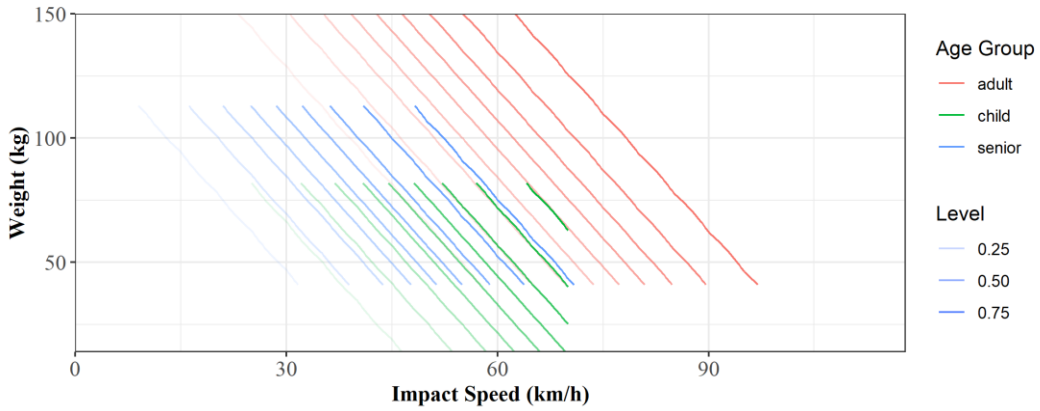

Figure 51. Risk of fatal injury contour lines for child (green), adult (red), and seniors (blue). Darker contour lines correspond to higher injury risk. Line length corresponds to the data available within each age group.

Figure 52 shows the risk of fatal injury for the adult, child, and senior age groups at each group's median weight. As shown in Figure 50 and Figure 51 seniors had the highest risk of injury followed by children and then adults.

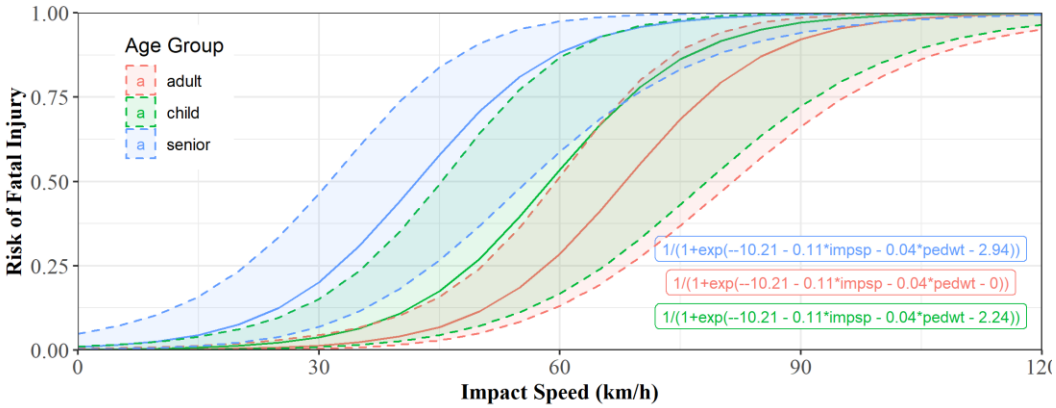

Figure 52. Risk of fatal injuries for the child, adult and senior groups. Weight was set as the median weight in each group: 70 kg for adult and senior and 37 kg for child. Dotted lines correspond to 95 percentile confidence intervals. Logistic regression equations are provided with the coefficients rounded to two decimal places.

The injury risk curves for MAIS 3+ F injury had different trends than the fatal injury risk curve

(

Figure 53). The senior age group still had the highest risk of injury, but the child age group had the lowest risk of injury. Although the child injury risk curves showed a lower risk than adults, this difference was not statistically significant.

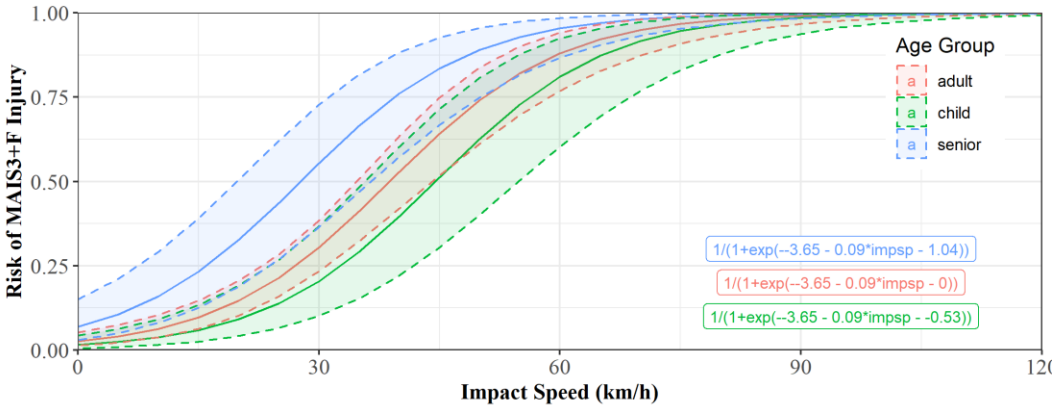

Figure 53. Risk of MAIS 3+F injury for child, adult and senior age groups. Dotted lines correspond to 95 percentile confidence intervals. Logistic regression equations are provided with the coefficients rounded to two decimal places.

Figure 54 shows the MAIS2+F injury risk curves. As with the previous models, the senior age group had the highest risk of injury. The child and adult injury risk curves were very similar. Although children are not adults, it is possible that analysis would have to be done at the body region level to elucidate differences in risk of MAIS2+F injury between these groups.

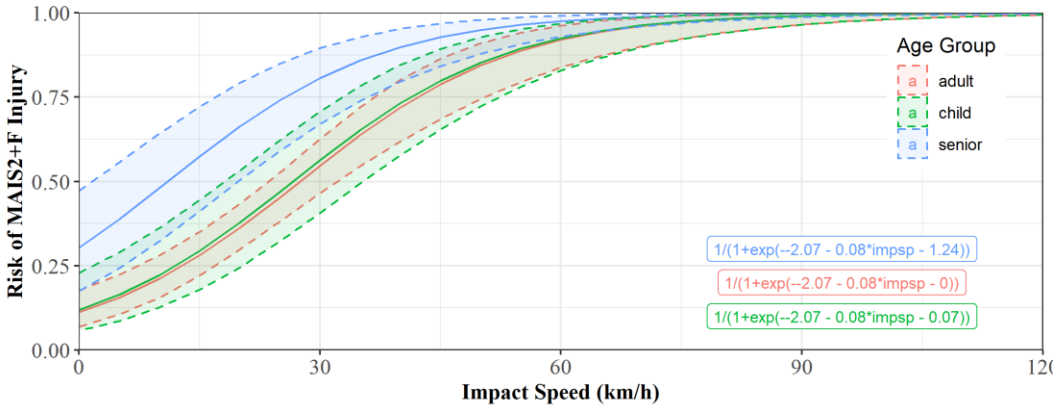

Figure 54. Risk of MAIS2+F injury for child, adult, and senior age groups. Dotted lines correspond to 95 percentile confidence intervals. Logistic regression equations are provided with the coefficients rounded to two decimal places.

Table 27. Odds ratios for the fatal, MAIS3+F, and MAIS2+F injury models.

Injury Model	Impact Speed	Child Age Group	Senior Age Group	Weight
Fatal	1.12	9.40	18.83	1.04
MAIS3+F	1.10	0.59	2.84	-
MAIS2+F	1.08	1.07	3.46	-

5.3.2.3 Injury Benefits Results

As shown in Figure 55 - Figure 57 and Table 28, the proportions of injuries prevented increased with sensor FOV and range. The reduction in injury probability ranged from 74.9% to 89.1%, 68.4% to 90.2%, and 58.0% to 90.8% for fatal, MAIS 3+F, and MAIS2+F injuries, respectively. The 25 m sensor prevented slightly less injuries than the 50 and 100 m sensor, although this difference was not statistically significant. The similarity in reduction of fatal injury probability was likely due to the low impact speeds of the unavoided cases meaning that the probability of fatal injury was also low or that the additional crashes avoidance by the better sensors were primarily low severity crashes.

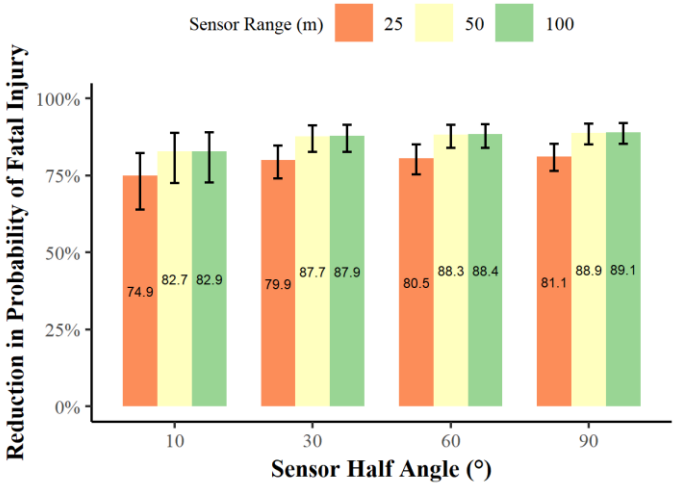

Figure 55. Proportion of fatal injuries prevented by P-AEB with 70%, 80%, 90%, and 100% sensors. Error bars represent one standard deviation change in the injury risk model.

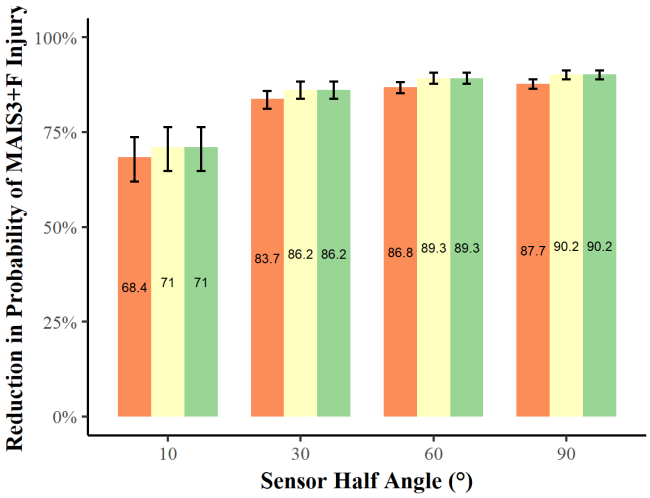

Figure 56. Proportion of MAIS3+F injuries prevented by P-AEB with 70%, 80%, 90%, and 100% sensors. Error bars represent one standard deviation change in the injury risk model.

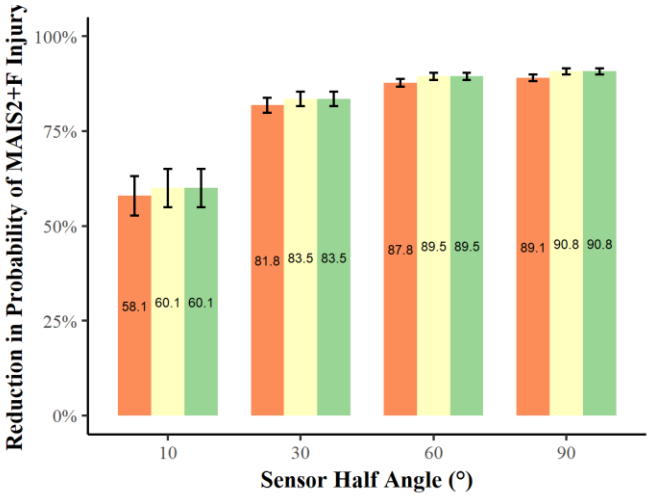

Figure 57. Proportion of MAIS2+F injuries prevented by P-AEB with 70%, 80%, 90%, and 100% sensors. Error bars represent one standard deviation change in the injury risk model.

Table 28. Change in fatal, MAIS3+F, and MAIS2+F injury risk.

Sensor Half Angle (°)	Sensor Range (m)	Fatal Injury		MAIS3+F Injury		MAIS2+F	
		Number of Injuries	Percent Change (%)	Number of Injuries	Percent Change (%)	Number of Injuries	Percent Change (%)
No System		24.8	-	90.5	-	158.6	-
10	25	6.2	74.9	28.6	68.4	66.6	58.0
	50	4.3	82.7	26.2	71.0	63.3	60.1
	100	4.2	82.9	26.2	71.0	63.3	60.1
30	25	5.0	79.9	14.7	83.7	28.8	81.8
	50	3.0	87.7	12.5	86.2	26.1	83.5
	100	3.0	87.9	12.5	86.2	26.1	83.5
60	25	4.8	80.5	11.9	86.8	19.4	87.8
	50	2.9	88.3	9.7	89.3	16.7	89.5
	100	2.9	88.4	9.7	89.3	16.7	89.5
90	25	4.7	81.1	11.1	87.7	17.3	89.1
	50	2.8	88.9	8.9	90.2	14.6	90.8
	100	2.7	89.1	8.9	90.2	14.6	90.8

5.3.3 DISCUSSION

In this study we compared different hypothetical sensor FOVs and ranges to estimate the effect of advanced sensors such as LiDAR and radar on crash avoidance and impact mitigation. Utilizing a TTC of 1.5 seconds and zero latency, the sensor ranges above 25 m were found to have little to no effect on estimated crash avoidance, but a small effect on impact mitigation. Sensor FOV was shown to have a larger effect on the estimated crash avoidance up to a FOV of ±60°.

Sensors with a 50 m and 100 m range only performed slightly better at crash avoidance than the sensor with a 25 m range. This could be due to the fact that the automatic braking did not activate until the TTC threshold was reached. Even if the pedestrian was visible 90 m out, the system did not brake until the vehicle was 1.5 seconds from the impact point. Cases with obstructions likely affected the system performance equally regardless of sensor range. A longer sensor range would not provide additional benefit if a pedestrian stepped out from behind parked cars just before impact.

Similar to results shown by Rosén, et al. [10] and Gruber, et al. [78], sensor ranges above 25 m were not found to have a significant effect on crash avoidance, but had a small effect on impact

mitigation. This is encouraging because the further away a pedestrian is, the harder they are to accurately detect and the harder it is to estimate their trajectory. Also, showing potential effectiveness at low ranges is encouraging for sensor systems that may be affected by lighting and weather conditions. Current systems often depend on both radar and cameras to detect pedestrians. While adverse weather may have only a small effect on radar and LIDAR, it has a large effect on camera detection. Furthermore, radar systems commonly have various FOVs and ranges within a system. For example they may have a long range radar with a small FOV coupled with a mid-range sensor with a larger FOV. This was not accounted for in the model. Future work could combine multiple sensors and vary effectiveness based on weather conditions.

Previous work has shown that as latency increased, effectiveness decreased, and as TTC threshold decreased effectiveness also decreased [2]. This study only examined one system latency and TTC threshold. The effectiveness values presented would likely be lower with a system that had a shorter TTC threshold and a longer latency value. It is also possible that sensor range could have a larger effect when combined with a different system latency and TTC threshold. TTC was calculated by dividing the distance to the original impact point (unit in meters) by the vehicle's current speed (unit in meters per second). This is a good estimation of TTC for cases in which the vehicle is traveling straight, but may underestimate the TTC in turning cases. This underestimation would cause the AEB system to activate sooner, due to the vehicle reaching the TTC threshold sooner, which could result in an overestimation of effectiveness for the turning cases.

The hypothetical sensors with FOVs of 60° and greater were estimated to avoid a greater percentage of cases in which the vehicle was turning than cases in which the vehicle was traveling straight. This is likely because the cases in which the vehicle was turning tended to have lower impact speeds than traveling straight cases. The median original impact speed of the curved cases was 3.6 m/s compared to a median impact speed of 8.6 m/s for traveling straight cases. Additionally, it was

assumed that the hypothetical P-AEB system was able to achieve the same maximum deceleration, regardless of the vehicle trajectory, which may have resulted in an overestimation of the crash avoidance potential in the cases in which the vehicle was turning. If a vehicle is turning, an AEB system may not be able to apply maximum deceleration to avoid the crash without resulting in loss of control.

For this study, we assumed an idealized hypothetical P-AEB system. We assumed that the sensors always detected the pedestrian when they were in the road and not obstructed and we assumed that the weather and lighting conditions had no effect on the system's ability to detect the pedestrian. Future work could incorporate the effect of weather, lighting conditions, and even pedestrian height on the sensor's ability to detect the pedestrian. We only examined sensor FOV and range. We did not consider differences in how various sensor systems would be able to detect the pedestrians. For example, LiDAR requires greater computational power than radar which could affect computational time. We did not consider differences in computational power, scanning time, or resolution in this study. Future work could vary the sensor system parameters to examine how differences amongst sensor detection parameters and associated computational and algorithmic requirements would change the results.

5.4 CONCLUSION

The first model treated the pedestrian as a wall, in that the crash is only considered avoided if the vehicle comes to a complete stop before reaching the impact point (temporal model), while the seconds model accounted for the fact that a crash could also be avoided if the vehicle slows sufficiently for the pedestrian to completely clear in front of the vehicle (spatiotemporal model).

The temporal model examined a variety of TTC threshold and latency values and found that shorter latency and longer TTC thresholds lead to increased avoidance potential. The temporal model estimated a lowest performing system, 33-37% effectiveness, was achieved by a system with 0.3

second latency and 0.5s TTC threshold. The highest performing system, 84-86% effectiveness, was achieved by the system with a 0s latency and a 1.5 s TTC. The spatiotemporal model further examined the highest performing system, latency of 0 seconds and a TTC threshold of 1.5 seconds, with a variety of sensor field-of-views and ranges. The spatiotemporal model predicted higher P-AEB performance than the temporal model at avoiding crashes when equipped with the ±90° and ±60° and sensor. This is likely because in the spatiotemporal model the vehicle did not need to come to a complete stop to successfully avoid the collision.

The temporal model injury reduction benefits closely mirrored the overall crash avoidance predictions. The spatiotemporal model saw a similar trend in the MAIS 2+F injury reduction estimates, but at more severe injury levels this trend was replaced with similar injury reduction estimates across sensor configuration.

A study examining real-world effectiveness of pedestrian AEB at reducing pedestrian bodily injuries found a 35% reduction in bodily injury claims [79], which is a substantially lower effectiveness than the idealized results presented here. Both models in this investigation presented an upper bound for vehicle-pedestrian crash avoidance because they assumed idealized sensors that were always accurately able to detect the pedestrian if they were within the sensor parameters. Additionally, both models in this investigation assumed the pedestrian was a threat and took on avoidance actions so the system did not have to determine the likelihood of collision or account for potential pedestrian actions.

6 PEDESTRIAN AEB PREDICTED BENEFITS

6.1 RESEARCH OBJECTIVE

The effectiveness estimates in chapter 5 assumed that all vehicles would be equipped with pedestrian AEB, but pedestrian AEB is a relatively new vehicle feature and therefore will take years to be widely deployed in the fleet. This chapter examines the potential benefits of AEB in a mixed fleet and predicts benefits of pedestrian AEB in future fleets.

6.2 APPROACH

The Insurance Institute for Highway Safety (IIHS) Highway Data Loss Institute (HLDI) has developed estimates of market penetration in the U.S. for various common active safety features. Figure 58 shows the 2015 IIHS estimated AEB U.S market penetration which was shifted to account for when pedestrian-AEB entered the U.S. market. We assumed that pedestrian–AEB entered the market in 2011 because this is when Volvo first released pedestrian crash mitigation in their new vehicles. The 2015 IIHS market penetration curve was used as a proxy because there was not a published pedestrian AEB market penetration curve. The 2015 AEB curve was chosen because this was before voluntary agreement by automakers to equip almost all new vehicles with forward collision warning by 2022 and requires similar technology as pedestrian AEB. Full deployment, which we defined at 95% adoption, was estimated to occur in 2053 (dashed line).

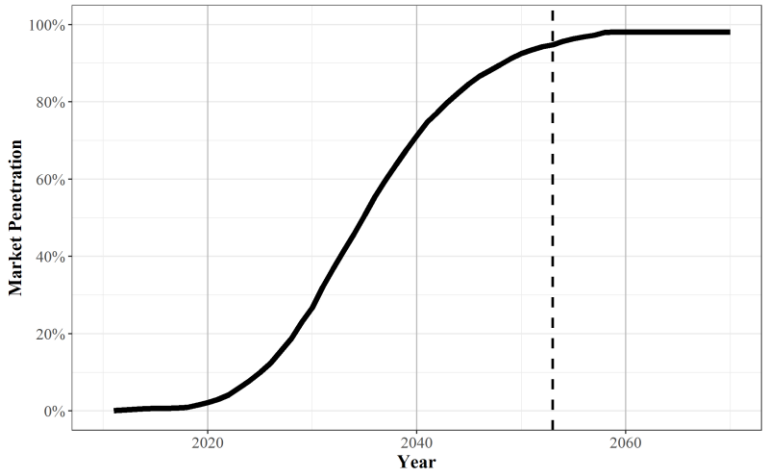

Figure 58. Estimated pedestrian-AEB market penetration based on the IIHS AEB market penetration estimates and shifted to reflect bicyclist-AEB entering the market in 2011.

We then applied the effectiveness numbers from chapter 5 to the market penetration values to get the crash reduction effectiveness at various market penetrations (Figure 59). The effectiveness values were multiplied by the likelihood that in a given vehicle-pedestrian crash the vehicle was equipped with P-AEB. Therefore, at low market penetration the effectiveness is low because very few vehicles are equipped with the system. As market penetration increases so does the effectiveness. To cover the range of effectiveness values from chapter 5, we applied the "best" and "worst" performing system effectiveness values for each model (Table 29).

Table 29. Effectiveness numbers for "best" and "worst" performing system from each AEB model.

Model	Performance	Crash Avoidance	Fatal Injury Avoidance	MAIS3+F Injury Avoidance
Temporal	Best	0.85	0.86	0.5
	Worst	0.35	0.36	0.36
Spatiotemporal	Best	0.92	0.89	0.90
	Worst	0.46	0.75	0.68

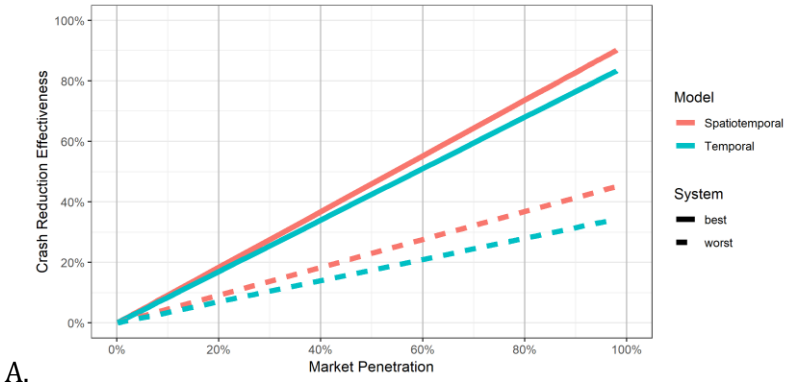

A.

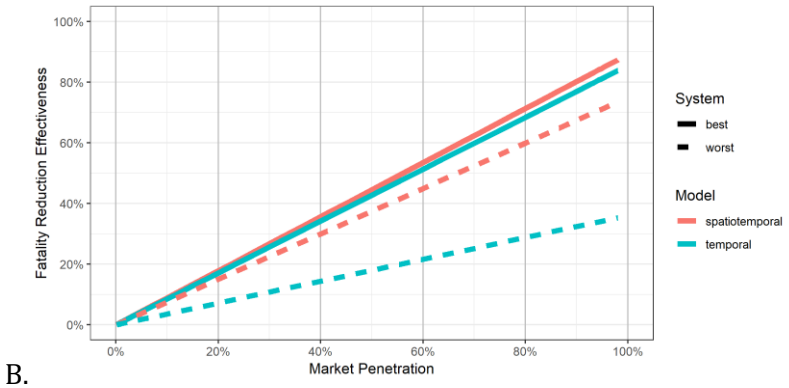

B.

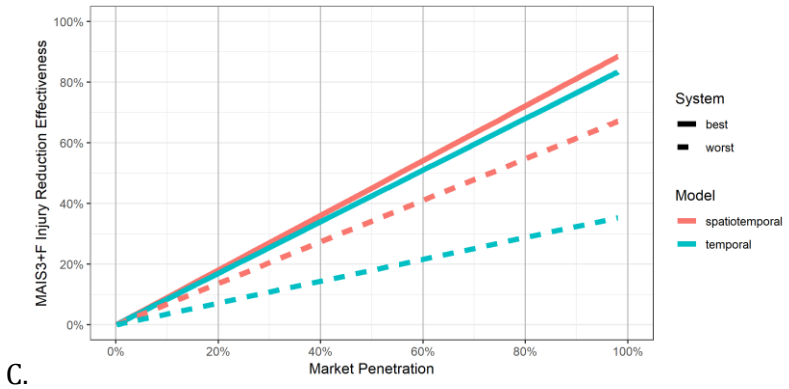

C.

Figure 59. Crash (A), fatal injury (B), and MAIS3+F injury (C) reduction effectiveness by market penetration.

The crash reduction effectiveness per market penetration was combined with the estimated market penetration over time to determine the crash reduction effectiveness over time (Figure 60). To estimate the residual crashes in 2025 and beyond, we estimated the incidence of target population vehicle-pedestrian crashes over time assuming they remained constant or increased linearly with

vehicle miles travelled. We assumed that vehicle miles traveled increased 1% annually in the growing VMT case [80].

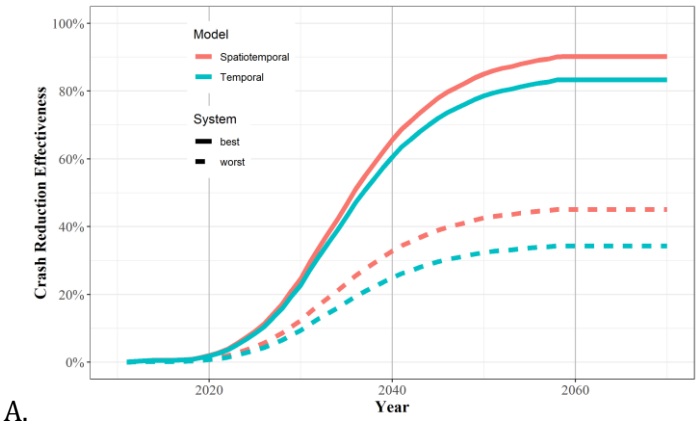

A.

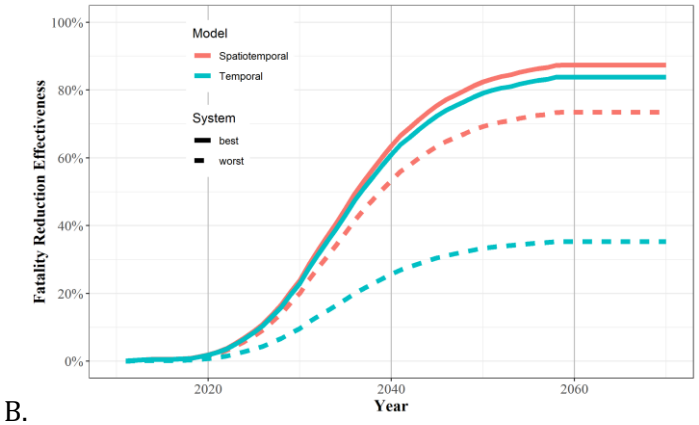

B.

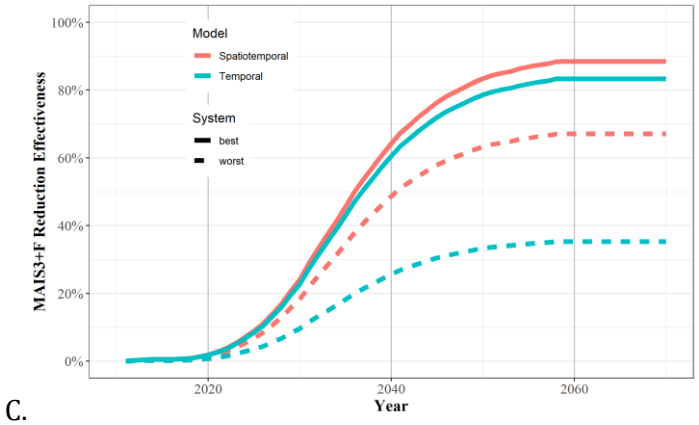

C.

Figure 60. Crash (A), fatal injury (B) and MAIS3+F injury (C) reduction effectiveness over time.

6.3 RESULTS

Figure 61, Figure 62, and Figure 63 (black line) show the estimated number of target population vehicle-pedestrian crashes, fatal injuries, and MAIS3+F injuries out to 2070 given that intervention does not occur. We then applied the effectiveness numbers by year to show the residual vehicle-pedestrian crashes and MAIS2+F injuries out to 2070 (Figure 61 blue and pink lines). The plots show that initially pedestrian AEB will have little effect due to the low market penetration, but by 2030 we expect some crash reduction effect.

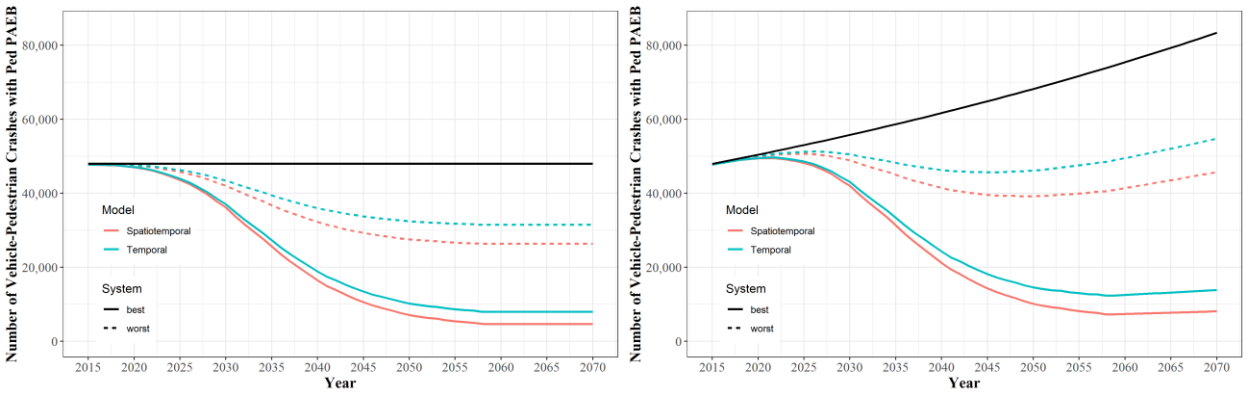

Figure 61. Estimate of vehicle-pedestrian crashes without pedestrian-AEB (black line) compared to spatiotemporal model (Pink line) and temporal model (blue line) with the "best" (solid line) and "worst" (dotted line) performing pedestrian-AEB. Assumed constant VMT (left) and growing VMT (right).

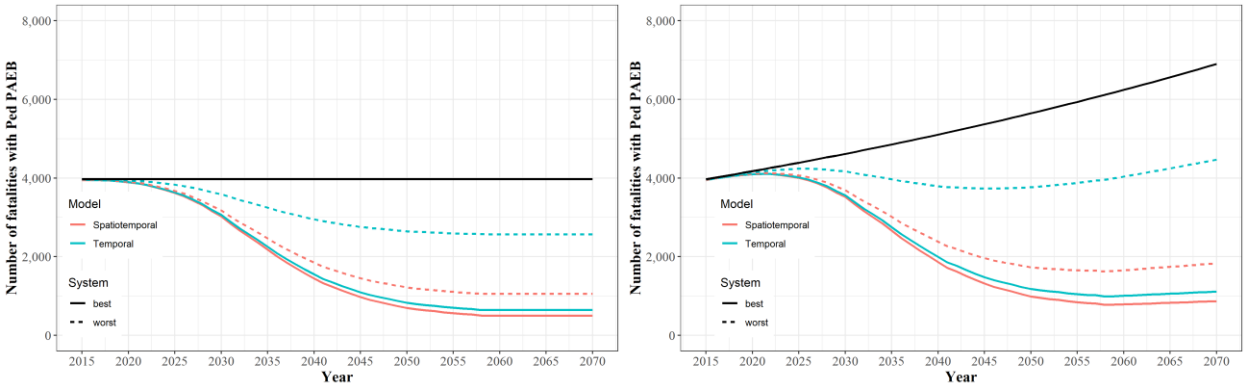

Figure 62. Estimate of vehicle-pedestrian fatal injuries without pedestrian-AEB (black line) compared to spatiotemporal model (Pink line) and temporal model (blue line) with the "best" (solid

line) and "worst" (dotted line) performing pedestrian-AEB. Assumed constant VMT (left) and growing VMT (right).

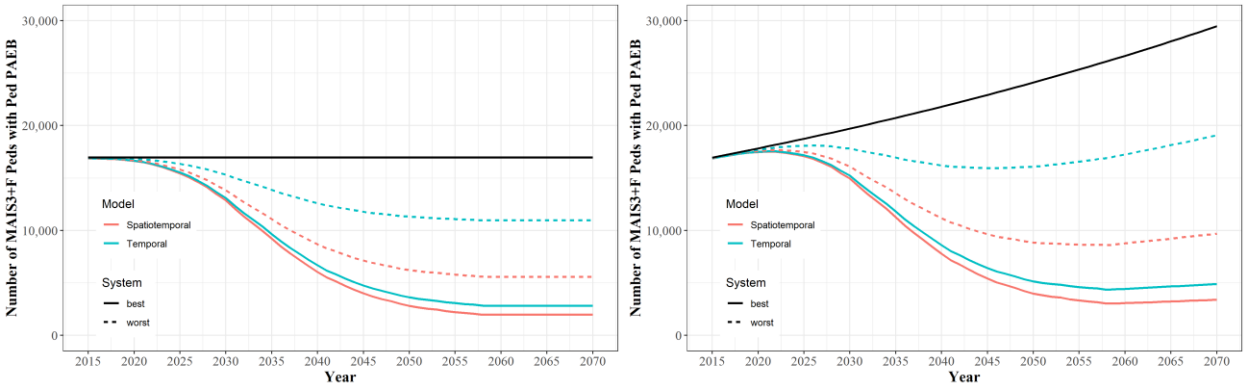

Figure 63. Estimate of vehicle-pedestrian MAIS3+F injuries without pedestrian-AEB (black line) compared to spatiotemporal model (Pink line) and temporal model (blue line) with the "best" (solid line) and "worst" (dotted line) performing pedestrian-AEB. Assumed constant VMT (left) and growing VMT (right).

6.4 DISCUSSION

This study predicted how P-AEB systems with a range of estimated effectiveness values could reduce vehicle pedestrian crashes, fatalities, and MAIS3+F injuries out to 2070. We assumed that P-AEB would follow a similar market penetration curve as standard AEB, although the penetration may be faster as standard AEB is already in most new vehicles in the US and P-AEB does not necessarily require additional equipment over standard AEB. Additionally, P-AEB could leverage a variety of sensor types, some of which are widely used in current vehicle platforms and may result in fast rates of adoption. For example, P-AEB could use video cameras to detect pedestrians which is a more cost effective approach than using expensive sensors such as LiDAR.

Due to low market penetration values, initially we see very little effect from pedestrian AEB prior to 2025. After 2025, we see a decrease in predicted pedestrian crashes and injuries that accelerates until about 2040 when the rate of decrease slows. Pedestrian crashes and injuries were

predicted to level off around 2060. While not all crashes or injuries are expected to be avoided, PAEB was predicted to decrease vehicle-pedestrian crashes and injuries substantially.

7 BICYCLIST AEB TARGET POPULATION

7.1 RESEARCH OBJECTIVE

The objective of this chapter was to characterize the target population of police-reported and fatal crashes for a bicyclist detecting AEB (bicyclist AEB) system. The target population was defined as the subset of bicyclist-vehicle impacts which might be avoided or mitigated by a bicyclist detecting AEB system. The characteristics of bicyclist, vehicle, environment, and driver conditions were examined for those crashes in the target population.

7.2 APPROACH

Similar to chapter 3 (pedestrian AEB target population), FARS and GES were filtered to include all vehicle-bicycle crashes from 2011-2015. The target population for bicycle-AEB was assumed to be vehicle-bicycle crashes in which the front of the car or LTV struck the bicycle and loss of control was not a factor. Bicycle collisions with heavy trucks, busses, and motorcycles were not considered. The proposed bicyclist AEB system would also be limited to single vehicle crashes as multi-vehicle crashes are too complex to determine if bicyclist AEB would affect the crash. For example, if vehicle 1 struck vehicle 2 and pushed vehicle 2 into the bicyclist, AEB would not prevent vehicle 2 from striking the bicyclist. Bicyclist AEB systems were assumed to only affect forward collisions, meaning that any crashes that were not forward collisions would not be mitigated by this system. Any bicyclist struck by the back or side of the vehicle would likely not be affected by a bicyclist AEB system. Bicyclist AEB systems would also be ineffective in a situation in which a vehicle

lost control and then struck a bicyclist. Delivering an alert to the driver or automatically braking in this situation would be unlikely to prevent the crash. Therefore, the data was filtered to only include cases in which the striking vehicle had a car or LTV body type (*body_typ* or *bdy_typ_im < 50)*, frontal impact (*impact1 = 11, 12, or 1*), and no loss of control (*p_crash2 > 9*).

Other factors such as weather or lighting conditions may also affect Bicyclist AEB effectiveness. These potential factors will be examined in this chapter as well as bicyclist and driver characteristics, environmental factors, and event factors.

7.3 RESULTS

As shown in Figure 64, vehicle-bicycle fatalities have increased by over 20% from 2011-2015, with a high of 869 fatalities in 2015. On the other hand, police reported vehicle bicycle fatalities have been relatively constant with an average 53,482 vehicle-bicycle crashes per year.

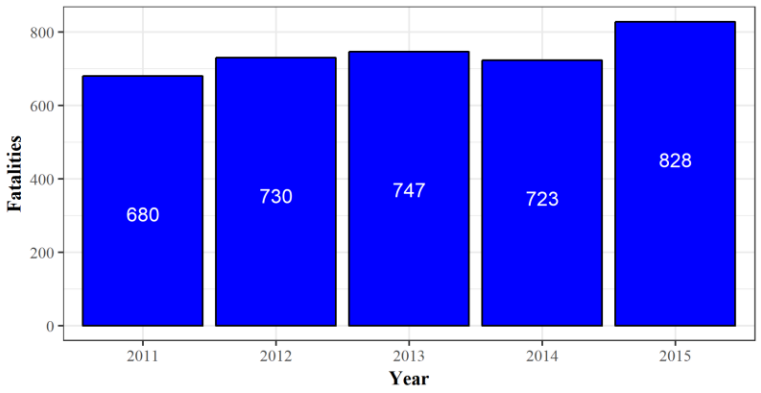

Figure 64. Vehicle-bicycle fatalities from 2011-2015 (FARS).

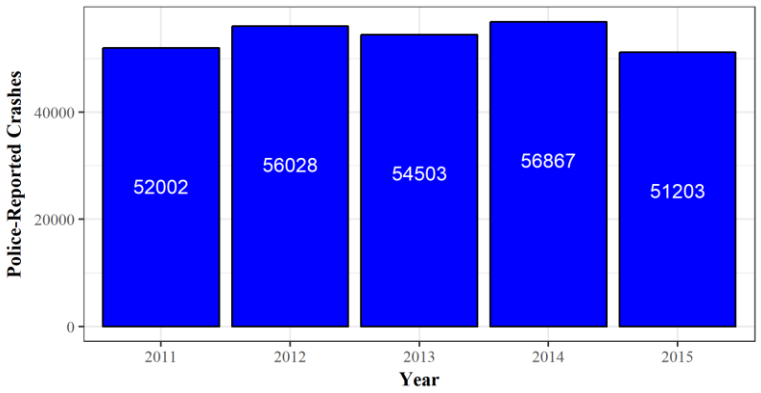

Figure 65. Vehicle-bicycle police-reported crashes from 2011-2015 (GES).

If a bicyclist AEB system uses a combination of forward facing radar, LiDAR and/or cameras to detect bicyclists then it would likely be effective for frontal impact crashes. For this reason, we assumed the target population for bicyclist-AEB would only consist of frontal impact crashes. As shown in Figure 66, most vehicle-bicycle fatalities and crashes were frontal impacts, but there was also a substantial number of right, left and back impacts. Frontal impact made up over 80% of fatal crashes (FARS) and 70% of police-reported crashes (GES).

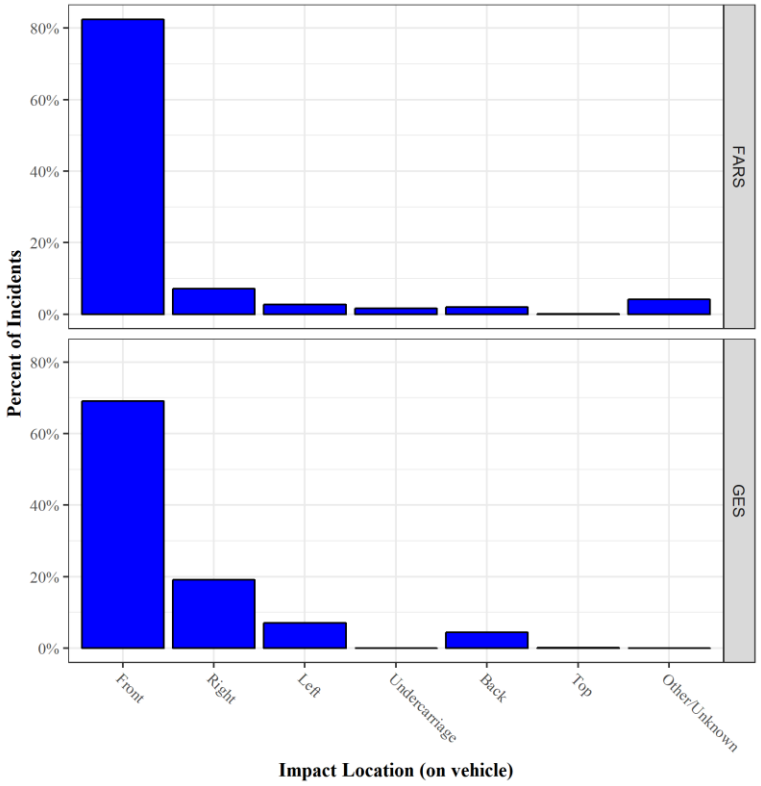

Figure 66. Distribution of impact locations vehicle-bicycle fatalities (FARS) and police-reported crashes (GES).

The following sections break down the target population and compare the distributions of vehicle-bicyclist collisions in terms of selected environmental and bicyclist-related variables. The tables highlight the trends, similarities, and differences between the distributions of FARS and GES (weighted). The trends, similarities, and differences are discussed individually in the following bicyclist characteristics, driver characteristics, and environmental characteristics sections.

7.3.1 TARGET POPULATION

The target population refers to that subset of vehicle-bicycle impacts which might be avoided or mitigated by a bicyclist AEB system. The AEB system in question is an active safety system designed to be integrated in cars, light trucks, and vans. It expected that it will only be effective in

single vehicle collisions. As shown in Table 30, when multi-vehicle crashes are excluded, there were 3,537 applicable fatal crashes and an estimated 264,359 applicable police-reported crashes from 2011 - 2015. The exclusion criteria are also depicted in Figure 67. The numbers are slightly different because a small number of cases involve multiple bicyclists, Table 30 shows the number of cases and Figure 67 shows the number of bicyclists.

An additional 578 fatal and 16,444 police-reported crashes involved non-passenger vehicles, and were excluded, as were another 346 fatal and 75,150 police-reported crashes since the proposed AEB system would only be effective in frontal impact scenarios. Frontal impacts made up the majority of impacts with only about 20% of fatal crashes and 30% of police-reported crashes occurring at non-frontal impact locations.

Finally, AEB would not be effective in situations in which there was loss of control of the vehicle. This criteria excluded an additional 12 fatal and 314 police-reported crashes resulting in a target population of 2,601 fatal and 172,451 police-reported vehicle-bicyclist crashes (Table 1).

Table 30. Breakdown of target population exclusion criteria for vehicle-bicycle crashes.

	FARS Cases (2011-2015)	GES Cases (2011-2015)	Weighted GES Cases (2011-2015)	Annual FARS Cases	Annual GES Cases
All Bicyclist Crashes	3,690	8,287	267,412	738	53,482
Inclusion Criteria	**Cases remaining**				
Single-vehicle crash	3,537	8,228	264,359	707	52,872
Struck by car or LTV	2,959	7,642	247,915	592	49,583
Frontal Impacts	2,613	5,158	172,765	523	34,553
No loss of control	2,601	5,150	172,451	520	34,490
Target Population	2,601	5,150	172,451	520	34,490

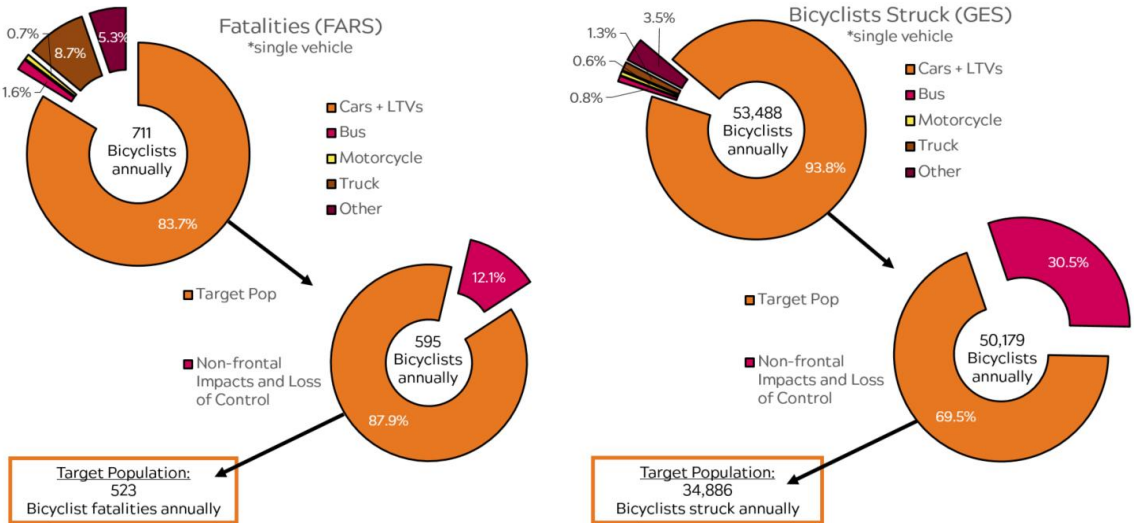

Figure 67. Breakdown of target population exclusion criteria for bicyclists.

Figure 68 and Figure 69 compare the total vehicle-bicycle fatal and crash populations to the target population for 2011-2015. The total population includes all vehicle types, multi-vehicle crashes, all impact locations, and cases with loss of control. Overall, the target population accounted for 70% of fatal and 64% of police-reported crashes. All analyses after this point are based on this target population.

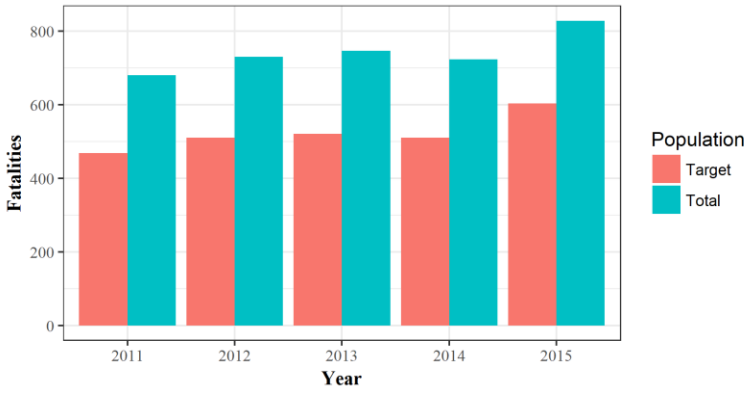

Figure 68. The total vehicle-bicycle fatalities (FARS) compared to the target population that could be affected by bicyclist AEB.

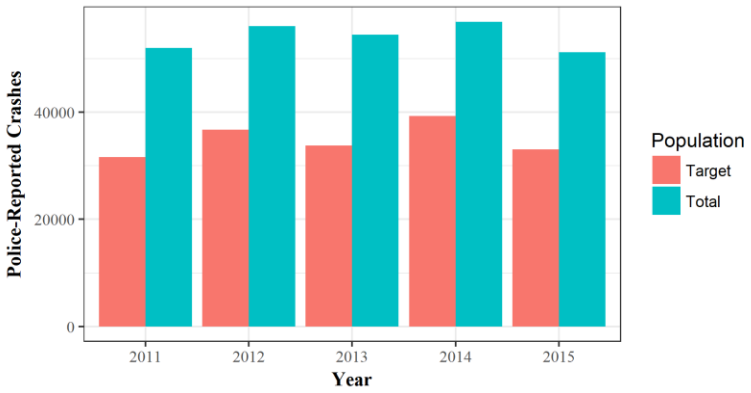

Figure 69. The total vehicle-bicycle crashes (GES) compared to the target population that could be affected by bicyclist AEB.

7.3.2 BICYCLIST CHARACTERISTICS

Bicyclist age had a bimodal distribution for both fatal and police reported crashes as shown in Figure 70 and Figure 71. Fatal crashes had a larger proportion of bicyclists over the age of 50 while police-reported crashes had a higher proportion of bicyclists under the age of 30. This difference could be due to the differences in injury tolerance between these age groups.

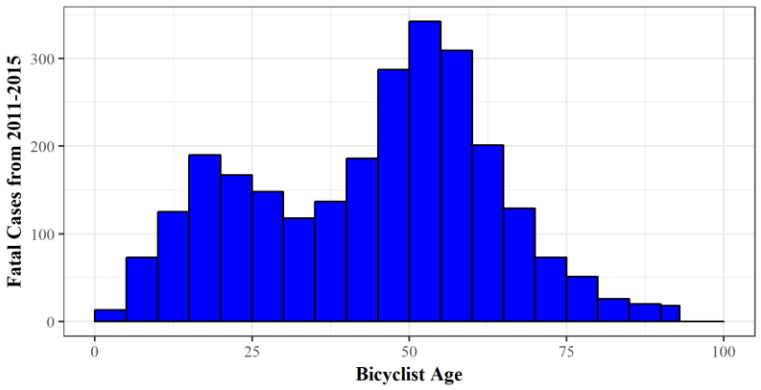

Figure 70. Distribution of bicyclist ages for vehicle-bicycle fatalities from 2011-2015 (FARS).

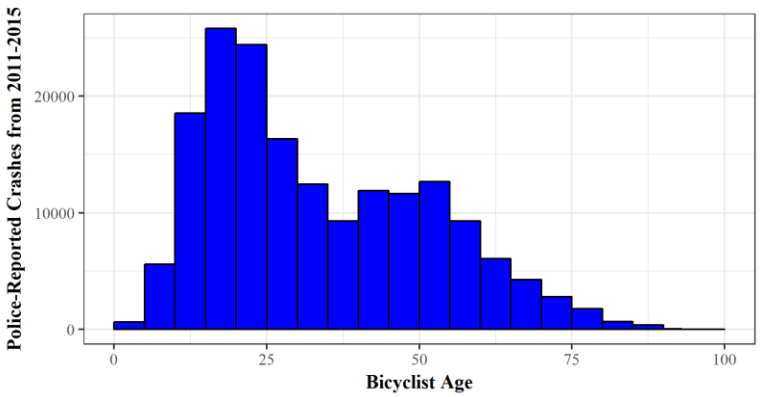

Figure 71. Distribution of bicyclist ages for vehicle-bicycle police-reported crashes from 2011-2015 (GES).

An overwhelming proportion of the struck bicyclists were male (Figure 72). Female bicyclists made up less than 25% of fatal and police-reported crashes. This difference could due to behavior differences (e.g. risk taking behavior) and/or gender differences in bicycle ridership in the US [81].

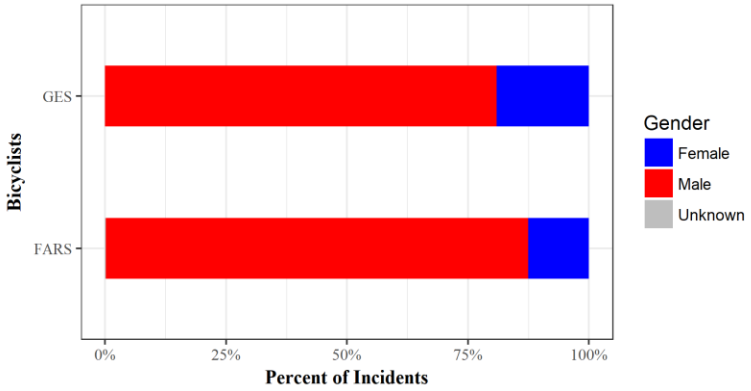

Figure 72. Distribution of bicyclist gender for all vehicle-bicyclist fatalities (FARS) and crashes (GES) from 2011-2015.

Bicyclist alcohol involvement did not make up a large proportion of vehicle-bicycle fatalities or crashes. As shown in Figure 73, about 12% of fatally injured bicyclists and only 2.4% of bicyclists involved in police-reported crashes had reported alcohol involvement. Despite the low proportions, the proportion of fatally injured bicyclists that were involved with alcohol was about 5 times higher

than bicyclists involved in police-reported crashes, although in a large proportion of fatal crashes the alcohol involvement was unknown.

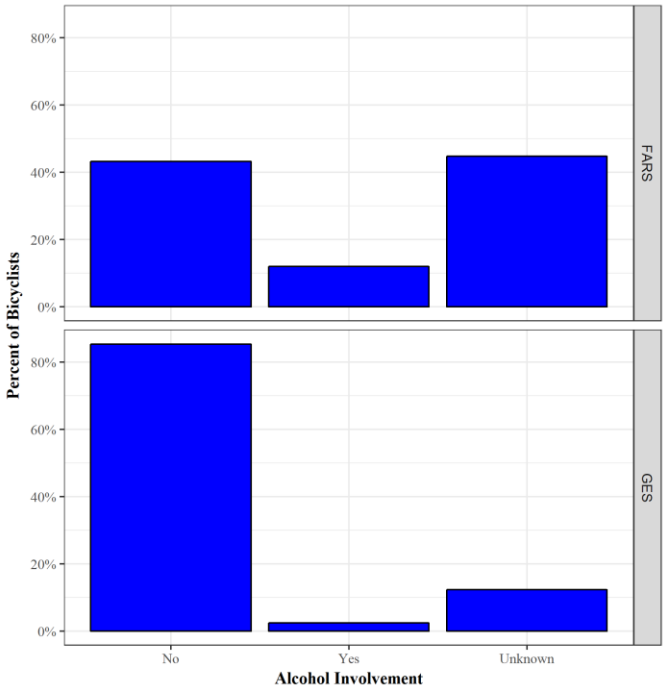

Figure 73. Distribution of bicyclists that had evidence of alcohol involvement for fatal (FARS) and police-reported crashes (GES) from 2011-2015.

7.3.3 DRIVER CHARACTERISTICS

As shown in Figure 74 and Figure 75, young drivers made up a higher proportion drivers involved in vehicle-bicyclist fatalities and crashes. Interestingly, there was an almost linear relationship between driver age and the number of bicycle fatalities and crashes.

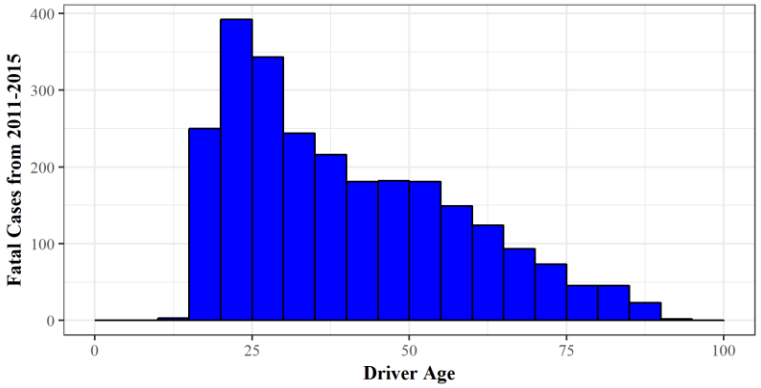

Figure 74. Distribution of driver ages for vehicle-bicycle fatalities from 2011-2015 (FARS).

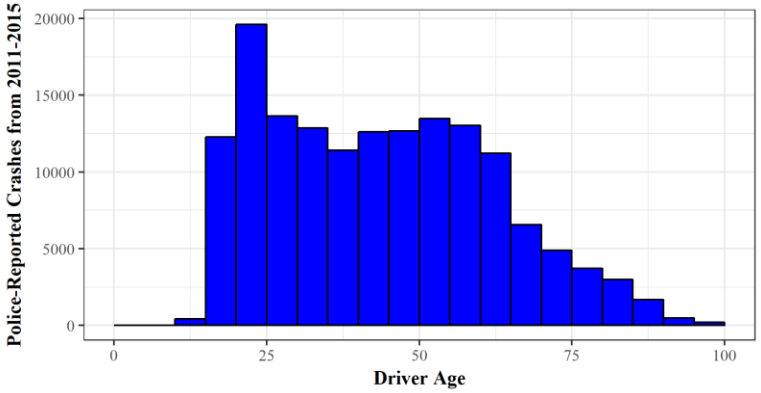

Figure 75. Distribution of driver ages for vehicle-bicycle crashes from 2011-2015 (GES).

Most drivers involved in vehicle-bicycle fatalities and crashes were male (Figure 76). A greater proportion of male drivers were involved in fatal crashes than police-reported crashes. Drivers were reportedly involved with alcohol in less than 1% of police reported crashes, but 11% of fatal crashes (Figure 77), although a large proportion (more than 20%) of the fatal crashes had unknown driver alcohol involvement.

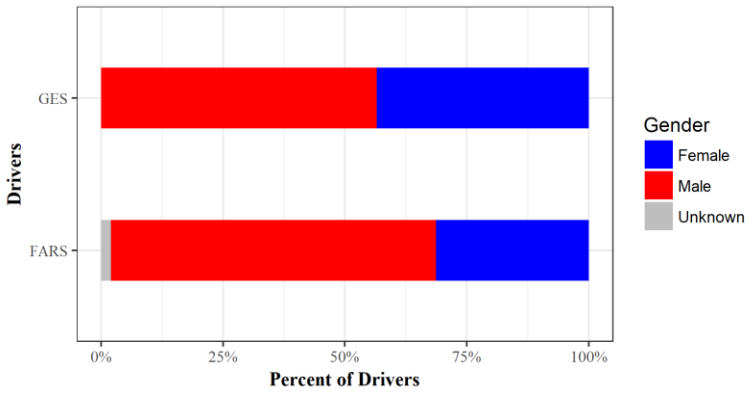

Figure 76. Distribution of driver gender for all vehicle-bicyclist fatalities (FARS) and crashes (GES) from 2011-2015.

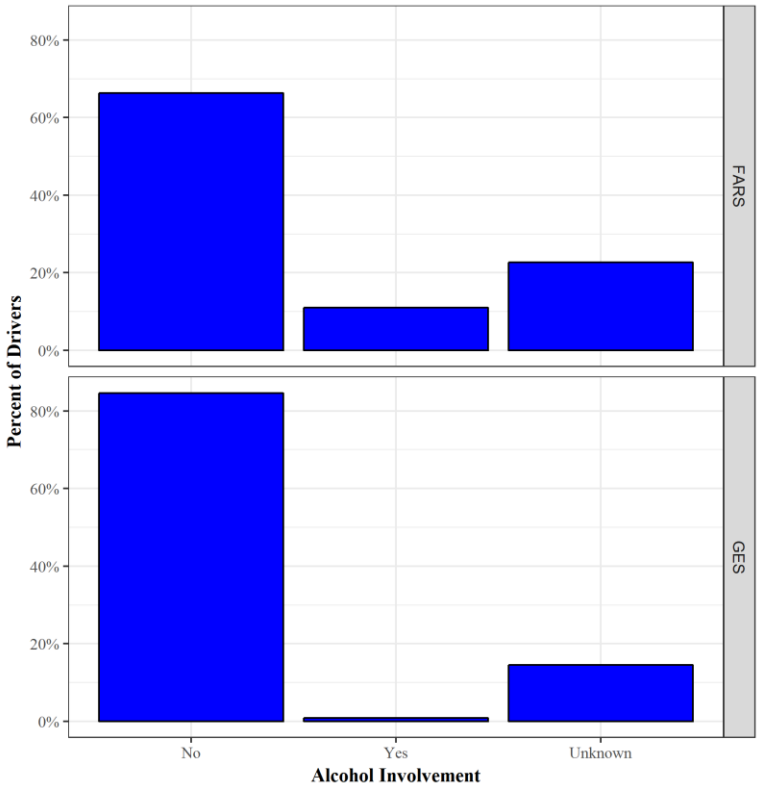

Figure 77. Distribution of drivers that had reported alcohol involvement for fatal (FARS) and police-reported crashes (GES) from 2011-2015.

7.3.4 *Environmental Characteristics*

As shown in Figure 78, the distributions of speed limits vary between fatal and police-reported crashes. Fatal crashes tended to have higher speed limits than police-reported crashes. Conclusions are difficult to draw from this information, however, because about 30% of police-reported crashes had either no limit or an unknown speed limit.

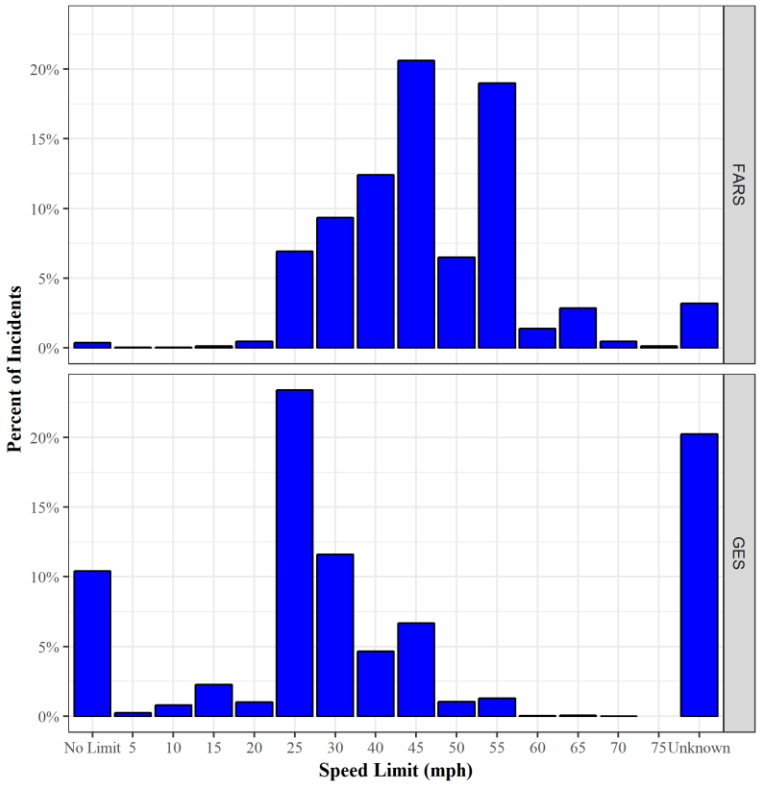

Figure 78. Distribution of speed limits for fatal (FARS) and police-reported crashes (GES) from 2011-2015.

The most common lighting condition for fatal and police-reported crashes was daylight which made up 49% and 76% of the sample, respectively. A large proportion of fatal crashes occurred during dark lighted or not lighted conditions with a combined proportion of 45% (Figure 79).

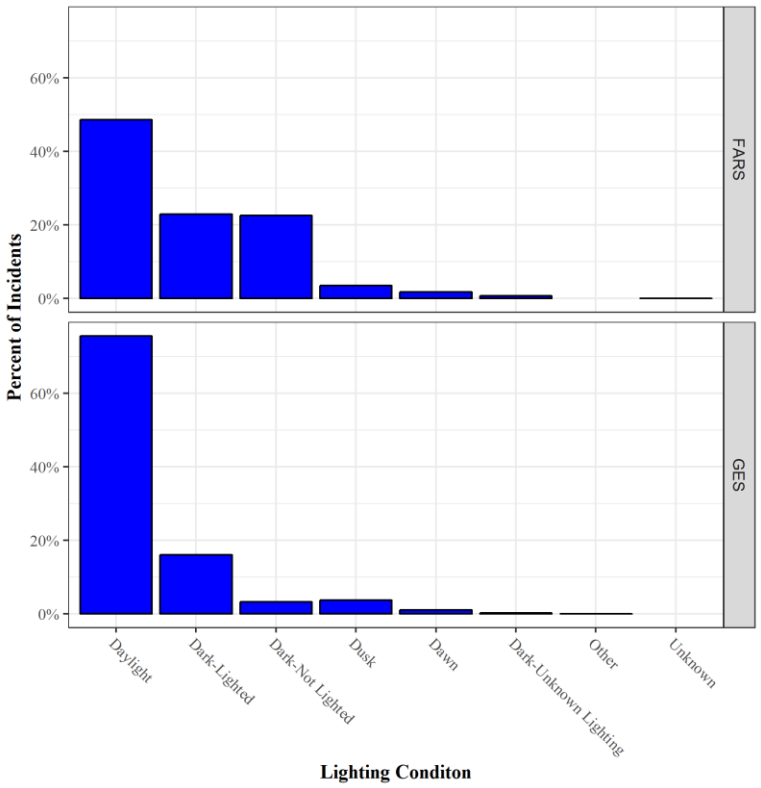

Figure 79. Distribution of lighting conditions for fatal (FARS) and police-reported crashes (GES) from 2011-2015.

For both fatal and police reported crashes clear weather conditions were present in the majority of cases (~80%) as shown in Figure 80. This is encouraging for sensor systems as adverse weather conditions could negatively affect an AEB sensor system's ability to detect a bicyclist.

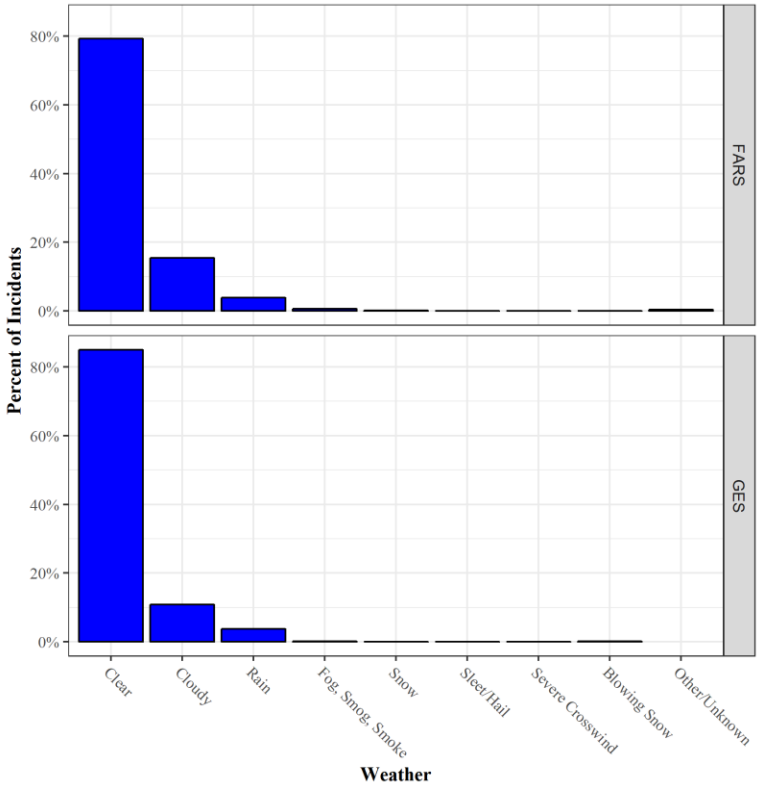

Figure 80. Distribution of weather conditions for fatal (FARS) and police-reported crashes (GES) from 2011-2015.

Almost all vehicle-bicycle fatalities and police reported crashes occurred on the roadway, 92% and 98%, respectively (Figure 81).

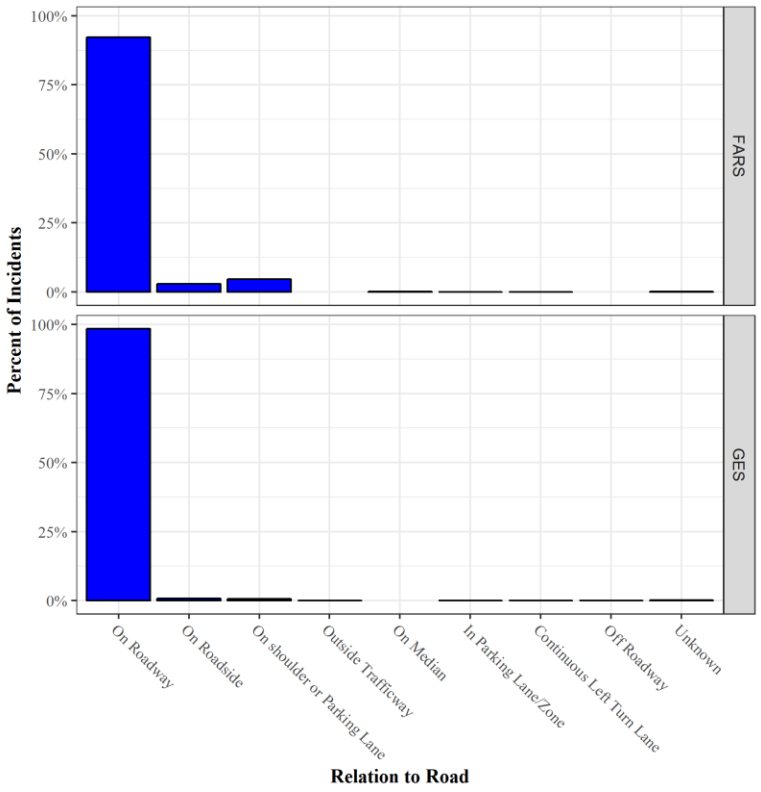

Figure 81. Distribution of bicyclist relation to the road for fatal (FARS) and police-reported crashes (GES) from 2011-2015.

As shown in Figure 82, most fatal vehicle-bicycle crashes occurred at non-junctions (60%), while most police-reported crashes occurred at intersections (37%) and intersection-related areas (32%). A higher proportion of fatal crashes may have occurred at non-junctions because the vehicles were likely traveling at faster speeds.

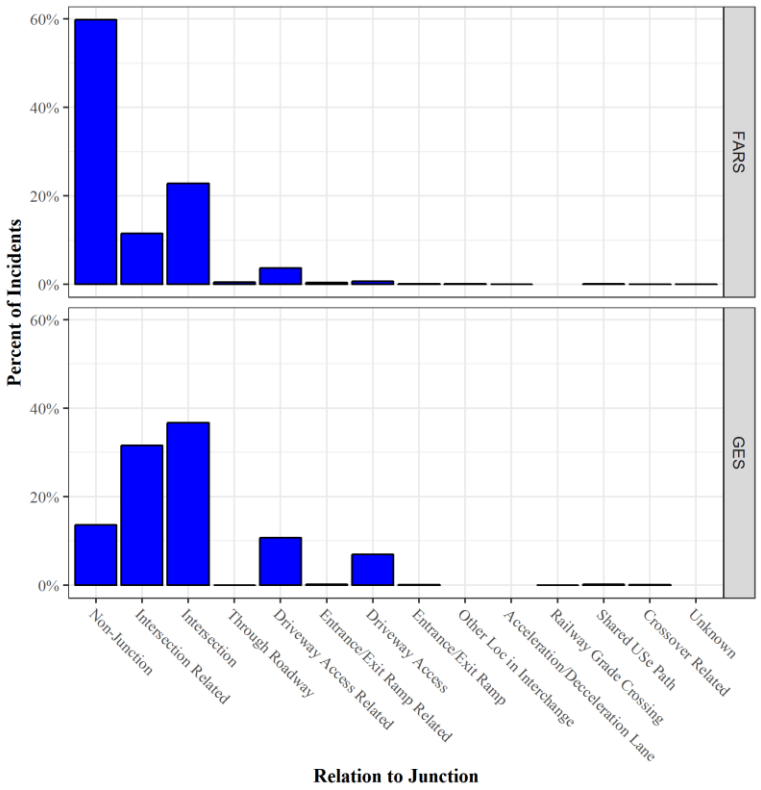

Figure 82. Distribution of crash location in relation to junction for fatal (FARS) and police-reported crashes (GES) from 2011-2015.

7.3.5 VEHICLE-BICYCLE EVENT CHARACTERISTICS

In 2014, NHTSA added a pedestrian and bicyclist table with more detailed information of factors specifically applicable to bicyclists and pedestrians. The following analyses are based on this data, and therefore are only presented for 2014-2015. As shown in Figure 83, bicyclists traveling with traffic were the most commonly present for both fatal and police-reported crashes. Police-reported crashes had a higher proportion of bicyclists facing traffic than fatal crashes. Similarly, 78% of fatal vehicle-bicycle crashes occurred when the bicyclist was in the travel lane, whereas the majority of police-reported crashes occurred when the bicyclist was in the travel lane or a sidewalk/crosswalk, 53% and 42%, respectively (Figure 84).

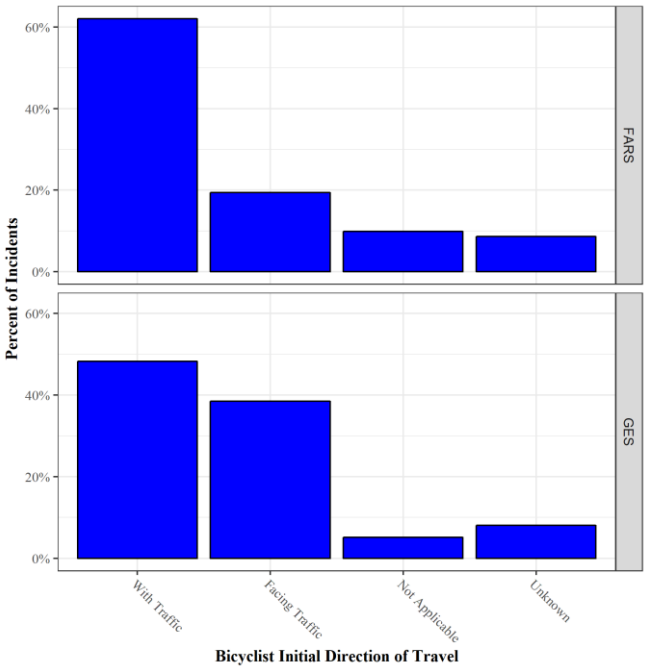

Figure 83. Distribution of bicyclist initial travel direction for fatal (FARS) and police-reported crashes (GES) from 2014-2015.

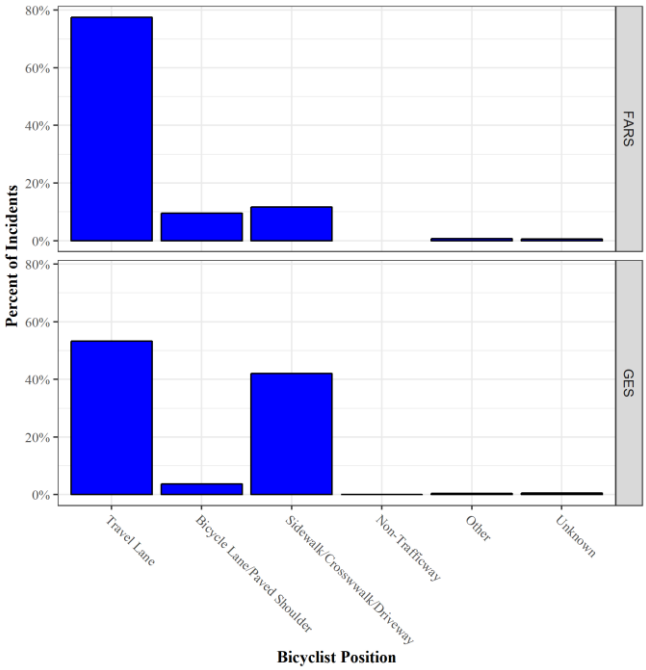

Figure 84. Distribution of bicyclist position for fatal (FARS) and police-reported crashes (GES) from 2014-2015.

There were a wide range of bicyclist crash groups for both fatal and police reported crashes (Figure 85). The bicyclist crash groups are simplified groups of the bicyclist crash types. Descriptions of the crash groups can be found on pages 99-102 of the PBCAT manual [82]. The most common fatal bicyclist crash group, accounting for 30% of fatal crashes, was when the motorist overtook the bicyclist. The most common police-reported bicyclist crash groups, accounting for 16% each, were loss of control/turning error and crossing path-other. Crossing path-other indicates that the bicyclist and vehicle were initially crossing paths, but no further classification can be made [83]. This may indicate that additional or better coding options are needed as a fairly large percentage fall into this category. As vehicle loss of control cases were excluded from this target population dataset, we can assume that any loss of control cases were loss of control by the bicyclist.

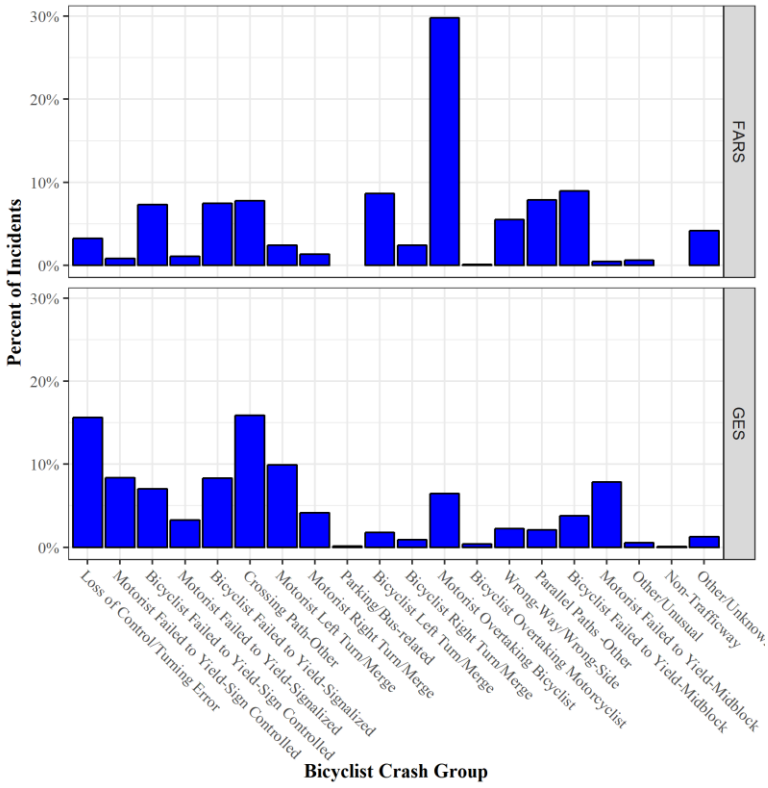

Figure 85. Distribution of bicyclist crash groups for fatal (FARS) and police-reported crashes (GES) from 2014-2015. Descriptions of the crash groups can be found on pages 99-102 of the PBCAT manual [82].

As shown in Figure 86, the majority vehicles were traveling straight prior to the fatal crashes (83%). The GES police-reported crashes were approximately split between traveling straight (44%) and turning (45%). In police reported crashes the vehicle was turning right or left, 27% and 18% respectively, prior to the crash. Scenarios in which the vehicle is turning could present a challenge for bicyclist AEB because it primarily uses forward sensors which may have a limited field of view. The limited field of view would make it difficult to detect bicyclists not directly in front of the vehicle

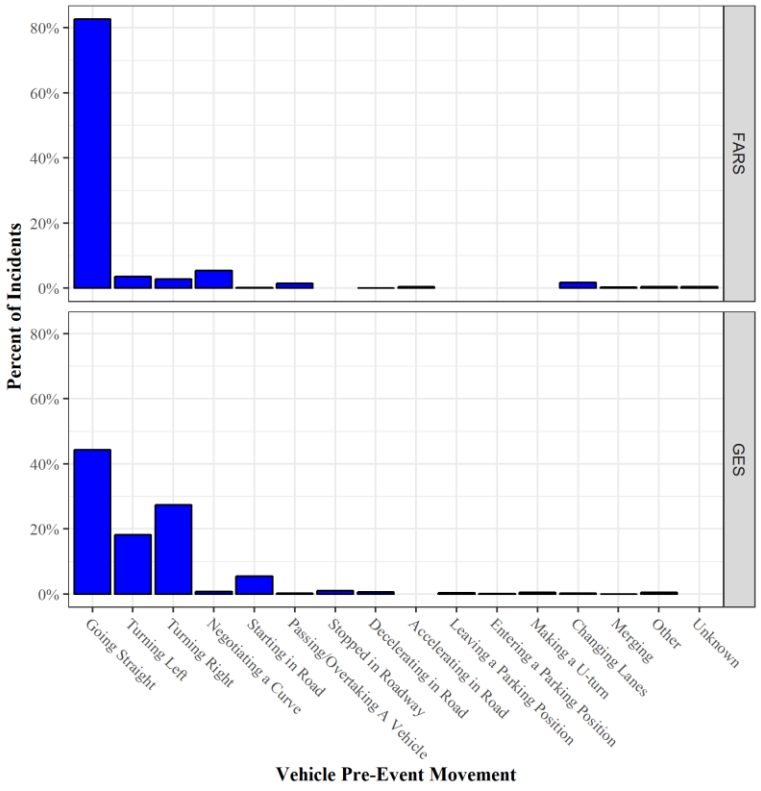

Figure 86. Distribution of pre-event vehicle movement for fatal (FARS) and police-reported crashes (GES) from 2014-2015.

As shown in Table 31, most fatal vehicle bicycle crashes occurred when the vehicle was traveling straight and the bicyclist was traveling with traffic. This crash type was also the most common police-reported vehicle crash configuration, but GES had an almost even split between the vehicle traveling straight and the vehicle turning. It should be noted that NHTSA defined traveling

with traffic as "the bicyclist was traveling with the flow of traffic for the side of the traffic way the bicyclist occupied prior to the crash." A bicyclist traveling with traffic does not necessarily imply that the vehicle and bicyclist were traveling the same direction. FARS and GES have limited information on vehicle-bicycle crashes which affects the ability to further distinguish crashes.

The data in Table 31 was condensed from the vehicle pre-event movement variable, therefore the "other" category included events coded as other and unknown as well as events in which the vehicle was merging, changing lanes, leaving or entering a parking spot, and negotiating a curve. Traveling straight included going straight, starting in road, stopped in road, accelerating/decelerating in road, and passing or overtaking another vehicle.

Table 31. Weighted distribution of case vehicle pre-event movement and bicyclist travel direction.

		Bicyclist – With Traffic	Bicyclist – Facing Traffic	Bicyclist – Other/Unknown
FARS (2014-2015)	Vehicle – Traveling Straight	588	169	184
	Vehicle – Turning Right	13	15	3
	Vehicle – Turning Left	26	11	3
	Vehicle – Other/Unknown	60	20	16
GES (2014-2015)	Vehicle – Traveling Straight	19,345	10,888	6,935
	Vehicle – Turning Right	5,474	12,768	1,448
	Vehicle – Turning Left	8,739	3,450	874
	Vehicle – Other/Unknown	1,101	494	215

7.4 DISCUSSION

This study examined two nationally representative data sources collected in the U.S., GES and FARS, to characterize the target population for a bicyclist pre-collision system (AEB). The target population was the population of crashes that a bicyclist AEB system may have had the ability to mitigate. The target population was defined as all vehicle-bicycle crashes that were single vehicle frontal crashes in which the striking vehicle was a car or LTV and there was no loss of control. The AEB-applicable vehicle-bicycle crashes accounted for 70% of fatal and 64% of police-reported crashes.

Bicyclist Characteristics: Male bicyclists constituted the majority of struck bicyclists (80-87%). Few bicyclists were involved with alcohol prior to the incident (2-12%). If unknowns are excluded 2.8-22% of bicyclists were reported involved with alcohol. The median age of struck bicyclists was 28 years, however the median age of fatally-injured bicyclists was 48 years reflecting the lower injury tolerance of older bicyclists.

Driver Characteristics: The age distribution of drivers who struck bicyclists had a median age of 37 in fatal crashes and 47 years old in all crashes. Furthermore, males made up 66% of the drivers involved in fatal crashes and 56% of drivers in police-reported crashes. Few drivers were involved with alcohol prior to the incident (0.8-11%). If unknowns are excluded 1-14% of drivers were reported involved with alcohol.

Environmental Characteristics: Most collisions occurred during the daylight (49-76%), however a larger proportion of fatalities occurred in dark conditions (46%, combined lighted and not lighted). Most collisions occurred when there were no adverse weather conditions (79-85%) and on the roadway (92-98%). Fatal crashes were more likely to occur at non-junction locations (60%) compared to police-reported crashes (14%).

Event Characteristics: Most crashes occurred when the bicyclist was in the travel lane and traveling with traffic. The reason for the crash varied between fatal crashes and police-reported crashes. Most fatal crashes were due to the motorist overtaking the bicycle and most police reported crashes were due either to loss of control/turning error or because the motorist and the bicyclist crossed paths. Most crashes occurred when the vehicle was traveling straight (52%), but in a large proportion the vehicle was turning (46%).

These observations will aid in the development of potential safety benefit models by indicating factors that increase risk of collisions and to estimate the number of crashes that may not be able to be avoided by a bicyclist AEB system. AEB systems may have limited effectiveness in adverse weather and low light conditions. Most crashes and fatalities occurred in clear weather conditions, but a large number of fatalities occurred in dark lighting conditions. AEB systems may have reduced effectiveness in turning scenarios. While in most fatal crashes the vehicle was traveling straight, a large proportion of all crashes involved a turning vehicle.

8 BICYCLIST EARLIEST DETECTION OPPORTUNITY

8.1 RESEARCH OBJECTIVE

The objective of this chapter was to estimate the earliest detection opportunity (EDO) of bicyclists using the WATS and SHRP 2 databases. Understanding the earliest detection opportunity can be used to further enhance the effectiveness of Automatic Emergency Braking (AEB) and tune system parameters.

8.2 POTENTIAL EFFECTIVENESS OF BICYCLE-AUTOMATIC EMERGENCY BRAKING USING THE WATS DATASET [4]

8.2.1 INTRODUCTION

Using European data, Rosén [67] examined the potential effectiveness of a range of AEB system designs to mitigate 607 vehicle-bicycle crashes extracted from the German In-Depth Accident Study (GIDAS) database. The four main factors that affected AEB effectiveness were found to be the vehicle speed, lighting conditions, time to collision, and deceleration ability. The study found that when the vehicle's braking system was applied at maximum capacity, 84% of the fatalities could have been prevented. When the vehicle's braking system was applied at minimal capacity, 19% of fatalities could have been prevented [67]. These estimates in fatality reduction with respect to braking demonstrate how applying the brakes at maximum capacity can better reduce the number of fatalities. Fredriksson and Rosén [84] used GIDAS to find a relationship between body region injury and impact location on the vehicle. Both of these studies relied on German crash data and therefore may not be directly applicable to U.S. crashes as the U.S. vehicle fleet and infrastructure may differ from Germany. For example, many US states allow "right turn on red" which is not permitted in Germany [85].

Unfortunately, little in-depth vehicle-bicycle crash data is available to study vehicle-bicycle crashes in the U.S. In lieu of in-depth crash data, U.S. vehicle-bicycle studies have examined naturalistic and government curated national databases. Sherony, et al. [86] used naturalistic data from the Transportation Active Safety Institute (TASI) 110-Car study to examine bicyclist motion during vehicle-bicycle interactions to aid in the design of AEB bicyclist detection systems. Haus and Gabler examined U.S. vehicle-bicycle near crashes in the second Strategic Highway Research Program (SHRP 2), a naturalistic driving study, and found that in about half of the cases the bicyclist was visible for at least one second which is promising for AEB as a mitigation strategy [7]. An analysis of U.S. national databases from 2014-2017 found that 71% of vehicle-bicycle crashes and 82% of fatal vehicle-bicycle crashes were frontal crashes and therefore potentially mitigatable by AEB [87].

The goal of this study was to elucidate U.S. vehicle-bicycle crashes and examine factors related to AEB effectiveness using in-depth vehicle-bicycle crash data.

8.2.2 METHODS

This study used a new dataset collected under the Washtenaw Area Transportation Study (WATS) conducted in southeast Michigan. This dataset was collected in collaboration with Toyota CSRC. First, WATS was compared to the Fatality Analysis Reporting System (FARS) and the General Estimate System (GES) to compare and contrast WATS findings with national observations. Then, the WATS database cases were examined to determine potential AEB effectiveness.

8.2.2.1 Data Sources

The data for this study was compiled from three data sources (shown in Table 32): the Washtenaw Area Transportation Study (WATS), the Fatality Analysis Reporting System (FARS), and the National Automotive Sampling System (NASS) General Estimate System (GES). A summary of the

three data sources is included in Table 32. As WATS is not necessarily nationally representative, the WATS data distributions were compared to those of FARS and GES for illustrative purposes.

Table 32. Overview of Data Sources.

Dataset	WATS	FARS	GES
Injury Severity	All Injury Levels	Fatal	All Injury Levels
Years	2011-2013	2011-2015	2011-2015
Total Cases (unweighted)	100	3,554	8,353
Weighted	No	No	Yes
Nationally Representative	No	Yes	Yes
Sample	Sample of crashes in southeast Michigan	Census of US Fatal Crashes	All US Police Reported Crashes
Scene Diagram	Yes	No	No
Imputed Variables	No	No	Yes

8.2.2.2 Calculate Earliest Detection Opportunity

The effectiveness of AEB depends on the ability of the sensors to detect the bicyclist, but this information is not available in publically available US databases. Therefore, we utilized the WATS scene diagrams and associated crash event records to estimate time to collision, i.e., how long the bicyclist was in the road before the crash.

The estimated time to collision, referred to here as the Earliest Detection Opportunity (EDO), was calculated by dividing the distance the bicyclist traveled in the road by the bicyclist riding velocity as shown in Equation 1:

$$EDO = \frac{distance}{velocity_{bicyclist}} \quad (1)$$

For a bicyclist crossing scenario, the distance the bicyclist travelled in the road prior to impact was measured from the crash scene diagrams. As shown in Figure 87, each crash scene diagram was uploaded into AutoCAD and scaled to proper dimensions. The bicyclist's path was then measured from the edge of the road to the impact point.

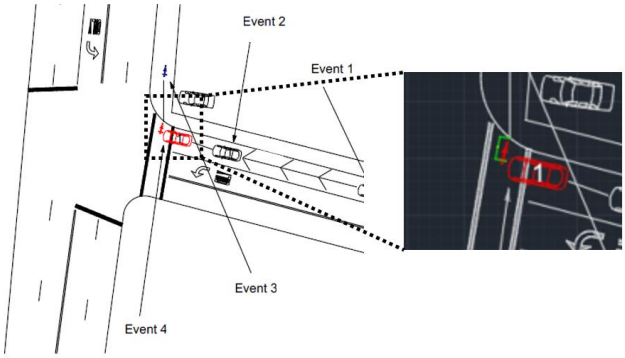

Figure 87. Sample crash scene diagram and CAD measurement. Green bracket indicates the measured distance the bicyclist traveled on the road.

For bicyclists riding along the road, relative speed was used instead of the bicyclist's speed. The bicyclist was assumed to be visible for 40 m as a conservative estimate, although current radar systems can detect pedestrians at ranges upwards of 90m in ideal conditions [62]. Bhagavathula, et al. [58] found that bicyclists were detected by drivers an average of 85 m away in unlit conditions, although this study only tested crossing bicyclists and not bicyclists travelling with traffic. A detection range of 40 m was chosen because camera based detection and non-ideal conditions can reduce pedestrian detection ranges [64, 76]. The relative speed was the difference between the bicyclist's estimated speed and the vehicle's estimated speed as shown in Equation 2. In our study, the posted speed limit was used as a surrogate for the vehicle speed as the actual travel speed of the vehicle was not reported in the WATS dataset.

$$EDO = \frac{distance}{velocity_{vehicle} - velocity_{bicyclist}} \quad (2)$$

The speeds of the bicyclists were assumed to depend on age, gender, and crossing behavior. Age and gender were available directly from the WATS database. Bicyclist crossing behavior was determined based on the crash scene diagram and associated event information. Bicyclist crossing behavior was grouped into three categories: riding along the road, riding through an intersection, or turning left/right (Figure 88).

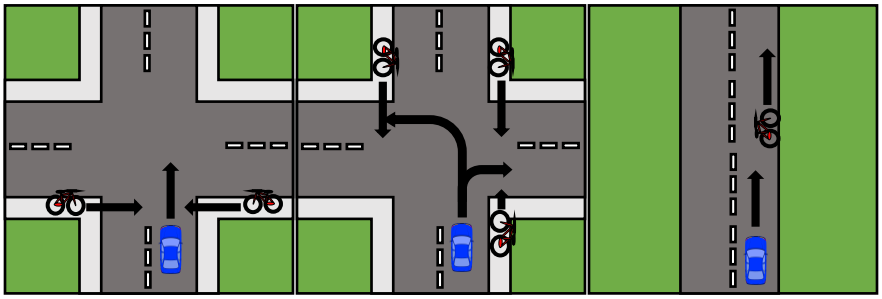

Figure 88. Ride through (left), turning left/right (center), and ride along (right) diagrams.

Thompson, et al. [88] reported the bicyclist's speed as a function of age and gender. The findings were based on radar-gun measurement of the speed of 152 children and adults riding bicycles on a closed road. Ling and Wu [89] calculated the speeds for bicyclists turning left through analysis of video surveillance of 531 bicyclists at intersections. Sherony, et al. [90] determined the speeds of 895 bicyclists riding through/along and at certain parts through the road from an analyzing the TASI 110. The TASI 110 car study was a one year naturalistic driving collection conducted in the greater Indianapolis area **[34]**. For this study, the 50th percentile speed was used for each characteristic of the bicyclist since it represents the average rider. The bicyclist values used are shown in Table 33 and Table 34

Table 33 Average Bicyclist Speeds for Riding along the Road and Turning [88, 89].

	Sample Size	**Male**	**Female**	**Unknown Gender**
≤ 13 years old	107	4.11 m/s	3.84 m/s	3.97 m/s
≥ 14 years old	45	4.69 m/s	4.04 m/s	4.33 m/s
Unknown Age	152	4.29 m/s	3.93 m/s	5.6 m/s
Turning Left	531	3.58 m/s	3.73 m/s	3.66 m/s

Table 34. Average Bicyclist Speeds for Riding through an Intersection [91].

Sample Size: 280	Starting Stationary	Constant Speed
25 % across road	3.35 m/s	4 m/s
50 % across road	3.77 m/s	5.2 m/s
75 % across road	3.85 m/s	6.3 m/s
Riding through	-	5.2 m/s

8.2.3 RESULTS

8.2.3.1 WATS comparison to GES and FARS

Table 35, Table 36, Table 37, and Table 38 summarize the results from the WATS data for driver/bicyclist, environment, and event characteristics. The percentages in the column that are bolded are the highest percentage of the specific category. GES cases were weighted and rounded to the nearest whole number. A chi-squared goodness of fit test was conducted to compare WATS to GES. We assumed GES values were the expected values and the WATS values were the observed. The test was run with a 90% and a 95% confidence interval. If the p-value was less than 0.1 or 0.05 there was no statistically significant difference between the datasets and it was assumed they were sufficiently similar. Variables with P-values greater than 0.1 were denoted with ** and variables with p-values greater than 0.05 were denoted with *. For all groupings, unknown variables and variables with zero GES cases were excluded and denoted with °.

8.2.3.1.1 Driver Characteristics

One-quarter (25%) of drivers in WATS vehicle-bicycle crashes were under the age of 24. This may be due to younger drivers tending to have less driving experience. FARS and GES drivers under the age of 26 and 29, respectively, accounted for 25% of vehicle-bicycle crashes. In WATS, male drivers were involved in 48% of vehicle-bicycle crashes. FARS and GES male drivers accounted for 66% and 57.5%, respectively. In WATS, 1% of the drivers were involved with alcohol and the rest had no reported alcohol involvement (96%) or it was unknown (3%). FARS and GES had reported that 9.1% and 0.9%, respectively, of drivers were involved with alcohol.

Table 35. Results for Driver Characteristics.

Driver Characteristics	WATS Cases	WATS Percentage	FARS Cases	FARS Percentage	GES Cases	GES Percentage
Total	100	100%	3,690	100%	267,412	100%
Gender*						
Male	48	48%	2,435	66.0%	153,762	57.5%
Female	41	41%	1,000	27.1%	113,650	42.5%
Unknown°	11	11%	255	6.9%	-	-
Alcohol Involvement **						
Drinking	1	1%	334	9.1%	2,313	0.9%
Not Drinking	96	96%	2,380	64.5%	220,013	82.3%
Unknown°	3	3%	976	26.4%	45,085	16.9%
P-values greater than 0.1 were denoted with **. P-values greater than 0.05 were denoted with *. Excluded variables denoted with °.						

8.2.3.1.2 Bicyclist Characteristics

In WATS, FARS, and GES, bicyclists that were struck by a passenger vehicle had a median age of 37, 46, and 47, respectively, and the WATS sample was younger than either FARS or GES. Males accounted for the majority (64%) of the bicyclist crashes in the WATS dataset, which also matched the trends in GES and FARS. Only 1% of bicyclists were involved with alcohol in WATS. Nearly half (42%) of bicyclists in WATS did not wear a helmet and those riders tended to have more severe injuries. However, both fatally-injured riders in WATS were wearing their helmets.

Table 36 Results for Bicyclist Characteristics.

Bicyclist Characteristics	WATS Cases	WATS Percentage	FARS Cases	FARS Percentage	GES Cases	GES Percentage
Total	100	100%	3,895	100%	273,829	100%
Gender						
Male	64	64%	3,372	84.6%	222,747	81.3%
Female	29	29%	513	31.3%	51,082	18.7%
Unknown°	7	7%	10	2%	0	0%
Alcohol Involvement**						
Drinking	1	1%	432	11.1%	7,002	2.6%
Not Drinking	95	95%	1,659	42.6%	230,771	84.3%
Unknown°	4	4%	1,804	46.3%	36,056	13.2%
Helmet Usage°						
Worn	31	31%	-	-	-	-
Not Worn	42	42%	-	-	-	-
Unknown	27	27%	-	-	-	-
Injury Severity (KABCO Scale)**						
Killed	2	2%	3,895	100%	2,855	1.0%
Incapacitating	5	5%	-	-	29,450	10.8%
Non-incapacitating	49	49%	-	-	122,735	44.8%
Possible Injury	21	21%	-	-	85,358	31.2%
No Injury	12	12%	-	-	28,608	10.4%
Unknown°	11	11%	-	-	4,823	1.8%
P-values greater than 0.1 were denoted with **. P-values greater than 0.05 were denoted with *. Excluded variables denoted with °.						

8.2.3.1.3 Environmental Characteristics

In WATS, nearly three-fourths (72%) of bicyclists were struck by drivers in the daylight and 20% were struck in darkness, either lighted or unlighted. This is similar to GES, in which 76.5% of bicyclists were struck in daylight and 18.2% were struck in dark-lighted/unlighted. By contrast, FARS reported that half (50.1%) of fatal bicyclist crashes occurred during daylight conditions and 43.2% in dark-lighted/unlighted conditions. In WATS, the majority of the collisions (70%) occurred when the weather was clear and 26% of the collisions occurred when there were adverse weather conditions (rain, cloudy, fog). Likewise, FARS and GES reported that struck bicyclists were riding in clear weather for 79.2% and 83.9% of the crashes, respectively. Dry road conditions were present in 90% of WATS driver-bicyclist collisions. FARS and GES reported that 91.4% and 84.8%, respectively,

of bicyclists were riding on dry roads. In WATS, 46% of crashes occurred in a speed limit zone of 25 mph (roughly 40 km/h) and 60% occurred at an intersection.

Table 37 Results of Environmental Characteristics.

Environmental Characteristics	WATS Cases	WATS Percentage	FARS Cases	FARS Percentage	GES Cases	GES Percentage
Total	100	100%	3,690	100%	267,412	100%
Weather Type						
Clear	70	70%	2,922	79.2%	224,480	83.9%
Cloudy	22	22%	522	15.0%	29,904	11.2%
Rain	3	3%	147	4.0%	11,956	4.5%
Sleet/Hail	-	-	2	0.05%	88	0.03%
Fog/Smoke	1	1%	27	0.07%	298	0.1%
Snow/Blowing Snow	-	-	7	0.02%	588	0.02%
Severe Wind	-	-	1	0.002%	26	0.001%
Other/Unknown	4	4%	28	0.08%	-	-
Road Surface Condition**						
Dry	**90**	**90%**	**3,373**	**91.4%**	**226,652**	**84.8%**
Wet	6	6%	251	6.8%	15,807	5.9%
Snow/Ice/Frost/etc.	0	0%	13	0.4%	511	0.2%
Other/Unknown	4	4%	53	1.4%	24,442	9.1%
Lighting**						
Dawn	2	2%	89	2.4%	3,457	1.3%
Daylight	72	72%	1,850	50.1%	204,567	76.5%
Dusk	5	5%	123	3.3%	10,037	3.8%
Dark-Lighted	13	13%	817	22.1%	39,167	14.6%
Dark-Unlighted	7	7%	777	21.1%	9,629	3.6%
Dark-Unknown Lighting	0	0%	24	0.7%	541	0.2%
Other/Unknown°	1	1%	10	0.3%	15	0.006%
Road Type°						
Non-freeway Intersection	43	43%	-	-	-	-
Non-freeway Straight	27	27%	-	-	-	-
Intersection Related Other	13	13%	-	-	-	-
Non-freeway Driveway	11	11%	-	-	-	-
Intersection Driveway	4	4%	-	-	-	-
Non-freeway Curved	1	1%	-	-	-	-
Other	1	1%	-	-	-	-
Intersection**						
Intersection	**60**	**60%**	1,393	37.8%	**171,569**	**64.2%**
Non-Intersection	40	40%	**2,297**	**62.2%**	95,843	35.8%
Traffic Control**						
Signal	33	33%	613	16.6%	74,154	27.7%
Stop Sign	24	24%	162	4.4%	49,814	18.6%
Yield Sign	2	2%	7	0.2%	1,254	0.5%
Other Regulatory Sign	-	-	37	1.0%	239	0.09%
Warning Sign	-	-	22	0.6%	493	0.2%

Environmental Characteristics	WATS Cases	WATS Percentage	FARS Cases	FARS Percentage	GES Cases	GES Percentage
Railway Crossing Device	-	-	1	0.05%	40	0.001%
None	41	41%	2,819	76.4%	129,201	48.3%
Other/Unknown	-	-	29	0.8%	12,217	4.6%
P-values greater than 0.1 were denoted with **. Excluded variables denoted with °.						

8.2.3.1.4 Event Characteristics

Most WATS vehicle-bicycle collisions were impacts to the front of the vehicle (81%). Likewise, most impacts in FARS and GES were to the front of the vehicle and accounted for 82.4% and 69.1%, respectively. Before the crash, in WATS, 31% of the drivers were traveling straight, 26% were turning left, and 23% were turning right. FARS and GES reported that vehicles traveling straight accounted for 78% and 40.6% of collisions, respectively. The presence of visual obstructions was not recorded in most cases, but when known, the most commonly reported in WATS were hills (5%) and traffic (6%).

Table 38 Results for Event Characteristics.

Event Characteristics	WATS Cases	WATS Percentage	FARS Cases	FARS Percentage	GES Cases	GES Percentage
Total	100	100%	3,690	100%	267,412	100%
Vehicle First Impact Location*						
Front	81	81%	3,042	82.4%	184,831	69.1%
Back	5	5%	71	1.92%	11,944	4.4%
Left	1	1%	99	2.6%	19,018	7.1%
Right	12	12%	263	7.1%	51,123	19.1%
Undercarriage	0	0%	58	1.5%	124	0.046%
Top	0	0%	2	0.054%	284	0.1%
None°	1	1%	4	0.1%	76	0.028%
Other/Unknown°	0	0%	151	4%	12	0.0046%
Vehicle Pre-event Movement**						
Going Straight	31	31%	2,880	78.0%	108,537	40.6%
Slowing/Stopping	4	4%	6	0.2%	2,717	1.0%
Starting Up on Roadway	4	4%	16	0.4%	13,733	5.1%
Stopped on Roadway	2	2%	8	0.2%	6,789	2.5%
Turning Right	23	23%	187	5.1%	69,992	26.2%
Turning Left	26	26%	163	4.4%	42,676	16.0%
Accelerating in Road	0	0%	12	0.3%	127	0.05%
Overtaking or passing	0	0%	52	1.4%	2,498	0.9%
Leaving a parking position	0	0%	-	-	1,227	0.5%
Entering parking position	0	0%	-	-	1,230	0.5%
Making a U-Turn	0	0%	1	0.03%	2,455	0.9%
Negotiating a Curve	0	0%	219	5.9%	3,886	1.5%

Event Characteristics	WATS Cases	WATS Percentage	FARS Cases	FARS Percentage	GES Cases	GES Percentage
Changing Lanes	0	0%	59	1.6%	889	0.3%
Merging	0	0%	7	0.2%	127	0.05%
Successful Avoidance	0	0%	6	0.2%	39	0.01%
Other/Unknown°	10	10%	74	2.0 %	10,489	3.9%
P-values greater than 0.1 were denoted with **. P-values greater than 0.05 were denoted with *. Excluded variables denoted with °.						
Vehicle Visual Obstruction°						
Hill	5	5%	-	-	-	-
House/Building/Intersection	1	1%	-	-	-	-
Limited Sunlight	1	1%	-	-	-	-
Parked Vehicle	1	1%	-	-	-	-
Tree/Bushes/Fence	4	4%	-	-	-	-
Traffic	6	6%	-	-	-	-
Unknown	82	82%	-	-	-	-
P-values greater than 0.1 were denoted with **. P-values greater than 0.05 were denoted with *. Excluded variables denoted with °.						

8.2.3.2 WATS Analysis

Turning crashes may present a challenge for AEB systems as the vehicle-mounted sensors may have limited field of view to detect the bicyclists. In turning cases, the bicyclist often is not in the view until just before impact. As shown in Figure 89, most drivers were going straight or turning prior to the crash which likely resulted in front or side first impacts across all three datasets. The WATS data was similar to GES with about 30-40% of cars travelling straight and about 25% turning right. In FARS however, more than three-fourths (78%) of fatal crashes occurred when the vehicle was traveling straight and very few occurred when the motorist was turning left or right.

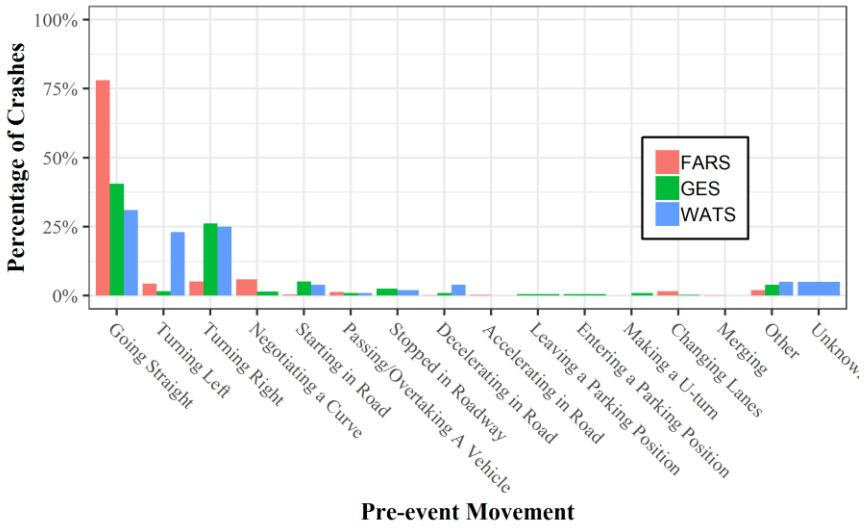

Figure 89. Distribution of vehicle pre-event movements before colliding with a bicyclist.

In addition to detecting the bicyclist, bicycle AEB systems must be able to predict the bicyclists' movement. This presents a challenge given the multitude of ways bicyclists and vehicles interact and the possibility that the bicyclist is on the road or on pedestrian pathways. Most vehicle-bicycle collisions in WATS occurred at intersections (76 of the 100 crashes). As shown in Figure 90, crashes that involved the bicyclist riding along the road only resulted in 20 collisions, which was approximately one-fourth the number of intersection crashes. There were only 3 cases in which the bicyclist was turning – 2 left turning cases and 1 right turning case. Turning left may put the bicyclist at a great risk of collision because the bicyclist had to cross another through lane, but this cannot be confirmed with this small sample of turning cases. The most common vehicle pre-crash movement was turning right, closely followed by turning left. Ride through and ride along vehicle travel paths indicate the vehicle was travelling straight through an intersection or straight on a non-junction, respectively.

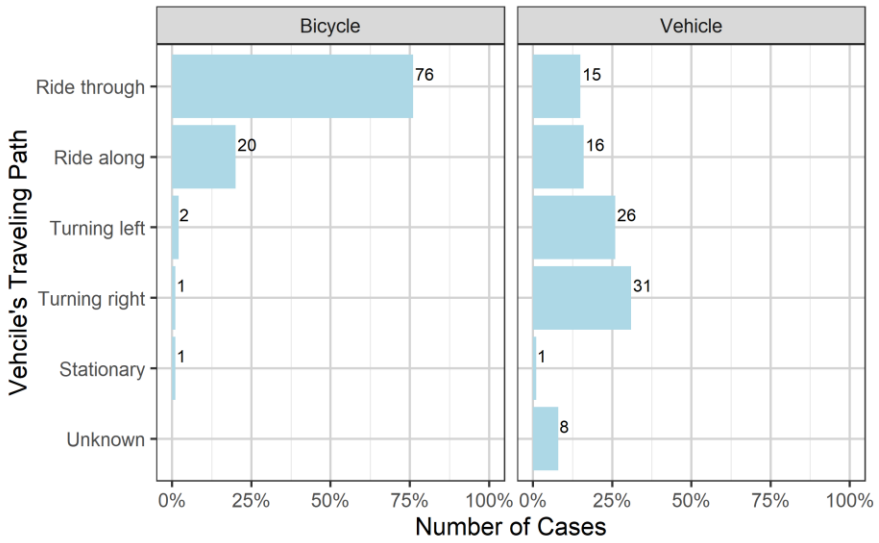

Figure 90. Percentage of crash cases for varying vehicle and bicycling traveling paths in WATS. The annotated number denotes the number of cases each bar represents.

Once the bicyclist is detected, the effectiveness of the AEB system largely depends on the time the system has to react. The longer a bicyclist is visible to an AEB system, the longer the system has to initiate braking and avoid the collision. As shown in Figure 91, the bicyclist ride along and ride through cases have similar distributions of earliest detection time. For ride along cases, the bicyclist was visible for at least half a second, 1 second, and 2 seconds for 25%, 45%, and 70% of the cases, respectively. For ride through cases, bicyclists were visible for at least half a second, 1 second, and about 2 seconds for 23%, 39%, and 69% of the cases, respectively. While AEB system parameters are highly proprietary and differ by manufacturer, one second is a commonly assumed threshold above which an AEB system could mitigate or avoid a crash. If an AEB system only needs one second to mitigate a crash, then about 60% of the crashes in the WATS database could potentially be mitigated.

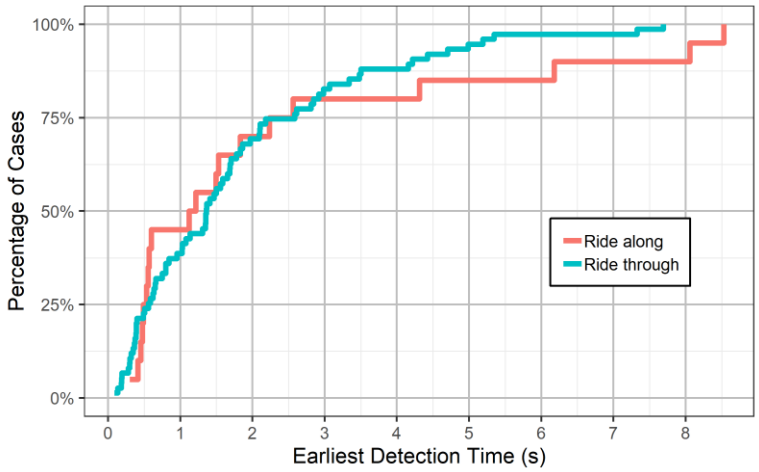

Figure 91. Cumulative distribution of earliest detection time for ride along and ride through cases in WATS.

8.2.4 DISCUSSION

This study examined vehicle-bicycle crashes investigated by Washtenaw Area Transportation Study (WATS) in southeast Michigan with support from Toyota CSRC. The goal of this study was to elucidate prevalent conditions for U.S. vehicle-bicycle crashes and examine factors that could be detrimental to AEB effectiveness. The data from WATS was able to provide many details about vehicle-bicycle crashes that are not available in national databases and could be very useful in research and further development of AEB.

Although WATS data collection was limited to southeast Michigan, WATS was broadly similar to the nationally representative GES. The two exceptions were weather and bicyclist gender which had statistically significant differences between WATS and GES. While weather conditions, e.g. rain, could affect AEB performance and was significantly different between the datasets, the distribution of road surface conditions, e.g. wet vs. dry pavement, was not significantly different. This counterintuitive finding may reflect actual differences in weather at the time of collision, but may also reflect how quickly investigators were able to visit the scene after the collision (which could be expected to have occurred, in some situations, after the weather had changed). WATS and GES also had significantly different distributions of bicyclist gender. Although bicyclist gender could affect

bicyclist speed, it would likely have little effect on crash causation factors or AEB detection capabilities.

The WATS database provides a unique dataset of in-depth investigation of vehicle-bicycle crashes in the U.S. which allows computation of important parameters such as earliest detection opportunity and distance travelled in the road. This study was limited by the number of cases (100) in the WATS dataset. Another limitation in the study was the lack of available travel speed data in the WATS dataset. For bicyclists riding along the road, our study used posted speed limits as a surrogate for the driver's travel speed. This assumption may affect the earliest detection calculation. For all cases, bicyclist speed was not known and therefore had to be estimated based on literature values. There were two cases where the bicyclist's speed and earliest detection time could not be calculated and were omitted from our calculations.

This work presents variables that can contribute to the potential effectiveness of AEB in reducing/mitigating vehicle bicycle crashes. In order to estimate effectiveness further research needs to examine the time requirements for braking, the effects of pavement conditions on maximum possible braking, and the effects of obstructions. WATS does not record impact speed or travel speed of the vehicle which make it difficult to simulate the crashes accurately. While WATS is more in-depth than publicly available vehicle-bicycle crash databases in the US, a national study that includes a larger sample size, crash reconstructions, and more detailed injury information would benefit AEB effectiveness estimations.

AEB is a promising active safety technology that may avoid or mitigate many vehicle-to-bicycle collisions. Bicyclists were on the road for more than one second prior to impact in 60% of the WATS cases. Assuming that an AEB system requires a minimum of one second for detection and brake activation, these collisions would be potentially detectable by an AEB system with sufficient time to take evasive action. However, for the remaining cases with less than one second of time to react (40%

of cases), an AEB system would be challenged to avoid or mitigate the collision. Collision type, such as straight crossing path or turning, could also affect AEB effectiveness.

8.3 CHARACTERISTICS OF VEHICLE-BICYCLE CRASHES AND NEAR-CRASHES USING NATURALISTIC DRIVING DATA [7]

8.3.1 INTRODUCTION

This study is motivated by a need to reduce the incidence of bicyclist injuries and fatalities from vehicle-bicycle collisions in the U.S. and examines the feasibility of automatic braking systems to accomplish this goal.

An important factor in bicyclist detection is the time the bicyclist is visible. If an automated braking system could detect a bicyclist, a crash could be avoided or injury decreased. Vehicle and bicycle speed before a crash and presence of visual obstructions have been shown to be significant factors in determining the severity of a crash, but can also affect the detectability of cyclists [92]. Studies are being conducted to model cyclist behavior with the goal of testing and improving pre-collision systems [86, 90, 93]. While these studies have successfully modeled much of the movement of a typical bicyclist, little has been reported on how effective these pre-collision systems would be in real world examples in the U.S. In Europe, the effectiveness of automated emergency braking systems in situations with pedestrians have been estimated to reduce fatalities by 11-40% and seriously injured persons by 14-27% [10, 94, 95]. For this reason, characterizing vehicle and bicyclist speeds and duration of visibility is necessary to determine whether and when the bicyclist would be detectable by active safety systems. The objective of this study was to characterize the types of interactions between vehicles and cyclists with the goal of determining if vehicle active safety features could potentially mitigate these vehicle-bicycle interactions.

8.3.2 *APPROACH*

This study used the Second Strategic Highway Research Program (SHRP 2) Naturalistic Driving Study (NDS) data to examine interactions between vehicles and bicycles. SHRP 2 vehicles are instrumented with five cameras, but for the purposes of this study only the forward facing video was examined. The forward facing camera is an analog standard definition camera that captures at a frame rate of 30 frames per second. The camera has a focal length of 3.6mm and a horizontal field of view of 67.4 degrees. The video is captured and scaled to 480x360 pixels for storage on the SHRP 2 data acquisition system.

The interactions were categorized by SHRP 2 data reductionists by type of interaction, severity, vehicle type, and driver distractions, among others. In our study, the data set was filtered to include only interactions with pedalcyclists (any severity was accepted) resulting in 65 events. A pedalcyclist was defined as bicyclists and other cyclists, including riders of unicycles, tricycles, and any other vehicle powered only by pedals [96]. For the remainder of this paper these road users will be referred to as bicyclists as all the cases involved bicycles. The data set consisted of 3 crashes, 61 near-crashes, and 1 non-subject conflict. In SHRP 2, an event was considered a crash if the subject vehicle made any contact with the bicyclist that results in kinetic energy measurably transferring or dissipating. An event was considered a near-crash if a rapid evasive maneuver by the subject vehicle or bicyclist was required in order to avoid a crash. A rapid evasive maneuver refers to a change in steering, braking, accelerating or any combination of these maneuvers. Three of the near crash events were missing video and were therefore excluded. The non-subject conflict event, an event in which the subject vehicle observed an incident with a bicyclist, did not have enough information for analysis and was excluded. The final dataset consisted of 61 cases (58 near-crashes and 3 crashes).

While not ideal, near crashes are acceptable surrogates for crashes because there is a positive relationship between the frequency of factors that contribute to crashes and near crashes [97]. Guo,

et al. [97] found that the inclusion of both near crash data and crash data increases the precision of contributing factor risk estimations.

8.3.2.1 Classification of Interaction Types

In each case, the factors which may have influenced the crash or near-crash were examined including, but not limited to the speeds of the vehicle, road conditions, light conditions, and the path of the vehicle and bicycle. These factors were compared to bicyclist crash data extracted from the General Estimates System (GES) and the Fatality Analysis Reporting System (FARS) to ensure that the SHRP 2 sample was representative of national vehicle-bicycle crash statistics. GES is a probability sample of about 60,000 police-reported crashes of all severities (no injury to fatal injury) that use weighting factors to scale case counts to match national figures. These weighting factors were incorporated in our analysis of the GES data. FARS is a census of all U.S. traffic crash fatalities. While these data sets are large, they do not contain the level of detail provided by the SHRP 2 sample. The SHRP 2 database records video of the incident which can provide information such as the path of the vehicle and bicyclist, speed of the vehicle and the bicyclist before the crash, and the duration the bicyclist was visible. These parameters are not available in the GES or FARS data. The paths of the vehicle and bicycle were recorded and compared to the data reductionist's analysis of each incident. The different types of vehicle and bicycle interactions are shown in Figure 92.

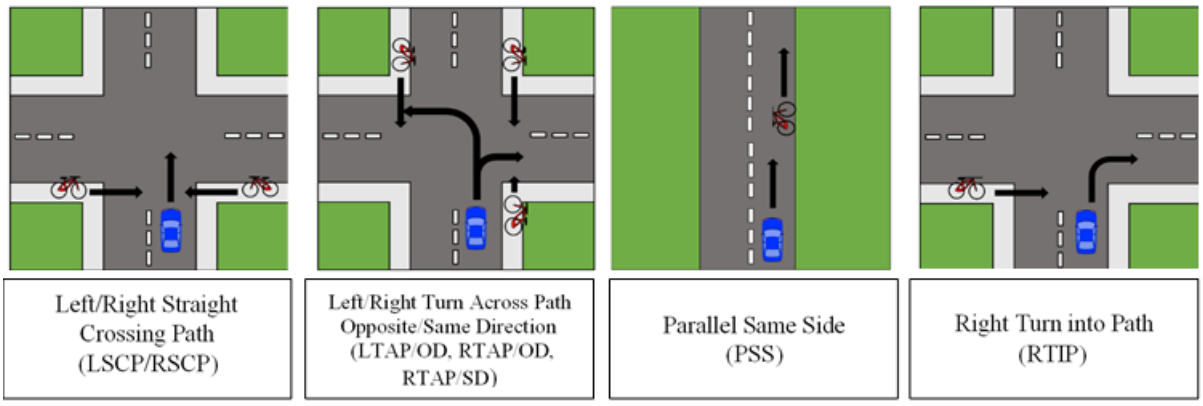

Figure 92. The most common vehicle-bicycle interactions found in the SHRP 2 NDS database.

8.3.2.2 Determine Duration Bicyclist was Visible

The duration that the bicyclist was visible was calculated using the timestamps provided in the SHRP 2 NDS videos. Both the total time duration visible and the on road duration visible were calculated. The total duration visible was considered to be the time from when the bicyclist was first visible to the forward facing camera until the proximity point. The on-road duration visible was considered to be the time from when the bicyclist first entered a travel lane or road as seen by the forward facing camera until the proximity point. As shown in Figure 93 (left), the total duration visible and the on-road duration visible will differ when, for example, a bicyclist was first visible on a sidewalk prior to beginning to cross the street. The on-road duration visible will always be less than or equal to the total time duration visible.

The proximity point was defined as the timestamp of when the vehicle and the bicycle first made contact or, in the absence of contact, when the vehicle and bicycle were the least distance apart [98]. This point was originally determined by the data reductionists who categorized the SHRP 2 dataset and then verified by the authors using both the forward facing video and the time series data. In a case where a bicyclist was obstructed, the time visible was considered to begin from that point at which the bicyclist was consistently visible as shown in Figure 93 (right).

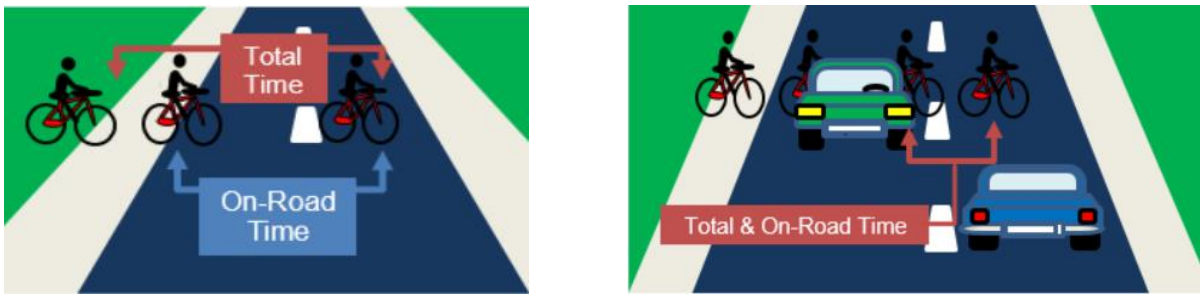

Figure 93. Visual depiction of time and total time in non-obstructed and obstructed cases.

8.3.2.3 Determine Speed of Bicyclist

The speed of the bicyclists was determined using video time stamps and standard lane widths. Typical lane widths range from 3-3.8m. Most of the cases occurred in urban or rural environments, rather than on the wider roads of the interstate highways. As we could not measure the lane width for each case, we assumed lane width to be 3m. By choosing a lane width estimate of 3m, the narrower end of the spectrum, the resulting bicycle speed measurements will more likely be overestimates of the actual speed.

If the bicyclist path was perpendicular to the vehicle, the timestamps were used to record how long it took for the bicyclist to cross a specific number of lanes. In most cases, the bicyclist was only consistently visible for the length of one lane, but in those cases where bicyclists were visible for multiple lanes, the maximum number of possible lanes was utilized. The speed was assumed to be constant for all cases as the measurement technique could not accurately measure acceleration.

If the bicyclist path was parallel to the vehicle, multiple methods were used to determine the speed of the bicycle. First, if at any point in the video the vehicle and the bicycle were traveling at the same speed, then the bicycle speed was concluded to be the same as the network speed indicated by the on-board network of the vehicle at that point. If that approach was not possible, then the time it took for the bicyclist to cross a side entrance to the road, such as a cross street, entrance to a parking lot, or a driveway was used. We assumed that the side entrance had roughly the same width as a lane and the method that was used for the bicycles with a perpendicular path was then also used to determine the speed of the bicyclist on a parallel path. If there were no side entrances that the bicycle passed within the span of the video, then road markings were used to estimate the distance the bicycle traveled. This was only necessary in one case within the sample set. For this instance, we determined that the distance between the raised pavement markers was 12.2 m (40ft) [99]. This distance and the time required for the bicyclist to travel from one pavement marker to the other was used in conjunction to determine the speed of the bicyclist.

The bicyclists were then categorized as either going slow, moderate or fast based on average bicycling speeds in different scenarios [90]. A moderate speed was considered to be any speed between 10-20 km/h, slow was defined to be any speed less than 10 km/h, and fast was considered to be any speed greater than 20 km/h.

8.3.2.4 Time Series Data Analysis

The SHRP 2 time series data was used to analyze driver reaction, specifically acceleration/deceleration, speed, and braking application.

Speed at both the proximity point and one second prior to the proximity point were calculated using the time series data. The time series sampling rate for speed differed between vehicles and was not synchronized with the video frame rate. Therefore, linear interpolation was used to estimate the speed at the specific proximity point collected from the video.

The acceleration data was noisy resulting in higher deceleration values than we would expect. To smooth the acceleration curves we interpolated the network speed velocity and differentiated to calculate the acceleration over the event. While true deceleration may be noisy, the smoothed acceleration data calculated from the change in velocity results is an averaged deceleration which may be more useful for developing simplified driver braking profiles. The maximum deceleration was determined by taking the minimum acceleration value from the event. If a driver did not decelerate then their maximum deceleration was reported as zero.

8.3.3 RESULTS

The SHRP 2 NDS dataset contained a combined 61 vehicle-bicycle near-crashes and crashes. This SHRP 2 subset roughly follows the trends of larger datasets such as bicyclist crashes in the FARS and GES databases. As shown in Table 39, the SHRP 2 data set, similar to GES and FARS, has a majority of cases that involve male bicyclists and adult riders. Additionally, like the GES and FARS data sets,

most of the SHRP 2 cases occurred during daylight hours and in clear weather. The SHRP 2 data set differed in the most common vehicle types, crash locations, and bike positions.

Table 39. Composition of the SHRP 2 data compared to 2015 GES and FARS bicycle crash data.

Variable	SHRP 2 Count	Percent of Total	GES Count	Percent of Total	FARS Count	Percent of Total
Total Number of Events	61	-	51,203	-	817	-
Bicyclist Gender						
Male	42	69%	40,175	78.5%	697	85.3%
Female	12	20%	9,481	18.5%	120	14.7%
Unknown	4	7%	1,547	3%	-	-
Mu1tiple Riders	3	5%	-	-	-	-
Age						
Adult	56	92%	43,547	85%	767	94%
Child (<16)	5	8%	7,657	15%	50	6%
Vehicle Type						
Car	50	82%	28,173	55%	318	38.9%
Light Truck or Van (LTV)	11	18%	19,123	37.3%	351	43%
Other/Unknown	-	-	3,907	7.6%	148	18.1%
Lightning Condition						
Daylight	47	77%	38,406	75%	366	44.8%
Dusk	7	11%	1,980	3.9%	32	0.1%
Dark – Lighted	5	8%	7,619	14.9%	173	21.2%
Dark- Not Lighted	2	4%	2,415	4.7%	181	22.2%
Missing/Unknown	-	-	783	1.5%	65	8%
Weather						
Clear	51	84%	40,221	78.6%	622	76.1%
Cloudy	4	7%	7,530	14.7%	113	13.8%
Rain	6	10%	2,891	5.6%	27	3.3%
Other	-	-	561	1.1%	55	6.7%
Crash Location						
At intersection	42	69%	29,715	58%	227	27.8%
Intersection-Related	6	10%	3,911	8%	74	9.1%
Not at Intersection	13	21%	17,479	34%	508	62.2%
Unknown/Other	-	-	98	0.2%	8	1%
Bike Position						
Travel Lane	33	54%	29,352	57.3%	640	78.3%
Sidewalk/Crosswalk	24	39%	17,654	34.5%	85	10.4%
Bicycle Lane/ Paved Shoulder	2	3%	3,165	6.2%	76	9.3%
Unknown/Other	-	-	1,033	2%	16	2%

Based on the SHRP 2 NDS sample, the most common vehicle-bicycle near crash scenarios were the left and right straight crossing path (RSCP, LSCP) interaction with a combined 54% incidence rate and, respectively, a 33% and 21% incidence rate. This was followed closely by the turn across path/opposite direction scenario with a combined incidence rate of 23%. Left and right turn across path/opposite direction (LTAP/OD, RTAP/OD) had incidence rates of 15% and 8%, respectively. The parallel same side scenario (PSS) had an incidence rate of 10%, the right turn into path scenario (RTIP) had an incidence rate of 5%, and the right turn across path/same direction (RTAP/SD) scenario had an incidence rate of 3%. The "Other" category consisted of incidents that were considered irregular and therefore did not fit into any of the previously mentioned categories. The incidence rates are shown graphically in Figure 94.

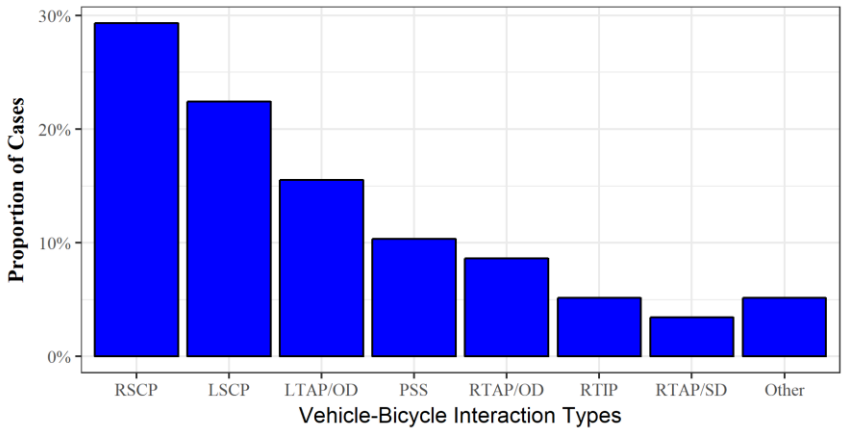

Figure 94. Breakdown of the incidence of the different vehicle bicycle interaction types by percentage of total cases.

The average duration the bicyclists were visible on or off of the road before the proximity point was 2.2 seconds. The average duration the bicyclist was both visible and on the road was 1.8 seconds. As shown in Figure 95, only 31% of the bicyclists were visible for less than 1 second prior to the proximity point which included time the bicyclist was not on the road. If only the time the bicyclist was on the road is considered, then 51% of bicyclists were visible for less than 1 second.

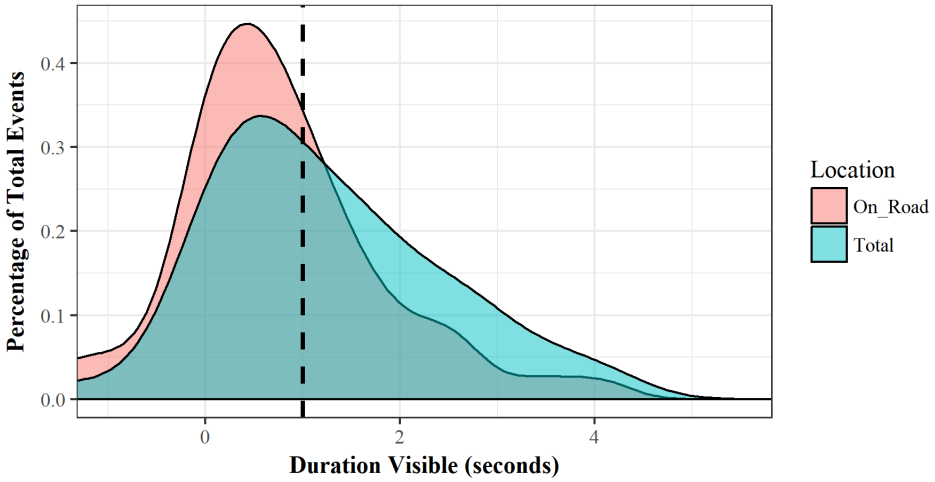

Figure 95. Distribution of duration of bicyclist visibility (seconds) before the proximity point (blue) compared to the duration the bicyclist was both visible and on the road (pink). The dashed line marks the one second threshold.

The average speed of the bicyclist was faster when the bicyclist was traveling parallel to and in the same direction as the subject vehicle (PSS). As shown in Figure 96, the PSS vehicle-bicycle interaction type resulted in much higher bicyclist speed while the other interaction types resulted in relatively similar bicyclist speeds.

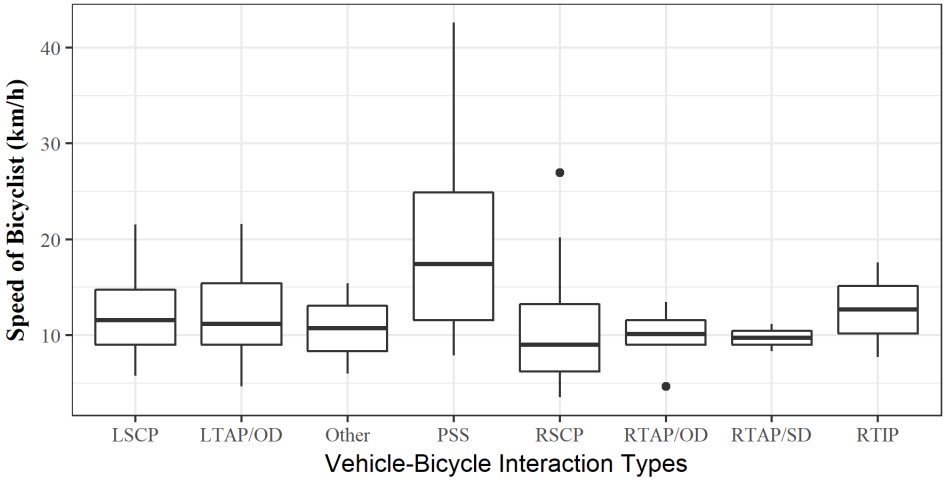

Figure 96. Box plots of the speed bicyclists were travelling grouped by the vehicle-bicycle interaction type.

The bicyclists traveling parallel to and in the same direction as the subject vehicle (PSS) was also visible for a longer duration than bicyclists interacting with vehicles in other ways

(Figure 97). The PSS group also had the largest variability, particularly in the 3rd quadrant, which indicates that the distribution was left skewed. As shown in Figure 97, the RTAP/SD interaction type had the lowest average duration of visibility.

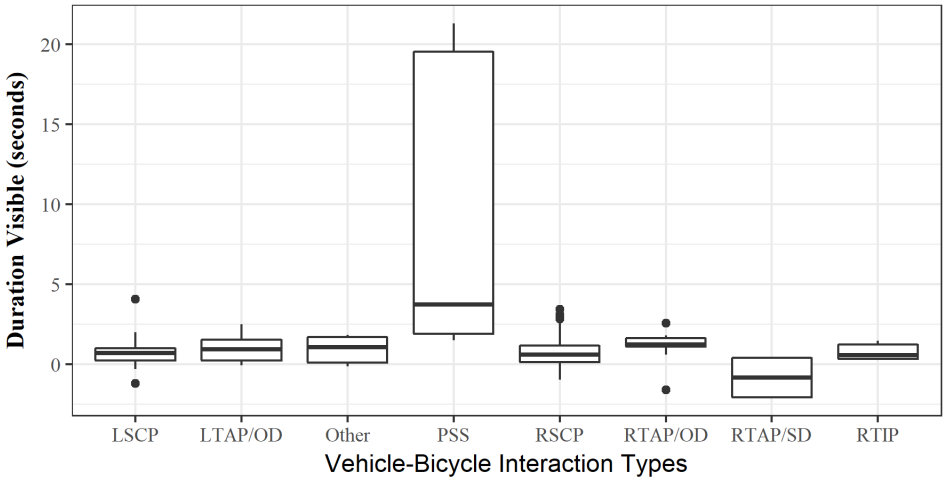

Figure 97. Box plot of the duration bicyclists were both visible and on the road grouped by the vehicle bicycle interaction type.

The vehicle operator's response was quantified by comparing the vehicle's speed 1 second before the proximity point to the vehicle's speed at the proximity point. As shown in Figure 98, the majority of the vehicle operators reduced their speed, by an average of 8.55 km/h (2.38 m/s), in the 1 second leading up to the proximity point. This reduction in speed corresponds to an average of 0.208g of deceleration over the one second prior to impact.

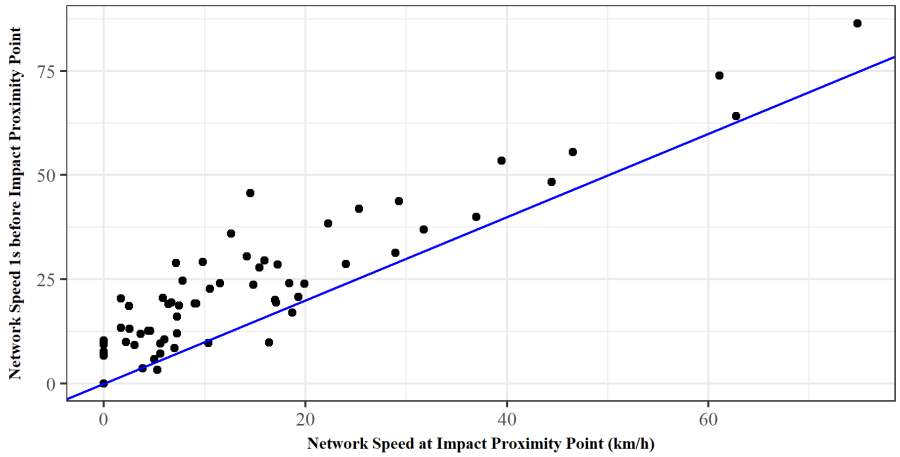

Figure 98. The speed in km/h between vehicles 1 second before proximity point and at the proximity point. The horizontal distance between the data point and the no brake line (blue) indicates the increase or decrease in speed.

In all of the SHRP 2 cases, the driver decelerated prior to the proximity point. Figure 99 shows the extent to which the drivers braked during the event. AEB is expected to reach approximately 0.8g of braking, but no SHRP 2 drivers applied braking near 0.8G. The median value of all maximum longitudinal decelerations for SHRP 2 drivers was 0.25g.

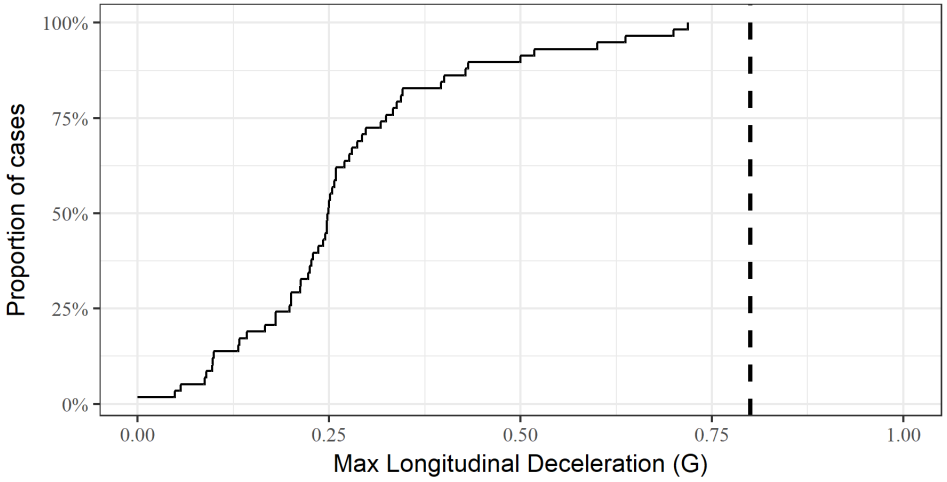

Figure 99. Cumulative distribution plot of the maximum longitudinal deceleration for each event.

8.3.4 DISCUSSION

The SHRP 2 NDS case studies had over three times as many male bicyclists as female bicyclists. This is consistent with the U.S. bicyclist fatality data as males are more likely to have a crash with a vehicle. The National Highway Traffic Safety Administration, reports that male bicyclists have a fatality rate about six times higher than that of females and an injury rate about 4 times higher than females [96]. The SHRP 2 cases followed the trends of the GES and FARS data with a few notable exceptions. The SHRP 2 data set had relatively more cars involved in incidents than the GES and FARS data sets. This may be because the SHRP 2 data set comes from instrumented personal cars and light trucks and vans (LTVs), while the GES and FARS data sets include heavy trucks and other

commercial vehicles. The SHRP 2 crash locations and bike positions were relatively more similar to the GES data than the FARS data. This may be because the GES data contains bicyclist collisions of all severities, while the relevant FARS data consists of bicyclist fatalities. The SHRP 2 data set examined dealt mostly with near crashes and was therefore expected to be more similar to the GES data distributions than the FARS distributions.

The observed vehicle-bicycle interactions can be split into 6 main categories with the most frequent cases being left/right straight crossing path (LSCP/RSCP) and left turn across path/opposite direction (LTAP/OD). This distribution of cases is consistent with studies conducted on European bicyclist crash data (*6*). The major difference between vehicle-bicycle interactions and vehicle-vehicle interactions is that bicycles can ride on the road (or bike path) like a vehicle or on the sidewalk like a pedestrian. This creates additional scenarios such as PSS in which a bicycle and a vehicle are sharing a lane or RTAP/OD in which the bicyclist is traveling on the right shoulder in the opposite direction of the vehicle.

The speed of the vehicle one second before the proximity point compared to the speed at the proximity point indicates whether the driver took evasive actions before the proximity point. In all near-crash cases in our dataset the driver braked before reaching the proximity point. In some cases, the driver accelerated in the one second prior to the proximity point. This generally occurred when the driver was stopped at an intersection and a bicyclist crossed in front of the vehicle while the vehicle was accelerating. This measurement demonstrates the cases that the driver was aware of the cyclist with enough time to avoid them. The cases that fall below the no brake line (Figure 98) indicate that the driver was unaware of the cyclist until less than one second before the proximity point. It is in these cases that an automated braking system would be extremely helpful by alerting the driver of the bicyclists' presence.

An important factor in bicyclist detection is the time the bicyclist is visible. If an automated braking system could detect a bicyclist at an early enough point, a crash could be avoided or mitigated. Impact speed is correlated with injury severity meaning that the higher the impact speed, the more likely the pedestrian or bicyclist is to be injured [10]. Studies have shown that initiating automatic braking one second before collision can decrease the injury severity substantially [10]. As shown in Figure 95, bicyclists were visible and on the road for less than 1 second in 51% of the cases. This suggests that in 49% of the cases an automated braking system could have helped mitigate injury severity or avoided the incident altogether.

In the cases where the bicyclists were traveling perpendicular to the vehicles (LSCP and RSCP), the average time visible is lower than bicyclists traveling in paths parallel to vehicles. This is due, in part, to the fact that this study only looks at views of a forward facing camera. Often in perpendicular cases, the cyclist was out of view of the camera until near the proximity point. Potential bicyclist detecting automated braking systems with a camera configuration similar to SHRP 2 may also have limited field of views [14]. It may be difficult for such safety systems to detect these perpendicular traveling pedestrians with enough time to initiate braking or other safety features.

Obstructions are another potential challenge for early detection of bicyclists. In one specific case, a bicyclist crossed an intersection in the crosswalk from the left (LSCP). The bicyclist was visible when first crossing the road, but was then obstructed by a large stopped truck in the adjacent lane. The bicyclist was out of the driver's view for approximately 1.5 seconds and then reappeared 1.1 seconds before the proximity point. Many current automated braking systems are not designed to track objects that have gone out of view for extended periods of time.

This study provides valuable insights into designing bicyclist detection systems. As shown in Figure 95, bicyclists were generally visible for longer than they were on the road. Automakers can gain additional warning time by tracking bicyclists prior to their entering the roadway. Additionally,

in some cases the duration the bicyclists were visible may have been artificially low because only the front camera was examined. Automakers may want to consider additional sideways facing sensors, or sensors with larger FOVs to increase the detection range of their systems. The implications for regulatory agencies include improving both vehicle impact testing scenarios to account for a wider range of possible vehicle-bicycle interaction types and automatic emergency braking tests for bicyclist detection.

This study is limited by the small available sample set and is based solely on forward facing cameras and smoothed time series data. An improved analysis would consider driver attention through examination of driver facing cameras. This analysis could pinpoint when the bicyclist became visible to the driver and when the driver reacted after seeing the bicyclist. Another limitation is in the method required to estimate bicyclist speed. The use of video processing and simulation techniques to track the speed and location of the bicyclists in relation to the subject vehicles would aid in determining if bicyclists would be detectable using current automatic braking systems.

This study aimed to classify the various vehicle-bicycle interactions in the U.S. and determine whether the introduction of active safety features could mitigate vehicle-bicycle interactions. The circumstances of the interaction, the speed of the vehicle and the bicycle, and the duration of bicycle visibility were all examined as these factors affect a pre-collision system's ability to detect a bicyclist. It was found that the most prevalent vehicle-bicycle incidents occurred when the bicycle traveled straight across the path of the vehicle or when the vehicle turned left across the path of the bicyclist. The average time visible was dependent on the path and speed of the bicyclist with the bicyclists traveling in the same direction remaining visible for longer than the bicyclists traveling across the path of the vehicle. While other factors such as the angle of the cyclist relative to the vehicle need to

be considered, the time visible measurement indicates that, in 49% of the cases, automated braking would have the potential to decrease the severity of the crash or avoid the crash altogether.

8.4 Conclusion

Overall, data from WATS and SHRP 2 indicated that most bicyclists were visible for longer than one second, which is promising for bicyclist AEB as the system would often have sufficient time to detect the bicyclist and take action to avoid the crash. The SHRP 2 duration visible cumulative distribution plots were shifted slightly to the left of the WATS curves meaning that the SHRP 2 bicyclists were visible for a shorter duration than WATS (Figure 100). However, this difference could be due to the differences in calculation methods. The SHRP 2 duration visible was calculated using a forward facing camera which has a limited field of view. The bicyclist was not considered visible until they entered the field of view of the camera. Human drivers have a wider field of view, and could have potentially seen the bicyclists at an earlier time. Additionally, the WATS duration visible calculations were completed based on crash scene diagrams, field of view was not considered and the calculations depended on average bicyclists speeds.

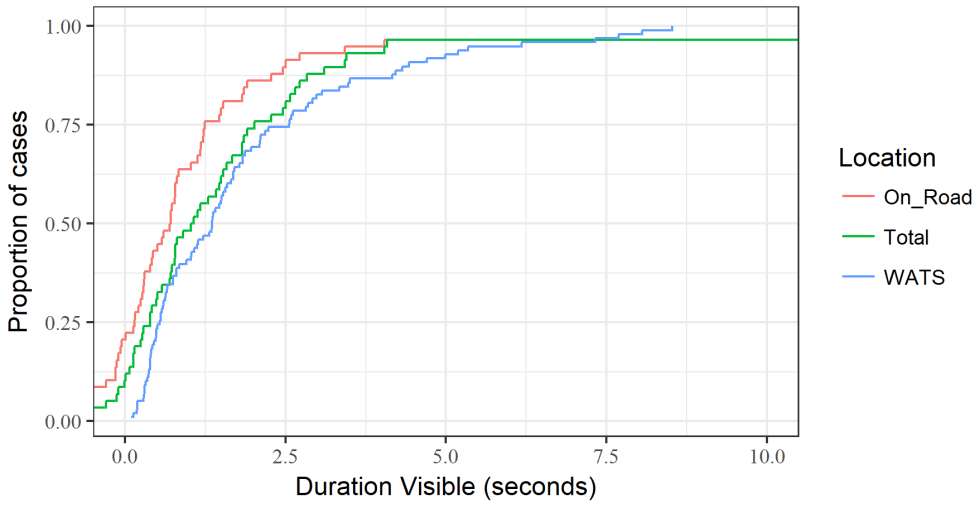

Figure 100. Cumulative distribution plot of the total and on-road time the bicyclist was visible before the proximity point (SHRP 2) compared to the WATS estimated earliest detection opportunity.

9 BICYCLIST AEB EFFECTIVENESS

9.1 RESEARCH OBJECTIVE

The objective of this chapter was to use the earliest detection opportunity estimated in Chapter 8 and the posted speed limit collected in WATS to estimate the effectiveness of a prototypical bicyclist AEB system on impact speeds.

9.2 APPROACH

9.2.1 DATA SOURCE

This study utilized the WATS database to examine the potential effectiveness of bicyclist AEB. We assumed that the system would only be effective in frontal collisions. Therefore, we filtered out crashes in which the first impact location of the vehicle was the front Table 40. WATS only examined cases involving passenger vehicles

Table 40. WATS Case Exclusion Criteria.

Case Exclusion Criteria	Number of Cases Remaining
None	100
Missing Speed Limit or Earliest Detection Opportunity	97
Non-Frontal Impact	78

9.2.2 BICYCLIST AEB MODEL

The bicyclist-AEB model followed a similar approach to the pedestrian-AEB temporal model presented in chapter 5. The AEB system model had two components: 1) bicyclist detection and 2) evasive braking. The system has a latency period, which was defined as the time required for the system to prepare the vehicle for braking. It was assumed the system instantaneously identified the object as a pedestrian and determined the pedestrian was on a collision course with the vehicle. The

latency period was applied to the time the bicyclist was visible. The time the bicyclist was visible was calculated using the scene diagrams from WATS (Chapter 8). The speeds of bicyclists were assumed to depend on age, gender, and crossing behavior. Bicyclists crossing behavior was defined as riding along the road, riding through an intersection, or turning left. Bicyclists were assumed to only be visible once they entered the road.

Once the vehicle was within the time-to-collision (TTC) threshold of the bicyclist and the latency time had elapsed, the bicyclist AEB model initiated evasive braking (Figure 101). The system constantly braked at the maximum braking force safely possible for the road conditions. The assumed braking force values, shown in Table 41, were dependent on road surface conditions[69]. We assumed the AEB achieved maximum braking with a jerk of 30 m/s^3 [23]. ABE systems currently on the market may deliver a warning to the driver prior to automatic braking, time-permitting, but this was not modeled in this study.

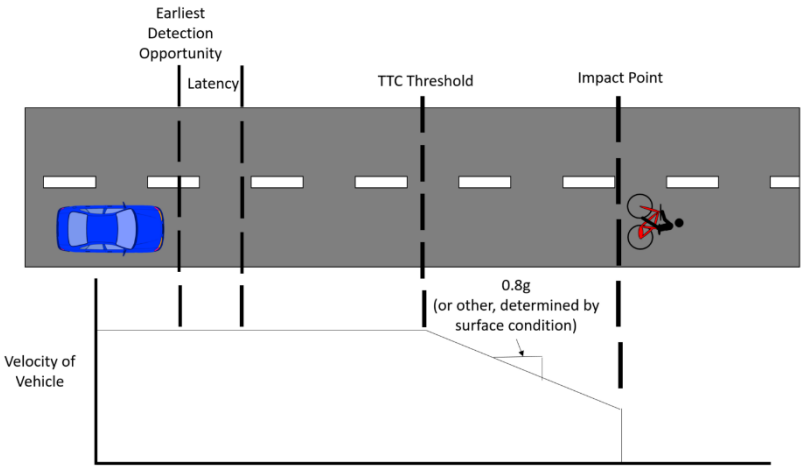

Figure 101. Diagram of AEB system modeled.

Table 41. Maximum system braking forces assumed based on road surface conditions [69].

Road Surface Condition	Braking Force (g)
Dry/Unknown	0.8

Wet	0.4

The travel speed of the vehicle is an important component in determining the impact speed (if an impact occurs) of the vehicle, but this variable was not reported in WATS. As a surrogate, the travel speed was assumed to be the posted speed limit as reported in the WATS database. Additionally, injury risk was not evaluated because WATS did not contain detailed injury information necessary for injury risk curve development.

9.3 RESULTS

As TTC values increase and latency values decrease, the percent of cases that could be avoided increases (Figure 102). The maximum number of cases that could be avoided within the range of TTC values and latency values presented was 50% for frontal only crashes. Not all events in which the bicyclist was detectable for longer than one second were avoidable. Unfavorable road surface conditions and high vehicle travel speeds increased the amount of time the vehicle needed to stop. Figure 102 shows that there was a substantial difference between TTC values above and below one second. No cases with a TTC value of 0.5 and 0.75 could be avoided regardless of the latency value.

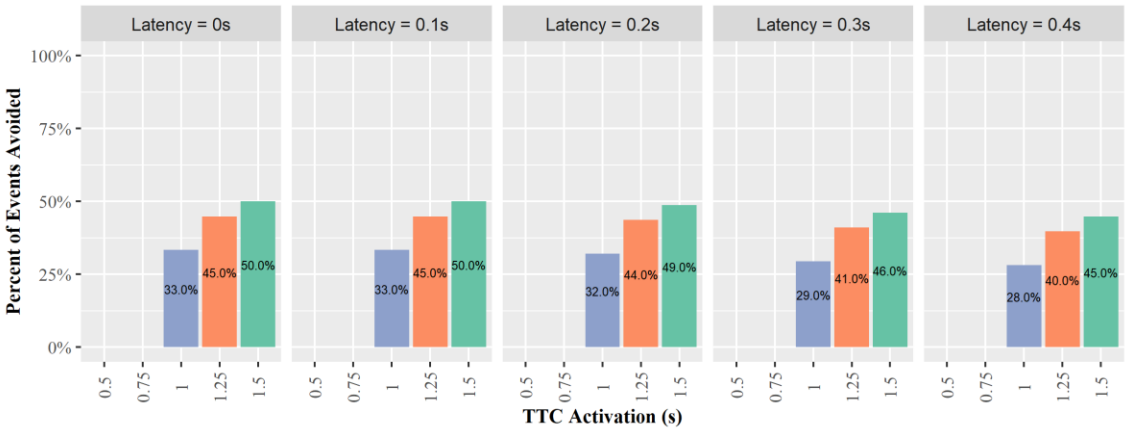

Figure 102. Events avoided through braking using differing latency and TTC values.

Figure 103 shows the average change in velocity experienced by the vehicles that were unable to avoid the collision. As expected, the longer the latency, the smaller the change in velocity. The average velocity change did not vary linearly with TTC values. This likely occurred because as TTC increased the remaining unavoided cases were more difficult to avoid due to adverse road surface conditions or a low bicyclist visibility.

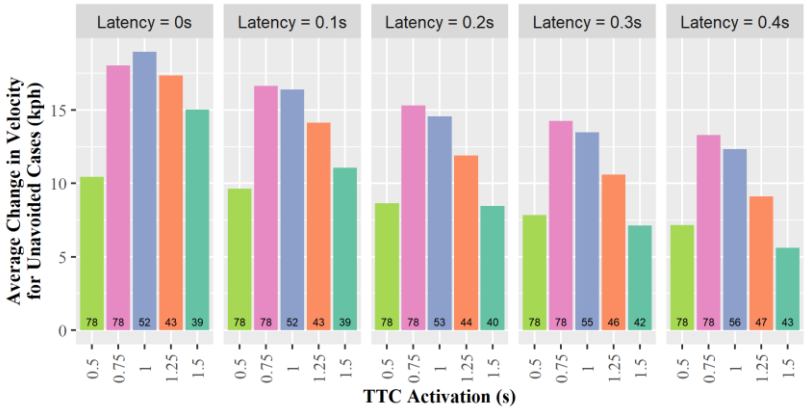

Figure 103. Average change in velocity for unavoided cases. The number in the bar corresponds to the number of unavoided cases for a given AEB system configuration.

Figure 104 examined the average change in velocity in wet (Mu=0.4) and dry (Mu=0.8) road surface conditions individually. The collisions that occurred in wet conditions had an increasing trend in change in velocity while the TTC increased, which is expected. These same four crashes that occurred during wet roadway conditions were unavoidable by all the tested system configurations. The non-linearity of the average change in velocity for dry conditions, shown in Figure 104, could be explained by the number of crashes remaining in each grouping (denoted by the number in the bar). The system with a TTC threshold of 1 second and a latency value of 0 seconds had 52 crashes that were unavoided compared to 78 unavoided crashes for the systems with TTC thresholds of 0.5 and 0.75. Although, a higher TTC threshold should translate to a greater change in vehicle speed, this trend was not seen because the number of cases in each group also changed as TTC increased. As TTC

increased, less crashes occurred and the crashes that remained were more difficult to avoid resulting in lower changes in vehicle speeds rather than higher.

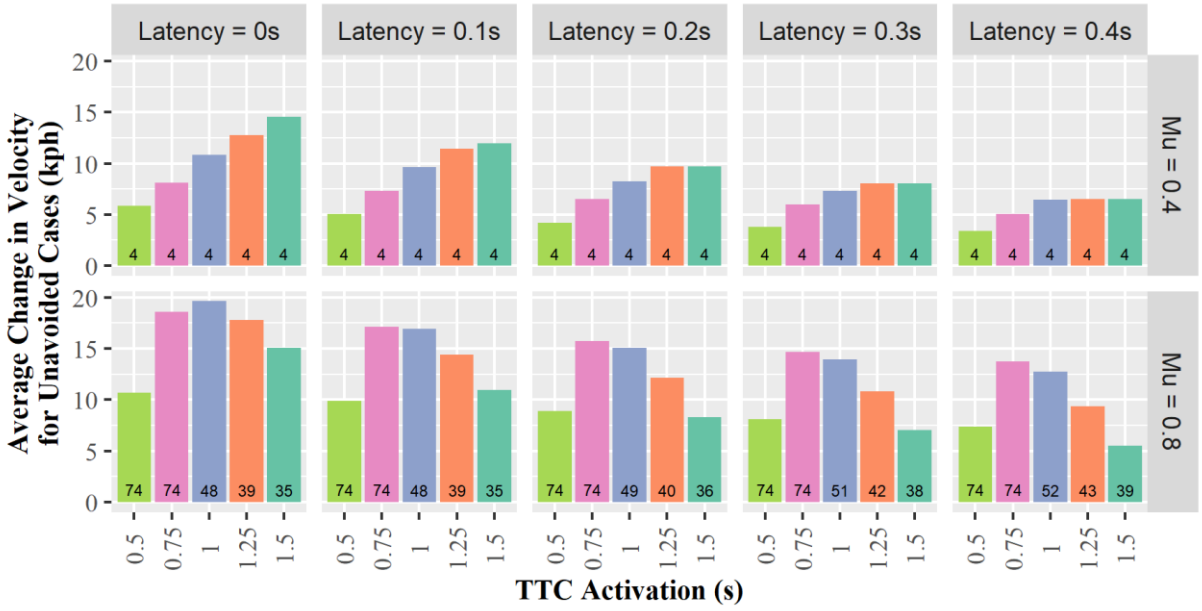

Figure 104. Comparison of average change in velocity for cases that could not be avoided from braking alone. Split by road surface conditions: Mu = 0.4 was assumed for wet road conditions, and Mu = 0.8 was assumed for dry road conditions. The number in the bar corresponds to the number of unavoided cases.

9.4 DISCUSSION

Even with the best AEB system, not all vehicle-bicycle crashes could be avoided. This model estimated that a bicyclist-AEB system with a TTC threshold of less than one second would not be effective in avoiding crashes and no examined systems were effective in adverse weather conditions. These results seem somewhat counterintuitive and may be connected to the assumption that the vehicle was travelling at the speed limit. While in non-junction areas this assumption may be accurate, near intersections we would expect vehicles to be traveling more slowly as they may be slowing down or speeding up from a stop. Intersection crashes made up 43% of the WATS database. The potential overestimation of travel speed likely reduced the effectiveness estimates as vehicles traveling faster require more time to come to a complete stop to avoid a collision.

Figure 105 shows the vehicle speed compared to earliest detection time. The curved line denotes the maximum earliest detection time needed to avoid a crash for a given travel speed. It should be noted that this does not account for the time increase due to braking. As the vehicle brakes, the speed is reduced, and the elapsed time increases. The dotted line did not capture this phenomenon, which explains why there are crashes that were avoided that are to the left of the line (Figure 105). Additionally the dotted line did not account for TTC or latency.

Figure 105. Vehicle speed (speed limit used as surrogate) compared to earliest detection time. The curved line denotes the maximum earliest detection time needed to avoid a crash for a given travel speed. The color of the point indicates whether that cases could be avoided (green) by a system with a 1.5 second TTC of braking and 0 second latency, or not avoided (red).

The model defined avoidance as the vehicle being able to stop completely before the point of impact. This is sometimes called “temporal avoidance”. The other alternative is “spatial avoidance” in which the vehicle does not stop completely, but slows sufficiently to allow the bicycle to pass without collision. Including both spatial and temporal avoidance in our model would likely increase our effectiveness estimate, but more complex spatiotemporal modelling requires additional

information that was not available in the WATS dataset. The WATS database contained crash scene diagrams which were instrumental in determining earliest detection opportunity, but did not reconstruct the crash to provide travel speed or impact speed and did not include detailed injury information. Due to these limitations, the speed limit was used as a surrogate for travel speed. Although we know that drivers are often driving above or below the speed limit, with the information present we could not accurately determine the true travel speed. Additionally, the database did not include specific impact location data or whether or not the driver braked prior to the collision which were necessary components in the spatiotemporal model developed to assess pedestrian AEB effectiveness. Without detailed injury information we could not make estimates of how the change in impact speed could affect bicyclist injury levels, therefore only crash avoidance was examined.

9.5 CONCLUSION

This study used the WATS database to estimate the potential effectiveness of bicyclist AEB in the US. Interestingly, there was no crash avoidance effectiveness at TTC thresholds less than 1 second and no crashes in adverse weather conditions were avoided. As TTC threshold increased and latency decreased there was increased estimated crash avoidance and greater potential for impact speed mitigation.

10 BICYCLIST AEB PREDICTED BENEFITS

10.1 RESEARCH OBJECTIVE

The effectiveness values estimated in chapter 9 assumed that all vehicles had bicyclist-AEB, but this is unlikely to occur given that bicyclist AEB is relatively new. Any new vehicle technology requires years to be widely deployed within the fleet, especially in the U.S. where the average vehicle is 11.8 years old [100]. This chapter aims to estimate the benefits of bicyclist in a mixed fleet and predicts benefits of bicyclist AEB in future fleets.

10.2 APPROACH

In order to estimate system effectiveness, we have to consider the market penetration of bicyclist-AEB. The Insurance Institute for Highway Safety-Highway Data Loss Institute (IIHS-HILDI) created market penetration predictions for a number of active safety features. As of the most recent report, bicyclist-AEB estimates were not included [101]. Therefore, vehicle AEB estimates were shifted to start in 2013 to reflect when bicyclist-AEB first entered the market. We used the 2015 curve for AEB market penetration because it was created prior to the agreement by car manufactures to have AEB standard in their vehicles by 2022 which would affect the penetration rate [102].

We then applied the bicyclist-AEB effectiveness numbers from chapter 9 to estimate the effectiveness of bicyclist-AEB at reducing crashes given the market penetration out to the year 2070. We used the effectiveness values from the best performing system, the system with a TTC of 1.5 seconds and a latency of 0, which had an estimated 50% avoidance effectiveness. The worst performing system had no crash avoidance effectiveness so they were not plotted, but would be represented by the crash number with no intervention.

Finally, we applied the effectiveness numbers for a given year to the estimated incidence rate of the target population from the present to 2070. Incidence was calculated as the number of crashes

in the target population over the number of vehicle miles travelled (VMT). The number of crashes in our target population was calculated using 2015 GES data. It was assumed that VMT would remain constant or increase approximately 1% annually, therefore causing the target population of crashes to increase as well [80].

10.3 RESULTS

Figure 106 shows the estimated market penetration of bicycle-AEB in the U.S. We assumed that bicyclist AEB entered the market in 2013 because that was when Volvo first released bicyclist detection in their new model year vehicles.

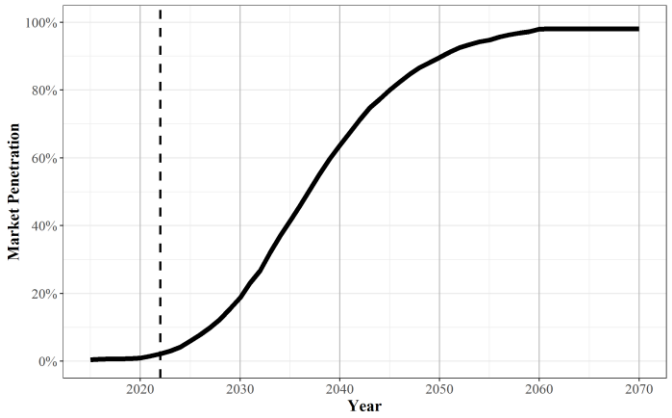

Figure 106. Estimated bicyclist-AEB market penetration based on the IIHS AEB market penetration estimates and shifted to reflect bicyclist-AEB entering the market in 2019.

We then applied the effectiveness numbers from chapter 9 to the market penetration values to get the crash reduction effectiveness at various market penetrations (Figure 107) and over time (Figure 108).

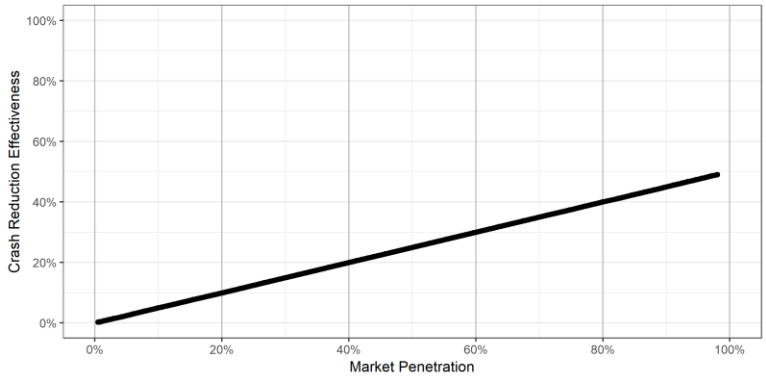

Figure 107. Crash reduction by market penetration.

Next we applied the crash reduction effectiveness per market penetration to the estimated market penetration over time to determine the crash reduction effectiveness over time (Figure 108).

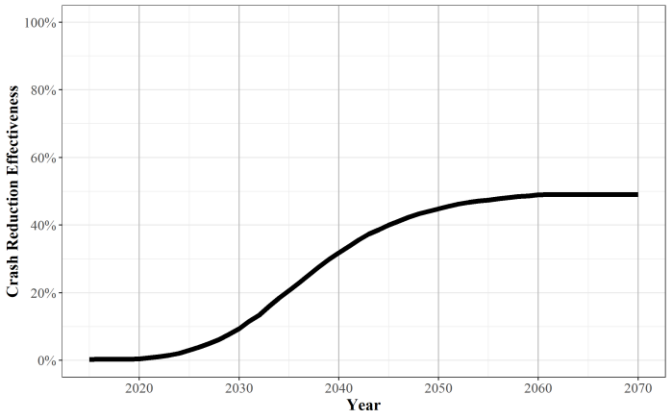

Figure 108. Crash reduction effectiveness by year.

To estimate the residual crashes in 2025 and beyond, we estimated the incidence of vehicle-bicycle crashes in the target population over time assuming they remained constant or increase linearly with vehicle miles travelled at a rate of 1% annually. Figure 61 (black line) shows the estimated number of target population vehicle-bicycle crashes out to 2050 given that intervention does not occur. We then applied the crash reduction effectiveness by year to show the residual

vehicle-bicycle crashes out to 2070 (Figure 61). The dotted line corresponds to the year in which there will be 95% adoption of bicyclist AEB which we estimated to occur in the year 2056. The estimated crash values with and without intervention can be found in Table 42. Initially, there was minimal crash reduction from bicycle AEB because when adoption is low, the likelihood that a vehicle-bicycle interaction occurs with a vehicle with bicyclist AEB is very low. As adoption increased the crash reduction potential also increased, although we see a leveling off of crash reduction around the year 2050 because the technology is in most vehicles meaning the crash reduction effectiveness is nearing its full potential.

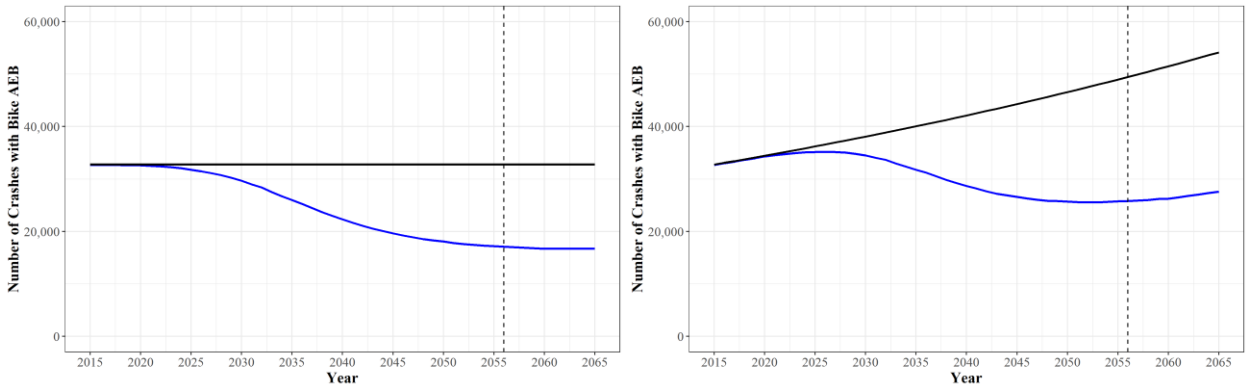

Figure 109. Estimate of vehicle-bicycle crashes without bicyclist-AEB (black line) compared to crashes with bicyclist-AEB (blue line) for the constant (left) and increasing (right) VMT assumptions.

Table 42. Estimated vehicle-bicycle crashes with and without bicyclist-AEB intervention for the constant and growing VMT assumptions.

Year	Constant VMT		Growing VMT	
	Without intervention	With intervention	Without intervention	With intervention
2020	32,759	32,603	34,447	34,283
2030	32,759	29,685	38,089	34,515
2040	32,759	22,329	42,115	28,707
2050	32,759	18,081	46,568	25,702
2060	32,759	16,707	51,491	26,260
2070	32,759	16,699	56,934	29,021

10.4 Discussion

This study used technology adoption curves developed by HILDI and IIHS to estimate the adoption of bicycle AEB into the US market. The 2015 estimation for AEB was used because this was before the voluntary agreement by vehicle manufacturers to include AEB as standard feature by 2022. While the voluntary agreement only applies to vehicle to vehicle AEB, the agreement may speed up adoption of bicycle AEB as well because bicycle AEB would not necessarily require additional sensors to be installed on the vehicle.

We used two different VMT assumptions to predict future crashes. One in which the VMT remains constant and one in which the VMT grows at 1% per year. These assumptions provide bounds for potential VMT growth as we did not account for potential fluctuations in VMT, as we saw in 2020 [103].

In-depth vehicle-bicycle crash data in the US is limited. WATS was used to estimate the effectiveness of bicyclist AEB in reducing crashes. While WATS is valuable due to the detailed crash scene diagrams, the crashes were not reconstructed meaning travel and impact speeds were unknown. Instead, the speed limit was used as a surrogate for travel speed. Additionally, WATS was not nationally representative and no weighting scheme was provided to compare WATS cases to national incidence.

10.5 Conclusion

In this chapter, future benefits of a bicyclist detection AEB system were predicted out to 2070. While bicyclist detecting AEB systems are a promising solution to mitigate or avoid vehicle-bicycle collisions, they could not avoid all vehicle-bicycle crashes. If a bicyclist AEB system could avoid 50% of vehicle-bicycle crashes we could see a 32% reduction in vehicle bicycle crashes by the year 2040 and nearly full benefits (95% adoption) by 2056.

11 UNDERSTANDING PEDESTRIAN BEHAVIOR IN CRASH AND NEAR-CRASH SCENARIOS

11.1 RESEARCH OBJECTIVE

In previous chapters we explored the potential for vehicle-pedestrian crash mitigation through vehicle based countermeasures with the assumption that the pedestrian did not take any evasive maneuvers, but this does not accurately represent real crash and near-crash scenarios. The goal of this chapter was to better understand pedestrian reactions during crashes and near crashes and propose a taxonomy for classification of these reactions.

11.2 INTRODUCTION

As vehicles become more advanced, the ability to quantify and predict pedestrian behavior is a vital component to reducing vehicle-pedestrian crashes. As shown in previous chapters, active safety features like AEB show great promise in avoiding vehicle-pedestrian crashes when it is assumed that the vehicle and pedestrian are on a collision course, but in reality this assumption isn't so simple. Pedestrians, more so than other road users, have the ability to change direction and speed quickly and often, making their movements less predictable than other road users.

A large collection of research has examined pedestrians as crosswalks and intersections paying special attention to when pedestrians decide to cross [104]. Additional work has used naturalistic data to identify situations that lead to increased conflict risk to pedestrians such as children traveling alone and adults in groups [36] [34].Other research has examined pedestrian pose in simulated crashes to understand what pedestrian do when they are struck by a vehicle [105]. While this information is useful it does not answer the question of how pedestrians respond when they are faced with an imminent crash or near crash scenario.

In this chapter we sought to understand what actions pedestrians take in response to a potential conflict with a vehicle. This information could help inform pedestrian behavior models and help make vehicle-pedestrian simulations more realistic.

11.3 METHODS

11.3.1 DATA SELECTION

Data for this study was taken from the Automated Mobility Partnership (AMP) database. The AMP database is a targeted and curated sample of driving scenarios from different naturalistic driving studies, including SHRP 2[106] . We specifically used trajectory data from SHRP 2 crashes and near crashes that had been incorporated into the AMP database.

For each case in which dynamic actor trajectories were able to be collected, the dataset provided the location, speed, and heading for the subject vehicle and the dynamic actors (which could include pedestrians, bicyclists, and other vehicles). For this study we were specifically looking for pedestrians that were involved in crashes or near crashes. We only examined the pedestrians that "interacted with the vehicle", which was defined as the pedestrian with which the vehicle had a crash or near crash interaction. To determine the interacting pedestrian/s, each case with multiple pedestrians was examined to ensure that the pedestrian being considered was relevant and not just a bystander to the interaction.

Of the 256 cases in which trajectories were collected and that involved pedestrians, 51 cases (involving 53 interacting pedestrians) were crashes or near-crashes. Of these 3 cases were crashes. One crash was excluded because "crash" resulted from the pedestrian intentionally kicking the subject vehicle after a disagreement with the subject vehicle driver, resulting in a total of 50 cases that were analyzed.

11.3.2 Reaction Classification

Pedestrian velocity profiles from the 50 cases were divided into categories based on the pedestrian's change in speed and heading over the event. If the pedestrian changed speed more than 0.3 m/s over the course of the event, the pedestrian reaction was either classified as speeding up or slowing down. The threshold of 0.3 m/s was chosen because it 25% of 1.2 m/s, which is the average adult pedestrian walking speed. Often pedestrians both accelerated and decelerated over the course of the event, therefore, to choose the appropriate reaction we identified the inflection points and chose the inflection point that was closest to the impact proximity point. The impact proximity point is the time at which the vehicle made first contact with the pedestrian or, in the case of a near crash, the time at which the vehicle was spatially the closest to the pedestrian [98]. The proximity point was previously identified by SHRP 2 data reductions and, in this study, aligned with the time series trajectory points by assuming the trajectory points started at the 'event start' time (also defined previously by the SHRP 2 data reductionists). If there were two inflection points equidistant from the impact proximity point, we chose the inflection point with the highest magnitude jerk value (i.e. the most rapid change in acceleration).

If the pedestrian heading changed more than 60°, the pedestrian reaction was classified as a change in direction. In all of the change in direction cases the pedestrian also had at least a 0.3 m/s change in speed, so these cases were classified as a change in speed and direction. If a pedestrian was not classified as reacting with a change of speed or direction, we assumed the pedestrian took no significant avoidance action and classified the case as "minimal reaction".

11.3.3 Reaction Parameters

The reaction classifications were examined across pedestrian location, pedestrian estimated age, and lighting conditions to discern if the pedestrian reactions were more likely in specific conditions. This is important for context-aware pedestrian behavior prediction.

To understand the parameters of the different pedestrian reactions the minimum, average, and maximum speeds, and the time the reaction took place relative to the impact proximity point were examined for each reaction classification. The starting point of the reaction time for the speed up and slow down reactions was based on the inflection point used for reaction classification. The starting point of the reaction time for change of direction and speed cases was based on either the inflection point or the time point at which the pedestrian heading had changed 10° from the original trajectory, whichever came first.

11.4 RESULTS

11.4.1 REACTION CLASSIFICATION

The most common pedestrian reaction was speeding up followed by slowing down, minimal response, and a change in speed and direction (Figure 110). The groupings were fairly evenly distributed. The distribution was dependent on the chosen thresholds. While thresholds were not optimized for an equal distribution, they were chosen such that each group had at least three events. No other optimization was conducted.

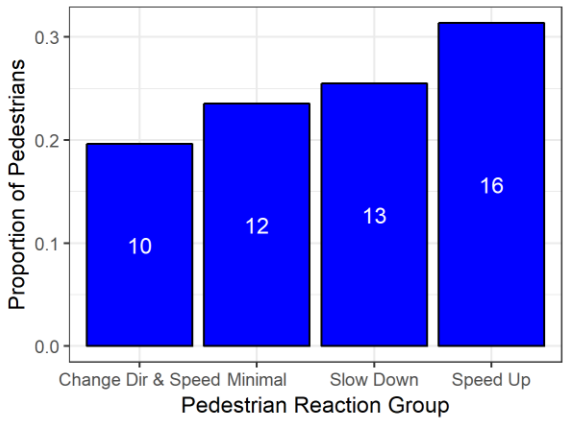

Figure 110. Distribution of pedestrian reactions. The number in the bar corresponds to the number of pedestrian trajectories.

As shown in Figure 111, in most of the speed up cases the pedestrian was initially stopped or travelling at a low speed and then sped up after the impact proximity point. In the cases in which the pedestrian slowed down, the pedestrians were not visible until after the impact proximity point and then slowed down or came to a stop. Although, the pedestrian was visible before the proximity point for many of the other reaction types, most of the noticeable changes in speed did not occur until about 4000ms after the proximity point.

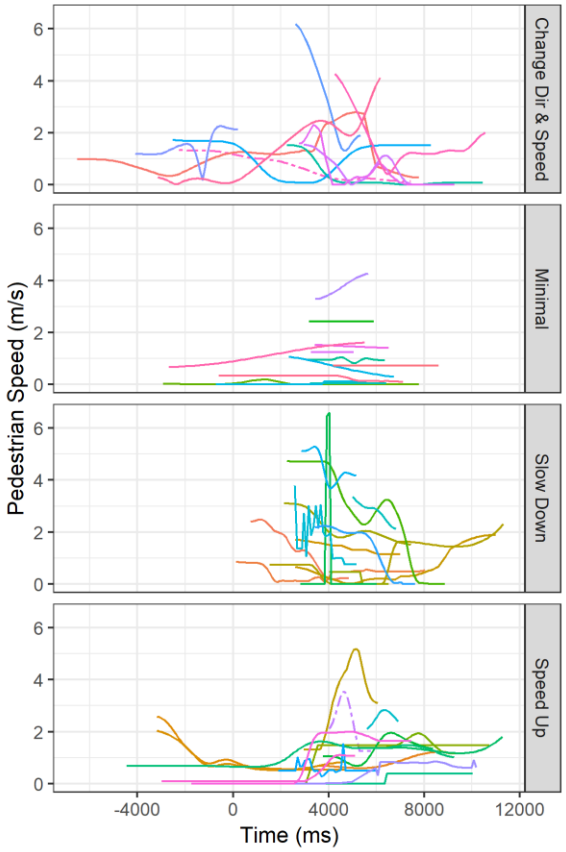

Figure 111. Pedestrian speed profiles for SHRP 2 crash and near crash events divided by pedestrian reaction group. A time of zero corresponds to the impact proximity point. Dotted lines represent events that were crashes.

The threshold for categorizing a pedestrian reaction as a change in direction was a difference of 60° in heading over the course of the event. As shown in Figure 112, most pedestrian reactions did not involve much change in heading. Most pedestrians that changed direction continued along their new path, although some returned to their original path presumably once they were no longer on a collision course with the vehicle. Similar to the change in speed, most pedestrians did not noticeably change direction until about 4000ms after the impact proximity point.

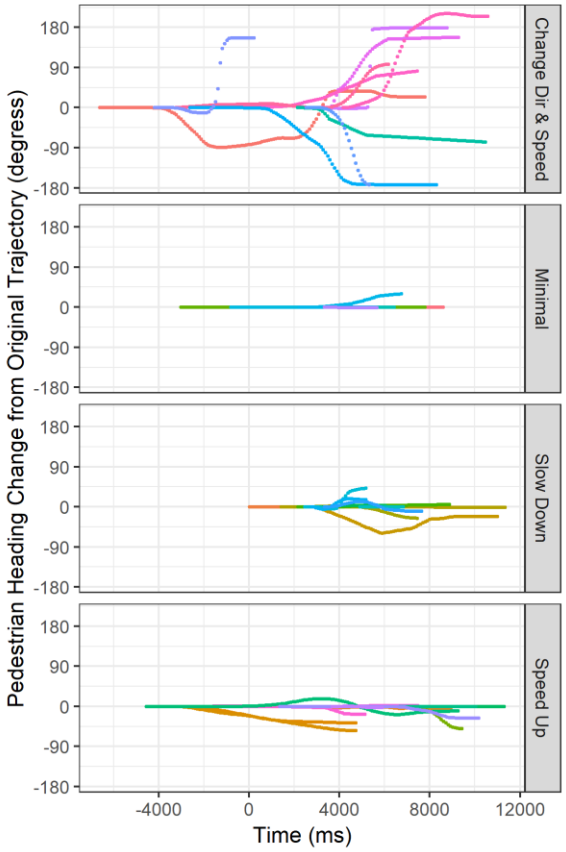

Figure 112. Pedestrian heading change from original trajectory for SHRP 2 crash and near crash events divided by pedestrian reaction group. A time of zero corresponds to the impact proximity point.

As shown in Figure 111 and Figure 112, the pedestrians in the minimal response category had very little change in speed or direction over the course of the event. Further video review revealed that these "minimal response" pedestrians often appeared to be aware of the vehicle, but trusted that the vehicle would not hit them. In two cases, the pedestrian backed up when the vehicle approached. In these cases, the pedestrian's heading did not noticeably change and their overall speed change was below the speed change threshold. Three additional cases involved a pedestrian exiting or entering a vehicle that was parked on the side of the road.

11.4.2 Reaction Conditions

As shown in Figure 113, most of the vehicle pedestrian interactions examined occurred when the pedestrian was in the travel lane, but not in a crosswalk. This was the prevalent pedestrian location for pedestrians that slowed down, changed speed and direction, and pedestrians that minimally reacted to the near crash situation. However, pedestrians that sped up were more likely to be located in crosswalks. Pedestrians with minimal reactions were disproportionately on the road shoulder or in a driveway which could explain why they did not change direction or speed.

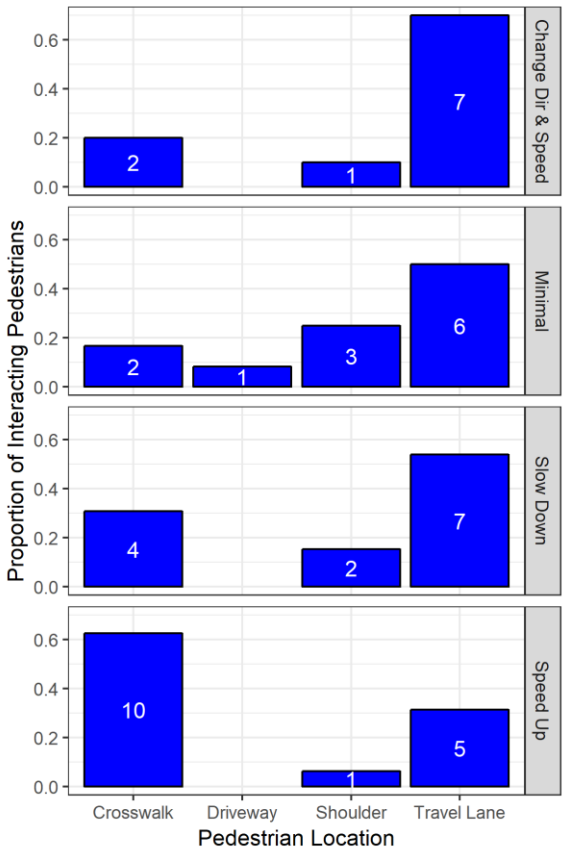

Figure 113. Distribution of pedestrian locations for each pedestrian reaction type. The number in the bar corresponds to the number of pedestrian trajectories.

The most common lighting condition for all the pedestrian reactions was daylight light conditions (Figure 114). This was not surprising as daylight conditions are the more prevalent among vehicle-pedestrian near-crashes in SHRP 2 [5]. The pedestrians that slowed down had the lowest proportion of cases that occurred during daylight (50%).

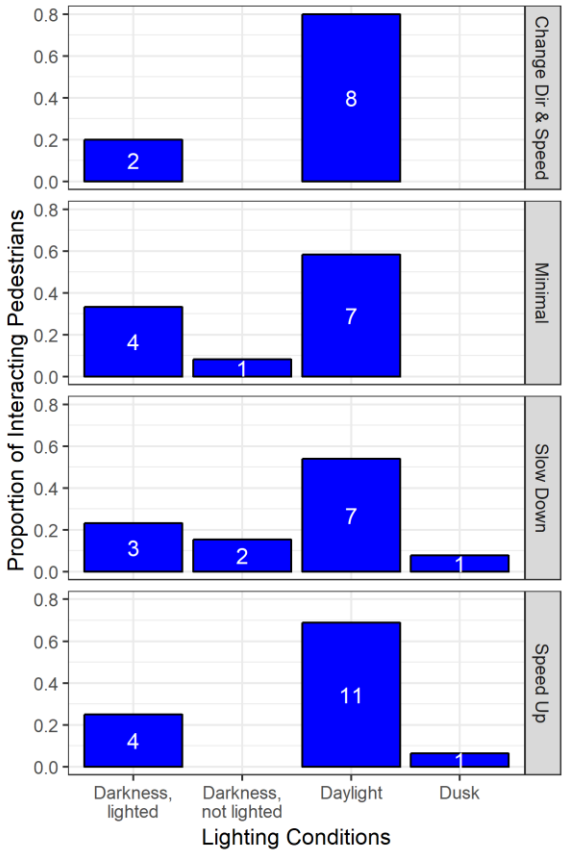

Figure 114. Distribution of lighting conditions for each pedestrian reaction type. The number in the bar corresponds to the number of pedestrian trajectories.

Adult pedestrians were the most common age group present in the examined cases. Young adults, the second most prevalent group were more likely to speed up or minimally respond (Figure 115). No young adults reacted by changing direction. The two senior pedestrians in the cases reacted by speeding up. It should be noted that this study was conducted on a small sample size of vehicle-pedestrian crashes and near crashes.

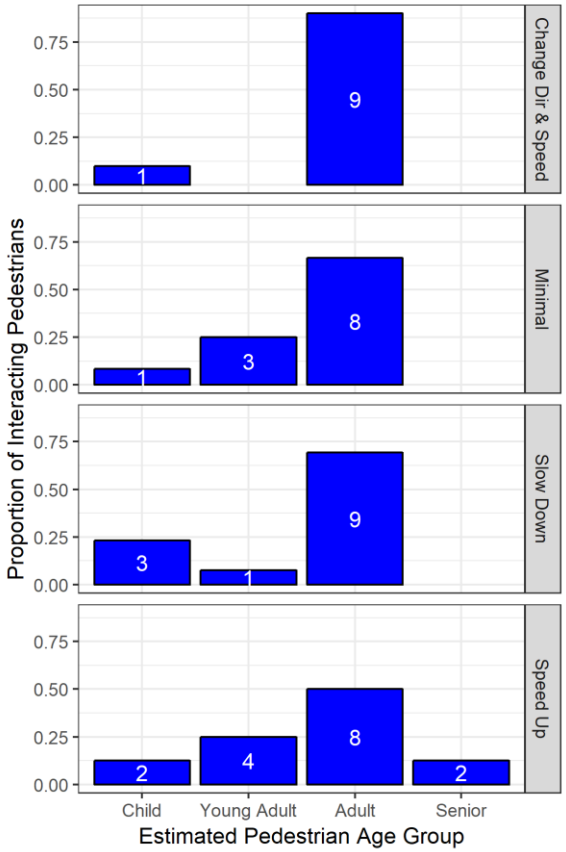

Figure 115. Distribution of estimated pedestrian age group for each pedestrian reaction type. The number in the bar corresponds to the number of pedestrian trajectories.

11.4.3 Reaction Parameters

Pedestrian speeds varied by pedestrian reaction type. Pedestrians that minimally reacted had the lowest average speed, with about 75% of these pedestrians walking at speeds of 1 m/s or below. These pedestrians also exhibited very little difference between their minimum and maximum speed, as expected. For the pedestrians that changed direction or slowed down, the maximum speed was above 2 m/s for 60 – 75% of the cases. According to Rotstein, et al. [107] the speed at which a walk becomes a run is about 2 m/s. About 33% of the cases in which the pedestrians slowed down had a

minimum speed of 0 m/s which indicates that they came to a stop. For the speed up cases, about 35% of the pedestrians had a minimum speed of 0 m/s, indicating that they accelerated from a stop.

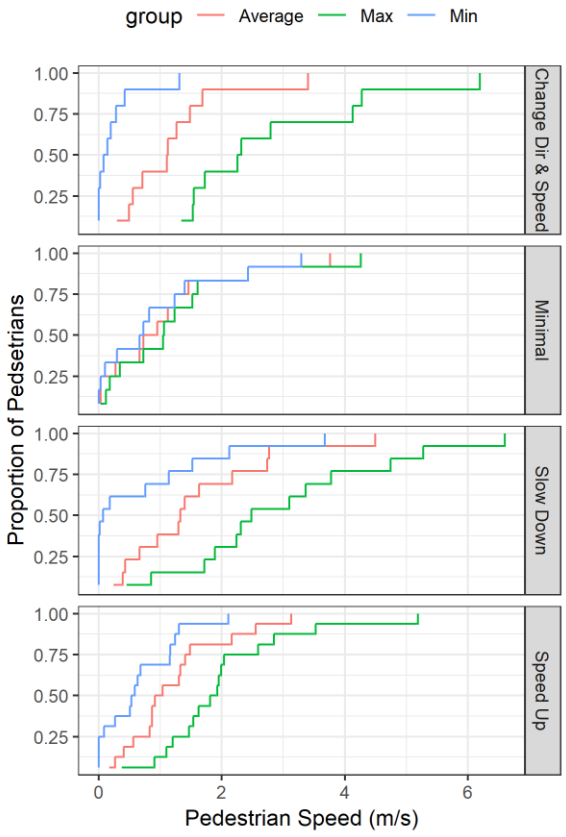

Figure 116. Cumulative distribution of minimum (blue), average (red), and maximum (green) pedestrian speed for each pedestrian reaction group.

Reaction time is very important for modeling behavior. As shown in Figure 117, pedestrians that changed direction and speed tended to begin their reaction earlier with about 25% of the pedestrians reacting before the impact proximity point and 50% reacting within 2.5 seconds of the impact proximity point. Pedestrians that sped up reacted slightly slower with about 12% reacting before the impact proximity point and 50% reacting within 5 seconds of impact proximity point. Pedestrians that slowed down were the slowest to react with no pedestrians reacting before the impact proximity point. This may be partly due to the fact that the pedestrians in the slow down

category did not have data available prior to the proximity point (e.g. due to limited or no pedestrian visibility in the video). Video analysis revealed that, in many of these cases, the vehicle reacted before the pedestrian, slowing down or coming to a stop before the pedestrian reacted.

Note that, as the majority of the cases were near-crashes the proximity point was used as an anchor. This approach may be subject to some error in the timing of the pedestrian reaction because a clear impact point does not exist, therefore, the time is simply an estimate of when the vehicle and the pedestrian were closest to each other. Therefore, if a vehicle stopped to avoid a pedestrian, the proximity point would be when the vehicle came to a stop (i.e. when the vehicle and pedestrian were physically the closest). Limitations in the data, such as limited visibility and increased radar inaccuracies under low/no speed conditions, may also have resulted in inaccuracies in the pedestrian speed and location near the impact proximity point, and may be partly responsible for some of these findings. Additionally, the trajectory data was not inherently time synced with the video. The event start time was estimated to align the events with the proximity point, and this estimation may have introduced some error into the analysis.

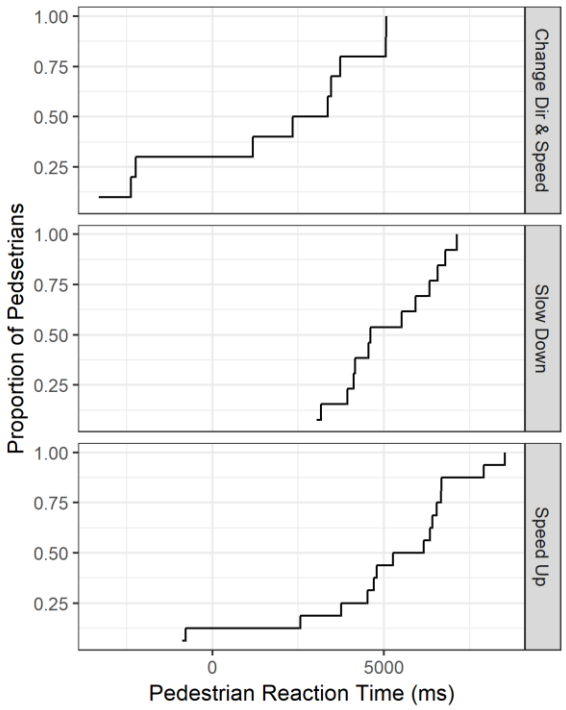

Figure 117. Cumulative distribution of pedestrian reaction time for each pedestrian reaction group. The minimal reaction group was not included as there was no estimated reaction time.

11.5 DISCUSSION

This study used pedestrian trajectory information to classify and characterize pedestrian reactions to an imminent vehicle-pedestrian crash or near-crash. Pedestrian reactions were grouped into four categories: minimal reaction, slow down, speed up, and change in speed and direction. For each category, we examined different characteristics including pedestrian age, relation to junction, pedestrian speed, and when the pedestrian reacted to the crash or near-crash.

The pedestrian reactions were categorized based on a completely automated process, which is beneficial because it would be scalable to larger datasets and doesn't rely on manual review of crash video. This automated process, however, may miss reactions that a human reviewer would see. The relevant reaction was chosen based on temporal closeness to the proximity point and the urgency of the reaction, but in certain situations it is possible that the reaction identified was not

related to the presence of the vehicle. Additionally, this method relies heavily on the pedestrian trajectories, which were collected from the vehicle instrumentation and video footage. Potential noise or errors in the instrumentation or algorithms to develop the trajectories could have affected the results.

This study provides a framework for classifying pedestrian reactions from trajectory data and outlines some characteristics that could be used for improving pedestrian models in vehicle-pedestrian crash simulations.

12 CONCLUSION

The purpose of this dissertation was to assess the potential effectiveness of AEB at mitigating or avoiding vehicle collisions with pedestrians and bicyclists. This was achieved through examination of the characteristics of the relevant crashes and near-crashes, quantifying the time an AEB system would have to react to a potential pedestrian or bicyclist, modeling and/or simulating real world crashes to assess the effect of a variety of AEB systems, and finally predicting how those effectiveness values would translate to crash reductions in the future.

To achieve these goals, we used a variety of datasets to assess AEB effectiveness because each dataset had its own limitations. Together, the datasets painted a much fuller picture of vulnerable road user crashes and allowed us to examine both individual crashes and near crashes in-depth along with trends in national crash data. This area of research would greatly benefit from new in-depth data in which relevant crashes were reconstructed to estimate impact speed. While naturalistic data has that capability, sample sizes of vehicle-pedestrian and vehicle-bicycle crashes tend to be low in that domain due to the rarity of these types of events and limited sizes of instrumented fleets.

This work assumed an idealized AEB system that was able to accurately and instantaneously detect pedestrians and bicyclists and always correctly identified them as potential collision partners. These assumptions overestimate the capabilities of current AEB systems. To address some of these limitations, the model could be modified to account for the sensor system detection accuracy, incorporate the time needed for the system to identify the pedestrian or bicyclist, and institute a measure of confidence that the pedestrian or bicyclist is a potential collision partner. These changes may provide a more accurate representation of the avoidance capability of AEB systems in non-ideal conditions than the current model.

Overall, we found that AEB has great potential to avoid and mitigate collisions with pedestrians and bicyclists, but it can't avoid all crashes even when assuming an idealized AEB system. Obstructions and adverse weather conditions are a challenging obstacle to AEB systems because they reduce the time that such a system has to respond and the braking ability of the system, respectively. Other mitigation strategies such as improved infrastructure, V2V and/or V2I communication, and hood airbags are some alternate technologies that may need to be explored in the future to achieve the ultimate goal of zero traffic fatalities.

REFERENCES

[1] National Center for Statistics and Analysis. (2019). *DOT HS 812 826, 2018 Fatal Motor Vehicle Crashes: Overview. (Traffic Safety Facts)*.

[2] S. H. Haus, R. Sherony, and H. C. Gabler, "Estimated benefit of automated emergency braking systems for vehicle–pedestrian crashes in the United States," *Traffic Injury Prevention,* vol. 20, no. sup1, pp. S171-S176, 2019/06/12 2019.

[3] S. H. Haus, R. Sherony, and H. C. Gabler, "Differential benefit of sensor system field-of-view and range in pedestrian automated emergency braking systems," *Traffic Injury Prevention,* pp. 1-5, 2021.

[4] S. H. Haus, R. M. Anderson, R. Sherony, and H. C. Gabler, "Potential Effectiveness of Bicycle-Automatic Emergency Braking using the Washtenaw Area Transportation Study Data Set," *Transportation Research Record,* 2021.

[5] S. H. Haus, R. Sherony, and H. C. Gabler, "Feasibility of using Naturalistic Driving Data to Characterise Vehicle-Pedestrian Crashes and Near Crashes," in *IRCOBI conference*, Athens, Greece, 2018.

[6] S. H. Haus, R. Sherony, and H. C. Gabler, "Automatic Emergency Braking Sensor Configuration Effect on the Detection of U.S. Pedestrians," in *IRCOBI Conference 2021*, Online, 2021.

[7] S. H. Haus and H. C. Gabler, "Characteristics of Vehicle-Bicycle Crashes and Near Crashes Using Naturalistic Driving Data," in *Transportation Research Board 97th Annual Meeting*, Washington DC, United States, 2018.

[8] M. G. Mohamed, N. Saunier, L. F. Miranda-Moreno, and S. V. Ukkusuri, "A clustering regression approach: A comprehensive injury severity analysis of pedestrian–vehicle crashes in New York, US and Montreal, Canada," *Safety Science,* vol. 54, pp. 27-37, 2013/04/01/ 2013.

[9] R. Fredriksson, E. Rosén, and A. Kullgren, "Priorities of pedestrian protection—A real-life study of severe injuries and car sources," *Accident Analysis & Prevention,* vol. 42, no. 6, pp. 1672-1681, 2010/11/01/ 2010.

[10] E. Rosén, J. E. Kallhammer, D. Eriksson, M. Nentwich, R. Fredriksson, and K. Smith, "Pedestrian injury mitigation by autonomous braking," *Accident Analysis and Prevention,* vol. 42, no. 6, pp. 1949-1957, 2010.

[11] T. Niebuhr, M. Junge, and E. Rosén, "Pedestrian injury risk and the effect of age," *Accident Analysis & Prevention,* vol. 86, pp. 121-128, 2016/01/01/ 2016.

[12] K. Mizuno and J. Kajzer, "Head Injuries in Vehicle-Pedestrian Impact," *SAE Transactions,* vol. 109, pp. 232-243, 2000.

[13] D. E. Lefler and H. C. Gabler, "The fatality and injury risk of light truck impacts with pedestrians in the United States," *Accident Analysis & Prevention,* vol. 36, no. 2, pp. 295-304, 2004/03/01/ 2004.

[14] R. Ono, W. Ike, and Y. Fukaya, "Pre-Collision System for Toyota Safety Sense," SAE Technical Paper 2016, Art. no. 2016-01-1458.

[15] A. Lopez, R. Sherony, S. Chien, L. Li, Y. Qiang, and Y. Chen, "Analysis of the Braking Behaviour in Pedestrian Automatic Emergency Braking," in *2015 IEEE 18th International Conference on Intelligent Transportation Systems*, 2015, pp. 1117-1122.

[16] M. Bareiss, "Effectiveness of Intersection Advanced Driver Assistance Systems in Preventing Crashes and Injuries in Left Turn Across Path/Opposite Direction Crashes in the United States," Virginia Tech, 2019.

[17] M. Bareiss, J. Scanlon, R. Sherony, and H. C. Gabler, "Crash and injury prevention estimates for intersection driver assistance systems in left turn across path/opposite direction

crashes in the United States," *Traffic injury prevention,* vol. 20, no. sup1, pp. S133-S138, 2019.
[18] L. E. Riexinger, R. Sherony, and H. C. Gabler, "Residual road departure crashes after full deployment of LDW and LDP systems," *Traffic injury prevention,* vol. 20, no. sup1, pp. S177-S181, 2019.
[19] J. A. Decker, S. H. Haus, R. Sherony, and H. C. Gabler, "Potential Benefits of Animal-Detecting Automatic Emergency Braking Systems Based on U.S. Driving Data," *Transportation Research Record,* p. 03611981211012416, 2021.
[20] M. E. Dean, S. H. Haus, R. Sherony, and H. C. Gabler, "Potential Crash Benefits of Motorcycle-Detecting Automatic Emergency Braking Systems."
[21] N. Lubbe and E. Rosén, "Pedestrian crossing situations: Quantification of comfort boundaries to guide intervention timing," *Accident Analysis & Prevention,* vol. 71, pp. 261-266, 2014/10/01/ 2014.
[22] N. Lubbe and J. Davidsson, "Drivers' comfort boundaries in pedestrian crossings: A study in driver braking characteristics as a function of pedestrian walking speed," *Safety Science,* vol. 75, pp. 100-106, 06/01 2015.
[23] N. Lubbe and A. Kullgren, "Assessment of Integrated Pedestrian Protection Systems with Forward Collision Warning and Automated Emergency Braking," *IRCOBI Conference Proceedings,* pp. 385-397, 2015.
[24] N. Lubbe, "Brake reactions of distracted drivers to pedestrian Forward Collision Warning systems," *Journal of Safety Research,* vol. 61, pp. 23-32, 2017/06/01/ 2017.
[25] C. Ho, N. Reed, and C. Spence, "Multisensory In-Car Warning Signals for Collision Avoidance," *Human Factors,* vol. 49, no. 6, pp. 1107-1114, 2007.
[26] M. Blommer, R. Curry, R. Swaminathan, L. Tijerina, W. Talamonti, and D. Kochhar, "Driver brake vs. steer response to sudden forward collision scenario in manual and automated driving modes," *Transportation research part F: traffic psychology and behaviour,* vol. 45, pp. 93-101, 2017.
[27] N. Lubbe, M. Edwards, and M. Wisch, "Towards an Integrated Pedestrian Safety Assessment Method," in *2012 IRCOBI Conference*, Dublin , Ireland, 2012.
[28] M. Edwards, A. Nathanson, and M. Wisch, "Estimate of Potential Benefit for Europe of Fitting Autonomous Emergency Braking (AEB) Systems for Pedestrian Protection to Passenger Cars," *Traffic Injury Prevention,* vol. 15, no. sup1, pp. S173-S182, 2014/09/26 2014.
[29] A. Millard-Ball, "Pedestrians, Autonomous Vehicles, and Cities," *Journal of Planning Education and Research,* vol. 38, no. 1, pp. 6-12, 2018.
[30] S. C. Stanciu, D. W. Eby, L. J. Molnar, R. M. St. Louis, N. Zanier, and L. P. Kostyniuk, "Pedestrians/Bicyclists and Autonomous Vehicles: How Will They Communicate?," *Transportation Research Record,* vol. 2672, no. 22, pp. 58-66, 2018.
[31] M. Detwiller and H. C. Gabler, "Potential Reduction in Pedestrian Collisions with an Autonomous Vehicle," presented at the 25th International Technical Conference on the Enhanced Safety of Vehicles (ESV), Detroit Michigan, United States, 2017.
[32] R. Kannan and R. C. Lasky, "Autonomous Vehicles Still Decades Away: 2019," in *2020 Pan Pacific Microelectronics Symposium (Pan Pacific)*, 2020, pp. 1-6.
[33] K. Yang, E. Y. Du, P. Jiang, Y. Chen, R. Sherony, and H. Takahashi, "Automatic categorization-based multi-stage pedestrian detection," in *2012 15th International IEEE Conference on Intelligent Transportation Systems*, 2012, pp. 451-456.
[34] R. Tian, L. Li, K. Yang, S. Chien, Y. Chen, and R. Sherony, "Estimation of the vehicle-pedestrian encounter/conflict risk on the road based on TASI 110-car naturalistic driving data collection," in *2014 IEEE Intelligent Vehicles Symposium Proceedings*, 2014, pp. 623-629.
[35] D. Belgiovane, C. Chen, M. Chen, S. Y. Chien, and R. Sherony, "77 GHz radar scattering properties of pedestrians," in *2014 IEEE Radar Conference*, 2014, pp. 0735-0738.

[36] E. Y. Du *et al.*, "Pedestrian behavior analysis using 110-car naturalistic driving data in USA," in *23rd International Technical Conference on the Enhanced Safety of Vehicles (ESV)*, Seoul, South Korea, 2013.
[37] R. Tian *et al.*, "Pilot study on pedestrian step frequency in naturalistic driving environment," in *2013 IEEE Intelligent Vehicles Symposium (IV)*, 2013, pp. 1215-1220.
[38] S. Chien, L. Dong, Q. Yi, Y. Chen, R. Sherony, and H. Takahashi, "Joint Motion Pattern of Limb Moving Mannequins for Active Safety Vehicle Tests," in *23rd International Technical Conference on the Enhanced Safety of Vehicles (ESV)*, Seoul , South Korea, 2013.
[39] D. Kim, "The transportation safety of elderly pedestrians: Modeling contributing factors to elderly pedestrian collisions," *Accident Analysis & Prevention,* vol. 131, pp. 268-274, 2019/10/01/ 2019.
[40] Insurance Institute for Highway Safety, "Pedestrian Autonomous Emergency Braking Test Protocol (Version 1)," Insurance Institute for Highway Safety, Ruckersville, VA2018.
[41] National Highway Traffic Safety Administration, "NHTSA Announces Coming Upgrades to New Car Assessment Program," ed. Washington, D.C. , October 16, 2019.
[42] M. van Ratingen *et al.*, "The European New Car Assessment Programme: A historical review," *Chinese Journal of Traumatology,* vol. 19, no. 2, pp. 63-69, 2016/04/01/ 2016.
[43] European New Car Assessment Programme (Euro NCAP), "Test Protocol - AEB VRU Systems," Version 2.0, 2017.
[44] J. Strandroth, M. Rizzi, S. Sternlund, A. Lie, and C. Tingvall, "The Correlation Between Pedestrian Injury Severity in Real-Life Crashes and Euro NCAP Pedestrian Test Results," *Traffic Injury Prevention,* vol. 12, no. 6, pp. 604-613, 2011/12/01 2011.
[45] European New Car Assessment Programme (Euro NCAP), "Assessment Protocol - Pedestrian Protection," June 2014, vol. Version 8.0.
[46] European New Car Assessment Programme (Euro NCAP), "Euro NCAP 2025 Roadmap," in *In Pursuit of Vision Zero*, ed, 2017.
[47] National Highway Traffic Safety Administration, "Fatality Analysis Reporting System (FARS) Analytical User's Manual (1975-2017) " 2018.
[48] (2018). *DOT HS 812 320, National Automotive Sampling System General Estimates System analytical user's manual, 1988-2015*.
[49] (2019). *DOT HS 812 688, Crash Report Sampling System: Design Overview, Analytic Guidance, and FAQs*.
[50] NHTSA, "Pedestrian Crash Data Study 1996 Data Collection, Coding, and Editing Manual," Washington1996.
[51] M. Detwiller and H. C. Gabler, "Potential Reduction in Pedestrian Collisions with an Autonomous Vehicle," in *Enhanced Safety of Vehicles*, Detroit, 2017.
[52] J. F. Antin, S. Lee, M. A. Perez, T. A. Dingus, J. M. Hankey, and A. Brach, "Second strategic highway research program naturalistic driving study methods," *Safety Science,* vol. 119, pp. 2-10, 2019.
[53] A. S. Trigell, M. Rothhämel, J. Pauwelussen, and K. Kural, "Advanced vehicle dynamics of heavy trucks with the perspective of road safety," *Vehicle System Dynamics,* vol. 55, no. 10, pp. 1572-1617, 2017/10/03 2017.
[54] National Highway Traffic Safety Administration. (March 2020). *DOT HS 812 850, Pedestrians: 2018 Data*.
[55] N. Lubbe and E. Rosen, "Pedestrian crossing situation: Quantification of comfort boundaries to guide intervention timing," *Accident Analysis and Prevention,* vol. 71, pp. 261-266, 2014.
[56] T. Niebuhr, M. Junge, and E. Rosen, "Pedestrian injury risk and the effect of age," *Accident Analysis and Prevention,* vol. 86, pp. 121-128, 2016.
[57] A. Bartsch, Fitzek, F., and Rasshofer, R.H., "Pedestrian recognition using automotive radar sensors," *Advances in Radio Science,* pp. 45-55, 2012.

[58] R. Bhagavathula, R. Gibbons, and C. Edwards, *Effect of Static and Moving Objects on Driver Eye Movements and Detection Distances*. 2012.
[59] T. J. Gates, D. A. Noyce, A. R. Bill, and N. Van Ee, "Recommended Walking Speeds for Pedestrian Clearance Timing Based on Pedestrian Characteristics," *TRB Annual Meeting,* no. 06-1826, 2006.
[60] T. J. Gates, D. A. Noyce, A. R. Bill, and N. Van Ee, "Recommended Walking Speeds for Pedestrian Clearance Timing Based on Pedestrian Characteristics," *TRB Annual Meeting,* 2006, Art. no. 06-1826.
[61] K. D. Kusano and H. C. Gabler, "Safety Benefits of Forward Collision Warning, Brake Assist, and Autonomous Braking Systems in Rear-End Collisions," *IEEE Transactions on Intelligent Transportation Systems,* vol. 13, no. 4, pp. 1546-1555, 2012.
[62] ETSI, "System Reference document (SRdoc); Transmission characteristics; Technical characteristics for radiodetermination equipment for ground based vehicular applications within the frequency range 77 GHz to 81 GHz," 2020, vol. 1.1.1 Available: https://www.etsi.org/deliver/etsi_tr/103500_103599/103593/01.01.01_60/tr_103593v010101p.pdf.
[63] S. H. Haus, R. Sherony, and H. C. Gabler, "Differential Benefit of LiDAR and Current Sensor Systems in Pedestrian Automated Emeregency Braking Systems," *Traffic Injury Prevention,* vol. In Press, 2021.
[64] A. S. Mohammed, A. Amamou, F. K. Ayevide, S. Kelouwani, K. Agbossou, and N. Zioui, "The Perception System of Intelligent Ground Vehicles in All Weather Conditions: A Systematic Literature Review," (in eng), *Sensors (Basel),* vol. 20, no. 22, pp. 8-22, Nov 15 2020.
[65] J. Lenard, R. Welsh, and R. Danton, "Time-to-collision analysis of pedestrian and pedal-cycle accidents for the development of autonomous emergency braking systems," *Accident Analysis & Prevention,* vol. 115, pp. 128-136, 2018/06/01/ 2018.
[66] M. S. A. Hardy and D. Cebon, "An Investigation of Anti-Lock Braking Strategies for Heavy Goods Vehicles," *Proceedings of the Institution of Mechanical Engineers, Part D: Journal of Automobile Engineering,* vol. 209, no. 4, pp. 263-271, 1995.
[67] E. Rosén, "Autonomous Emergency Braking for Vulnerable Road Users," in *IRCOBI Conference*, Gothenburg, Sweden, 2013.
[68] (2007). *FHWA-SA-07-011, Mitigation Startegies for Design Exceptions*.
[69] J. M. Scanlon, R. Sherony, and H. C. Gabler, "Injury mitigation estimates for an intersection driver assistance system in straight crossing path crashes in the United States," *Traffic Injury Prevention,* vol. 18, no. sup1, pp. S9-S17, 2017/05/29 2017.
[70] K. D. Kusano and H. Gabler, "Method for Estimating Time to Collision at Braking in Real-World, Lead Vehicle Stopped Rear-End Crashes for Use in Pre-Crash System Design," *SAE International Journal of Passenger Cars - Mechanical Systems,* vol. 4, no. 1, pp. 435-443, 2011.
[71] D. E. Lefler and H. C. Gabler, "The fatality and injury risk of light truck impacts with pedestrians in the United States," *Accident Analysis & Prevention,* no. 36, pp. 295-304, 2004.
[72] R Core Team, "R: A Language and Environment for Statistical Computing," ed. Vienna, Austria: R Foundation for Statistical Computing, , 2017.
[73] E. Rosén and U. Sander, "Pedestrian fatality risk as a function of car impact speed," *Accident Analysis and Prevention,* vol. 41, pp. 536-542, 2009.
[74] A. B. Chidester and R. Isenberg, "FINAL REPORT - THE PEDESTRIAN CRASH DATA STUDY," in *International Technical Conference on the Enhanced Safety of Vehicles*, Amsterdan, Netherlands, 2001.
[75] National Highway Traffic Safety Administration, "National Automotive Sampling System: General Estimates Data System: Analytical User's Manual (1988-2015)," 2018.

[76] A. A. Belyaev, T. A. Suanov, I. O. Frolov, and D. O. Trots, "The Range of Pedestrian Detection with Automotive Radar," in *2019 Radiation and Scattering of Electromagnetic Waves (RSEMW)*, 2019, pp. 432-435.
[77] L. Tang, Y. Shi, Q. He, A. W. Sadek, and C. Qiao, "Performance Test of Autonomous Vehicle Lidar Sensors Under Different Weather Conditions," *Transportation Research Record,* vol. 2674, no. 1, pp. 319-329, 2020/01/01 2020.
[78] M. Gruber *et al.*, "The Effect of P-AEB System Parameters on the Effectiveness for Real World Pedestrian Accidents," in *International Technical Conference on the Enhanced Safety of Vehicles* Eindhoven, Netherlands, 2019.
[79] K. Wakeman, M. Moore, D. Zuby, and L. Hellinga, "Effect of Subaru Eyesight on pedestrian-related bodily injury liability claim frequencies," in "Bulletin," Arlington, VA December 2017, vol. 34.
[80] Office of Highway Policy Information, "FHWA Forecasts of Vehicle Miles Traveled (VMT): Spring 2019," 2019.
[81] K. Wang and G. Akar, "Gender gap generators for bike share ridership: Evidence from Citi Bike system in New York City," *Journal of Transport Geography,* vol. 76, pp. 1-9, 2019/04/01/ 2019.
[82] (2006). *FHWA-HRT-06-089, Pedestrian and Bicycle Crash Analysis Tool (PBCAT): Version 2.0 Application Manual*.
[83] National Highway Traffic Safety Administration. (2018). *DOT HS 812 564, 2017 FARS/CRSS Pedestrian Bicyclist Crash Typing Manual: A guide for Coders Using the FARS/CRSS Ped/Bike Typing Tool*.
[84] R. Fredriksson and E. Rosén, "Priorities for Bicyclist Protection in Car Impacts - a Real life Study of Severe Injuries and Car Sources," in *IRCOBI Conference*, 2012.
[85] *Road Traffic Regulations (Straßenverkehrs-Ordnung, StVO) Section 37.(2).1*, 2016.
[86] R. Sherony, R. Tian, S. Chien, L. Fu, Y. Chen, and H. Takahashi, "Pedestrian/Bicyclist Limb Motion Analysis from 110-Car TASI Video Data for Autonomous Emergency Braking Testing Surrogate Development," *SAE International Journal of Transportation Safety,* vol. 4, no. 1, pp. 113-120, 2016.
[87] S. H. Haus and H. C. Gabler, "The Potential for Active Safety Mitigation of US Vehicle-Bicycle Crashes," in *Future Active Safety Technology Towards Zero Traffic Accidents (FAST-Zero)*, Blacksburg, VA, 2019.
[88] D. C. Thompson, V. Rebolledo, R. S. Thompson, A. Kaufman, and F. P. Rivara, "Bike speed measurements in a recreational population: validity of self reported speed," *Injury Prevention,* vol. 3, no. 1, p. 43, 1997.
[89] H. Ling and J. Wu, *A Study on Cyclist Behavior at Signalized Intersections*. 2005, pp. 293-299.
[90] R. Sherony *et al.*, *Development of Bicycle Carrier for Bicyclist Pre-Collision System Evaluation* (SAE 2016 World Congress and Exhibition). Detroit, Michigan, 2016.
[91] R. Sherony and C. Zhang, "Pedestrian and Bicyclist Crash Scenarios in the U.S," in *2015 IEEE 18th International Conference on Intelligent Transportation Systems*, 2015, pp. 1533-1538.
[92] E. Robartes and T. D. Chen, "The effect of crash characteristics on cyclist injuries: An analysis of Virginia automobile-bicycle crash data," *Accident Analysis & Prevention,* vol. 104, pp. 165-173, 2017/07/01/ 2017.
[93] Q. Yi *et al.*, "Development of Bicycle Surrogate for Bicyclist Pre-Collision System Evaluation," 2016. Available: https://doi.org/10.4271/2016-01-1447
[94] H. Liers and L. Hannawald, "Benefit estimation of secondary safety measures in real-world pedestrian accidents," in *22st International Technical Conference on the Enhanced Safety of Vehicles (ESV 2011)*, 2011, no. 11-0300.
[95] M. Lindman, A. Ödblom, E. Bergvall, A. Eidehall, B. Svanberg, and T. Lukaszewicz, "Benefit estimation model for pedestrian auto brake functionality," 2010.

[96] National Highway Traffic Safety Administration. (March 2017). *DOT HS 812 382, Traffic Safety Facts: Bicyclists and Other Cyclists 2015 Data*. Available: https://crashstats.nhtsa.dot.gov/Api/Public/ViewPublication/812382
[97] F. Guo, S. G. Klauer, J. M. Hankey, and T. A. Dingus, "Near Crashes as Crash Surrogate for Naturalistic Driving Studies," *Transportation Research Record Journal of the Transportation Research Board,* vol. 2147, no. 1, pp. 66-74, 2010.
[98] J. M. Hankey , M. A. Perez, and J. A. McClafferty, "Description of the SHRP 2 Naturalistic Database and the Crash, Near-Crash, and Baseline Data Sets," 2016.
[99] U.S. Department of Transportation. (2016). *FHWA-RD-97-152, Guidelines for the Use of Raised Pavement Markers*. Available: https://www.fhwa.dot.gov/publications/research/safety/97152/ch01.cfm
[100] IHS Markit, "Average Age of Cars and Light Trucks in U.S. Rises Again in 2019 to 11.8 Years, IHS Markit Says," ed. Southfield, Mich, 2019.
[101] Highway Loss Data Institute, "Predicted availability and fitment of safety features on registered vehicke - a 2018 update," Arlington, VA. 27, September 2018, vol. 35.
[102] Highway Loss Data Institute, "Predicted availability of safety features on registered vehicle - a 2015 update," in "Loss Bulletin," Arlington, VASeptember 2015, vol. 32.
[103] (May 2021). *DOT HS 813 115, Early Estimate of Motor Vehcile Traffic Fatalities in 2020*. Available: https://crashstats.nhtsa.dot.gov/Api/Public/ViewPublication/813115
[104] A. Rasouli, I. Kotseruba, and J. K. Tsotsos, "Understanding Pedestrian Behavior in Complex Traffic Scenes," *IEEE Transactions on Intelligent Vehicles,* vol. 3, no. 1, pp. 61-70, 2018.
[105] A. Soni, T. Robert, F. Rongiéras, and P. Beillas, "Observations on Pedestrian Pre-Crash Reactions during Simulated Accidents," 2013. Available: https://doi.org/10.4271/2013-22-0006
[106] "Automated Mobility Partnership Database," V. T. T. Institute, Ed., ed. https://vtti-amp.org/.
[107] A. Rotstein, O. Inbar, T. Berginsky, and Y. Meckel, "Preferred transition speed between walking and running: effects of training status," (in eng), *Med Sci Sports Exerc,* vol. 37, no. 11, pp. 1864-70, Nov 2005.